

HETEROGENEITY OF DUTCH RAINFALL

J.V. Witter

CENTRALE LANDBOUWCATALOGUS



0000 0060 0631

Promotoren: dr.ir. L.C.A. Corsten, hoogleraar in de Wiskundige
Statistiek
ir. D.A. Kraijenhoff van de Leur, hoogleraar in de
Hydraulica, de Afvoerhydrologie en de Grondmechanica

J.V. WITTER

HETEROGENEITY OF DUTCH RAINFALL

Proefschrift

ter verkrijging van de graad van
doctor in de landbouwwetenschappen,
op gezag van de rector magnificus,
dr. C.C. Oosterlee,
in het openbaar te verdedigen
op woensdag 12 december 1984
des namiddags te vier uur in de aula
van de Landbouwhogeschool te Wageningen

ISBN: 217 786-02

TABLE OF CONTENTS

ACKNOWLEDGEMENTS

NOTATIONS AND ABBREVIATIONS

1. INTRODUCTION	1
2. HOMOGENEITY OF DUTCH RAINFALL RECORDS	4
2.1. Introduction	4
2.2. Rainfall levels	6
2.3. Time-inhomogeneity of rainfall	10
2.4. Local differences in rainfall level and in rainfall trend	16
2.4.1. Kriging method	16
2.4.2. Local differences in rainfall level	22
2.4.3. Local differences in rainfall trend	26
2.5. Partitions of the Netherlands based on rainfall	29
2.5.1. Possible partitions	31
2.5.2. Testing the statistical significance of the partitions	33
2.5.3. The hydrological significance of the partitions	36
2.6. Effect of urbanization and industrialization on precipitation	45
2.6.1. Urban effects in the Netherlands	49
3. STATISTICAL AREAL REDUCTION FACTOR ARF	88
3.1. Introduction	88
3.2. Prediction of areal rainfall	92
3.2.1. The order k and the estimation of the semi-variogram	93
3.2.2. Comparison of the kriging, Thiessen, and arithmetic mean predictors	102
3.3. ARF for daily rainfall and its dependence on location, season, and return period	108

3.3.1. Methods to estimate ARF	109
3.3.2. Estimates of ARF_{24} for three areas of 1000 km ² in the Netherlands	115
3.3.3. Variance of ARF for daily rainfall	124
3.4. ARF for hourly rainfall	128
3.4.1. The distribution of hourly areal rainfall	129
3.4.2. Estimates of ARF_1	130
3.5. Storm-centred areal reduction factor SRF	133
4. SUMMARY AND CONCLUSIONS	162
SAMENVATTING EN CONCLUSIES	167
APPENDICES A. Data and supplementary results of the study on homogeneity	173
B. Data and supplementary results of the study on ARF	192
REFERENCES	195
CURRICULUM VITAE	204

ACKNOWLEDGEMENTS

This study was carried out under the supervision and guidance of Professor L.C.A. Corsten, and Professor D.A. Kraijenhoff. I would like to thank them for their advice and stimulating and critical discussions. I am also grateful to Dr. M.A.J. van Montfort for his support throughout this study. Dr. T.A. Buishand and Dr. J.N.M. Stricker made valuable comments on the manuscript.

I would like to thank also: Mrs. H.J. West, for revising the English text; Mr. A. van 't Veer for preparing the numerous drawings in the manuscript; and Mrs. J. Heijnekamp-van de Molen and Mrs. W.B.J. Korte-Bayer for typing the manuscript.

NOTATIONS AND ABBREVIATIONS

An estimate of a particular parameter is denoted by a caret above the parameter. Thus $\hat{\alpha}_1$ is an estimate of α_1 . However, estimates of correlation coefficients (ρ) are denoted by r and estimates of the variance (σ^2) are denoted by s^2 . Stochastic variables are underlined. The expectation operator is denoted by E , and a frequency of, for instance, two events per year is written as 2 (# year⁻¹). Means of variables with two subscripts $x_{i,j}$ are denoted by $x_{i.}$, $x_{.j}$, or $x_{..}$, where a point indicates the suffix with respect to which the mean has been taken.

Although notations are introduced as they are used, some symbols appear throughout this study, and are listed here for convenience.

A	area
C	symmetric N by N covariance matrix
cc	coefficient of covariation
cv	coefficient of variation
D	duration of rainfall
F_{ℓ}^S	annual frequency of exceedance in summer (beginning of May to the end of September) of a certain threshold of daily rainfall depth ℓ (mm), for instance F_{15}^S
F_{ℓ}^W	annual frequency of exceedance in winter (beginning of October to the end of April) of a certain threshold of daily rainfall depth ℓ (mm)
h	distance
I	intensity of rainfall
i	suffix indicating station number
j	suffix indicating year number
K	symmetric N by N generalized covariance matrix
N	number of sample points
n	length of record
N(h)	number of paired data in a particular distance class
L	dimension of a region V, in particular the maximum distance occurring between sample points

q exceedance of a threshold or peak
 q_T peak quantile corresponding to a T-year return period
 R total annual rainfall
 $r(h)$ estimate of the correlation coefficient $\rho(h)$
 s estimate of the standard deviation σ
 s_r residual standard error
 \underline{T} test statistic
 T return period
 t time co-ordinate
 u spatial co-ordinate vector
 V region
 \underline{x}_A variable, denoting mean areal rainfall
 \underline{x}_S variable, denoting point rainfall at point S
 x_p quantile (eventually written as $x_{A,p}$ or $x_{S,p}$)
 $Z(u)$ intrinsic random function located at u
 $z(u)$ realization at u of an intrinsic random function $Z(u)$

α significance level
 Γ symmetric N by N matrix of semi-variances γ_{ij}
 $\gamma(h)$ semi-variance at distance h
 $\rho(h)$ correlation coefficient at distance h
 σ standard deviation
 σ_E^2 squared estimation error
 σ_K^2 squared kriging error

Frequently used abbreviations

ACN Aitken condensation nuclei
 ARF statistical areal reduction factor
 BLUP best linear unbiased predictor
 CCN cloud condensation nuclei
 cdf cumulative distribution function
 df degrees of freedom
 D14 data set consisting of 14 long-term daily rainfall records
 for the period 1906-1979

D32 data set consisting of 32 daily rainfall records for the period 1932-1979
 D140 data set consisting of 140 daily rainfall records for the period 1951-1979
 edf empirical distribution function
 GMT Greenwich mean time
 H12 data set consisting of 12 hourly rainfall records
 IRF-k intrinsic random function of order k
 KNMI Koninklijk Nederlands Meteorologisch Instituut (Royal Netherlands Meteorological Institute)
 LS least squares
 MM method of moments
 ML maximum likelihood
 ms mean of squares
 OLS ordinary least squares
 POT peaks-over-threshold
 pdf probability density function
 SRF storm-centred areal reduction factor
 UTC universal time co-ordinated

1. INTRODUCTION

The object of this study is to investigate heterogeneity of rainfall in time and space in the Netherlands. The length scale considered is several hundreds kilometres in Chapter 2, in which possible partitions of the Netherlands into regions on the basis of local differences in rainfall are investigated, and a few tenths of a kilometre in Chapter 3, in a study of spatial variability of time-aggregated rainfall (over an hour or a day) at the basin scale. The time scale considered in Chapter 2 is a year, divided into a summer period (May to September) and a winter period (October to April). As alternatives to homogeneity in rainfall series, trends and jumps are considered in Chapter 2.

The absence of homogeneity of rainfall may have relevance for hydrological design. For instance, the possible effects of urbanization and industrialization on precipitation, may have design implications. Also, the question may be raised as to whether it would be preferable for a particular design to use rainfall data from a nearby site instead of rainfall data measured at the Royal Netherlands Meteorological Institute (KNMI) at De Bilt. In addition, because of rainfall variation in time and space, consideration may be given to whether an areal reduction factor is applicable in a design. Therefore, rainfalls with rather low return periods were studied. Because the object was to include as many rainfall records as possible, which were of good and even quality, the study was almost completely confined to rainfall data collected and published by the KNMI. As the network of rainfall recorders in the Netherlands is very sparse, the study is concerned mainly with daily records, but some hourly rainfall records have also been used.

Homogeneity of Dutch rainfall records is investigated in Chapter 2, and in Chapter 3 the statistical areal reduction factor (ARF) is estimated for daily and hourly rainfall. In the introduction to each chapter a number of issues is raised, which are dealt with in the subsequent sections. Conclusions are presented within each section and not in a separate section at the end of the chapter.

All equations, tables and figures are numbered consecutively within each chapter; equations and tables are to be found in the appropriate place in the text, and figures at the end of the relevant chapter.

A survey of the rainfall data used in this study is given in the Appendices A.1 and B.1. The geographical location of the rainfall stations and regions used throughout this study are given in Figure 1.1; and a list of all provinces and rainfall stations together with their KNMI code numbers is presented in Table 1.1.

PROPOSITIONS

1. The Netherlands may be assumed to be inhomogeneous with regard to daily rainfall level. A partition of the Netherlands based on the combined effects of friction, topography, differential heating, and urban precipitation enhancement, and a partition based on mean annual rainfall, show significant inhomogeneities.
[This thesis]
2. The effect of urbanization on heavy daily rainfall in summer increases with rainfall depth.
[This thesis]
3. Statistical areal reduction factors depend *inter alia* on climate and on season.
[This thesis]
4. Present theories about the causes of urban precipitation enhancement stress the influence of thermodynamic and mechanical processes rather than the influence of additional condensation and freezing nuclei from urban aerosols. This does not support the assumption of Petit-Renaud (1980) that there was an urban effect due to coal-based industrialization in northern France in the second half of the nineteenth century.
[Petit-Renaud, G., 1980. Les principaux aspects de la variabilité des précipitations dans le nord de la France. Recherches Géographiques à Strasbourg no. 13-14: 31-38]
5. The areal reduction factors for discharge presented in the "Cultuurtechnisch Vademecum" are unnecessarily high.
6. The choice of a design rainfall intensity of $60-90 \text{ l}\cdot\text{s}^{-1}\cdot\text{ha}^{-1}$ is partly a consequence of uncertainties about the actual performance of a sewerage system. Thus firstly, evaluation of actual performance is necessary.

7. The method which is currently used for estimating the generalized covariance is *ad hoc*, and it is by no means certain that it provides asymptotically efficient parameter estimates.
[Barendregt, L.G., 1983. Maximum-likelihood schatting van de gegeneraliseerde covariantie, in: Enkele kanttekeningen bij de stochastische interpolatiemethode 'kriging'. IWIS-TNO, 's-Gravenhage]
8. The sole criterion of a maximum overflow frequency is inappropriate for the design of centrally operated, regional sewage water transport systems. However, in order to include other criteria, certain technical, legal, and financial obstacles must be overcome.
9. Strategies for the Third World, such as, 'small farmers approach' and 'intermediate technology' reflect, *inter alia*, too academic an attitude and paternalism.

J.V. Witter. Heterogeneity of Dutch rainfall. Wageningen,
12 December 1984.

2. HOMOGENEITY OF DUTCH RAINFALL RECORDS

2.1. INTRODUCTION

Rainfall series can be seen as realizations of a process $\{x(u,t)\}$, where the co-ordinate vector of the sample points is denoted by u and time is denoted by t . Although such a process can be homogeneous in several ways, in this chapter, only two types of homogeneity are investigated:

homogeneity in time: given a location U , the probability distribution of the process $\{x(U,t)\}$ is independent of time;

homogeneity in space: given a time co-ordinate T , the probability distribution of the process $\{x(u,T)\}$ is independent of location.

As rainfall series exhibit periodicities, the homogeneity of the following seven annual rainfall characteristics are investigated:

- total annual rainfall R ;
- annual frequency of exceedance F of a certain threshold ℓ of daily rainfall depth,
 - . in summer F_{ℓ}^S , the summer being defined as the period from the beginning of May to the end of September
 - . in winter F_{ℓ}^W , the winter being defined as the period from the beginning of October to the end of April
 - . three thresholds were chosen for the annual frequency of exceedance, 1, 15, 25 mm.

Total annual rainfall R , and annual frequency of exceedance of 1 mm in summer (F_1^S) and in winter (F_1^W) give a general indication of rainfall level: its long-term mean value. Annual frequencies of exceedance of 15 and 25 mm, which are of more relevance to hydrological practice, are also useful in investigating the effect of industrialization and urbanization on rainfall trend. Convective rather than frontal rainfall events are more susceptible to modification, and severe weather phenomena (thunderstorms) are likely to be affected in particular (Oke, 1980).

The existence of regional differences in rainfall depths has been reported by various investigators, (e.g., Buishand and Velds, 1980), and also regional differences in rainfall trend have been reported

(e.g., Kraijenhoff and Prak, 1979; Buishand, 1979). These differences in trend have been attributed to the anthropogenic effects of industrialization and urbanization. Therefore, it has been suggested (Werkgroep Afvoerberekeningen, 1979) that more stringent design criteria should be used for urban than for rural areas. Earlier investigations of homogeneity in time of Dutch rainfall records have focused mainly on total monthly and annual rainfall, except Kraijenhoff and Prak (1979), who established the inhomogeneity in time of the annual frequency of daily rainfall exceeding 30 mm in summer. Jumps in the mean seasonal and annual rainfall of Dutch rainfall series roughly for the period 1925-1970, have been studied by Buishand (1977a). Departures from homogeneity in 24 Dutch long-term monthly and annual rainfall records were reported by Buishand (1981), who also investigated departures from homogeneity in 264 Dutch records of annual rainfall for the period 1950-1980 (Buishand, 1982a). In all three studies, strong indications of a change in the mean were found for large numbers of records.

In this chapter the following issues are dealt with:

- . In Section 2.2, mean values of the rainfall characteristics defined above for the Netherlands are determined from daily rainfall records for the period 1951-1979 for 140 rainfall stations of the Royal Netherlands Meteorological Institute (KNMI). This data set is denoted as D140 (Appendix A.1). These mean values are compared with mean values determined from the long-term records for the period 1906-1979 for 14 KNMI rainfall stations considered to be of good quality (Buishand, 1982b). This data set is referred to as D14 (Appendix A.1).
- . In Section 2.3, time-inhomogeneity of rainfall in the Netherlands is considered. Use is made of data set D140 for the period 1951-1979 and of data set D14 for the period 1906-1979.
- . In Section 2.4, local differences in rainfall level and rainfall trend between Dutch rainfall stations are investigated. Use is made of data set D140.

- . In Section 2.5, consideration is given to whether such local differences in rainfall level and in rainfall trend justify a partition of the Netherlands on the basis of rainfall. Use is made of data sets D140, D14, and H12, that is hourly records of 12 KNMI rainfall stations (Appendix A.1).
- . In Section 2.6, statistical evidence for the effect of urbanization and industrialization on rainfall in the most urbanized and industrialized part of the Netherlands, namely the Randstad, is investigated. Use is made of data set D32, which consists of daily rainfall records of 32 KNMI rainfall stations for the period 1932-1979 (Appendix A.1).

The geographical location of all rainfall stations is shown on the map in Figure 2.1.

2.2. RAINFALL LEVELS

In this section, mean values of each of the seven rainfall characteristics defined in the introduction to this chapter are determined. Let $x_{i,j}$ be the value of one characteristic under investigation at station i ($i = 1, \dots, 140$) in year j ($j = 1, \dots, 29$), then the station means \bar{x}_i can be calculated. Their mean \bar{x} , together with the unbiased estimate s of their standard deviation and the corresponding coefficient of variation cv are presented in Table 2.1.

As a check on the consistency of these results, \bar{x} , s , and cv were also calculated for data set D14 (Table 2.2). Although in the longer series D14 all mean values are somewhat smaller, the values of the characteristics F_{15} and R differ considerably.

Disregarding any correlation in the data between stations and between years, a first indication of the occurrence of inhomogeneities in mean total annual rainfall may be obtained from a comparison of components in an analysis of variance and a cross classification of the factors years and stations (Table 2.3). The effects between years and between stations are considerable.

Table 2.1. Mean \bar{x} , standard deviation s , and coefficient of variation cv of rainfall characteristics for data set D140

Rainfall character- istic	Mean \bar{x}		Standard deviation s		Coefficient of variation cv (%)	
	Summer	Winter	Summer	Winter	Summer	Winter
Exceedance frequency						
1 mm (F_1)	52.4	80.5	2.6	2.6	4.9	3.2
15 mm (F_{15})	4.7	3.5	0.5	0.6	11.2	16.4
25 mm (F_{25})	1.15	0.48	0.25	0.13	21.9	27.4
Total annual rainfall (R)	775.8 (mm)		36.4 (mm)		4.7	

Table 2.2. Mean \bar{x} , standard deviation s , and coefficient of variation cv of rainfall characteristics for data set D14

Rainfall character- istic	Mean \bar{x}		Standard deviation s		Coefficient of variation cv (%)	
	Summer	Winter	Summer	Winter	Summer	Winter
Exceedance frequency						
1 mm (F_1)	50.6	78.1	3.2	3.0	6.3	3.9
15 mm (F_{15})	4.2	3.1	0.5	0.3	11.6	10.6
25 mm (F_{25})	1.03	0.45	0.14	0.07	13.2	16.8
Total annual rainfall (R)	732.0 (mm)		32.8 (mm)		4.5	

Table 2.3. ANOVA table for between years and between stations effects for total annual rainfall

Source of variation	df	ms(mm ²)
Between years	28	2.21×10^6
Between stations	139	3.83×10^4
Residual	3892	3.47×10^1
Total	4059	

In order to obtain a general impression of daily rainfall level at a Dutch rainfall station, peaks-over-threshold series (POT series) were extracted for each station in the D140 data set for summer, winter, and the total year, and with a mean annual number of threshold exceedances of two. To assure independence of the exceedances, these had to be separated by at least one day without rain. Mean order statistics were obtained by taking the mean of peaks of equal ranking. It was assumed that both the POT series for an individual station, and the series of mean peaks q were exponentially distributed. Thus, a probability density function was fitted according to

$$f(q) = \frac{1}{\beta} \exp[-(q-q_0)/\beta], \quad (q > q_0) \quad (2.1)$$

where

q_0 : parameter for location
 β : parameter for scale.

The maximum likelihood (ML) estimators of β and q_0 , corrected for bias, are (NERC, 1975; Vol. 1)

$$\hat{\beta} = \frac{n}{n-1}(\bar{q} - q_l), \quad (2.2)$$

and

$$\hat{q}_0 = q_l - \hat{\beta}/n, \quad (2.3)$$

where

n : sample size (58)
 q_l : lowest peak in the sample
 \bar{q} : sample mean of peaks.

Estimates of β and q_0 are given in Table 2.4.

Table 2.4. Maximum likelihood estimates of β and q_0 in Equation 2.1 for POT series of daily rainfall in the Netherlands (mean annual number of threshold exceedances: 2)

Period	$\hat{\beta}$ (mm)	\hat{q}_0 (mm)
Year	8.1	23.1
Summer	8.5	20.1
Winter	5.8	16.8

These mean POT series have been plotted and are presented, together with the fitted exponential distributions in Figure 2.2. For the plotting position of the order statistics $q_{(i)}$, with $q_{(1)} \leq \dots \leq q_{(n)}$, the following equation was used

$$E(Y_{(i)}) = \sum_{j=1}^i (n+1-j)^{-1}, \quad (2.4)$$

where

$Y_{(i)}$: order statistic of a standard-exponential variate with density $f(y) = e^{-y}$ ($y \geq 0$).

The assumption of an exponential distribution was tested in the following way. Let the order statistics $q_{(1)} \leq \dots \leq q_{(n)}$ be samples of a truncated exponential distribution, then the standardized increments

$$L_i = i(q_{(n-i+1)} - q_{(n-i)}), \quad i = 1, \dots, n-1 \quad (2.5)$$

are independent exponential variates. After eliminating the location parameter, the scale parameter is eliminated. Let

$$\underline{s} = \sum_{i=1}^{n-1} L_i, \quad (2.6)$$

and

$$\underline{z}_i = \sum_{j=1}^i L_j / \underline{s}, \quad i = 1, \dots, n-2 \quad (2.7)$$

The series (z_1, \dots, z_{n-2}) is distributed as an ordered sample of size $n-2$ from a uniform distribution on $(0,1)$ (Durbin, 1961). Thus, a test statistic \underline{T} can be used, where

$$\underline{T} = -2 \sum_{i=1}^{n-2} \ln z_i. \quad (2.8)$$

Under the null hypothesis of exponentially distributed peaks, \underline{T} has a χ^2 -distribution with parameter $2(n-2)$. As lack of fit with regard to the exponential distribution can lead to high as well as to low values of \underline{T} , a two-sided test is used. Very long tails give low values of \underline{T} , and very short tails high values. Realizations of \underline{T} for the total year, summer, and winter for the POT series were 95.9, 99.8, and 94.6, respectively. As these values are not significant (two-sided test, significance level $\alpha = 0.10$), the exponential distribution fits the POT series reasonably well.

2.3. TIME-INHOMOGENEITY OF RAINFALL

In this section, time-inhomogeneity of mean values of the seven rainfall characteristics defined in the introduction to this chapter is considered. Let $\underline{x}_{.j}$ be the mean value of a rainfall characteristic for all rainfall stations considered in year j ($j=1, \dots, n$). For rainfall characteristics F_ℓ^S and F_ℓ^W , the $\underline{x}_{.j}$ are means of transformed variates $\underline{x}_{i,j}$, where the transformation is according to

$$p = \sqrt{\tilde{p}} + \sqrt{(\tilde{p}+1)}, \quad (2.9)$$

the untransformed \tilde{p} being any positive integer. This transformation has a variance stabilizing and normalizing effect on Poisson variates, resulting in that case in a variance of almost 1 (see Appendix A.2).

In this section, consideration is given only to a possible change in the expected mean $\underline{x}_{.j}$, described by either a linear trend

$$E(\underline{x}_{.j}) = \mu_j = \mu + j\delta, \quad (2.10)$$

or

$$E(\underline{x}_{.j}) = \mu_j = \begin{cases} \mu & j = 1, \dots, m \\ \mu + \delta, & j = m+1, \dots, n \end{cases} \quad (2.11)$$

that is, a jump at $j = m+1$ with m unknown. Under the null hypothesis H_0 of a homogeneous series, $\delta = 0$. Note that for data set D140, $n=29$ and for data set D14, $n=74$.

When anthropogenic effects on rainfall are being studied, it is logical to look for a trend. However, since there are many factors affecting rainfall and rainfall measurements, including climatologic fluctuations or changes in methods of measuring rainfall, it is also necessary to consider jumps. Test statistics are needed which are powerful for the alternatives H_{1a} (Equation 2.10) and H_{1b} (Equation 2.11), both with $\delta \neq 0$ (the power of a test is defined as the probability of rejection of H_0 in favour of the alternative H_1).

The homogeneity of the series $\underline{x}_{.j}$ was tested by the three test statistics described below.

Von Neumann ratio Q

$$Q = \frac{\sum_{j=1}^{n-1} (\underline{x}_{.j+1} - \underline{x}_{.j})^2}{\sum_{j=1}^n (\underline{x}_{.j} - \underline{x}_{..})^2}. \quad (2.12)$$

A monotonic trend or slow oscillations in level tend to produce low values of Q ; and rapid oscillations in the mean may yield high values of Q . For the alternatives H_{1a} and H_{1b} , a left-sided critical region of Q seems adequate. An advantage of the statistic Q is its sensitivity for a great variety of inhomogeneities. A table of percentage points of Q for normally distributed samples is given by Abrahamse and Koerts (1969).

Student's statistic T for a linear time trend

$$T = \frac{\underline{r} \sqrt{(n-2)}}{\sqrt{(1-\underline{r}^2)}}, \quad (2.13)$$

where

\underline{r} : the sample correlation coefficient between the variate $\underline{x}_{.j}$ and time.

The statistic \underline{T} is an adequate tool for testing homogeneity when H_{1a} is the alternative. Under the null hypothesis \underline{T} is a Student variate with $n-2$ degrees of freedom. The test is two-sided, since an increasing trend gives high positive values of \underline{T} , and a decreasing trend, high negative values.

The maximum or minimum \underline{M} of weighted rescaled adjusted partial sums

For a series $\underline{x}_{.j}$ ($j=1, \dots, n$), the adjusted partial sum is defined as

$$\underline{S}_k = \sum_{j=1}^k (\underline{x}_{.j} - \bar{\underline{x}}), \quad k = 1, \dots, n-1 \quad (2.14)$$

and $S_0 = S_n = 0$. The adjusted partial sums are rescaled to scale invariance by dividing \underline{S}_k by the sample standard deviation \underline{s}_x

$$\underline{S}_k^* = \underline{S}_k / \underline{s}_x, \quad k = 1, \dots, n-1. \quad (2.15)$$

The weighted rescaled adjusted partial sums \underline{S}_k^{**} are defined as

$$\underline{S}_k^{**} = \{k(n-k)\}^{-\frac{1}{2}} \underline{S}_k^*, \quad k=1, \dots, n-1. \quad (2.16)$$

Because of the multiplication factor $\{k(n-k)\}^{-\frac{1}{2}}$

$$\text{var}(\underline{S}_k^{**}) = \frac{1}{n-1}, \quad k=1, \dots, n-1 \quad (2.17)$$

independent of k (Appendix A.3). The test statistic is

$$\underline{M} = \max_{k=1, \dots, n-1} |\underline{S}_k^{**}|. \quad (2.18)$$

A particular advantage of this test procedure is that it gives a value of k , say k^* , which maximizes $|\underline{S}_k^{**}|$. In case of H_{1b} , k^* is

the maximum likelihood (ML) estimate of m (Buishand, 1981). Because there is a unique relationship between \underline{M} and Worsley's \underline{W} (Worsley, 1979)

$$\underline{W} = (n-2)^{\frac{1}{2}} \underline{M} / (1-\underline{M}^2)^{\frac{1}{2}}, \quad (2.19)$$

percentage points of \underline{W} were used in the test, which is two-sided (Appendix A.3).

The power of a test can be determined directly by solving the power function only in a few cases. Here, the power of the test statistics \underline{Q} , \underline{T} , and \underline{M} for alternatives according to Equations 2.10 and 2.11 was investigated by means of Monte Carlo methods with 2000 samples of 29 normal variates; for each sample the test statistics were calculated for

a linear trend: $\delta = 0 \left(\frac{1}{58}\sigma \right) \frac{6}{58}\sigma$,

a jump : $\delta = 0 \left(\frac{1}{3}\sigma \right) \frac{9}{3}\sigma$, and $m = 7, 14$.

The simulated power functions of \underline{Q} , \underline{T} , and \underline{M} are presented for alternative H_{1a} in Figure 2.3A, for alternative H_{1b} ($m=7$) in Figure 2.3B, and for alternative H_{1b} ($m=14$) in Figure 2.3C.

Simulated powers of \underline{Q} and \underline{M} for H_{1b} have been given by Buishand (1982a) for $n = 30$, $\alpha = 0.05$ and $m = 5$, and 15; and those given in Figure 2.3B and 2.3C compare well with his results. It may be concluded from Figure 2.3 that the statistic \underline{T} has favourable characteristics when trends or jumps according to Equation 2.10 or 2.11 have to be detected. For other types of inhomogeneities, however, \underline{Q} may be superior to both \underline{T} and \underline{M} .

For data sets D140 and D14, values of the test statistics \underline{Q} , \underline{T} and \underline{M} , determined for the rainfall characteristics total annual rainfall R and annual exceedance frequencies for summer and winter $F_2^{s,w}$, are presented in Table 2.5.

Table 2.5. Realizations of the statistics \underline{Q} , \underline{T} , and \underline{M} and of the estimated jump point k^*

Rainfall characteristic	Data set D140				Data set D14			
	\underline{Q}	\underline{T}	\underline{M}	k^*	\underline{Q}	\underline{T}	\underline{M}	k^*
Exceedance frequency								
Summer								
1 mm (F_{15}^S)	2.03	-1.29	0.35	18	2.19	0.39	0.16	69
15 mm (F_{15}^S)	1.74	-1.93°	0.48°	24	1.81	0.45	0.30	70
25 mm (F_{25}^S)	1.85	-2.03°	0.50°	25	1.92	0.64	0.30	67
Winter								
1 mm (F_{15}^W)	2.03	0.84	-0.24	14	1.90	0.87	-0.20	59
15 mm (F_{15}^W)	1.16°°	0.68	-0.40	9	1.63	1.96°	-0.33°	19
25 mm (F_{25}^W)	1.18°°	-0.34	-0.33	9	1.65	1.15	-0.26	23
Total annual								
rainfall (R)	1.92	-0.55	0.30	20	1.78	1.62	-0.26	44

° Indicates values inside the critical region for $\alpha = 0.10$.

°° Indicates values inside the critical region for $\alpha = 0.05$.

The test statistics \underline{T} and \underline{M} lead to very similar conclusions. The Von Neumann ratio \underline{Q} , however, is very clearly sensitive to other types of inhomogeneities. The values of k^* indicate a jump towards the end of the summer series during the period 1970-1975, while in the winter series the jump points are more evenly spread throughout.

The positive trend of the D14 series is very likely to be affected by improvements in rainfall measurements, notably the introduction of standardized measurement practice at the beginning of this century, and the lowering of the rain gauge from 150 to 40 cm above ground level in the period 1946-1950 (Deij, 1968). Buishand (1977a) concluded that this last improvement resulted in an increase in measured rainfall of about 10% for coastal rainfall stations (see also Braak, 1945), and an increase of about 2% for stations at a distance from the coast.

The hypothesis that improvements in rainfall measurements are the main reason for the positive trend of the D14 series is supported by the higher values of \underline{T} for the winter. The lowering of the gauge has led to a reduction of the wind-field deformation around the gauge, which causes a loss of catch. This loss, however, is smallest in summer because raindrops are relatively large as a consequence of the rainfall intensity in this season.

The observed inhomogeneities may also be affected by the general circulation pattern during the period of the records used. The circulation pattern is described by distinct circulation types, the frequency of which is known to fluctuate. Each period is characterized by the predominance of certain circulation types (Barry and Perry, 1973), each having its own probability of rainfall.

A record of daily circulation types for the Netherlands in the period 1881-1976 has been compiled by Hess (1977); data for 1977 and 1978 have been supplied by KNMI. In addition, the rainfall probability, given the occurrence of a certain circulation type, has been worked out for five KNMI stations (Bijvoet and Schmidt, 1958, 1960). The effect of circulation types on rainfall trend was investigated by calculating the expected annual number of days in a certain rainfall class, according to the above-mentioned rainfall probabilities. In this study only the rainfall class in excess of 5 mm has been considered. The series of expected annual numbers of days was compared to the series of actual numbers of days in this rainfall class for the period 1956-1978, because the 1881-1955 data were used to calculate the rainfall probabilities. Both series are shown in Figure 2.4A (summer) and Figure 2.4B (winter) for the rainfall station Den Helder/De Kooy.

From Figure 2.4 it can be concluded that there is some evidence of the effect of the general circulation on rainfall trend. This effect is illustrated by the high values of k^* in Table 2.5 for most rainfall characteristics. This seems to be an immediate consequence of the wet sixties. This may also be concluded from Figure 2.5, where 10-year moving averages and the weighted rescaled adjusted partial sums are shown for total annual rainfall R for data set D14. The

10-year moving average of summer rainfall for the period 1734-1960 is given in Figure 2.5C (Wind, 1963).

2.4. LOCAL DIFFERENCES IN RAINFALL LEVEL AND IN RAINFALL TREND

In this section local differences in rainfall level and in rainfall trend are investigated as follows. Let $\underline{x}_{i,j}$ be the value in year j at station i of one of the rainfall characteristics: (i) exceedance frequency (in summer F_{ℓ}^S , with $\ell=1, 15$, or 25 mm; and in winter F_{ℓ}^W , also with $\ell=1, 15$, or 25 mm), (ii) total annual rainfall R . Local differences in rainfall level are studied by comparing the station means \underline{x}_i for each rainfall characteristic (Section 2.4.2), and local differences in rainfall trend by analysing the time series $\underline{x}_{i,j}$ for each particular rainfall station and each rainfall characteristic (Section 2.4.3). Use is made of data set D140. To give an impression of the local differences, maps of the Netherlands, showing the geographical distribution of station means and trend statistics, are presented. These maps were derived by the kriging method, which is a best linear unbiased predictor (BLUP). Firstly, the kriging method is discussed in Section 2.4.1.

2.4.1. Kriging method

Let $Z(u)$ be an intrinsic random function (IRF) which is defined in every point with co-ordinate vector u of a region V , and let $z(u)$ be a realization of $Z(u)$, known at the N sample points $u_i \in V$. For example, the set of station means \underline{x}_i for data set D140 is a realization $z(u)$, known at the 140 sample points.

A best linear unbiased predictor (BLUP) $\hat{z}(u_0)$ of $z(u)$ at some point u_0 is defined as

$$\hat{z}(u_0) = \sum_{i=1}^N \lambda_i z(u_i), \quad (2.20)$$

where:

λ_i : coefficients to be determined.

This BLUP $\hat{z}(u_0)$ is in fact the kriging prediction of $z(u_0)$. The kriging method holds, if the following intrinsic hypothesis is valid

$$\begin{cases} E[Z(u)-Z(u+h)] &= 0 \\ \text{Var}[Z(u)-Z(u+h)] &= 2\gamma(h), \end{cases} \quad \begin{matrix} (2.21a) \\ (2.21b) \end{matrix}$$

where

h : distance.

The function $\gamma(h)$ in Equation 2.21b is called the population semi-variogram. If Equation 2.21 holds, then $Z(u)$ is an IRF of order zero (IRF-0).

The condition for Equation 2.20 to be unbiased implies that the prediction error $z(u_0) - \hat{z}(u_0)$ will be a contrast. The variance of this contrast, σ_E^2 , equals

$$\sigma_E^2 = 2 \sum_{i=1}^N \lambda_i \gamma(u_i - u_0) - \sum_{i=1}^N \sum_{j=1}^N \lambda_i \lambda_j \gamma(u_i - u_j), \quad (2.22)$$

and Equation 2.22 has to be minimized. This leads to the kriging equations (Matheron, 1971) which can be deduced from the minimum variance and unbiasedness condition of the BLUP $\hat{z}(u_0)$

$$\begin{cases} \Gamma \lambda + \mu 1_N = r \end{cases} \quad (2.23a)$$

$$\begin{cases} 1_N' \lambda = 1, \end{cases} \quad (2.23b)$$

where Γ is a symmetric N by N matrix (γ_{ij}) , $\gamma_{ij} = \gamma(u_i - u_j)$, $r' = (\gamma(u_1 - u_0), \gamma(u_2 - u_0), \dots, \gamma(u_N - u_0))$, $1_N' = (1, 1, \dots, 1)$, $\lambda' = (\lambda_1, \lambda_2, \dots, \lambda_N)$, and μ is a Lagrange multiplier. The resulting minimum variance σ_K^2 of the kriging prediction equals

$$\sigma_K^2 = \sum_{i=1}^N \lambda_i \gamma(u_i - u_0) + \mu, \quad (2.24)$$

which follows from inserting Equation 2.23a into Equation 2.22. As will become clear in the following chapter, point to area interpolation requires some of the semi-variances in Equations 2.22, 2.23 and 2.24 to be replaced by certain types of mean semi-variances.

The weights λ_i in Equations 2.20 and 2.24 can be determined if the semi-variances are known. For an IRF-0 these semi-variances can be estimated by

$$\hat{\gamma}(h) = \frac{1}{2N(h)} \sum_{i=1}^{N(h)} [z(u_i) - z(u_i + h)]^2, \quad (2.25)$$

where $N(h)$ is the number of paired data points at mutual distance h , particularly suitable if sampling has been done according to a regular grid. For a random sample, paired data are grouped according to distance classes and $N(h)$ is the number of paired data in a particular class. Note that $\sum_h N(h) = N(N-1)/2$. Because of Equation 2.21a, $\hat{\gamma}(h)$ is an unbiased estimator.

A population semi-variogram $\gamma(h)$ may be fitted to $\hat{\gamma}(h)$ according to a parametric model, for instance a linear model

$$\gamma(h) = C\delta + \alpha_1 h, \quad (2.26a)$$

or an exponential model

$$\gamma(h) = C\delta + \alpha_1 (1 - \exp(-h/\alpha_2)), \quad (2.26b)$$

where

- C : a parameter for the nugget effect
- δ : 0 ($h=0$) or 1 ($h \neq 0$)
- α_1, α_2 : parameters.

The nugget effect represents discontinuity of the semi-variogram at the origin, due to spatial variability at very small distances in relation to the working scale, resulting for example from measurement errors and/or the physical characteristics of the spatial process concerned.

The linear model described in Equation 2.26a corresponds to intrinsic random functions $Z(u)$ of order zero, for which an a priori variance or a covariance need not exist. The exponential model described in Equation 2.26b exhibits a limit or a sill, equal to $C+\alpha_1$, as $h \rightarrow \infty$. This sill is almost (for 95%) reached at a distance or range equal to $3\alpha_2$. Models exhibiting a sill may correspond to second-order stationary random functions $Z(u)$ with spatial correlation.

The fitted $\gamma(h)$ should not only resemble the sample function $\hat{\gamma}(h)$, but should also satisfy the condition for the variance of a contrast $\sum_i \lambda_i Z(u_i)$, with $\sum_i \lambda_i = 0$, to be possible for all λ_i

$$\text{var}(\sum_i \lambda_i Z(u_i)) = -\sum_i \sum_j \lambda_i \lambda_j \gamma(u_i - u_j) \geq 0, \quad (2.27)$$

furthermore

$$\gamma(0) = 0, \quad \gamma(h) = \gamma(-h) \geq 0. \quad (2.28)$$

As the Equations 2.26 imply independence of $\gamma(h)$ of orientation, it should be verified that $z(u)$ is isotropic. In case of anisotropy, additional modifications are possible, see Journel and Huijbregts (1978).

If the assumption according to Equation 2.21a holds, then the increase of a semi-variogram for $h \gg 0$ can be shown to be necessarily slower than that of h^2 , that is

$$\lim_{h \rightarrow \infty} \frac{1}{h^2} \gamma(h) = 0, \quad (2.29)$$

which can be deduced from Equation 2.27. Consequently, a sample variogram which increases at least as rapidly as h^2 for large distances h is incompatible with the intrinsic hypothesis, as stated in Equation 2.21. Such an increase very often indicates the presence of a drift defined as

$$E[Z(u)] = m(u). \quad (2.30)$$

Where only one realization $z(u)$ of $Z(u)$ is known, and $Z(u)$ is only intrinsic, $\text{var}[\hat{\gamma}(h)]$ becomes very large (Appendix A.4) for $h > L/2$, where L is the maximum distance between sample points in V . Therefore, only for distances $h < L/2$, $\gamma(h)$ is fitted to $\hat{\gamma}(h)$.

For a second-order stationary $Z(u)$, Equation 2.23 can also be written in terms of covariances instead of semi-variances. The advantage of using semi-variances is that assumptions can be weaker, for example, the a priori variance $\text{var}[Z(u)]$ need not exist. A disadvantage is that calculation of the λ_i according to Equation 2.23 involves inverting a $(N+1)$ by $(N+1)$ matrix with zeros at the main diagonal; some common inversion methods can not handle this. Thus in the actual calculations, the semi-variances $\gamma(h)$ in Equation 2.23 are replaced by pseudo-covariances $C(h) = A - \gamma(h)$, where A is a constant, exceeding the maximum of semi-variances occurring in Equation 2.23.

The kriging method developed by Matheron (1971) is very closely related to the method of optimum interpolation developed by Russian statisticians, such as Gandin (1965). This last method, however, is based on second-order stationary realizations $z(u)$, and no use is made of the concept of intrinsic random functions. As a result, all equations, such as 2.22 and 2.23 are in terms of correlation coefficients. For an application of this method, see De Bruin (1975). The connection between kriging and linear regression has been pointed out by Corsten (1982). The Equation 2.23 leads to

$$\begin{aligned} \hat{z}(u_0) = & z' \Gamma^{-1} r - (z' \Gamma^{-1} 1_N) (1_N' \Gamma^{-1} 1_N)^{-1} (1_N' \Gamma^{-1} r) + \\ & + (1_N' \Gamma^{-1} 1_N)^{-1} (z' \Gamma^{-1} 1_N). \end{aligned} \quad (2.31)$$

Defining $x' \Gamma^{-1} y$ as an inner product of the vectors x and y , Equation 2.31 becomes

$$\hat{z}(u_0) = (z' r) - (z' 1_N) (1_N' 1_N)^{-1} (1_N' r) + (1_N' 1_N)^{-1} (z' 1_N). \quad (2.32)$$

The last term in Equation 2.32 can be interpreted as the estimate $\hat{\mu}$ of $\mu = E[Z(u)]$. The other terms in the right-hand side of Equation 2.32 can then be written as $(z - \hat{\mu} \mathbf{1}_N)' \mathbf{r} = \mathbf{r}' \Gamma^{-1} (z - \hat{\mu} \mathbf{1}_N)$, where the $\mathbf{r}' \Gamma^{-1}$ may be termed the best linear approximation coefficients for $z(u)$ by $z(u_i)$, $i=1, \dots, N$. Working along the same lines, an alternative expression to Equation 2.24 is obtained for the kriging variance in Corsten (1982)

$$\sigma_K^2 = \mathbf{r}' \Gamma^{-1} \mathbf{r} - (1 - \mathbf{1}_N' \Gamma^{-1} \mathbf{r}) (\mathbf{1}_N' \Gamma^{-1} \mathbf{1}_N)^{-1} (1 - \mathbf{1}_N' \Gamma^{-1} \mathbf{r}). \quad (2.33)$$

The last term in Equation 2.33 is closely related to the variance of the estimate of the stationary expectation $E[z(u_0)]$, and the other term on the right-hand side is an estimate of the residual variance of $z(u_0)$ with regard to the best linear approximation.

The IRF-k theory

In the presence of drift as defined by Equation 2.30, use may be made of the IRF-k theory, (Delfiner, 1976; Kafritsas and Bras, 1981). Basically, the drift is described as

$$m(u) = \sum_{\ell=0}^k a_{\ell} g_{\ell}(u), \quad (2.34)$$

where $g_{\ell}(u)$ are known monomial functions (in the one-dimensional case with $k=2$: $g_0(u)=1$, $g_1(u)=u$, $g_2(u)=u^2$, and the a_{ℓ} ($\ell=0, \dots, k$) are coefficients which need not be estimated).

For an intrinsic random function $Z(u)$ of order k (IRF-k) the following now hold:

- Any generalized increment of $Z(u)$, that is $\sum_i \lambda_i Z(u_i)$ with coefficient vector λ not only perpendicular to $\mathbf{1}_N$ but to all columns of the matrix $U=(u_{i\ell})$, where $u_{i\ell}=g_{\ell}(u_i)$, will have expectation zero. In other words, a generalized increment is a new process for which a drift according to Equation 2.34 is filtered out.
- $\text{Var}(\sum_i \lambda_i Z(u_i))$ exists and equals $\lambda' K \lambda$, where K is a (symmetric) matrix of generalized covariances. Note that for $k=0$, $K=-\Gamma$.

The condition of unbiasedness of the estimator $\hat{z}(u_0)$ in this case leads to $k+1$ constraints

$$\sum_{i=1}^N \lambda_i g_\ell(u_i) - g_\ell(u_0) = 0, \quad \ell=0, \dots, k$$

which, in matrix notation, may be represented as

$$U'\lambda = g.$$

The modified form of Equation 2.23 is

$$\begin{cases} K\lambda + U\mu = \tilde{k} & (2.35a) \\ U'\lambda = g, & (2.35b) \end{cases}$$

where $\tilde{k}' = (K(u_1, u_0), \dots, K(u_N, u_0))$, and μ is a vector of Lagrange multipliers. Alternative expressions for $\hat{z}(u_0)$ and σ_K^2 , analogous to Equation 2.32 and Equation 2.33 for an IRF- k $Z(u)$ are given in Corsten (1982).

2.4.2. Local differences in rainfall level

In order to analyze local differences in rainfall level, at each station i the station mean $x_{i\cdot}$ was calculated for each of the rainfall characteristics for data set D140. Values for the characteristics F_ℓ^S, F_ℓ^W were not transformed, because the normality assumption is superfluous. To give a more complete picture of the rainfall differences between stations, the station means have been interpolated to a dense and regular grid (7.5 x 7.5 km) by the kriging method.

Semi-variances, estimated by Equation 2.25, for distance classes 0-10, 10-20, 20-30, ... km, are presented in Figure 2.6 for each rainfall characteristic. A tendency for anisotropy of the semi-variograms was investigated by classifying paired data according to their orientation: in the NW-NE sector or in the NE-SE sector (see also Figure 2.6). These two particular sectors were chosen

because the spatial structure of rainfall has been shown to vary between directions either parallel or perpendicular to the coast (e.g., Boer and Feteris, 1969; Kruizinga and Yperlaan, 1976; Buishand and Velds, 1980).

The sample variograms grow slowly to a sill value for distances exceeding 100 km. Thus the exponential variogram model (Equation 2.26b) seems adequate, although for the exceedance frequency in summer of 1 mm (F_1^S) and in winter of 25 mm (F_{25}^W) a linear and logarithmic model, respectively, may also be acceptable. For large distances the sample variograms fluctuate considerably, as may be expected from the estimation variance of a sample variogram for a completely known realization (Appendix A.4). It may also be concluded from Figure 2.6, that none of these rainfall characteristics exhibits a drift.

When a rather large area, that is the whole Netherlands is considered, as is the case here, there may be some evidence for anisotropy, especially in the summer when local effects are more important (Boer and Feteris, 1969). For two rainfall characteristics, F_1^S and F_1^W , the presence of anisotropy may be inferred from the semi-variograms. However, because this is not very pertinent here, and in order to avoid arbitrary choices, isotropy has been assumed in the following.

Exponential semi-variogram models were fitted to the sample variograms. Because of the paucity of data at short mutual distance, C in Equation 2.26b was set equal to zero. As only one realization is known for only 140 sample points, $\gamma(h)$ was fitted to distance class means of $\hat{\gamma}(h)$ for distances $h < 162.4$ km, which is half the largest inter-station distance occurring in the sample. The parameters α_1 and α_2 were estimated by the Levenberg-Marquardt method, which is a gradient method of least squares optimization (Abdy and Dempster, 1974). The resulting ordinary least squares (OLS) estimates $\hat{\alpha}_1$ and $\hat{\alpha}_2$ are presented in Table 2.6.

Table 2.6. Ordinary least squares estimates $\hat{\alpha}_1$ (-) and $\hat{\alpha}_2$ (km) in Equation 2.26b

Rainfall characteristic	Summer		Winter	
	$\hat{\alpha}_1$	$\hat{\alpha}_2$	$\hat{\alpha}_1$	$\hat{\alpha}_2$
Exceedance frequency				
1 mm (F_1)	11.94	139.16	7.25	38.98
15 mm (F_{15})	0.29	21.07	0.35	21.72
25 mm (F_{25})	0.065	14.62	0.018	28.01
Total annual rainfall ¹ (R)	1355.1 ($=\hat{\alpha}_1$)		23.65 ($=\hat{\alpha}_2$)	

¹ For rainfall characteristic R, $\hat{\alpha}_1$ has dimension mm^2 .

From a comparison of Table 2.6 with Table 2.1, it can be seen that the sill $\hat{\alpha}_1$ of the exponential semi-variogram model is of the same order as s^2 in Table 2.1. The usual variance estimator s^2 equals the mean of the estimates $\hat{\gamma}(h)$, because

$$\begin{aligned}
 s^2 &= \frac{1}{N-1} \sum_{i=1}^N (z(u_i) - \bar{z}(u))^2 \\
 &= \frac{1}{N(N-1)} \sum_{i>j}^N (z(u_i) - z(u_j))^2 \\
 &= \frac{1}{N(N-1)} \frac{N(N-1)}{2} \overline{\hat{\gamma}(h)} = \overline{\hat{\gamma}(h)}. \quad (2.36)
 \end{aligned}$$

As most estimated semi-variances have been calculated for pairs of sample points at large mutual distances, that is beyond the range, $\overline{\hat{\gamma}(h)} \approx \hat{\alpha}_1$, and because of Equation 2.36, $s^2 \approx \hat{\alpha}_1$.

The matrix Equation 2.23 was solved by using the fitted semi-variograms. A fixed neighbourhood, the complete set of observations, has been applied because with a random design and a range of considerable magnitude, as is the case here, it is simpler to invert the left-hand side of Equation 2.23 only once, and to solve the equation by this inverted matrix, each point u_0 leading to a different

right-hand side $(\gamma(u_1-u_0), \dots, \gamma(u_N-u_0), 1)'$. Application of a fixed neighbourhood implies assigning values to $\gamma(h)$ for $h > L/2$, that is for distances for which the semi-variogram model has not been fitted to the data. From Table 2.6 it can be seen that for rainfall characteristic F_1^S this casts doubts about semi-variances at large mutual distances.

The resulting maps are shown in Figure 2.7. Figure 2.7G for rainfall characteristic R is in accordance with the regional differences in total annual rainfall within the Netherlands described by Buishand and Velds (1980). They also indicated the regions with most abundant annual rainfall as the Veluwe and the extreme southern part of Limburg, followed by central Drenthe, the eastern part of Friesland, the hilly parts of Overijssel and Utrecht, and regions leeward of the dunes in Zuid-Holland and Noord-Holland. The driest parts of the Netherlands are the coast of Groningen, the islands of Zeeland and Zuid-Holland, narrow strips adjacent to the IJsselmeer, the eastern part of Noord-Brabant and the northern and central part of Limburg (for the location of these regions, see Figure 1.1).

This regional distribution of annual rainfall is not only consistent with that of Buishand and Velds (1980) based on 1941-1970 data, but it is also in close agreement with that of KNMI (1972) based on 1931-1960 rainfall records with some extended series. Thus, analysis of rainfall records for the three periods, 1931-1960, 1941-1970, and 1951-1979, have yielded much the same regional distribution of total annual rainfall.

The south-west to north-east oriented strip across the Netherlands with high frequencies of heavy daily rainfall in summer reported by Kraijenhoff and Prak (1979) for the period 1957-1975 is also visible in Figure 2.7B and 2.7C.

The regional distribution of relatively heavy daily rainfall in summer and winter is distinguishable in Figure 2.7B and 2.7E. Seasonal rainfall differences have been found to occur in the following regions:

- Rotterdam-Dordrecht region, extending into the western part of Noord-Brabant;

- Noord-Oost Polder;
- northern part of Noord-Holland;
- eastern parts of Overijssel and Groningen;
- a small area in the south-eastern part of Noord-Brabant.

From Figure 2.7A and 2.7B, it can be concluded that in summer, the regional distribution of heavy daily rainfall differs greatly from that of rainfall in excess of a low threshold value, particularly in:

- the Randstad and the north-western part of Noord-Brabant;
- eastern parts of Groningen, Drenthe, Overijssel, and Gelderland.

In the winter, these differences are considerably less (Figure 2.7D and 2.7E). Differences between Figure 2.7B and 2.7E, 2.7A and 2.7B, and 2.7D and 2.7E, may be of interest in studying the possible influences on rainfall by the processes of urbanization and industrialization.

2.4.3. Local differences in rainfall trend

As before, let $x_{i,j}$ be the value in year j at station i of a certain rainfall characteristic (F_ℓ^S , F_ℓ^W or R). In the case of F_ℓ^S and F_ℓ^W , the $x_{i,j}$ were transformed variates, according to Equation 2.9. Local differences in rainfall trend for data set D140 were investigated as follows. The time series $\{x_{i,j}, j=1, \dots, n\}$ for each station was reduced by the annual mean $\bar{x}_{.j}$ for each year

$$y_{i,j} = x_{i,j} - \bar{x}_{.j} \quad (2.37)$$

This reduction is useful because here the interest is in local rainfall trends with respect to the general rainfall trend over the whole of the Netherlands (Kraijenhoff and Prak, 1979). Furthermore, because of this reduction, $\text{var}(y_{i,j}) < \text{var}(x_{i,j})$, as there is a high positive correlation between $x_{i,j}$ and $\bar{x}_{.j}$ (Buishand, 1981).

For each series $y_{i,j}$ ($i=1, \dots, N$) the test statistics Q , T , M , and k^* defined in Section 2.3 were calculated and the results are presented in Appendix A.5. For each rainfall characteristic, the number

of series for which at least one of these statistics is significant ($\alpha = 0.10$) is given in Table 2.7. For all rainfall characteristics, many series exhibit inhomogeneities. This is in accordance with the findings of Buishand (1982a) who tested homogeneity of annual rainfall series at 264 Dutch rainfall stations.

Table 2.7. Number of series with at least one of the statistics to test homogeneity, Q , T , or M , significant ($\alpha = 0.10$; for Q the test was one-sided, for T and M two-sided)

Rainfall characteristic	Number of series	
	Summer	Winter
Exceedance frequency		
1 mm (F_1)	44	50
15 mm (F_{15})	43	45
25 mm (F_{25})	35	29
Total annual rainfall (R)	72	

For those rainfall series having a significant M , a check was made whether there was a preferred location for the estimated jump point k^* . For each rainfall characteristic, these values of k^* were classified in intervals: 1951-1959; 1960-1969; and 1970-1979. From the results, which are presented in Table 2.8, there is no evidence of non-randomness.

Table 2.8. Number of significant ($\alpha = 0.10$) jump points (data set D140) in three periods: 1951-1959; 1960-1969; and 1970-1979

Period	Rainfall characteristic						Sum	
	Exceedance frequency					Total annual rainfall		
	F ₁ ^S	F ₁₅ ^S	F ₂₅ ^S	F ₁ ^W	F ₁₅ ^W			F ₂₅ ^W
1951-1959	8	7	0	8	15	6	10	54
1960-1969	11	7	6	9	1	6	21	61
1970-1979	5	6	2	17	10	6	12	58
Sum	24	20	8	34	26	18	43	173

In order to obtain an overall picture of the distribution of local rainfall trends, that is, of the reduced series (Equation 2.37), the calculated \underline{T} statistics were interpolated by the kriging method (Figure 2.9). Sample semi-variograms were calculated according to Equation 2.25, and are depicted in Figure 2.8. Again, checks were made for indications of anisotropy in the sample semi-variograms, and again no evidence for anisotropy was found. Therefore, the parameters α_1 and α_2 in Equation 2.26b were estimated by the procedure outlined in Section 2.4.2, and the resulting OLS estimates $\hat{\alpha}_1$ and $\hat{\alpha}_2$ are presented in Table 2.9.

Table 2.9. Ordinary least squares estimates $\hat{\alpha}_1$ (-) and $\hat{\alpha}_2$ (km) in Equation 2.26b

Rainfall characteristic	Summer		Winter	
	$\hat{\alpha}_1$	$\hat{\alpha}_2$	$\hat{\alpha}_1$	$\hat{\alpha}_2$
Exceedance frequency				
1 mm (F_1)	1.62	17.07	2.43	17.21
15 mm (F_{15})	1.73	15.11	1.60	32.63
25 mm (F_{25})	1.41	25.11	1.70	75.02
Total annual rainfall (R)	$\hat{\alpha}_1 = 3.00$		$\hat{\alpha}_2 = 31.86$	

The ranges ($\approx 3\hat{\alpha}_2$) of the semi-variograms for local rainfall trends are rather limited and are of the same order as the ranges of semi-variograms for rainfall levels (Table 2.6).

From Table 2.9 a large variance of the \underline{T} statistic can be implied. Under the null hypothesis $\text{var}(\underline{T}) = \text{var}(\underline{t}_{n-2})$, where \underline{t}_{n-2} is a Student variate with $(n-2)$ degrees of freedom with $\text{var}(\underline{t}_{n-2}) = (n-2)/(n-4) = 1.08$. Thus, it may be concluded that \underline{T} is a non-central Student variate $\underline{t}_v^{\delta_i}$, where $v = n-2$ and with non-centrality parameter δ_i at station i . For $\underline{t}_v^{\delta_i}$, the following holds (Johnson and Kotz, 1970; p. 203, 204))

$$E\{\underline{t}_v^{\delta_i}\} = \delta_i (v/2)^{1/2} \Gamma(v/2) / \Gamma(v/2), \quad (2.38)$$

$$\text{var}(\underline{t}_v^{\delta_i}) = \frac{v}{v-2} (1 + \delta_i^2) - (E\{\underline{t}_v^{\delta_i}\})^2. \quad (2.39)$$

If $v=27$, then $E\{\underline{t}_v^{\delta_i}\} \cong \delta_i$, and when inserted into Equation 2.39 this yields

$$\text{var}(\underline{t}_v^{\delta_i}) = 1.08 + 0.0214 \delta_i^2. \quad (2.40)$$

From Figure 2.9, for winter rainfall series there seems to be a general positive trend along the coast and a negative trend along the eastern border of the Netherlands. For the summer series, the picture is rather complicated. For the characteristics F_{15}^S and F_{25}^S there are positive trends in the extreme north of Noord-Holland, in a north-south strip through the centre of the Netherlands, the Noord-Oost Polder, and parts of Zeeland. Negative trends occur along the eastern border, and in some parts of Friesland, Noord-Holland and Zeeland.

For F_1^S and F_1^W seasonal differences in rainfall trend occur in Groningen, Noord-Holland, Randstad, Utrecht, Noord-Brabant, and Zeeland. (Figure 2.9A and 2.9D). With higher threshold values, characteristics F_{15}^S and F_{15}^W (Figure 2.9B and 2.9E), these seasonal differences occur only in Noord-Holland, Randstad, Utrecht, and Noord-Brabant. Within-season differences are particularly pronounced in summer.

The regional distribution of trends in total annual rainfall R corresponds rather well to the regional distributions of trends in the winter series, that is, a positive trend along the coast and a negative trend along the eastern border of the Netherlands (Figure 2.9G).

2.5. PARTITIONS OF THE NETHERLANDS BASED ON RAINFALL

Figure 2.7 and Figure 2.9 suggest local rainfall differences. However, replacing the real data with correlated random variates and applying the same interpolation and plotting procedures as used for Figure 2.7 and 2.9 also results in maps suggesting local differences. To be sure that a partitioning of the Netherlands based on rainfall is realistic, the following two points are important:

- the variation of a rainfall characteristic between regions should be significantly different to the variation within regions;
- a partition resulting from a statistical procedure should lead to physically interpretable regions. Such a partition should be valid for several rainfall characteristics. For design criteria in particular, the partition should be valid for the frequency of heavy rainfall of short duration, that is, of five minutes up to one hour.

Such a partition has been devised for France, in which three regions are distinguished (Ministère de l'Intérieur, 1977), and one is further subdivided into two regions (CTGREF, 1979). The United Kingdom has been divided into two regions, England and Wales, and Scotland and Northern Ireland (NERC, 1975, Vol. 2), which are not homogeneous with respect to rainfall. Thus, the recognition of local rainfall differences is not sufficient to justify a partition.

The actual procedure for rainfall durations shorter than 48 hours used by NERC (1975; Vol. 2) is as follows: the threshold value of rainfall corresponding to a 5-year return period, q_5 , for the appropriate duration and location is related to the two day q_5 and the 60 minute q_5 values; these last two values can be derived from detailed maps showing their geographical distribution. Then the q_5 value for the appropriate rainfall duration is related to the two day and the 60 minute values by $q_5 = a/(1+bD)^n$, where q_5 is in mm/hour, D is the rainfall duration expressed in hours and the parameters a , b , and n are related to the ratio of the two day and the 60 minute values of q_5 . This relationship coincides with a relationship of these parameters to mean annual rainfall (see Section 2.5.3). Once the q_5 value is determined, the value of q_T for a T -year return period can also be determined by considering the growth factor: the ratio q_T/q_5 . These growth factors which were found to vary slightly with geographical location, have been tabulated for the two regions of the United Kingdom mentioned above.

In NERC (1975) it is also pointed out that for rainfall durations of at least 24 hours, quantile estimates of rainfall for a given return period and rainfall duration are proportional to mean annual rainfall. Without partitioning the country into regions, such proportionality is mentioned for possible use in Belgium (Nonclerq, 1982) and the Netherlands (Buishand and Velds, 1980). As a consequence of the rainfall increase in urban areas, reported by Kraijenhoff and Prak (1979), it is suggested in Werkgroep Afvoerberekeningen (1979) to divide the Netherlands into urban and rural regions.

Possible partitions of the Netherlands based on rainfall are suggested in Section 2.5.1 and tested statistically in Section 2.5.2. Finally, the implications of local differences for hydrological design are discussed in Section 2.5.3.

2.5.1. Possible partitions

When suggesting possible partitions with respect to rainfall of the Netherlands, it seems natural to start with a summary of the relevant publications of the Royal Netherlands Meteorological Institute (KNMI): Hartman (1913), Braak (1933), Timmerman (1963), Buishand and Velds (1980) and Buishand (1983); also maps showing the geographical distribution of certain rainfall characteristics can be found in KNMI (1972).

Maps showing the geographical distribution of mean annual rainfall from Hartman (1913), Braak (1933), and Buishand and Velds (1980) are reproduced in Figure 2.10. The absence of a rainfall maximum in the southern part of Limburg in Figure 2.10A is due to the use made of the Maastricht and Ubachsberg records, which are of a rather questionable quality (Braak, 1933). The mean annual rainfall in Figure 2.10B ranged from 597 mm at Kampen to 862 mm at Vaals; in the present study (Figure 2.7G) the range is from 706 mm at Stavoren to 916 mm at Vaals. There is a general trend towards higher mean annual rainfalls which can at least partially be ascribed to improved measurement practices (Buishand, 1977a). The local rainfall differences can be attributed mainly to the following (Timmerman, 1963):

- *Friction.* Convergence of air masses reaching the coastline from south-west to north is induced by the increasing roughness. This results in an increase in rainfall levels and frequencies with increasing distance from the coast up to a maximum of about 30-35 km from the coast.
- *Topography.* The forced ascent of the air leads to an increase in rainfall on the windward side of the hills of Utrecht, Overijssel, the southern part of Limburg and the Veluwe.
- *Differential heating.* Temperature differences between sea and land lead to a relative increase in rainfall levels and frequencies along the coast in the autumn, and a decrease in the spring and the early summer.

The effects of urbanization on rainfall have been mentioned by Timmerman (1963), but not in relation to the geographical distribution of rainfall in the Netherlands. Buishand and Velds (1980) have concluded that cities, such as Amsterdam and Rotterdam, may have an effect on rainfall.

Four partitions of the Netherlands, based on rainfall, are proposed:

- partition (i), based on rainfall differences from east to west, that is from inland to the coast, and from north to south (Figure 2.11A);
- partition (ii), based on the effects of friction, topography, and differential heating (Figure 2.11B);
- partition (iii), based on the effects of friction, topography, and differential heating, and on anomalies attributed to urban effects reported by Kraijenhoff and Prak (1979) (Figure 2.11C);
- partition (iv), based on mean annual rainfall for the period 1951-1979 (Figure 2.11D; the three isolated dry stations have been included in the group of normal stations).

Each station in data set D140 has been assigned to one of the sub-regions in each of the proposed partitions (see Appendix A.5).

Each partition is to some extent a *posteriori*. Particularly partition (iv), but the other partitions are also partly based on maps showing the geographical distribution of rainfall.

2.5.2. Testing the statistical significance of the partitions

An indication of the existence of significant local differences in mean annual rainfall has already been given in Section 2.2. Here, the effect of spatial correlation is considered. The following three null hypotheses are considered:

- H_1 : all the expectations of a certain rainfall characteristic in all rainfall stations considered in the Netherlands are equal. If this were true, then the Netherlands can be considered to be homogeneous with regard to rainfall;
- H_2 : after assigning the rainfall stations to regions, all resulting regions are homogeneous;
- H_3 : differences between internal homogeneous regions vanish.

The following rainfall characteristics are considered:

- rainfall levels: R , F_{15}^S , F_{15}^W , and F_{25}^S , because these are relevant for hydrological design;
- rainfall trends: F_{15}^S and F_{25}^S , because these give an indication of the importance of urban effects (see Section 2.6).

The following model is used to test spatial homogeneity (M.A.J. Van Montfort, pers. comm., 1981). Let $z=(z_1, \dots, z_N)'$ be a vector of measurements, and let $z \sim N(\xi, C)$, that is a N -dimensional normal distribution with expectation $\xi=(\xi_1, \dots, \xi_N)' \in R^N$, and a N by N covariance matrix C , where C is assumed to be known. Furthermore, R^N is the direct sum of two orthogonal subspaces

$$R^N = D + R,$$

where D is the space of vectors ξ for a given null hypothesis. Obviously, $\xi = \xi_D + \xi_R = \xi_D$, ξ_D and ξ_R are orthogonal projections of ξ on D and R , respectively.

With respect to the subspace D , H_1 is equivalent to $D_1 = \langle s \rangle$ and $s = 1_N$, a vector in R^N consisting of merely ones. Hypothesis H_1 will be tested by the omnibus statistic T_1 , where

$$\underline{T}_1 = \underline{z}'C^{-1}\underline{z} - \frac{(s'C^{-1}\underline{z})^2}{s'C^{-1}s} \hat{H}_1 \chi_{N-1}^2 \quad (2.41)$$

H_2 is equivalent to $D_2 = \langle e_1, \dots, e_d \rangle$, $\dim(D_2) = d$, and d is the number of regions into which the Netherlands is partitioned; the vector e_j ($j=1, \dots, d$) indicates by one or zero whether or not a station belongs to region j . The hypothesis H_2 is tested by \underline{T}_2 , where

$$\underline{T}_2 = \underline{z}'C^{-1}\underline{z} - \text{proj}^2 \hat{H}_2 \chi_{N-d}^2 \quad (2.42)$$

and proj^2 is the square of a special projection of \underline{z} on D_2 , to be obtained by inserting the solution of the normal equations

$$\begin{pmatrix} e_1'C^{-1}e_1 & \dots & e_1'C^{-1}e_d \\ & \ddots & \\ & & e_d'C^{-1}e_d \end{pmatrix} \begin{pmatrix} \beta_1 \\ \vdots \\ \beta_d \end{pmatrix} = \begin{pmatrix} e_1'C^{-1}\underline{z} \\ \vdots \\ e_d'C^{-1}\underline{z} \end{pmatrix} \quad (2.43)$$

into $\sum_{i=1}^d \beta_i e_i C^{-1} \underline{z}$.

H_3 is equivalent to $\zeta \in D_3$, where $D_3 = \langle s \rangle$, and the alternative hypothesis is H_2 . The test statistic \underline{T}_3 is the difference of the squares of the special projections of \underline{z} on D under H_3 and under H_2

$$\underline{T}_3 = \hat{\underline{z}}_{D_2}^2 - \hat{\underline{z}}_D^2 \hat{H}_3 \chi_{d-1}^2 \quad (2.44)$$

As the statistics \underline{T}_1 , \underline{T}_2 , and \underline{T}_3 tend to large values under the alternative, a right-hand sided critical region ($\alpha=0.05$) is used.

In the present application, standardized variables are used, so that in Equations 2.41, 2.42, and 2.44, $\zeta=0$ and $\sigma^2=1$. The Student variates used as trend characteristics (Section 2.3) have been

standardized by considering their ratio to the standard deviation, estimated as the square root of the sill value of the semi-variogram, that is $\sqrt{\hat{\alpha}_1}$, where $\hat{\alpha}_1$ is given in Table 2.9. Rainfall levels $x_{1.}$ have been standardized by subtracting $x_{..}$, followed by dividing by $\sqrt{\hat{\alpha}_1}$ (Table 2.6).

For rainfall levels, the normality assumption may be doubted, except for mean annual rainfall. However, the frequencies F_{15}^S , F_{15}^W , F_{25}^S could follow a binomial distribution and it is only by virtue of the Central Limit Theorem that the standardized values may have a normal distribution. For the Student variates, the normality assumption seems more plausible.

The covariance matrix $C=(c_{i,j})$ has been estimated as

$$c_{i,j} = \exp(-h/\alpha_2), \quad (2.45)$$

where α_2 has already been estimated. In Table 2.10 the values of $\hat{\alpha}_1$ and $\hat{\alpha}_2$ are reproduced, together with the results of the tests. The test statistics are obviously functions of $\hat{\alpha}_2$, but it has been verified that the conclusions to be drawn from Table 2.10 do not change within a reasonable range of $\hat{\alpha}_2$ values.

Table 2.10. The statistical significance of four partitions of the Netherlands (Figure 2.11); not significant values of T_2 , and significant values of T_1 and T_3 support inhomogeneities

Rainfall characteristic		PARTITION										
		$\hat{\alpha}_1$	$\hat{\alpha}_2$	T_1	(i)		(ii)		(iii)		(iv)	
					T_2	T_3	T_2	T_3	T_2	T_3	T_2	T_3
Trends	F_{15}^S	1.73	15.11	128.4	124.1	1.2	124.1	2.4	127.6	0.4	127.9	0.3
	F_{25}^S	1.41	25.11	193.1**	187.2**	1.1	192.3**	0.3	192.1**	0.4	191.8**	0.5
Levels of rainfall	F_{15}^S	0.29	21.07	142.2	138.5	0.9	131.7	5.5	127.0	8.2**	94.1	35.0**
	F_{15}^W	0.35	21.72	145.4	141.9	0.8	131.0	7.5**	135.4	5.1	107.1	24.3**
	F_{25}^S	0.065	14.62	135.3	133.4	0.5	129.8	2.9	122.1	7.4**	115.5	11.7**
	R	1355.1	23.65	157.9	154.6	0.7	143.8	6.7**	141.0	8.2**	89.8	52.0**

** Indicates values inside the critical region for $\alpha = 0.05$.

With respect to the Student variates it could be argued that, instead of standardizing on division by $\sqrt{\hat{\alpha}_1}$, division by the standard deviation of such Student variates under the null hypothesis is preferable. This, however, would lead to inconsistencies in the estimation of α_2 in Equation 2.45.

With regard to trends, it can be seen from the T_1 values in Table 2.10 that only for rainfall characteristic F_{25}^S , the hypothesis of inhomogeneity in space has statistical support. This is not surprising, as the alternative for hypothesis H_1 is quite general. With regard to rainfall levels it can be seen from the T_2 and T_3 values in Table 2.10 that, in spite of an insignificant value of T_1 , partitions (iii) and especially (iv) are statistically significant partitions of the Netherlands. Regional rainfall differences are to a certain extent the consequence of differences in time, for example, the distribution of rainfall over the seasons is different for inland and for coastal areas. Thus the attractive feature of partition (iv) is that it yields significant results for the year as a whole and for both winter and summer.

The adequacy of the partitions for rainfall levels but not for rainfall trends can be explained by the large differences between Figure 2.7C and 2.9C for levels and trends respectively of rainfall characteristic F_{25}^S . As the partitions have been suggested from maps of rainfall levels, the adequacy of the partitions for rainfall trends could be expected to be less.

2.5.3. *The hydrological significance of the partitions*

Of the four partitions of the Netherlands proposed in Section 2.5.2, only one explains successfully regional differences in rainfall levels, but none explains successfully regional differences in trends.

It is difficult to draw conclusions of relevance to hydrological practice about regional differences in rainfall trend. A significant trend for a particular series may very well reverse when the period of analysis is extended (Table 2.5 and Figure 2.5). This is the result of the pseudo fluctuations which many hydrological time series exhibit as a result of the infinite memory of hydrological processes, that is a small but not negligible autocorrelation of the process at very large time lags (Wallis and O'Connell, 1973). The physical cause of this infinite memory is the storage effect, which acts in many hydrological processes (Feller, 1951). Sample curves from such processes reveal seemingly periodic swings, and

as pointed out by Mandelbrot and Wallis (1969): "... such cycles must be considered spurious. (...) Such cycles are useful in describing the past but have no predictive value for the future" (p. 231). Note that the moving averages considered in Figure 2.5B and 2.5C also cause pseudo fluctuations.

On the other hand, the differences in trend are quite notable. For rainfall characteristic F_{25}^S , the stations with highest and lowest values of \underline{T} (Section 2.3) are Medemblik and Vroomshoop, respectively. If a simple linear regression line is fitted to the untransformed frequencies F_{25}^S for these stations, the difference in slope is $0.06 - (-0.07) = 0.13 \text{ \# year}^{-1}$. For rainfall characteristic F_{15}^S , the stations with highest and lowest values of \underline{T} are Dordrecht and Leeuwarden, respectively, and the difference in slope of the regression lines is $0.06 - (-0.16) = 0.22 \text{ \# year}^{-1}$.

These are extremes, and for a more general picture, a partition (v) of the Netherlands, suggested by Figures 2.9B and 2.9C, is presented in Figure 2.12 (see also Appendix A.5). Let $x_{i,j}$ be the annual frequency F_{15}^S at station i in year j , and \bar{x}_j the annual mean for year j , then for each rainfall station in D140, the estimate \hat{b}_i of the slope parameter of the regression line of $(x_{i,j} - \bar{x}_j)$ on j has been calculated. It has been verified by the test procedures given in Section 2.5.2 that the partition was statistically sound. For each of the three subregions of the partition, the average slope parameter $\hat{\beta}$ has been estimated by Equation 2.43. The covariance matrix C of the \hat{b}_i in Equation 2.43 has been estimated from the semi-variogram of the \hat{b}_i . Results for F_{15}^S are

$$\hat{\beta}_1 = 0.041, \hat{\beta}_2 = -0.037, \hat{\beta}_3 = -0.002 \text{ (\# year}^{-1}\text{)}.$$

Application of this procedure to rainfall characteristic F_{25}^S yields

$$\hat{\beta}_1 = 0.005, \hat{\beta}_2 = -0.016, \hat{\beta}_3 = 0.001 \text{ (\# year}^{-1}\text{)}.$$

An indication of the homogeneity in time of the partition has been obtained by calculating the slope \hat{b}_i for the D14 series (1906-1979) for rainfall characteristics F_{15}^S and F_{25}^S . For data set D14, only

three rainfall stations were assigned to region 1 (Den Helder/De Kooy, Vlissingen, and Kerkwerpe), and only two stations to region 3 (West Terschelling and Heerde). Results for rainfall characteristic F_{15}^S are

$$\hat{\beta}_1 = -0.008, \hat{\beta}_2 = 0.003, \hat{\beta}_3 = -0.004 (\# \text{ year}^{-1}),$$

and for F_{25}^S

$$\hat{\beta}_1 = -0.003, \hat{\beta}_2 = 0.002, \hat{\beta}_3 = -0.005 (\# \text{ year}^{-1}).$$

These results were obtained as the mean $\hat{\beta}_i$ value for a particular region. Note that this partition has been designed to give a positive $\hat{\beta}_1$, a negative $\hat{\beta}_2$, and an approximately vanishing $\hat{\beta}_3$. Furthermore, values of $\hat{\beta}$ for data set D14 are considerably smaller than those for data set D140, which reflects the fact that the trends studied here are not constant in time. Therefore, it can be concluded that the partition with regard to trends is only valid for data set D140.

Kraijenhoff et al. (1981) present a map of the Netherlands (their Figure 5), showing the geographical distribution of the change $\Delta F = \sum_1 F_{30}^S - \sum_2 F_{30}^S$, where the symbol \sum_i refers to a summation over the period, 1933-1956 (excluding 1945) for $i=1$, and 1957-1979 for $i=2$. These changes ΔF were calculated as the means of such changes for all stations within a moving, square grid area of 1000 km^2 . The order of magnitude of the change ΔF in rainfall characteristic F_{30}^S , as reported in Kraijenhoff et al. (1981), corresponds to that for rainfall characteristic F_{25}^S (data set D140) in the present study. However, the pattern of regions with positive and with negative trends is very distinct. In fact, the map in Kraijenhoff et al. (1981) suggests an effect of urbanization and industrialization on rainfall.

With regard to regional differences in rainfall levels, the spatial distribution of annual frequencies of heavy rainfall seems, from a hydrological point of view, more interesting than that of mean annual rainfall. As an example, the estimated difference between rainfall levels for F_{25}^S in the wet and the dry region of partition

(iv) (Section 2.5.1) is 1.14 times per year. As before, this difference has been estimated by Equation 2.43.

Such local differences in frequency of heavy daily rainfall have been pointed out by Braak (1933) with a map of the Netherlands, showing the geographical distribution of deviations in the annual frequency of daily rainfall in excess of 20 mm. This map is reproduced here as Figure 2.13, together with an updated version, based on data set D140. Braak concluded that "local differences appear to be rather large" (p. 36), but continued that such maps should be interpreted with care. Above a certain rainfall level the relative change in the mean number of exceedances in a year is larger than the relative change in rainfall level itself, see also Figure 2.14. As a consequence, rainfall levels for a given low frequency of exceedance will show less local differences than the frequencies of exceedance themselves.

In statistical terms, it can be stated that confidence intervals for quantiles (x_p) are relatively smaller than those for probabilities (p). Consider for example, a level with number of exceedances k_e during the whole period of observation (29 years for data set D140). The number of exceedances has a binomial distribution with parameters n and p , and could be approximated by a Poisson distribution with expectation $\lambda=np$, for which confidence intervals can easily be constructed. In addition, distribution free confidence intervals for x_p given p can be constructed from an ordered sample of daily rainfalls. From the results given in Table 2.11, it can be seen that for levels which are exceeded rather frequently, confidence intervals for x_p are narrow. This is not true for low values of k_e . The level of 20 mm is attained or exceeded about 3.55 times a year (data set D140).

Table 2.11. Confidence intervals for the expected number of exceedances and for quantiles x_p at confidence level 0.90

k_e	Expected number of exceedances	$365 \cdot 29 \cdot p$	x_p (mm)
58	(45.5, 70.5) ¹	58	(22.8, 25.4)
29	(20.8, 39.6)	29	(27.1, 30.6)
6	(2.6, 11.9)	6	(36.0, 66.2)

¹ Estimated by using the normal approximation.

Maps of the Netherlands showing the geographical distribution of \hat{q}_5 , \hat{q}_{10} , and \hat{q}_{30} for daily rainfall for the months, February, April, June, August, October, and December have been presented in KNMI (1972), where \hat{q}_5 denotes the estimated threshold value of rainfall of the appropriate duration and for a 5-year return period. Here, such maps are produced for $\hat{q}_{0.5}$ (that is, the event with a 0.5-year return period) and \hat{q}_5 for the summer (Figure 2.15), the winter period (Figure 2.16), and for the whole year (Figure 2.17). These were obtained by maximum likelihood estimation of $q_{0.5}$ and q_5 from data set D140, in particular the POT series of daily rainfall from Section 2.2 (for a particular series $\hat{q}_{0.5}$ simply equals the estimate \hat{q}_0 of the location parameter). A test on the exponentiality of the individual series has been carried out. The hypothesis of an exponential distribution was rejected by the test outlined in Section 2.2, at significance level 0.10, for 34 year series, for 27 summer series, and for 39 winter series. For a relatively large number of series the test statistic is small, indicating too long a tail of the POT series.

Although local differences in daily rainfall are important for drainage design for rural areas in the Netherlands, this is not necessarily so for urban areas: the order of magnitude of the time lag between the centres of the hyetograph and the hydrograph for an urban drainage system is about one hour. Thus, it should be verified that a partition also holds for this duration of rainfall. Buishand (1983) found that there are only small differences between the quantiles of the distribution of hourly rainfall for the series

Den Helder/De Kooy, Eelde, De Bilt, Vlissingen, and Beek. Furthermore, somewhat larger differences may very often be the result of seasonal effects on rainfall distribution.

Consequences of differences in level of hourly rainfall have been investigated, by using the hourly rainfall data (data set H12) as input into a simulation model of urban runoff, STORM (HEC, 1977). This model operates as follows. The basin excess is calculated for each hourly interval as the sum of the dry weather flow and the net rainfall (evaporation and depression storage being taken into account) multiplied by a coefficient. The basin excess is routed to the outlet of the basin by the Soil Conservation Service triangular unit hydrograph. Storage, treatment, and overflow quantities are calculated by means of a simple bookkeeping system.

The model has been calibrated for a particular urban basin in the Netherlands (Leenen and Groot, 1980), and the resulting values of the input parameters of STORM have been used in the present study, together with the hourly rainfall of the twelve series of data set H12. The 12 stations have been assigned to each of the three regions within partition (iv) (Figure 2.11D). The mean annual number (\bar{N}) and total quantity (Q) of overflows, calculated for the period 1975-1980, are presented in Table 2.12. This partition is not particularly convincing. This is partly due to the difficulty of deciding which of the three regions is most appropriate for a particular rainfall station, for example, Volkel. The proposition of a certain partition necessitates not only a dense network of rainfall stations but also meteorological insight.

Furthermore, a partition based on the level of mean annual rainfall, and which also appeared to be valid for daily rainfall, may not be adequate for hourly rainfall. The reason for this is that the behaviour of quantiles of hourly and of daily rainfall with respect to mean annual rainfall may be different, as can be illustrated with results of NERC (1975).

Table 2.12. Mean annual number (\bar{N}) and total quantity (Q) of overflows over the period 1975-1980, calculated with the STORM model (the partitioning into regions is in accordance with Figure 2.11D)

Rainfall station	\bar{N} (# year ⁻¹)	Q (mm)
Region 1	2.00	51.53
Schiphol	1.50	11.23
Rotterdam	2.50	91.82
Region 2	2.00	53.16
Vlissingen	1.67	59.32
Volkel	2.33	46.99
Region 3	1.96	39.01
Soesterberg	2.17	43.34
Den Helder/De Kooy	2.17	80.87
Valkenburg	1.33	18.74
Beek	2.00	53.83
De Bilt	2.17	30.17
Eelde	1.67	15.79
Leeuwarden	2.67	37.60
Twente	1.50	31.73

A model for relating rainfall intensities of equal probability of exceedance to durations from some minutes to some days is

$$I = \frac{a}{(D+b)^n}, \quad (2.46)$$

where

I : intensity (mm/hour)

D : duration (hour)

a, b, n : parameters to be estimated.

Quantiles q for rainfall durations of one minute to 48 hours have been described by a somewhat different equation, $I = a/(1+bd)^n$ in NERC (1975; Vol. 2). The approximate relation of the parameters a , b , and n to mean annual rainfall as presented in NERC (1975; Vol. 2, p. 26) was used to estimate q_5 for rainfall durations of one and 24 hours (Table 2.13). For a rainfall duration of one hour, q_5 is rather insensitive to variations of mean annual rainfall, and as far as there is a relationship to mean annual rainfall, it is opposite to the relationship of q_5 for a rainfall duration of 24 hours to mean annual rainfall.

Table 2.13. Quantiles q_5 according to NERC (1975) for rainfall durations of 1 and 24 hours, as a function of mean annual rainfall

Mean annual rainfall (mm)	q_5 (mm)	
	1 hour	24 hours
500 - 600	19.6	41.3
600 - 800	20.6	47.8
800 - 1000	19.0	50.9
1000 - 1400	18.6	60.0
1400 - 2000	18.5	67.1

Define a depth-duration ratio as the ratio of two quantiles of rainfall of different duration, but with equal probability of exceedance. Such a ratio for durations D_1 and D_2 can be written as

$$\frac{D_1}{D_2} \left(\frac{D_2+b}{D_1+b} \right)^n$$

If local differences in these depth-duration ratios were totally absent, geographical variation in mean annual rainfall would be a perfect indicator of geographical variation of rainfall for all durations. However, Equation 2.46 is only valid for rainfall durations up to a few days, and for these durations, the total absence of local differences of depth-duration ratios also implies the absence of local differences of the coefficients b and n in Equation

2.46. But in fact, these have been found to vary locally with mean annual rainfall, as does the coefficient a in Equation 2.46, giving rise to the phenomenon illustrated in Table 2.13. Only for durations up to two hours, there is very little geographical variation in depth-duration ratios (Hershfield, 1961; Bell, 1969).

On the other hand, the impression offered by Table 2.13 does not seem to be typical. This may be concluded from comparing the maps showing the geographical distribution of the one-hour and 24-hour rainfall of a T -year return period for the United States (Hershfield, 1961). The one-hour maps in Hershfield (1961) have been extracted from the data of 200 US Weather Bureau first-order stations with a mean length of record of 48 years. Taking into consideration the reduced number of rainfall stations on which the one-hour rainfall maps are based in relation to the 24-hour rainfall maps, the patterns of isolines in both maps can be considered to agree very well.

For all of the H12 series, POT series have been extracted for durations of one hour and 24 hours (daily rainfall for each 24-hour period ending at 8h UTC), with a mean annual number of threshold exceedances of two. To assure independence, peaks had to be separated by a time gap of at least ten hours for rainfall durations of one hour (Buishand, 1983), and for daily rainfall by a dry period of 24 hours. Quantiles $\hat{q}_{0.5}$ have been estimated as the location parameter in Equation 2.3, for the summer, winter, and the whole year, and are plotted in Figure 2.18 as a function of mean seasonal or annual rainfall.

Especially when the year is divided into seasons, there is a significant positive correlation of quantiles of both hourly and daily rainfall and mean seasonal rainfall (one-sided t -test at significance level 0.05). There is not a very pronounced difference in the behaviour of quantiles of hourly and daily rainfall with respect to mean annual rainfall, and such differences cannot explain completely the unconvincing results presented in Table 2.12 of the partition of the Netherlands. Further, the total number and quantity of overflows tend to correlate positively with mean annual rainfall, although not statistically significant (both correlation coef-

ficients 0.16). A third explanation for the unconvincing results of the partition is, that only six of the 12 rainfall stations in the data set H12 have been used in designing the partition (iv), from which Twente has an atypically low mean annual rainfall for the period 1975-1980, as compared to the period 1951-1979 considered when designing the partition. Finally, the STORM model does not seem sensitive enough to yield large differences in overflow parameters, given the spatial differences in rainfall.

Thus it can be concluded that the proposed partition of the Netherlands based on rainfall trend (Figure 2.12) is only valid for the most recent period (data set D140), and for the particular rainfall characteristic considered, that is, the exceedance frequency of heavy daily rainfall in summer. The partition based on rainfall levels (Figure 2.11D) has considerably more support.

2.6. EFFECT OF URBANIZATION AND INDUSTRIALIZATION ON PRECIPITATION

The effect of urbanization and industrialization on precipitation is an aspect of urban climatology, which requires an understanding of the whole urban climate because of the interaction between the climatic elements. This understanding, however, is far from complete. For example, little is known about the physical mechanisms governing urban enhancement of precipitation. According to Oke (1980), the impact of cities upon precipitation is still a topic of some controversy, concerning both the proof that effects exist and the nature of the processes involved. The present consensus is that there is reasonable statistical and other support for the hypothesis of precipitation enhancement by large cities but that proof including knowledge of the governing physical mechanisms remains to be demonstrated. According to this consensus, the maximum effect is usually about 20-40 kilometres downwind of the city, and convective events are more susceptible to modification than frontal events. Effects increase with increasing intensity of rainfall, but this should not be interpreted as being restricted only to a few large rainstorms. Presumably such effects extend to rainstorms which, if unaffected, would be of rather modest size (Braham, 1978). It should be emphasized, however, that not everyone agrees with the above-mentioned consensus view (Hershfield, 1979).

The step from measurements to hypotheses about causal relationships is extremely complicated in urban climatology, because of the complexity of the system. For example, in the spatial definition of the urban system, not only is the urban surface involved, but also a certain part of the atmosphere, as evidenced by city-induced changes in wind, temperature, precipitation, and also pollution. The vertical extension of this part of the atmosphere, usually divided into an urban canopy layer, that is below roof level (UCL), and an urban boundary layer, that is above roof level (UBL), depends on meteorological conditions, for example, stability. To complicate matters further, a part of the soil is also involved, and there is considerable import to the system, including advected heat, imported water, etc.

Possible causes of urban enhancement of precipitation are suggested in two reports on urban climatology to the World Meteorological Organization by Oke (1974, 1979), and by Bornstein and Oke (1980) and Oke (1980); and methodology on statistical research into urban precipitation enhancement is suggested by Lowry (1977). These references are used in this introduction.

Thermodynamic and mechanical processes rather than the extra provision of condensation and freezing nuclei by urban aerosols and the extra supply of water vapour in the city due to combustion and cooling processes, lead to the urban enhancement of precipitation. The uplift associated with the heat island, mass convergence due to frictional retardation of the airflow and to heat island induced circulations, the barrier effect of the physical presence of the city, and increased mechanical and thermal turbulence, could well be sufficient to permit urban clouds to penetrate stable layers in the mid-troposphere and to reach glaciation levels, or to produce greater instability in general, or to produce confluence zones of preferred activity (Oke, 1980).

Two other processes sometimes mentioned as affecting urban precipitation are urban emissions of condensation nuclei and the extra supply of water vapour in the city, but these are considered to be less important by Oke. With regard to the former, in the urban atmosphere, Aitken condensation nuclei (ACN, with radius

$r: 4 \cdot 10^{-3} < r < 0.1 \mu\text{m}$) and the larger cloud condensation nuclei (CCN) in the background atmosphere are added to greatly by urban emissions. These emissions are supplemented by gas-to-particle conversions, especially from pollutant gases, such as, SO_2 and NO_x . These conversions result in particles of ACN size, which can grow by further absorption to CCN sizes. This leads to urban clouds having much higher drop concentrations than non-urban clouds, so that urban clouds are characterized by a very large number of small droplets.

Thus, if the mechanism responsible for precipitation is coalescence of cloud droplets rather than the formation and growth of ice particles, then there appears to be a negative urban microphysical effect on raindrop growth, and therefore on precipitation. The balance is at least partially redressed, however, with the discovery that certain industrial sources produce ultra-giant nuclei and thus provide an appropriate distribution of droplets for droplet growth. But, even where the appropriate seeding of nuclei from urban-industrial sources is present, it is likely that more than microphysical modification of clouds will be necessary for significant precipitation enhancement (Oke, 1980).

In this context numerous observations made downwind of isolated power-generating plants have not revealed significant increases in convective rainfall (Huff and Vogel, 1979). Although precipitation enhancement by cloud seeding has been accepted, seeding should take place under appropriate conditions, and even then the increase in rainfall is only modest (Rogers, 1979). In the case of power-generating plants, continuous cloud seeding may very well lead to occasional suppression of rainfall. Apart from that, the cloud seeding material emitted by these plants may not be very effective.

With the exception of daytime values during summer, absolute humidity in a city tends to be higher than in the surrounding rural area. In cloud physics, however, relative humidity is often a more important factor than the actual moisture concentration.

The difficulty of discriminating between controlling factors and the natural variability in time and in space of the precipitation, has allowed widely used estimators of urban effects, such as urban-rural and upwind-downwind rainfall differences, to become open to criticism (Lowry, 1977). Let \bar{x}_{itu} be the mean measured rainfall at location u on days within a period t given weather type i during those days, then the expectation of \bar{x}_{itu} may be considered to be the sum of three components (Lowry, 1977)

$$E\{\bar{x}_{itu}\} = E\{\underline{c}_{iu}\} + E\{\underline{l}_{iu}\} + E\{\underline{e}_{itu}\}, \quad (2.47)$$

where the component \underline{c} refers to the background climate, \underline{l} to the local landscape and \underline{e} to local urbanization. The variables \underline{c} and \underline{l} are assumed to be time-independent

$$\underline{c}_{it_j u} = \underline{c}_{it_k u} = \underline{c}_{iu}; \quad \underline{l}_{it_j u} = \underline{l}_{it_k u} = \underline{l}_{iu}. \quad (2.48)$$

Furthermore, it is assumed that prior to urbanization and industrialization, at period $t=0$, there is no urban effect: $E\{\underline{e}_{i0u}\} = 0$.

As pointed out by Lowry (1977), estimators of the urban effect, $E\{\underline{e}_{itu}\}$, such as urban-rural and upwind-downwind differences are subject to doubt. Consider, for example, urban-rural differences, $\delta(C,R)$. The recognition of urban effects beyond the urban boundary motivates the specification of areas C (city), R (rural), and Z (zone of influence beyond the urban area) (Figure 2.19). Because the location of the boundary between R and Z is one of the objects of study, it is not certain whether or not the urban-rural differences refer in fact to differences between the urban area and area Z : $\delta(C,Z)$. However, even if this were not so, then

$$\delta(C,R) = (E\{\underline{c}_{ic}\} - E\{\underline{c}_{ir}\}) + (E\{\underline{l}_{ic}\} - E\{\underline{l}_{ir}\}) + E\{\underline{e}_{itc}\}, \quad (2.49)$$

and it is by no means self-evident that the first two terms within brackets on the right-hand side of Equation 2.49 vanish.

Instead of the afore-mentioned indicators of the urban effect in the space domain, Lowry (1977) advocates the use of indicators in the time domain: estimated differences, for one station or for a

network of stations, between observations from urban and pre-urban periods, stratified by synoptic weather type

$$\delta_i(t,0) = E\{\bar{x}_{itu}\} - E\{\bar{x}_{iou}\}. \quad (2.50)$$

The estimate $\delta_i(t,0) = \bar{x}_{itu} - \bar{x}_{iou}$ is unbiased, because of the assumptions in Equation 2.48.

Although the estimate $\delta_i(t,0)$ is an improvement on, for instance, urban-rural differences, the assumptions in Equation 2.48 remain questionable. There may be within-circulation type precipitation changes (Barry and Perry, 1973) and/or geographical shifts of climatic zones. However, as already stated in Section 2.3, rainfall can be predicted to a certain degree from weather type. In addition, if the importance of these factors is stressed, then the urban effect is measured by the local differences in rainfall which have been considered in Section 2.4.

Urban enhancement of precipitation in the Netherlands has been investigated by Yperlaan (1977), Buishand (1979), Kraijenhoff and Prak (1979), and Kraijenhoff et al. (1981). With some caution it may be concluded from these studies that cities, such as Rotterdam and Amsterdam, do have an effect. These effects are not only present in summer but also in winter (Yperlaan, 1977; Buishand, 1979).

In this section the effects of urbanization and industrialization on precipitation with regard to daily rainfall levels and frequencies of heavy rainfall are investigated using the statistical procedure of Lowry (1977).

2.6.1. Urban effects in the Netherlands

As already stated, mechanical and thermal processes are considered to be the most effective agents in urban precipitation enhancement. In this context, the Rotterdam area must be considered to be the urban/industrial area par excellence in the Netherlands. Even though Amsterdam has a larger population than Rotterdam (CBS, 1980), the gross energy consumption of these cities in 1980 was 30 W/m^2 and

70 W/m² respectively, and incoming solar radiation was estimated to be 109 W/m² (Können, 1983). Not all of the gross energy consumption results in direct heat production, but say about 60%. Neither does all incoming solar radiation result in heat production. Only 50%-65% is converted into net radiation, of which only 25% results in direct heat production: about 18 W/m². Furthermore, both gross energy consumption and incoming solar radiation vary throughout the day and throughout the year.

The high energy consumption in the Rotterdam area is undoubtedly the result of the concentration of industry and to a lesser extent of other activities, such as, commerce and transport. This may be inferred from Table 2.14, which gives the emissions of sulphur dioxide, carbon monoxide and hydrocarbons in the Amsterdam and Rotterdam areas. The emissions of sulphur dioxide give a good indication of the degree of industrialization, and emissions of carbon monoxide of transport activities. Gross energy consumption in the Netherlands for the period 1946-1979 is presented in Figure 2.20. The gross energy consumption is unknown for the period 1932-1946; available data on the production of electricity and gas suggest a very slight increase during this period (CBS, 1979).

Table 2.14. Emissions of pollutants in the Rotterdam and in the Amsterdam area¹

	Sulphur dioxide (10 ³ t/y)	Carbon monoxide (10 ³ t/y)	Hydrocarbons (10 ³ t/y)
Rotterdam (1974)	149	61	50
Amsterdam (1975)	7	38	28

¹ Data: Ministerie van Volksgezondheid en Milieuhygiene, 1978, 1980. The Rotterdam area corresponds to blocks F6, G6, H6, I6, J6, I7, and J7 of the 1978 publication, the Amsterdam area to blocks F4, G4, H4, F5, G5, H5, E6, and G6 of the 1980 publication.

As the urban effects are considered to be greater in summer, it is important that heat production, for example in industry and transport, occurs throughout the year in contrast to heat production for the heating of buildings, which occurs mainly during the winter. Further, the heat produced by petro-chemical industries in and around Rotterdam is very often released from chimneys more than 100 m tall. Indeed, at these petro-chemical complexes, the combined effects of heat production, of its release at considerable heights, and of friction, create an important local circulation pattern over these areas: upward currents above its centres and downward movements in the immediate surroundings (Schmidt and Boer, 1962).

While the Rotterdam area is the most industrialized part of the Netherlands, it is by no means the only urban area in the country. In fact, the presence of several smaller urban industrial centres, the smallness of the country in relation to the scale of the meteorological processes (wind at a velocity of 10 m/s crosses the country in three to eight hours), and the large quantities of pollutants from neighbouring countries (for instance, the Dutch contribution to the mean sulphur dioxide level over the Netherlands is only 30%, see also Figure 2.21, reproduced from KNMI/RIV, 1982), all indicate that most of the Netherlands belongs in varying degree to area 2 of the classification presented in Figure 2.19.

In order to provide information about the rainfall stations in data set D32 which has been used in this section, data on local emissions of pollutants together with the number of inhabitants in the municipality in which the station is located are given in Appendix A.6. The pollutant data have been extracted from publications of the Ministry of Public Health and Environmental Hygiene, which give total emissions over 5 x 5 km grid areas. Here, for each rainfall series the grid area in which the rainfall station is located has been considered.

In the application of Lowry's procedure, the weather type occurring on a given day has been extracted from Hess (1977), and classified according to one of the ten "Grosswettertypen" (Types of

large-scale weather patterns) of Hess and referred to as circulation types.

The grouping of rainfall stations into urban affected and urban unaffected depends upon wind direction. In the classification of the circulation types, 500 mbar level maps have been used to represent the steering of tropospheric disturbances. An investigation into the relationship between prevailing wind direction at De Bilt at ground level and circulation type (Bijvoet and Schmidt, 1958) has shown that for a given circulation type, the pattern of flow remains characteristic at considerable heights. The most frequently occurring wind direction at ground level for each circulation type (Bijvoet and Schmidt, 1958) is given in Table 2.15. Wind direction at ground level for circulation types 4 and 5 is extremely variable. Circulation types 2, 3, 5, 7, 8 and 9 were not analysed statistically because they occurred rather unfrequently, being virtually absent in some years, or for short spells only (Table 2.15). The spell length is important because rainfall is measured in 24-hour intervals ending at 7.55 h UTC, whereas circulation types hold for calendar days.

It is difficult to assign rainfall stations to the three areas, C, Z, and R, in Figure 2.19 mainly because of:

- difficulties in determining the predominant wind direction;
- uncertainties about the regional effect of various urban industrial centres, especially the smaller centres;
- uncertainties about the urban industrial rainfall enhancement in general.

Difficulties in determining the predominant wind direction include the frictional drag exerted by the earth surface. Wind direction in, say, the lowest 0.5 km of the atmosphere deviates from the dominant winds at the 500 mbar level by about 30° in a counter-clockwise direction in the northern hemisphere (McIntosh and Thom, 1978). For example, if for a certain circulation type the dominant wind direction at the 500 mbar level is west, the wind direction measured at ground level will tend to be west-southwest. Storms tend to move in correspondence with wind at the 700 mbar level,

instead of with that at the 500 mbar level or at ground level. Further, there may be local circulations, which are quite different to the large-scale pattern.

Table 2.15. Most frequently occurring wind direction at ground level at De Bilt measured at 13.40 GMT, period 1881-1955 (Bijvoet and Schmidt, 1958)

Circulation type	Wind direction	Mean frequency (# year ⁻¹)		Mean spell length (days)	
		Summer	Winter	Summer	Winter
1. West (Zonal)	S-SW	40.1	54.3	5.6	6.0
2. South West	S-SW NW-W ¹ ¹	6.5	13.3	4.0	4.0
3. North West		13.3	14.1	4.2	3.7
4. High Middle Europe		24.3	33.9	4.1	4.1
5. Low Middle Europe		3.4	5.3	3.3	3.6
6. North	NW-NE NNE (Meridional) E-NE E-SE SE-SW	24.4	33.9	4.5	4.2
7. North East		10.8	6.8	4.0	2.8
8. East		12.3	18.4	4.5	4.9
9. South East		2.4	11.3	3.3	4.2
10. South		13.9	19.3	3.8	3.9
Unknown		1.6	1.6	1.2	1.0

¹ Highly variable wind directions.

In full recognition of the difficulties, an attempt has been made to identify for each circulation type the stations or groups of stations with and without a potential urban effect. For these stations, differences between mean daily rainfall for the period 1956-1979 and 1932-1955 for the given circulation type are presented in Table 2.16. In this table, stations have been classified as urban affected or urban unaffected, using information about the predominant wind direction, once the circulation type is known.

Table 2.16. Differences (0.1 mm) in mean daily rainfall, given circulation type and season, between the period 1956-1979 and 1932-1955, according to Equation 2.51

Rainfall station	Circulation types							
	1		10		4		6	
	Summer	Winter	Winter	Summer	Winter	Summer	Winter	
	Urban affected				Urban unaffected			
Delft, Bergschenhoek,	+2.6	+5.9 ^{°°}	-2.8	-1.4	+0.6	+3.0	+1.9	
Boskoop, Leiden								
	Urban unaffected							
Den Helder, West	+0.2	+3.6 ^{°°}	-4.2 ^{°°}	-1.3	-0.3	+0.1	+0.8	
Terschelling, Gronin-								
gen, Ter Apel, Dwin-								
gelo, Heerde, Dene-								
kamp, Winterswijk,								
Arnhem, Vlissingen								
	Urban affected							
Schellingwoude	+1.2	+5.1 ^{°°}	+2.6	-1.7	-0.3	+1.6	+2.1	
Amsterdam	+1.8	+5.4 ^{°°}	+0.3	-2.7	-0.4	+1.8	+0.5	
IJsselmonde	+5.7	+6.1 ^{°°}	-1.9	-2.4	+0.2	+3.9	+3.3	

°° Indicates values inside the critical region for $\alpha = 0.05$; there are no differences significant at the 5-10% level.

The differences $\delta_i^!(0, t)$ in Table 2.16 have been calculated as

$$\delta_i^!(0, t) = \bar{x}_{i,2}^! - \bar{x}_{i,1}^!, \quad (2.51)$$

where

$$\bar{x}_{i,1}^! = \frac{1}{24} \sum_{t=1}^{24} \bar{x}_{itu}$$

$$\bar{x}_{i,2}^! = \frac{1}{24} \sum_{t=25}^{48} \bar{x}_{itu}$$

Thus, $\bar{x}_{i,2}^!$ is the arithmetic mean of the observations \bar{x}_{itu} for period II (1956-1979), while $\bar{x}_{i,1}^!$ is the arithmetic mean for

period 1. Denote the standard deviation of the observations \bar{x}_{itu} by s_i , then realizations of a test statistic T can be calculated as

$$T = \frac{\bar{x}_{i,2} - \bar{x}_{i,1}}{\sqrt{(\frac{1}{24} + \frac{1}{24})s_i}}. \quad (2.52)$$

For samples from a normal distribution and for $H_0 : \mu_1 - \mu_2 = 0$

$$\frac{T}{\sqrt{H_0}} \sim t_{48-2}. \quad (2.53)$$

For the normal distribution to be valid, the observations \bar{x}_{itu} have been transformed according to Equation 2.9.

Table 2.16 should be read in conjunction with Figure 2.22A-J, which shows differences in mean daily rainfall between the period 1956-1979 and 1932-1955 for given circulation type and season for all rainfall stations. At this point a remark on the computations has to be made. A comparison of Table 2.16 and, for example, Figure 2.22A, shows that there are small divergencies, because the differences $\delta_i(t,0)$ in Figure 2.22A-J are differences of weighted averages

$$\delta_i(t,0) = \bar{x}_{i,2} - \bar{x}_{i,1}, \quad (2.54)$$

where

$$\bar{x}_{i,1} = \frac{1}{N_1} \sum_{t=1}^{24} n_{it} \bar{x}_{itu} \quad (2.55)$$

$$N_1 = \sum_{t=1}^{24} n_{it}$$

n_{it} : frequency of occurrence of circulation type i in year t ,

and the weighted means $\bar{x}_{i,2}$ are defined analogously. The statistical significance of the differences $\delta_i(t,0)$ cannot be tested. As an estimate of $\delta_i(t,0)$ in Equation 2.50, however, the estimate according to Equation 2.54 is preferable to the estimate according

to Equation 2.51. Figure 2.23 presents the differences in seasonal rainfall for the two periods considered. In accordance with the conclusions of Section 2.3, total summer and winter rainfall is higher for the more recent period for most rainfall stations in data set D32.

Although the differences in Figure 2.22 should be interpreted with caution, some observations can be made. Firstly, there are large differences between some stations classified as urban unaffected. This may indicate either local within-circulation type climatic changes, or effects other than industrialization and urbanization. Any conclusions, however, should also be based on the station history of all selected rainfall records.

Furthermore, Table 2.16 and Figure 2.22 suggest that there is an urban effect for circulation types 1, 6 and 10; but for circulation type 4, the results are not in accordance with an urban effect for summer and inconclusive for winter. Figure 2.22 shows that results for the remaining circulation types are somewhat inconclusive. The results for circulation type 5 and 10 are of special relevance to the present study, because on summer days with these circulation types, relatively many heavy daily rainfalls occurred.

In summary, for all circulation types, and including days with the circulation type not specified, it can be seen from Figure 2.23 that for the entire Randstad area, there is an increase in total summer rainfall, with maximum increases for rainfall stations near Amsterdam and Rotterdam, and in Leiden. It is somewhat doubtful whether the increase for the Leiden rainfall station can be attributed to industrialization and urbanization only. There are also high rainfall increases at the rainfall stations Roermond and Axel. For winter, the situation is more or less the same, with increases in total winter rainfall for the Randstad area exceeding those for other parts of the Netherlands. Again, there are several maxima within the Randstad, for which it is doubtful whether they can be attributed to industrialization and urbanization only.

Figure 2.23 is useful for assessing the relative contribution of each circulation type to seasonal rainfall. The differences, Δ , presented in this figure, can be calculated as

$$\Delta = \sum_i \{ \delta_i(t,0) \min(n_{i,1}, n_{i,2}) + (n_{i,2} - n_{i,1}) \bar{x}_{i,k} \}, \quad (2.56)$$

where

- $n_{i,1}$: mean annual frequency of circulation type i in period I
- $n_{i,2}$: mean annual frequency of circulation type i in period II
- $\bar{x}_{i,k}$: the mean of \bar{x}_{itu} (as in Equation 2.55 for period k , where k refers to the period with maximum N_j ($j=1,2$) in Equation 2.55).

The first term of the right-hand side of Equation 2.56 vanishes when either $n_{i,2}$ or $n_{i,1}$ is equal to zero, and the second term vanishes when $n_{i,2}$ is equal to $n_{i,1}$. Equation 2.56 shows that comparing the differences Δ for a rural and an urban station is not particularly suitable for assessing urban effects on rainfall, because Δ is dependent on \bar{x}_{itu} through $\bar{x}_{i,k}$. Recognition of this dependence must have been Lowry's starting point.

An indication whether urban effects extend to rainfall which, if urban unaffected, would be rather moderate, has been obtained by registering the numbers of rainfalls in excess of 15 mm at each station for both periods, pre-urban (1932-1955) and urban (1956-1979). Their differences, which are presented in Table 2.17, indicate that for most circulation types, there are no consistent inter-station differences, except for circulation types 1, 6, 8 (in summer), and 10 where there are indications of an urban effect.

For circulation type 4 (in summer) and 9 the results are not in accordance with the hypothesis of an urban effect. Furthermore, it can be seen from the last two columns of this table that during the period 1956-1979 stations in urbanized regions increased their effectivity in realizing an already potential heavy daily rainfall, in relation to stations in other regions. This is also concluded by Kraijenhoff et al. (1981) for daily summer rainfalls in excess of 30 mm.

Table 2.17. Differences in numbers of days with measured rainfall ≥ 15 mm between the periods 1956-1979 and 1932-1955

Rainfall station	Circulation type																							
	1		2		3		4		5		6		7		8		9		10		Sum			
	S ¹	W ²	S	W	S	W	S	W	S	W	S	W	S	W	S	W	S	W	S	W	S	W		
Rotterdam and Amsterdam area:																								
Schellingwoude	+6	+8	+12	+3	-3	-6	-2	-1	-5	0	0	0	+2	-1	+7	+2	-3	-1	+13	+9	+27	+13		
Amsterdam	+4	+16	+12	+6	-5	-2	-4	-3	-5	+2	-1	+2	+4	-3	+5	+4	-3	-1	+13	+13	+20	+34		
IJsselmonde	+22	+6	+11	+9	-2	+1	-6	-2	-6	+1	+2	+8	-1	-1	+5	+1	-1	-1	+9	+7	+33	+29		
Randstad area:																								
Cruquius	-3	+9	+12	+4	-9	0	-4	0	-3	0	-4	+1	-1	-2	+7	0	-1	-2	+5	+9	-1	+19		
Sassenheim	-1	-2	+5	+4	-5	-5	-6	-1	-6	+2	-3	0	0	-3	+6	+2	-3	-2	+1	+8	-12	+3		
Hoofddorp	0	+10	+10	+3	-5	-3	-5	-2	-3	-2	-1	+2	0	-1	+6	-1	-1	-2	+6	+11	+7	+15		
Oude Wetering	+2	-1	+8	+4	-6	-6	-4	-3	-1	-4	+3	+3	-2	-2	+7	+2	-1	-1	+8	+5	+12	+10		
Lisse	+7	+14	+8	+5	-3	-4	-4	-1	-4	+3	+1	+4	-2	-1	+6	+1	-3	-3	+7	+7	+14	+25		
Boskoop	+2	+7	+9	+6	-5	-3	-7	+1	-5	+4	+3	+1	-5	-2	+5	-3	-3	-2	+6	+2	0	+11		
Delft	+4	+7	+8	+8	-10	-2	-4	-1	-11	-1	+2	-1	-1	0	+8	+3	-4	-4	+10	+6	+2	+15		
Bergschenhoek	+14	+6	+9	+2	-8	+1	-2	0	-6	0	0	+2	0	-1	+10	0	-3	-1	+10	+5	+24	+14		
Leiden	+13	+10	+10	+4	-4	-1	-2	0	-5	+5	+2	+2	+1	-1	+11	+2	-1	-1	+3	+4	+28	+24		
Zegveld	+9	+6	+6	+7	-2	-2	-12	-1	-6	+2	-4	+9	+3	-1	+13	0	-1	0	+7	+3	+13	+23		
Other parts of the Netherlands:																								
Den Helder	-10	+9	+7	+3	-2	-1	+3	+1	-2	-1	-2	-2	0	-1	+4	0	0	-1	+3	+4	+1	+11		
West Terschelling	-6	-15	+12	+6	-3	0	+4	0	-2	0	-2	-1	0	0	+7	-1	0	0	-2	-4	+1	-14		
Groningen	-14	+3	+10	+3	0	+2	-2	-3	-6	-1	-9	+1	+2	0	+7	0	-1	0	+6	-2	-6	+2		
Ter Apel	-12	-3	+7	+6	-6	-2	-3	-4	-4	-1	-4	+4	-3	-1	+4	0	0	-1	-1	0	-22	-2		
Dwingelo	-12	-4	+9	+7	-3	+1	-5	-2	-4	0	0	0	-3	-2	+4	-1	-1	0	+3	-3	-12	-4		
Heerde	-13	-4	+8	+9	-7	-5	-1	-3	-5	-4	0	+3	0	-2	+3	+3	0	-2	+4	+1	-11	-4		
Denekamp	+7	-1	+7	+6	-6	-6	-7	-4	-1	0	5	+1	-1	0	0	0	-1	-1	+5	0	+8	-5		
Arnhem	+10	+5	+8	+10	-6	0	-1	-5	-3	-3	+3	+2	+1	-3	+5	+1	-3	-2	+10	-2	+18	+3		
Winterswijk	+2	0	+7	+7	-5	-4	-3	-4	-1	-3	+1	+4	+3	-1	+3	-1	-1	0	+13	0	+19	-2		
Castricum	-15	+9	+8	+5	-9	-2	-2	+1	-2	-1	-6	+1	-3	-1	+7	+4	0	0	+5	-22	+21			
Zandvoort	-22	+6	+7	+4	-4	-3	-7	0	-2	+1	-13	+6	+2	-1	+4	+2	-4	-3	+3	+8	-36	+20		
Hoorn	-14	+2	+7	+8	-2	+1	-4	-1	0	0	-4	+5	+1	-1	+1	0	-2	-1	+5	+10	-12	+23		
Mookhoek	+16	+5	+12	+11	-4	+1	-1	-2	-4	0	+7	+10	+2	-1	+3	-2	-1	0	+5	+3	+35	+25		
Oostvoorne	+2	+4	+9	+9	-9	-1	-4	-2	-13	-4	0	-2	-1	-1	+2	+4	-4	+1	+8	+3	-10	+11		
Vlissingen	+2	+4	+11	+7	-7	-4	-8	-2	-9	-3	+3	0	-2	-1	+9	+1	-1	0	+9	+4	+7	0		
Kerkwerve	-6	+1	+10	+5	-2	-4	-3	-3	-11	-2	-3	+1	-1	0	+10	+2	-2	-2	+3	+5	-5	+3		
Axel	0	-1	+9	+3	-2	+1	+1	-4	-5	-3	-4	+6	-4	0	+12	+1	-3	-3	+4	+6	+8	+12		
Oudenbosch	+6	+12	+8	+2	-2	-2	-2	-3	-2	-3	0	+2	+1	-1	+8	0	-1	-2	-2	+7	+14	+12		
Roermond	+15	-12	+7	+4	-2	-2	0	-1	-4	-2	-1	0	-3	0	+6	-2	+2	-1	+7	+3	+27	-13		
Mean frequency	41.7	46.8	3.0	5.1	9.3	6.7	8.4	3.7	7.2	3.2	14.0	7.3	3.4	1.2	4.1	1.6	2.4	1.4	13.3	6.1				
1932-1955	42.2	50.2	11.8	10.7	4.7	4.7	5.1	2.0	2.6	2.8	12.9	9.8	3.0	0.0	10.0	2.4	0.8	0.2	18.9	10.4				
1956-1979																								

1 Summer.

2 Winter.

In order to verify whether urban effects increase with increasing rainfall intensity, the following procedure could be followed. Register daily rainfall at each station for those days only on which at least at one station rainfall exceeded 15 mm. Then the mean of these daily rainfalls should be compared for the two periods considered, the circulation type and the season taken into account, and the difference between the two means obtained. Especially for those circulation types not occurring frequently, this method of sampling leads to results which are very much affected by chance. This can also be inferred from the last two rows in Table 2.17, which give the number of occurrences during both periods of days with a certain circulation type and rainfall in excess of 15 mm, averaged over all stations in data set D32.

Finally, in order to investigate whether urban effects result in a shift of the probability mass towards the right tail of the distribution, considered as the interval $[15 \text{ mm}, \infty)$, each rainfall series of data set D140 has been analysed in the following way. The interval $[15 \text{ mm}, \infty)$ has been divided into two subintervals, each with equal probability mass when averaged over the complete data set. The two subintervals were found to be $[15 \text{ mm}, 19.7 \text{ mm})$ and $[19.7 \text{ mm}, \infty)$ for the summer, and $[15 \text{ mm}, 18.4 \text{ mm})$ and $[18.4 \text{ mm}, \infty)$ for the winter. The period of record of data set D140, 1951-1979, roughly coincides with the industrialized period 1956-1979, analysed above for data set D32. A weighted difference of the frequencies in both subintervals has been calculated according to

$$\underline{z}_i = \frac{n_{1,i} - n_{2,i}}{\sqrt{(n_{1,i} + n_{2,i})}}, \quad i = 1, \dots, 140 \quad (2.57)$$

where

$\underline{n}_{1,i}$: frequency in subinterval $[15 \text{ mm}, 19.7 \text{ mm})$ or $[15 \text{ mm}, 18.4 \text{ mm})$ for station i

$\underline{n}_{2,i}$: frequency in subinterval $[19.7 \text{ mm}, \infty)$ or $[18.4 \text{ mm}, \infty)$ for station i .

The choice of subintervals gives approximately

$$\underline{z}_i \overset{H_0}{\sim} N(0,1), \quad (2.58)$$

where H_0 states that for each rainfall series, the probability mass is equally distributed over the two subintervals ("expectation of all \underline{z}_i zero").

The null hypothesis has been tested by the statistic \underline{T}_1 from Equation 2.41, where the covariance matrix $C=(c_{i,j})$ has been estimated as $c_{i,j}=\exp(-h/\alpha_2)$, according to Equation 2.45. Also, the statistics \underline{T}_2 in Equation 2.42, and \underline{T}_3 in Equation 2.44 have been calculated, after partitioning the country into urban affected and urban unaffected regions (partition (vi) in Appendix A.5; see also, Figure 2.24). For the summer, the tests indicated that the partition reflected the regional pattern of the \underline{z}_i (\underline{T}_1 and \underline{T}_2 not significant, \underline{T}_3 significant at the 5% level). Thus in summer, urban effects increase with rainfall depth (see also Kraijenhoff et al. 1981). For the winter, however, the tests did not yield a positive result, although the level of \underline{z}_i was slightly lower in the affected regions than in the other parts of the Netherlands, indicating a shift of the probability mass towards the right tail of the distribution also for the winter. Figure 2.25 shows the distribution of the $\underline{n}_{1,i}$, $\underline{n}_{2,i}$ and \underline{z}_i in Equation 2.57 over the Netherlands, for both the summer and the winter.

Thus in conclusion, it can be stated that, when assessing the effects of urbanization and industrialization on precipitation, comparisons have to be made of differences between mean rainfall over two periods: an urbanized and a pre-urbanized period. To avoid biased estimates of the differences, caused by changes in frequency of occurrence of large-scale weather types over the two periods, the data should be stratified according to weather type (Lowry, 1977). On the other hand, evaluating these time differences in mean rainfall at one site only could lead to erroneous conclusions, for example, because of all types of changes in measurement practices, and also because of within-circulation type changes, processes on a local scale other than urbanization and industrialization

affecting rainfall, and sample effects due to rainfall variability in time and space. In view of Equation 2.56, however, spatial analysis of these differences should be carried out with caution.

Thus with regard to statistical evidence for the effect of urbanization and industrialization on rainfall in the Randstad area, the following can be concluded:

- Although the results in the present study are sometimes inconclusive or even contrary to the hypothesis of an urban effect on rainfall, for the circulation types 1, 6, 10, and 8 (in summer only) there are indications of an urban effect. This supports the possibility of an urban effect on rainfall, already put forward by Yperlaan (1977), Buishand (1979), Kraijenhoff and Prak (1979) and Kraijenhoff et al. (1981).
- Urban effects are not only restricted to a few large rainstorms (Table 2.17). For the summer, urban effects seem to increase with rainfall depth (Figure 2.25C).
- A quantitative estimation of the urban effect on rainfall is given in Huff and Changnon (1973). In the Netherlands, this should be undertaken by using the statistical procedure suggested by Lowry (1977). This would require data over a sufficiently long period from groups of stations, preferably located in and near Rotterdam and to the north-east of Rotterdam, complemented with data on the local wind field. An additional complication to such an estimation is the effect of changes in measurement practices (Buishand, 1977a).

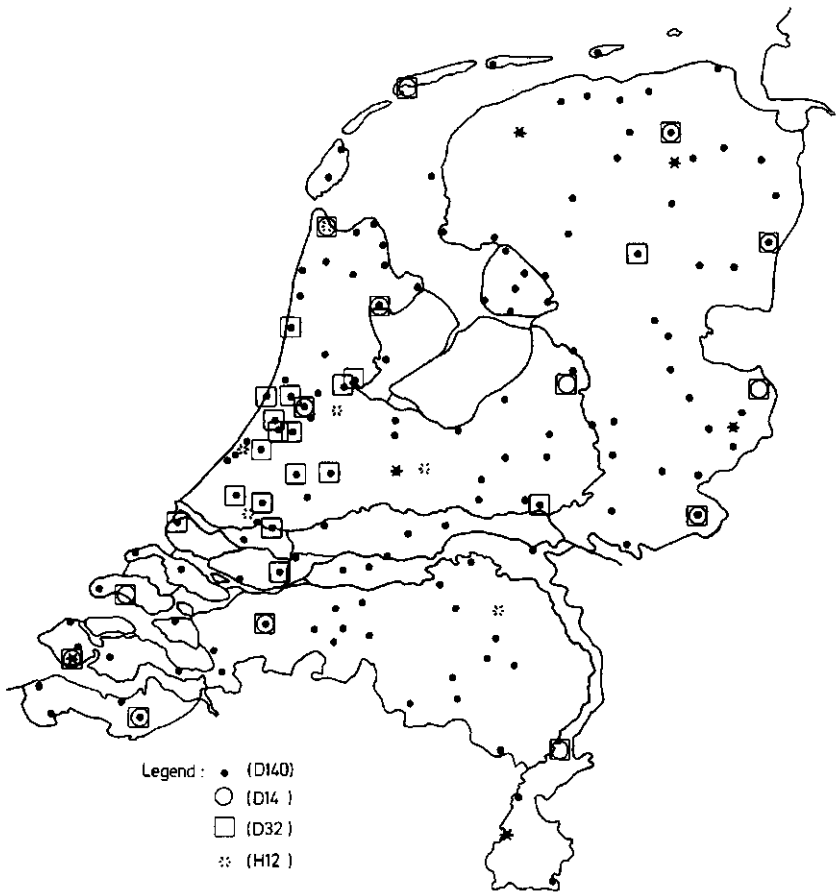


Fig. 2.1. Geographical location of rainfall stations considered in Chapter 2.

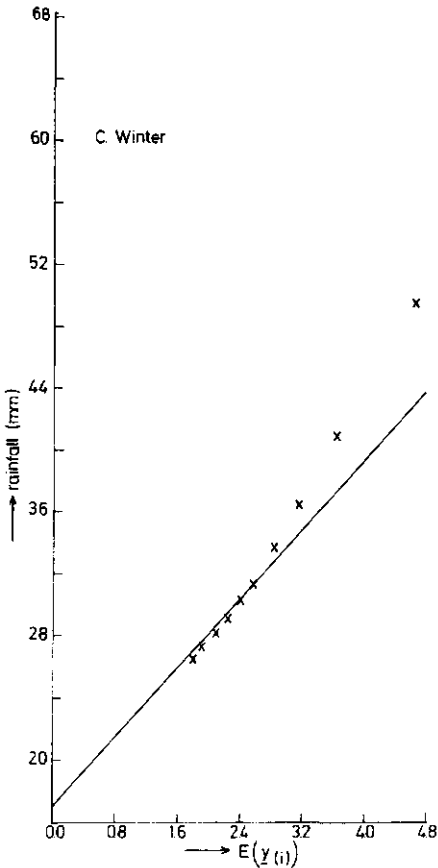
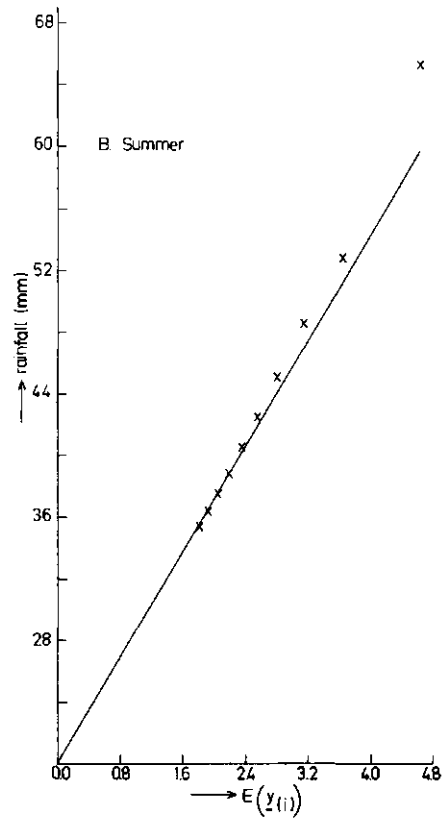
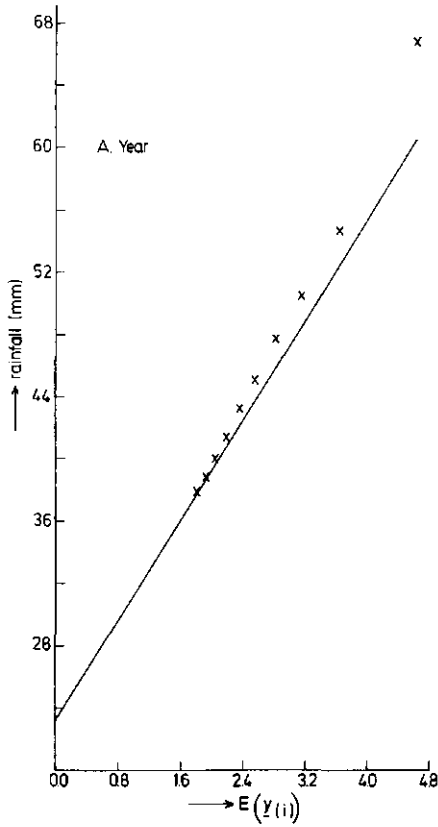


Fig. 2.2. Ten highest peaks (out of 58) of average POT series of daily rainfall and fitted exponential pdfs, for the complete year (A), for the summer (B) and the winter (C) with an average of two exceedances each season or year.
Plotting position $E(Y_{(i)}) = \sum_{j=1}^i (n+1-j)^{-1}$

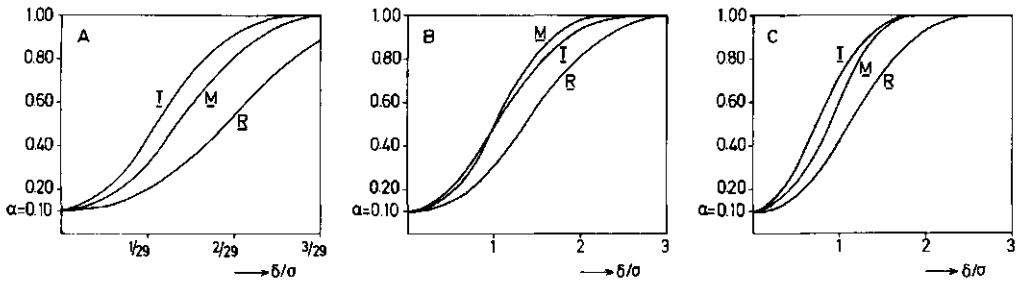


Fig. 2.3. Power curves of the test statistics for alternatives H_{1a} (A) and H_{1b} ($m=7:B$; $m=14:C$).

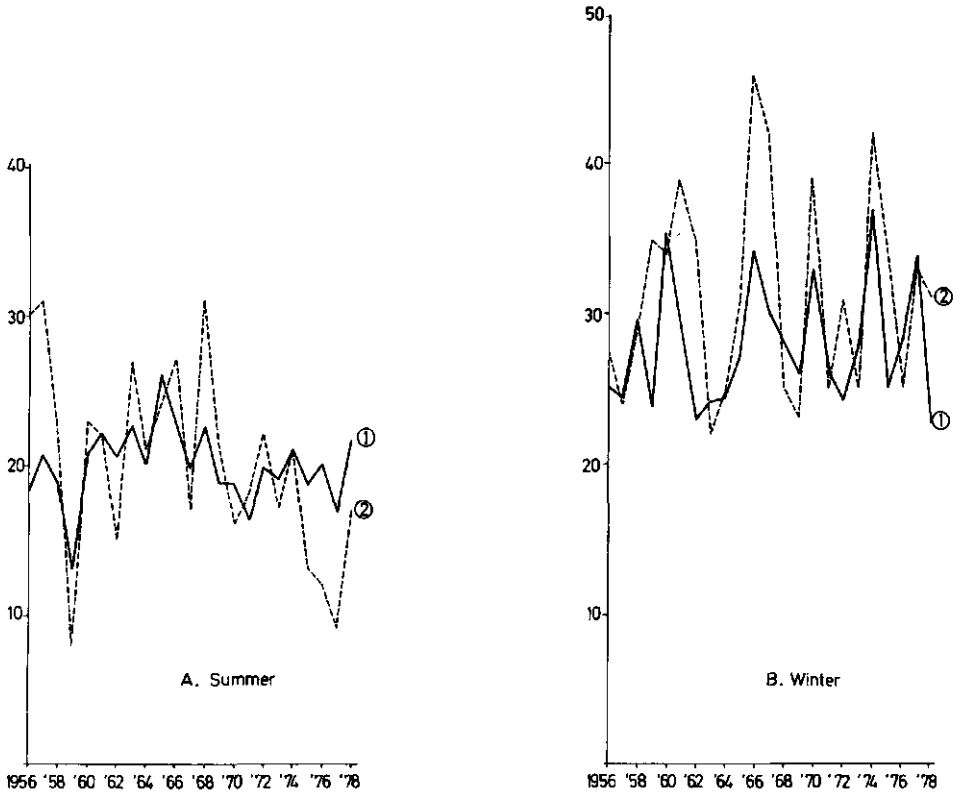


Fig. 2.4. Expected annual number of days with rainfall in excess of 5 mm ① and the actual number ②. Rainfall station: Den Helder (1956 - 1972) / De Kooy (1973 - 1978).

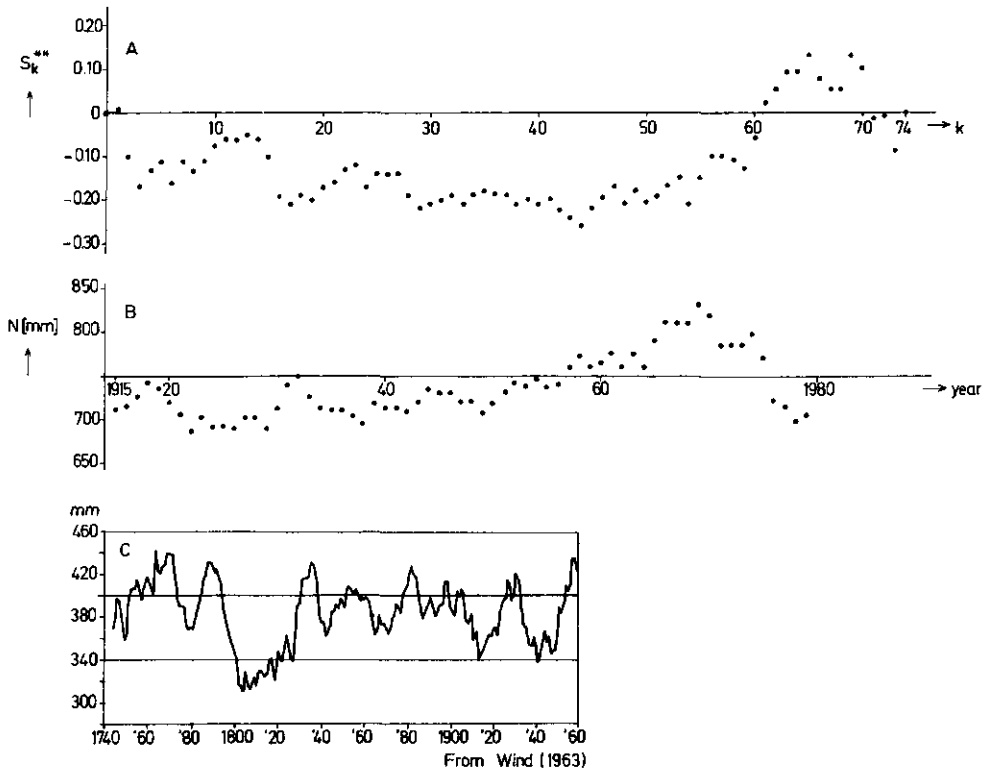
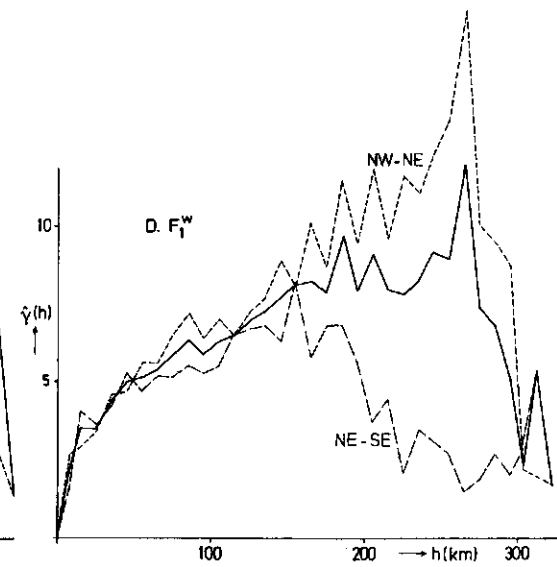
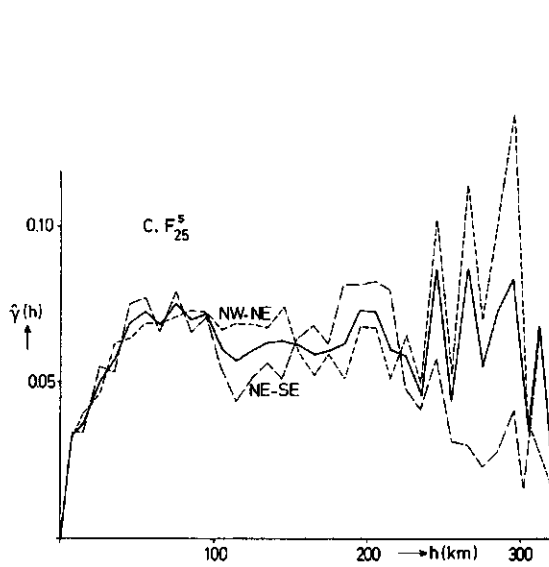
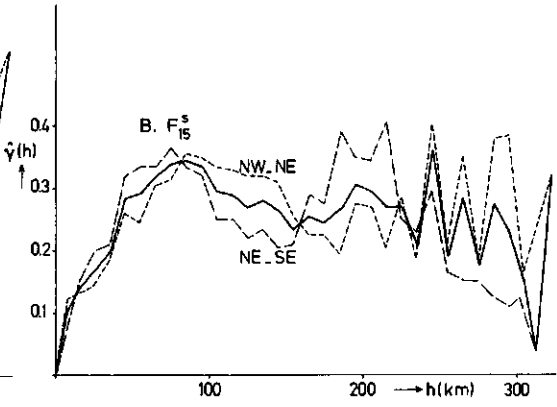
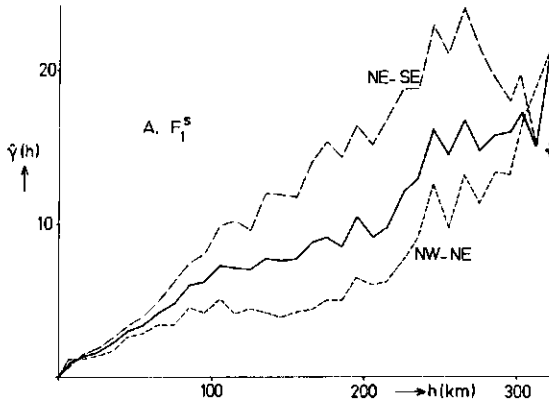


Fig. 2.5. Weighted rescaled adjusted partial sums S_k^{**} for annual rainfall (A), and 10-year moving averages of annual rainfall (B) (data set D 14); Figure C shows 10-year moving averages of summer rainfall for 1734-1960, and is reproduced from Wind (1963).



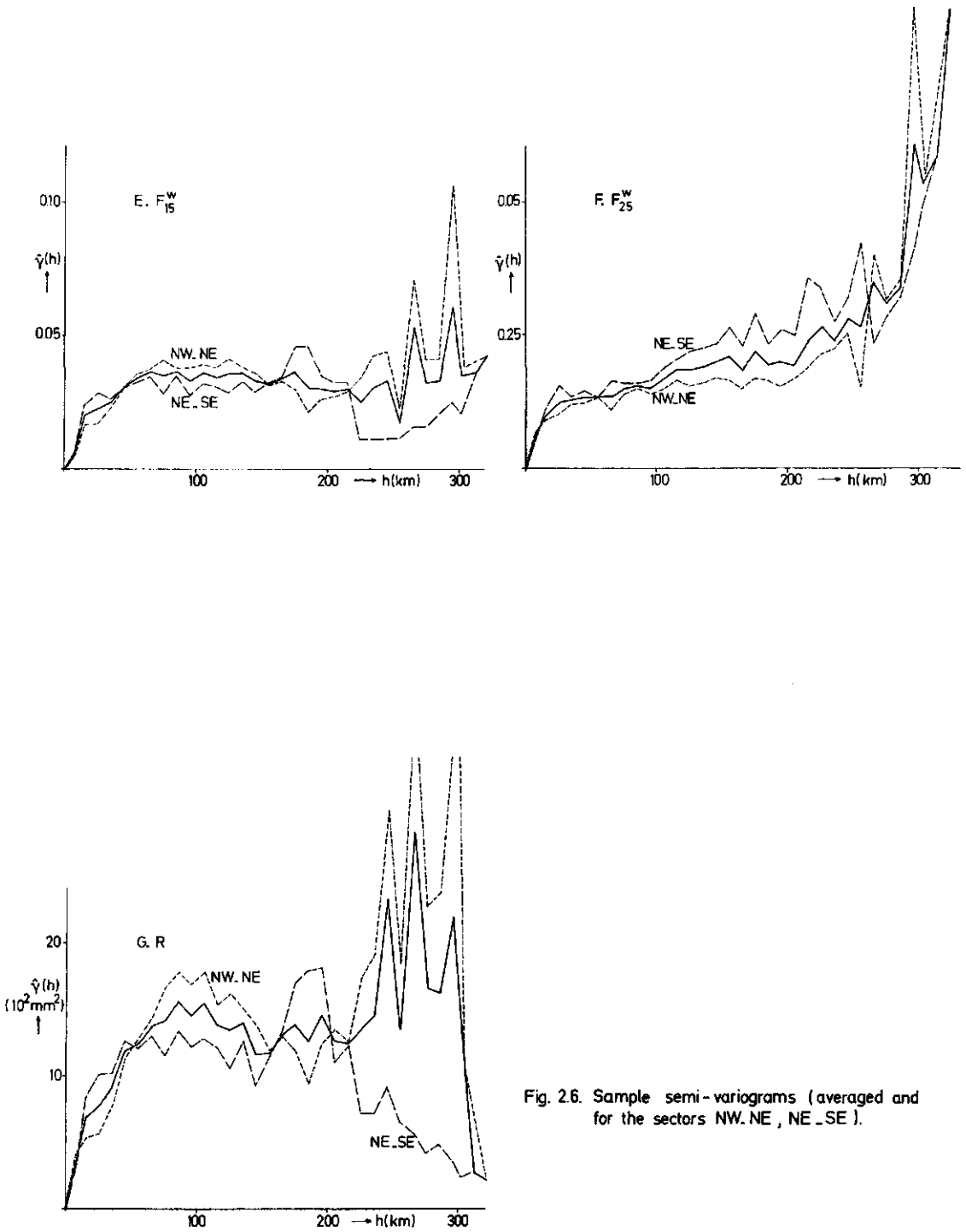
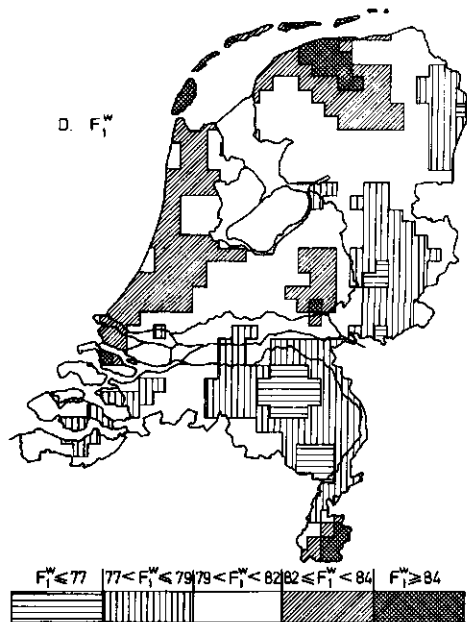
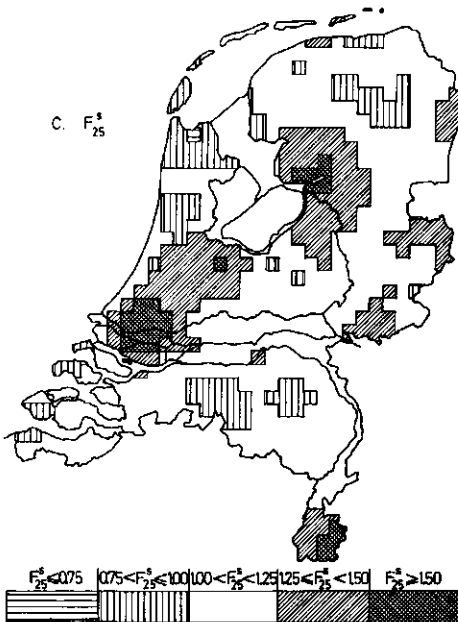
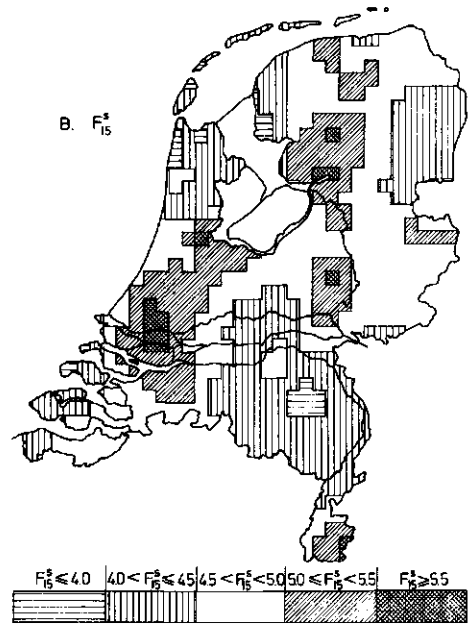
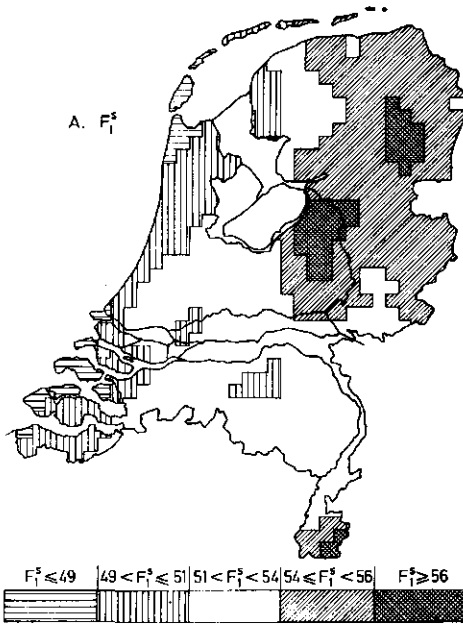


Fig. 2.6. Sample semi-variograms (averaged and for the sectors NW.NE, NE.SE).



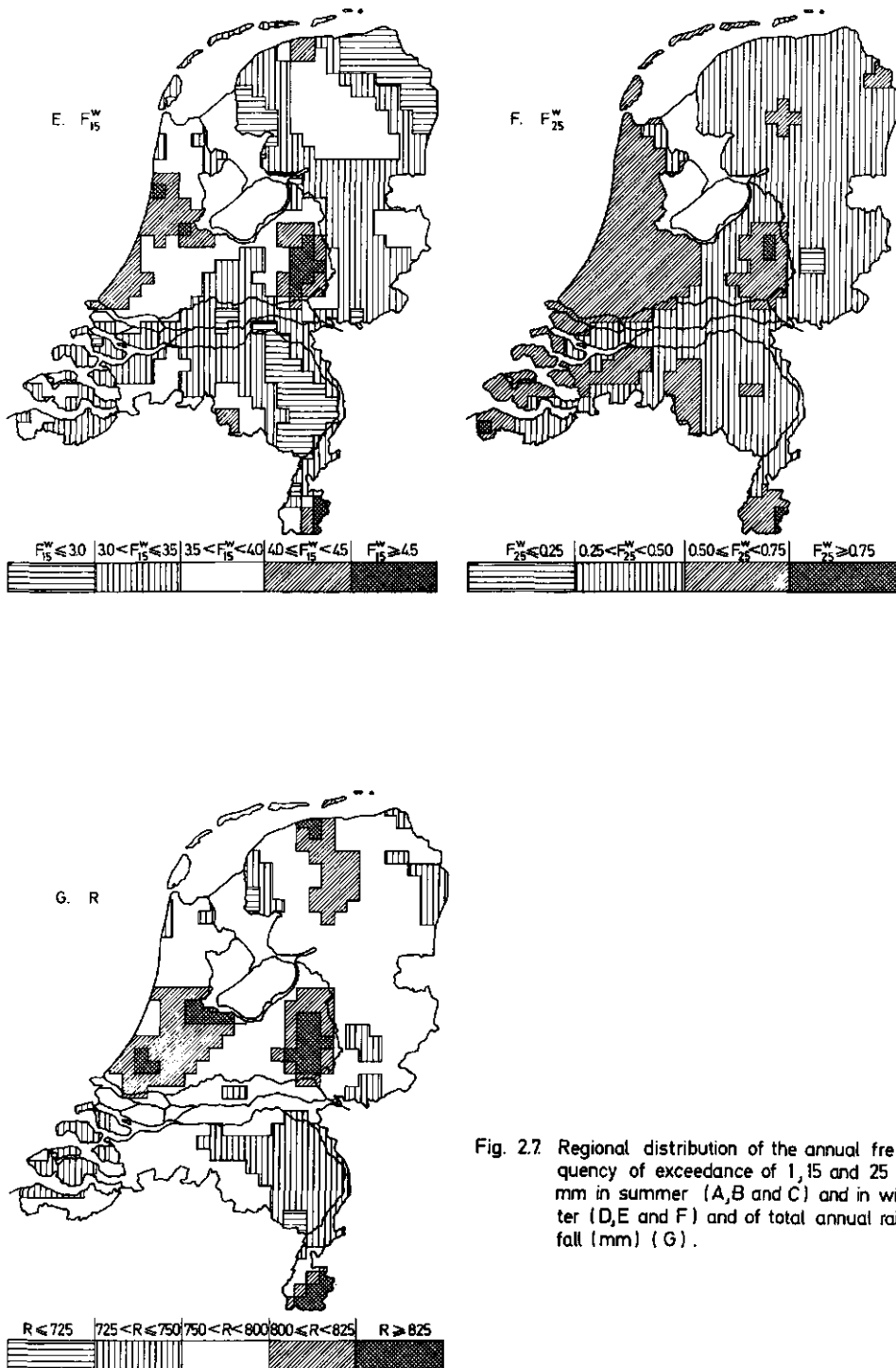
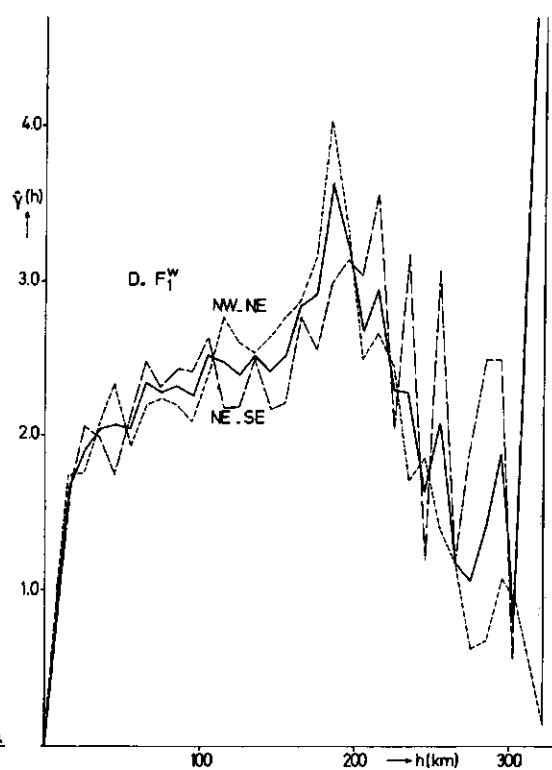
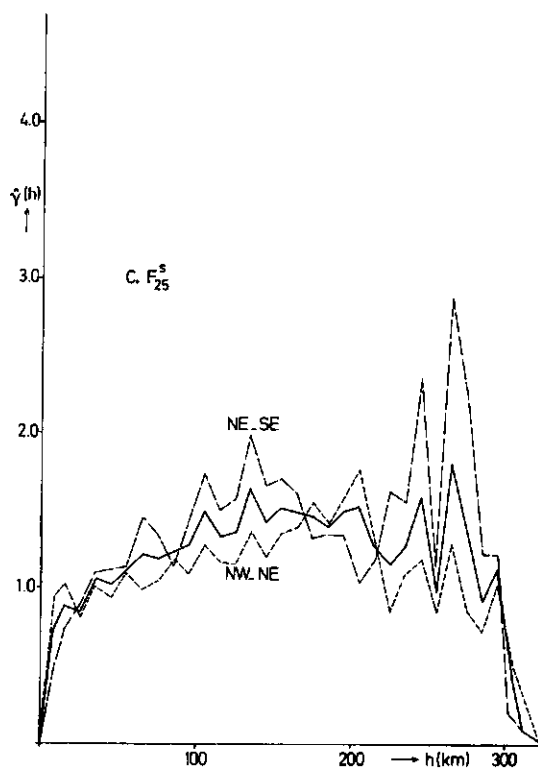
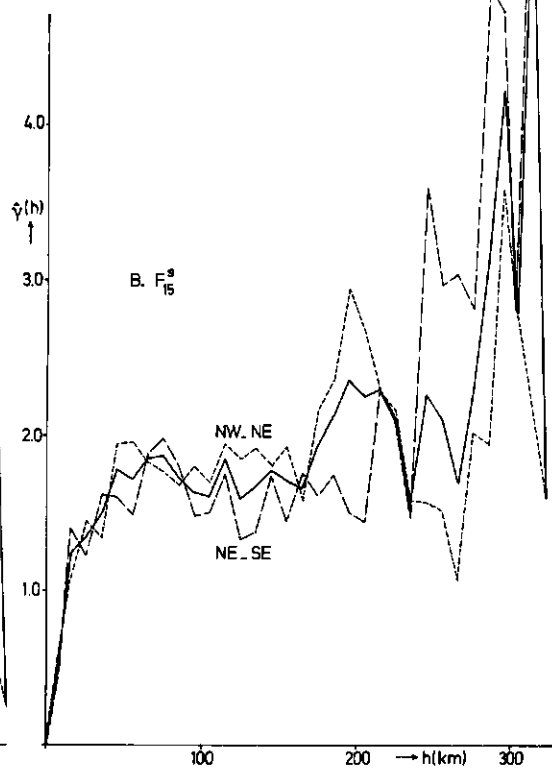
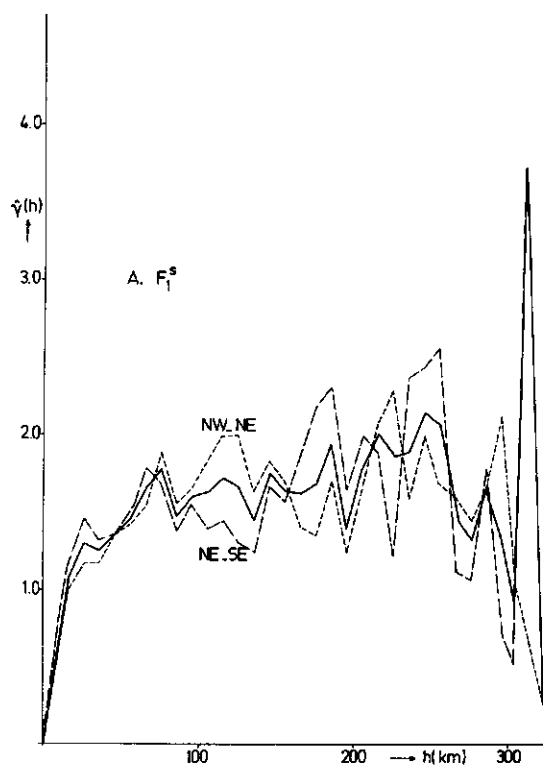


Fig. 2.7 Regional distribution of the annual frequency of exceedance of 1, 15 and 25 mm in summer (A, B and C) and in winter (D, E and F) and of total annual rainfall (mm) (G).



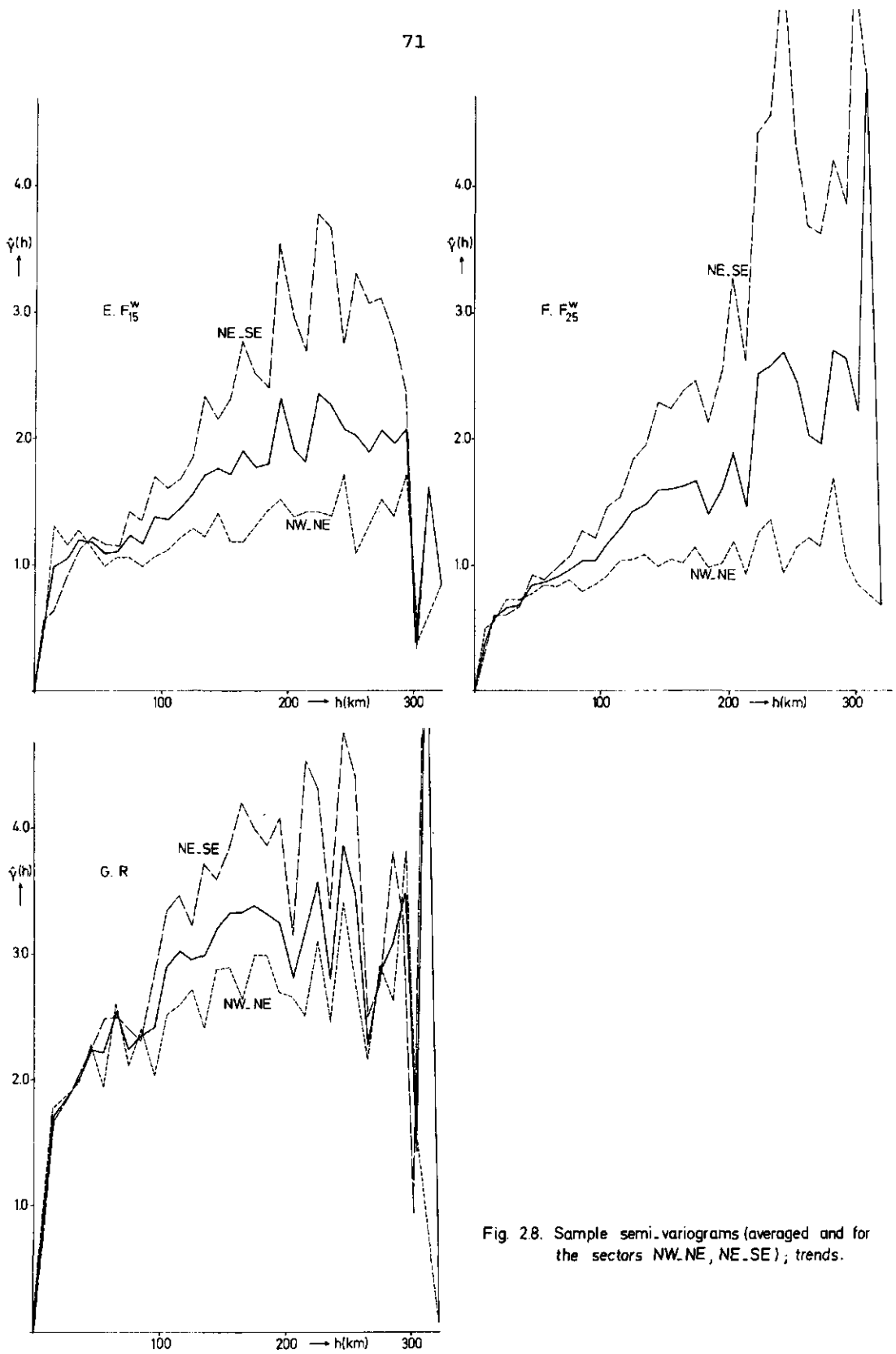
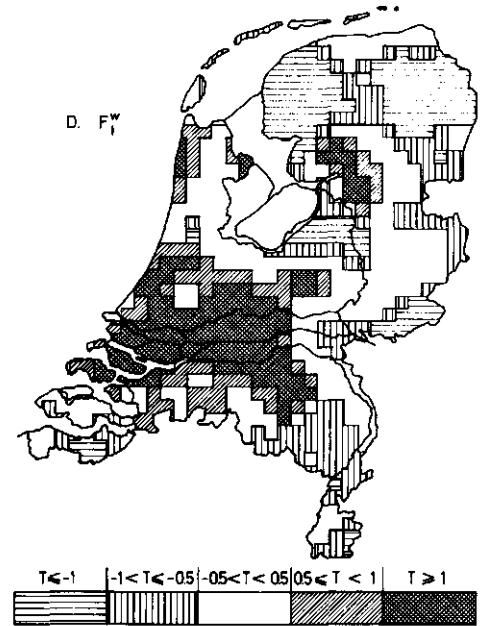
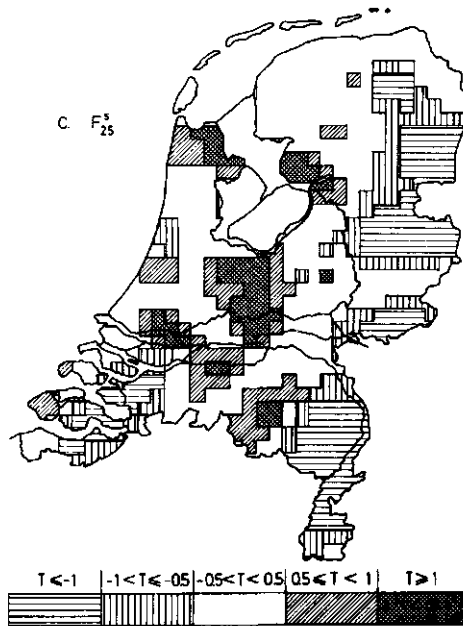
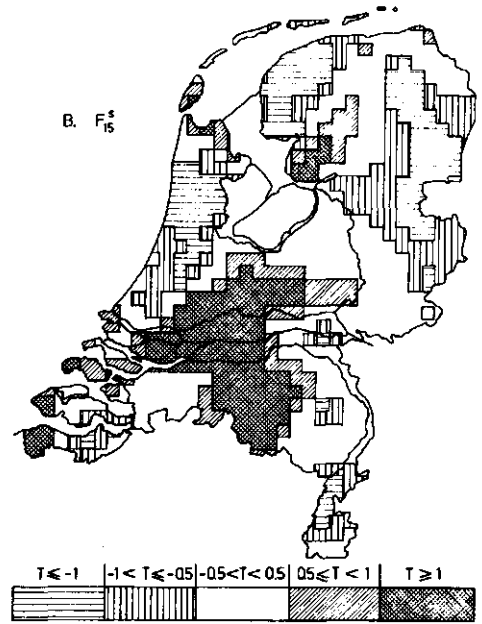
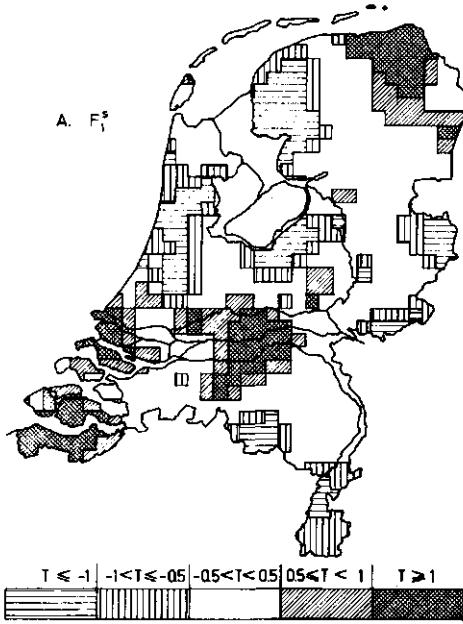


Fig. 28. Sample semi-variograms (averaged and for the sectors NW.NE, NE.SE); trends.



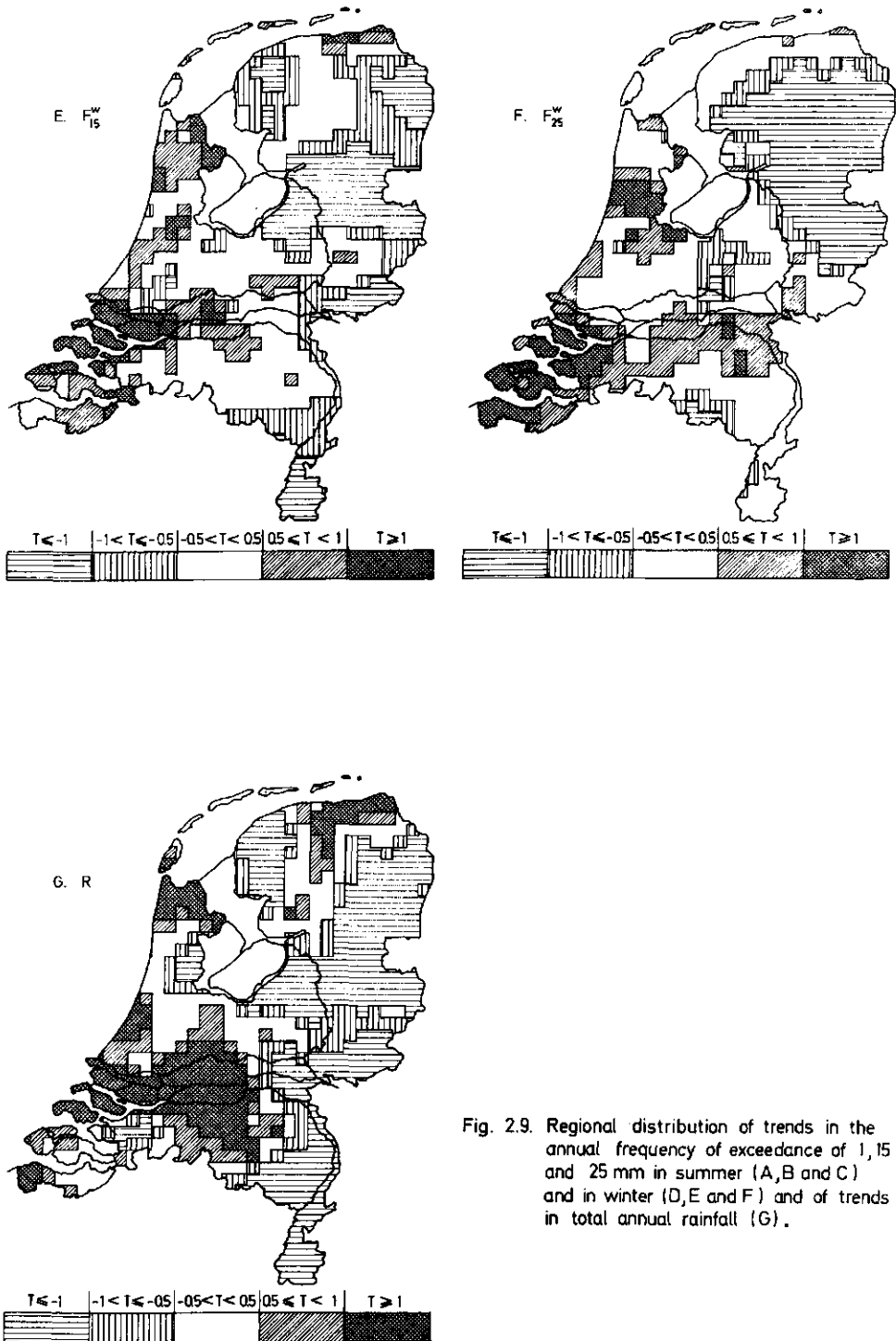


Fig. 2.9. Regional distribution of trends in the annual frequency of exceedance of 1, 15 and 25 mm in summer (A, B and C) and in winter (D, E and F) and of trends in total annual rainfall (G).

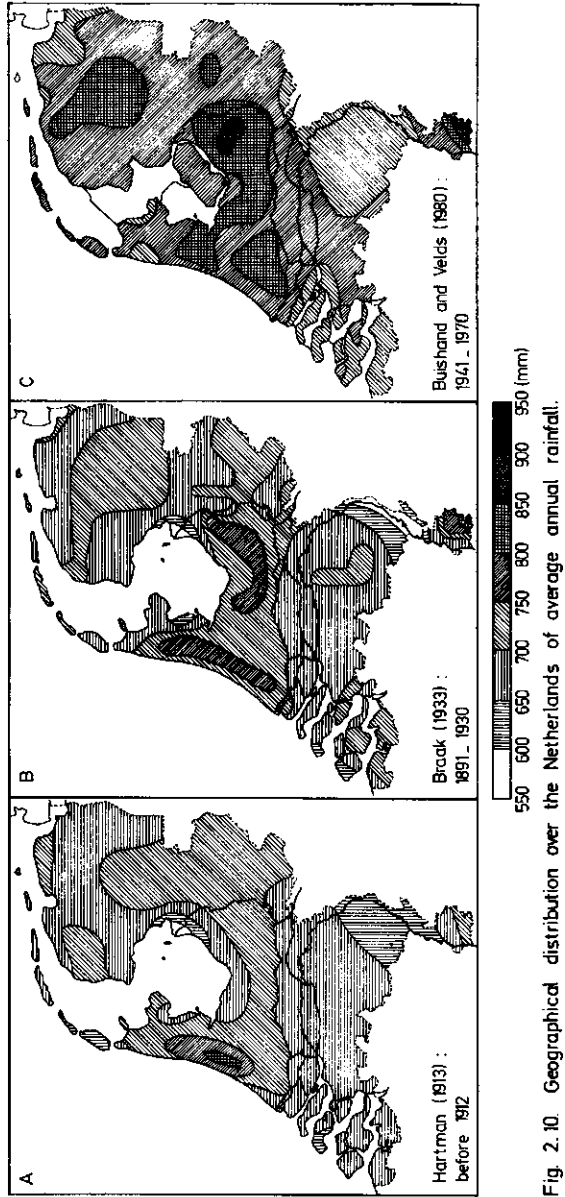


Fig. 2.10. Geographical distribution over the Netherlands of average annual rainfall.



Fig. 2.11. Partitions of the Netherlands. Figure A presents a partition based on distance from the coast and on north-south differences. Figure B is based on the influence of frictional effects and topography. Figure C includes the effects of urbanization, as reported in Kraijenhoff and Prak (1979). Figure D is based on average annual rainfall (in this figure "1" denotes a wet region, and "2" a dry region).



Fig. 2.12. A partition of the Netherlands with regard to trends in frequency of heavy summer rainfall :
 (1) positive trends
 (2) negative trends
 (3) no trend.

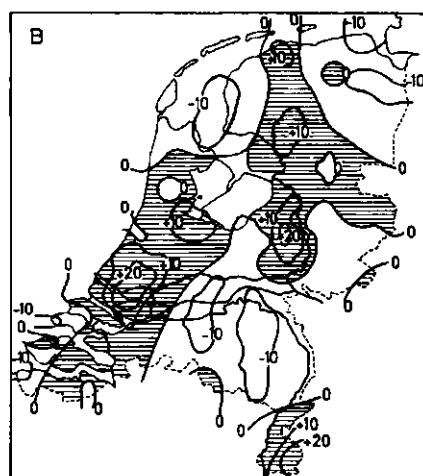
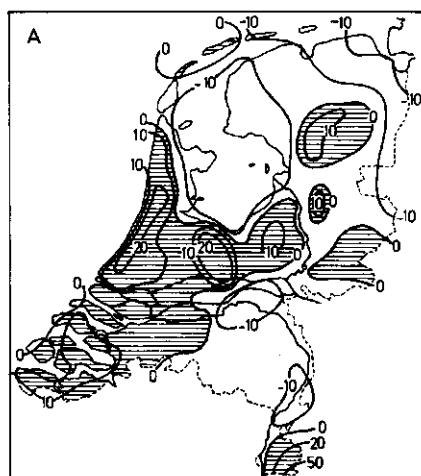


Fig. 2.13. Deviations (%) of annual frequency of daily rainfall in excess of 20 mm according to Braak (1933) (A) and according to data set D140 (B).

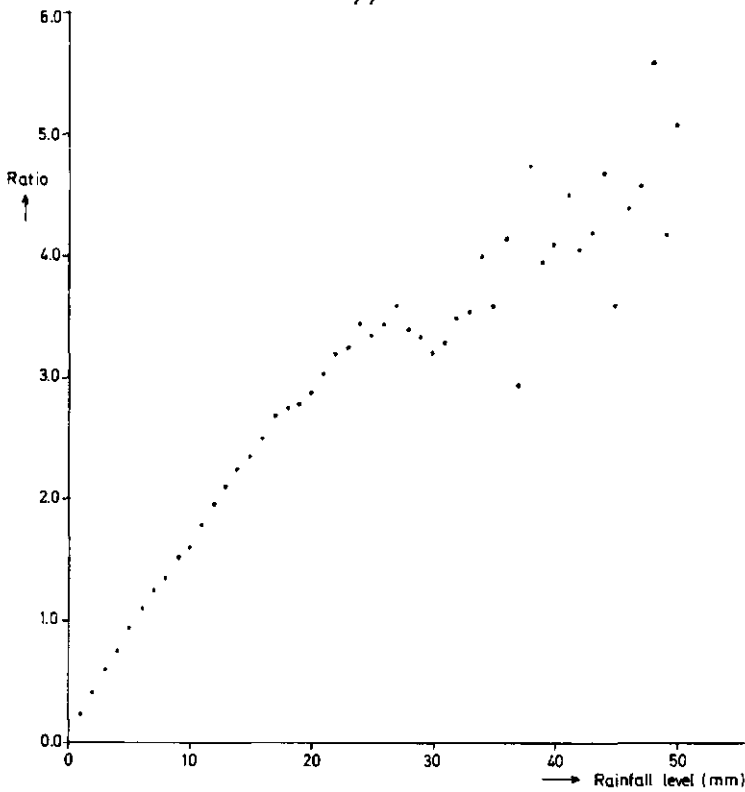


Fig. 2.14. Ratio of the relative decrease in no. of exceedances to the relative increase in rainfall level due to an increase of one millimetre in rainfall level, as a function of rainfall level (mm).

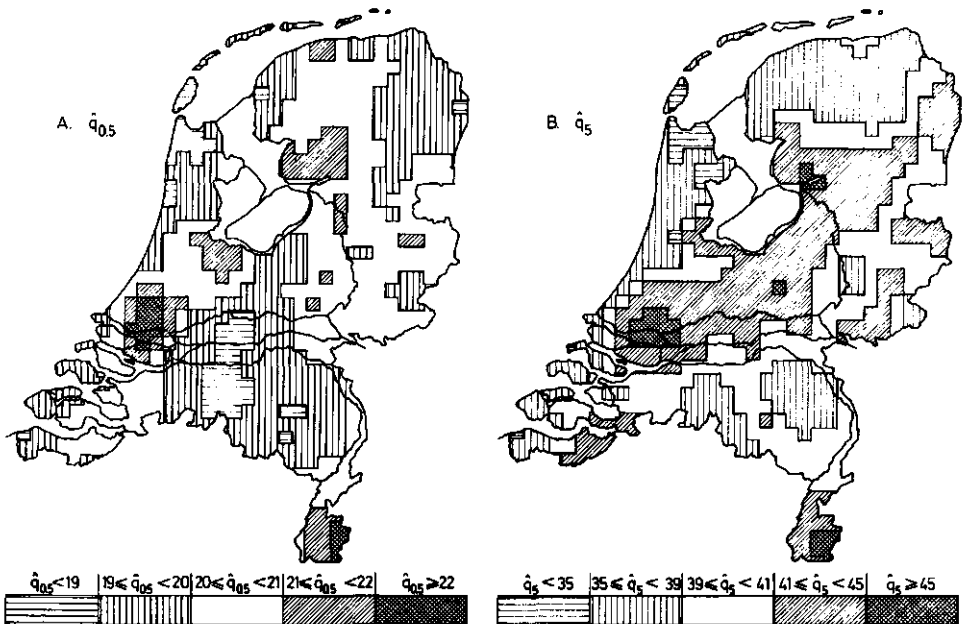


Fig. 2.15. Geographical distribution of summer daily rainfall (mm) for a 0.5-year return period (A), and for a 5-year return period (B).

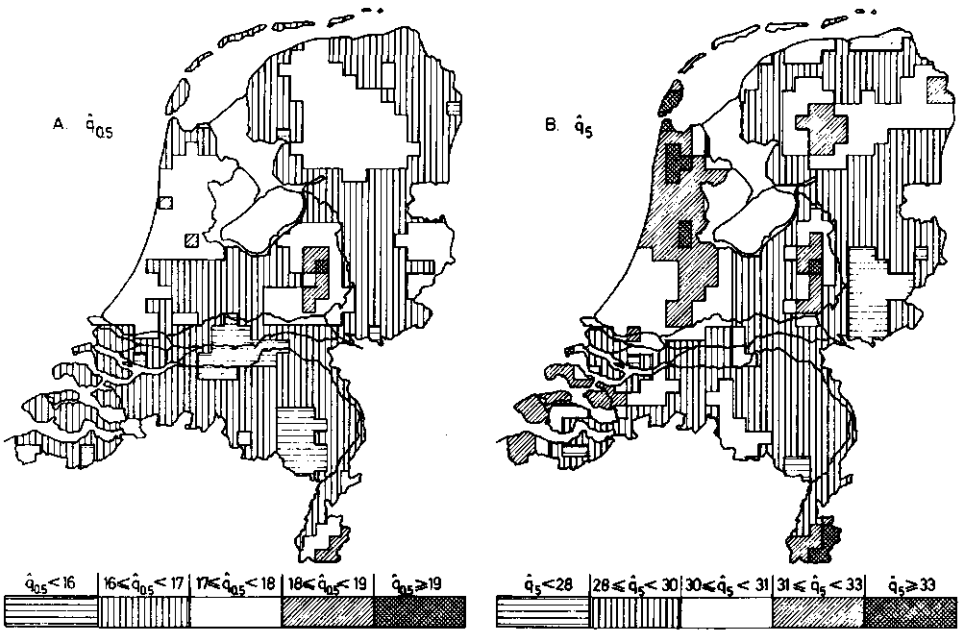


Fig. 2.16. Geographical distribution of winter daily rainfall (mm) for a 0.5-year return period (A), and for a 5-year return period (B).

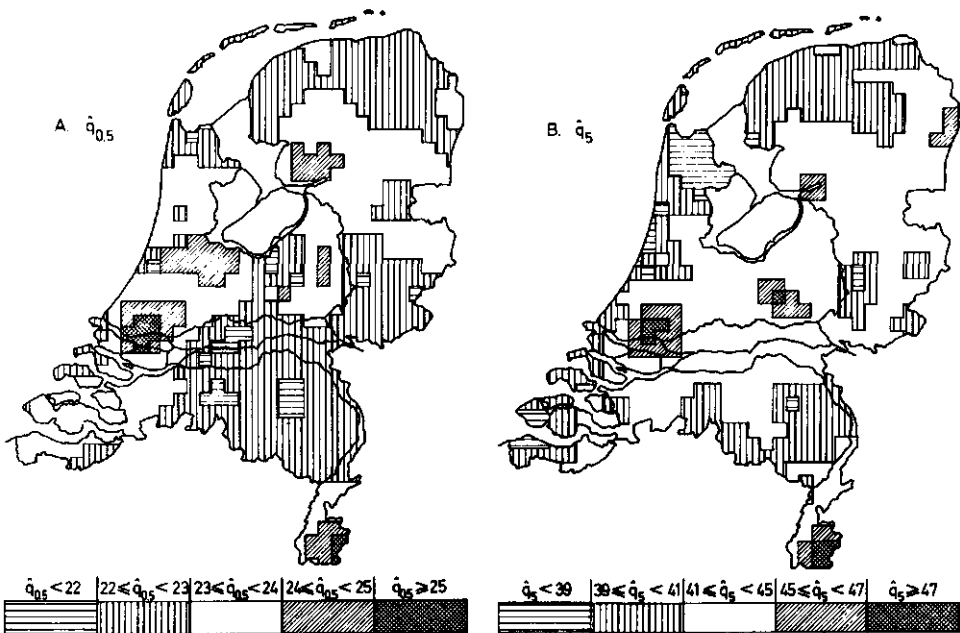


Fig. 2.17. Geographical distribution of daily rainfall (mm) for a 0.5-year return period (A), and for a 5-year return period (B).

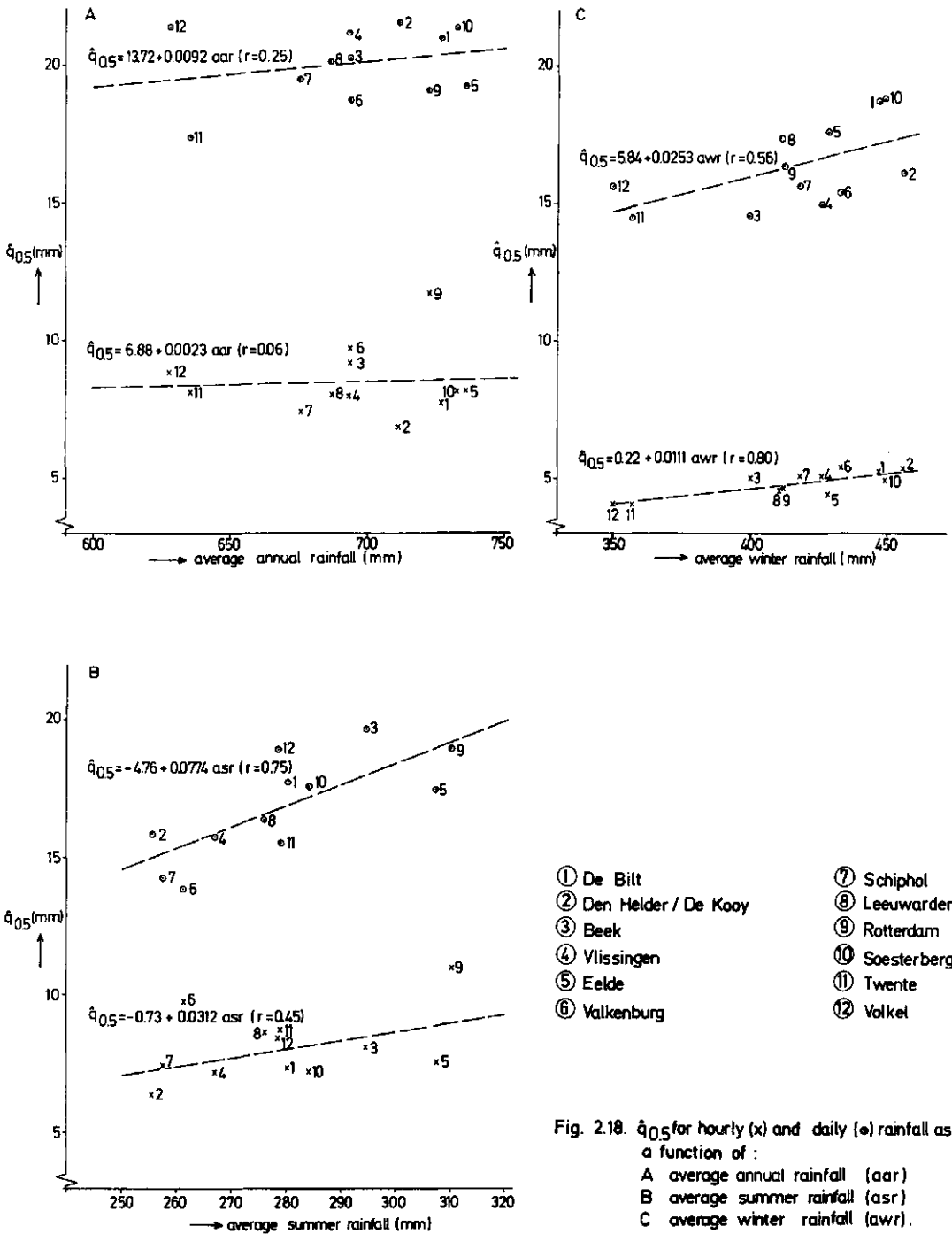


Fig. 2.18. $\hat{q}_{0.5}$ for hourly (x) and daily (o) rainfall as a function of:

- A average annual rainfall (aar)
- B average summer rainfall (asr)
- C average winter rainfall (awr).

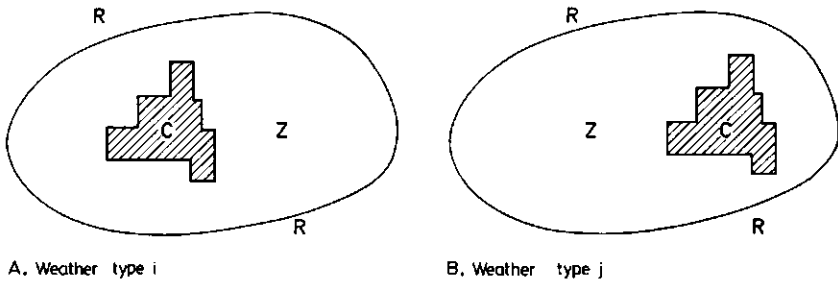


Fig. 2.19. Hypothetical relationships between area C (City), Z (Zone of influence) and R (Rural) during weather types i (A) and j (B).

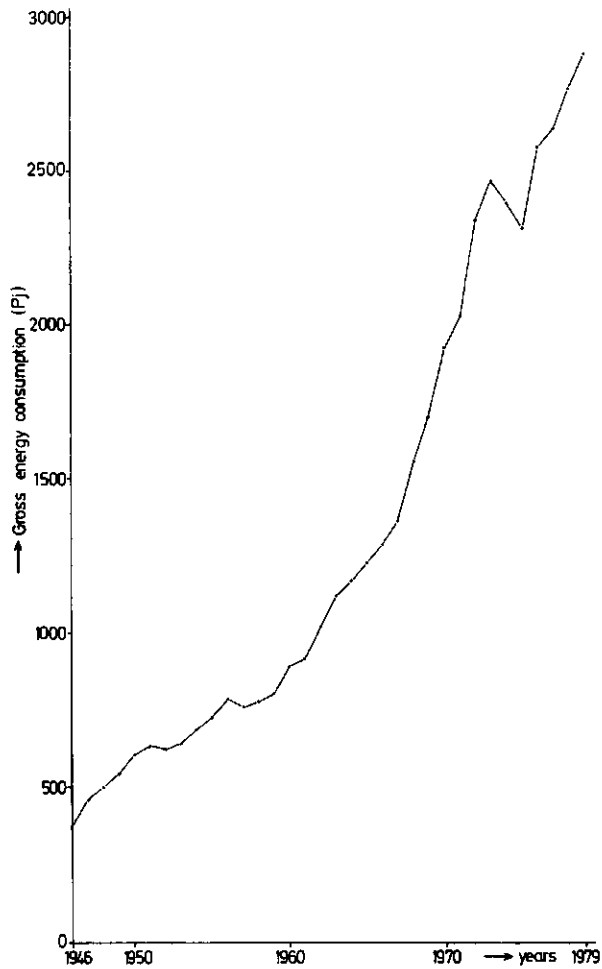


Fig. 2.20. Gross energy consumption in the Netherlands (CBS, 1979).

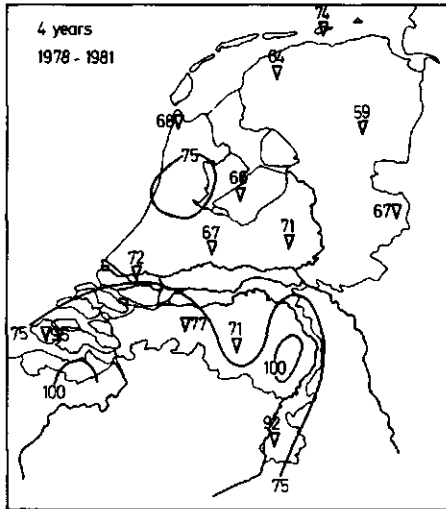
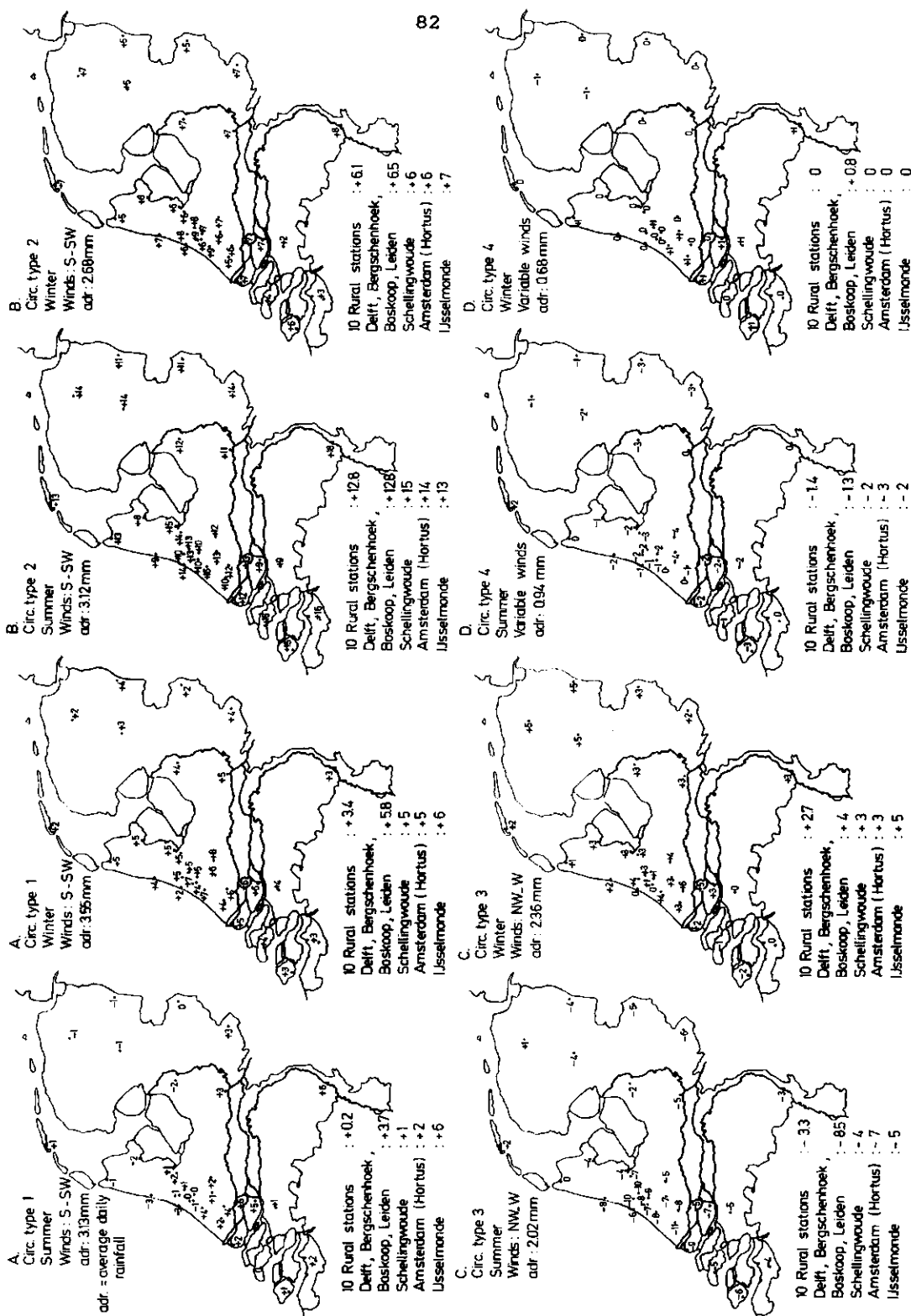
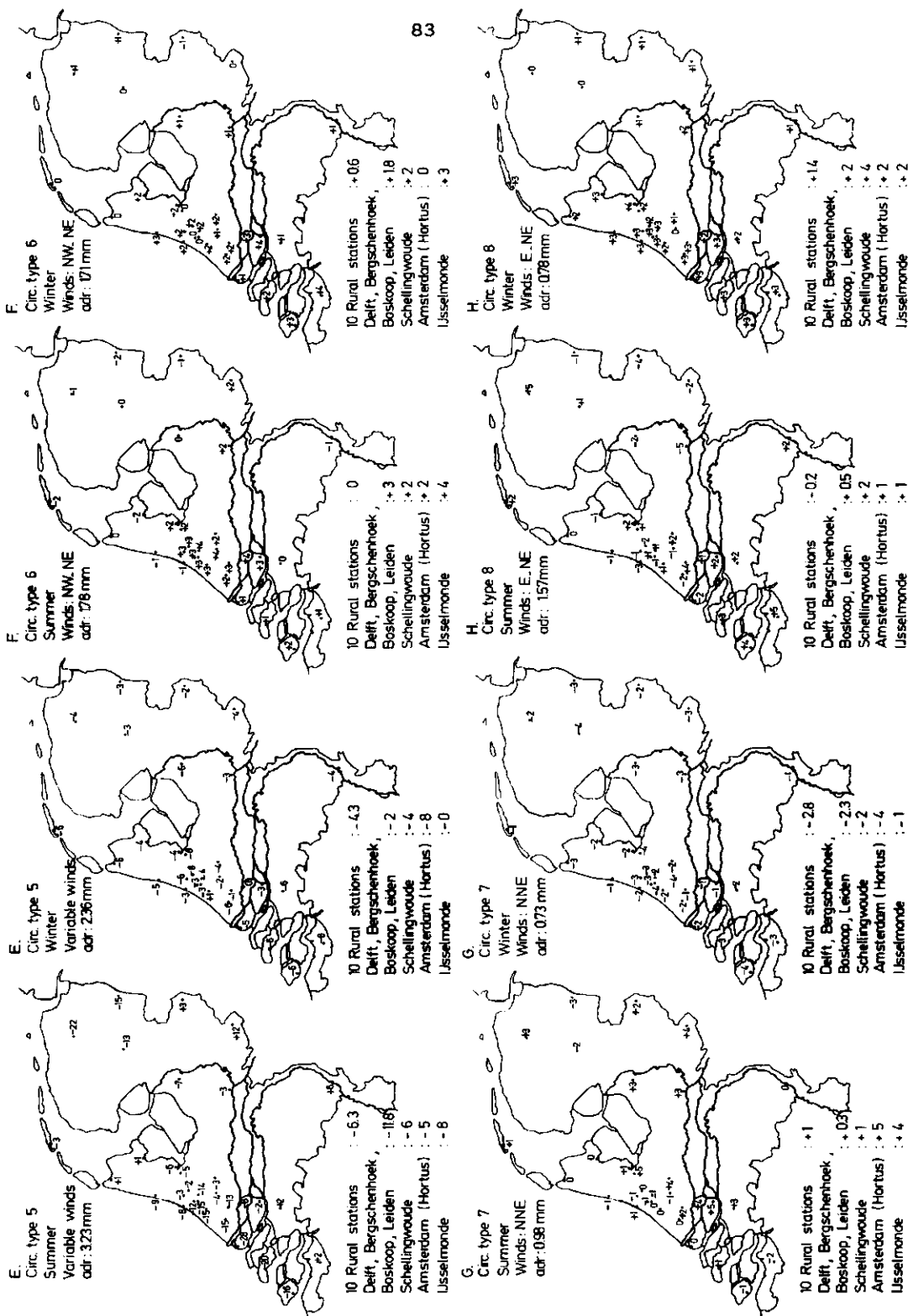


Fig. 2.21. Average SO_4^{2-} concentration in $\mu\text{mol/l}$ of precipitation over the Netherlands for the period 1978-1981 (reproduced from KNMI / RIV, 1982).





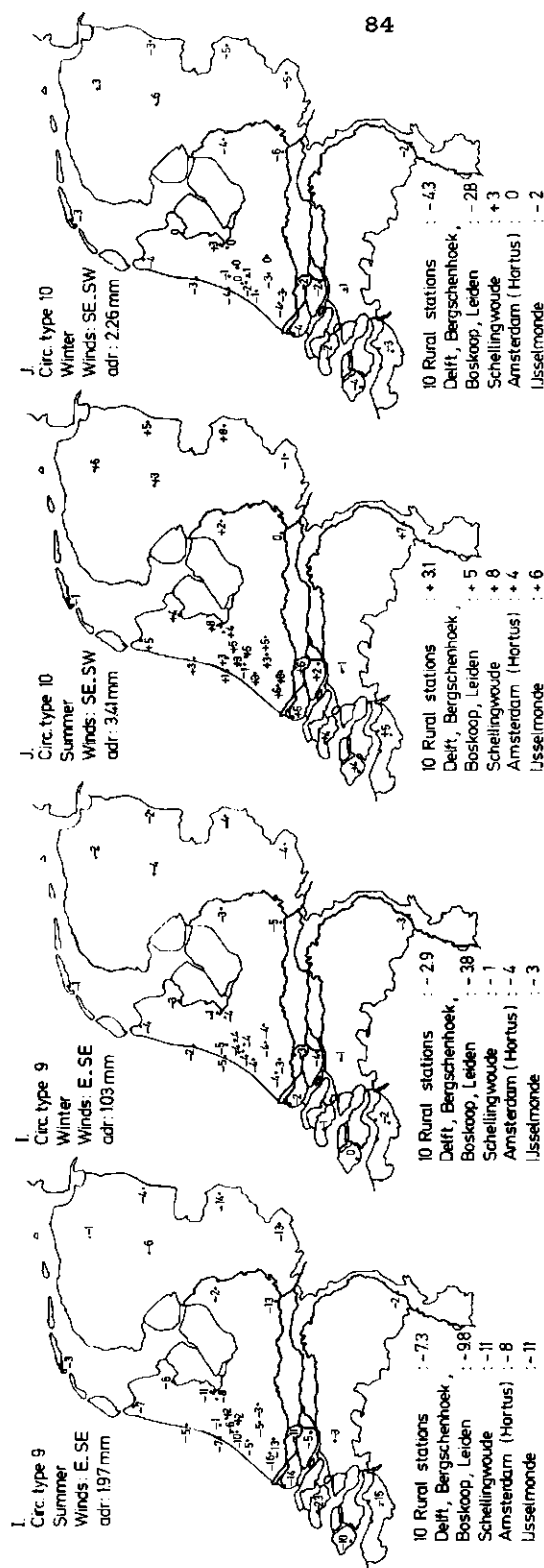


Fig. 2.22 A-J. Increase in average daily rainfall (1 mm) during period II (1956-1979) in relation to period I (1932-1955), given circulation type and season. In the charts has been indicated:

- the most frequently occurring wind directions at ground level at De Bilt, for the circulation type considered;
- daily rainfall (mm), averaged over both periods and over all of the D 32 rainfall series, given circulation type and season (adr).

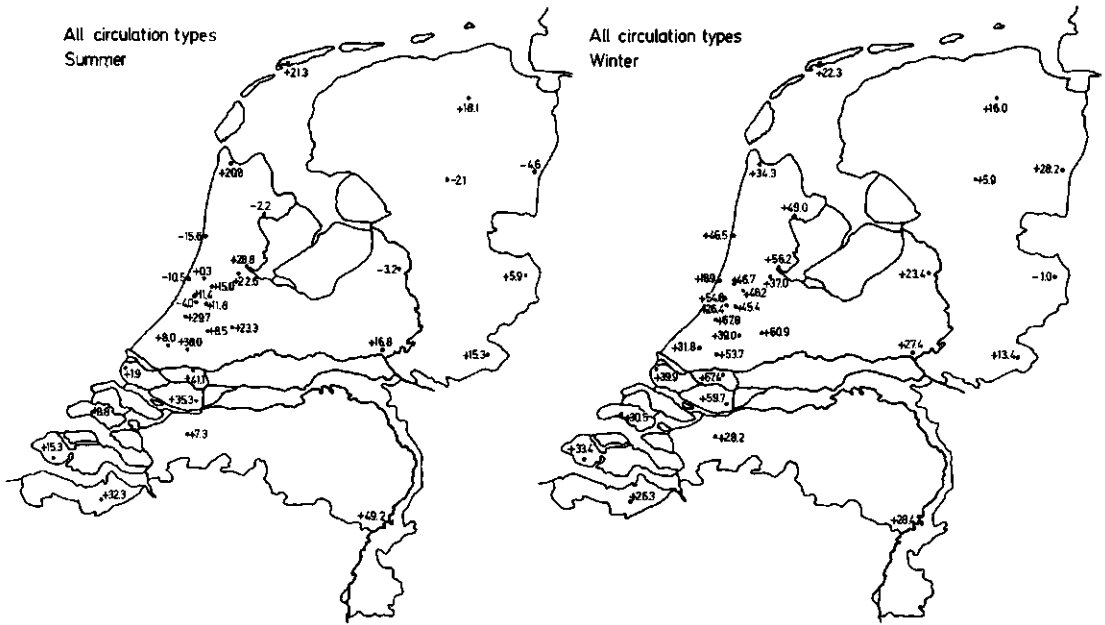
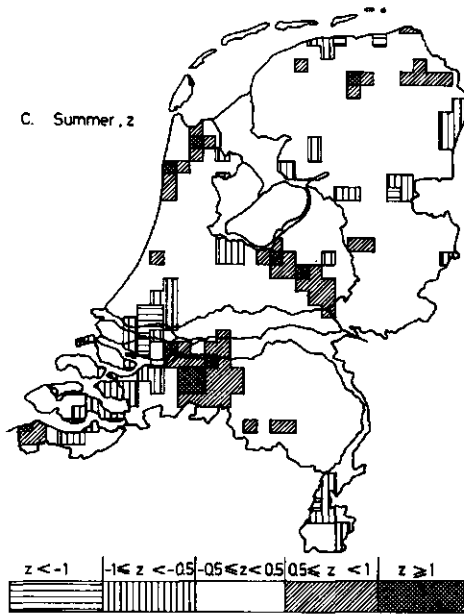
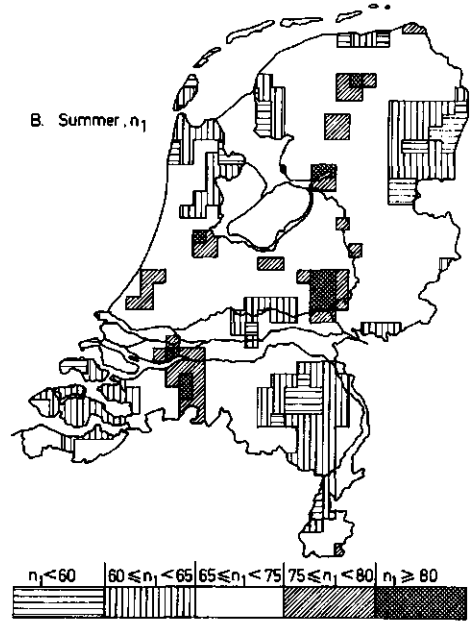
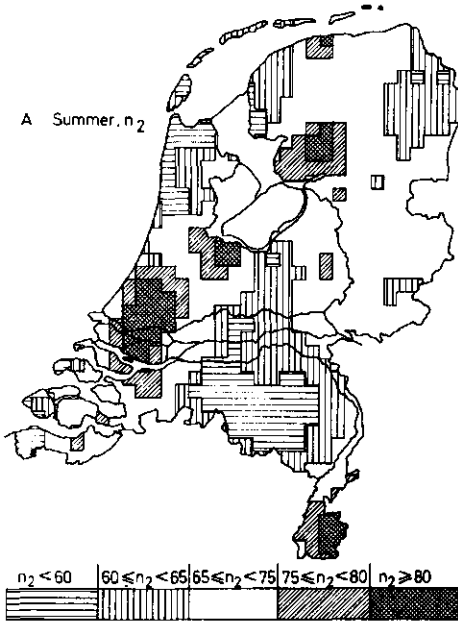


Fig. 2.23. Differences (mm) between average summer/winter rainfall for periods I and II (Average seasonal rainfall over both periods and over all stations : 334.5 mm (summer) and 432.7 mm (winter)).



Fig. 2.24. Partition of the Netherlands with regard to the degree of influence of urbanization and industrialization: (1) affected, (2) unaffected.



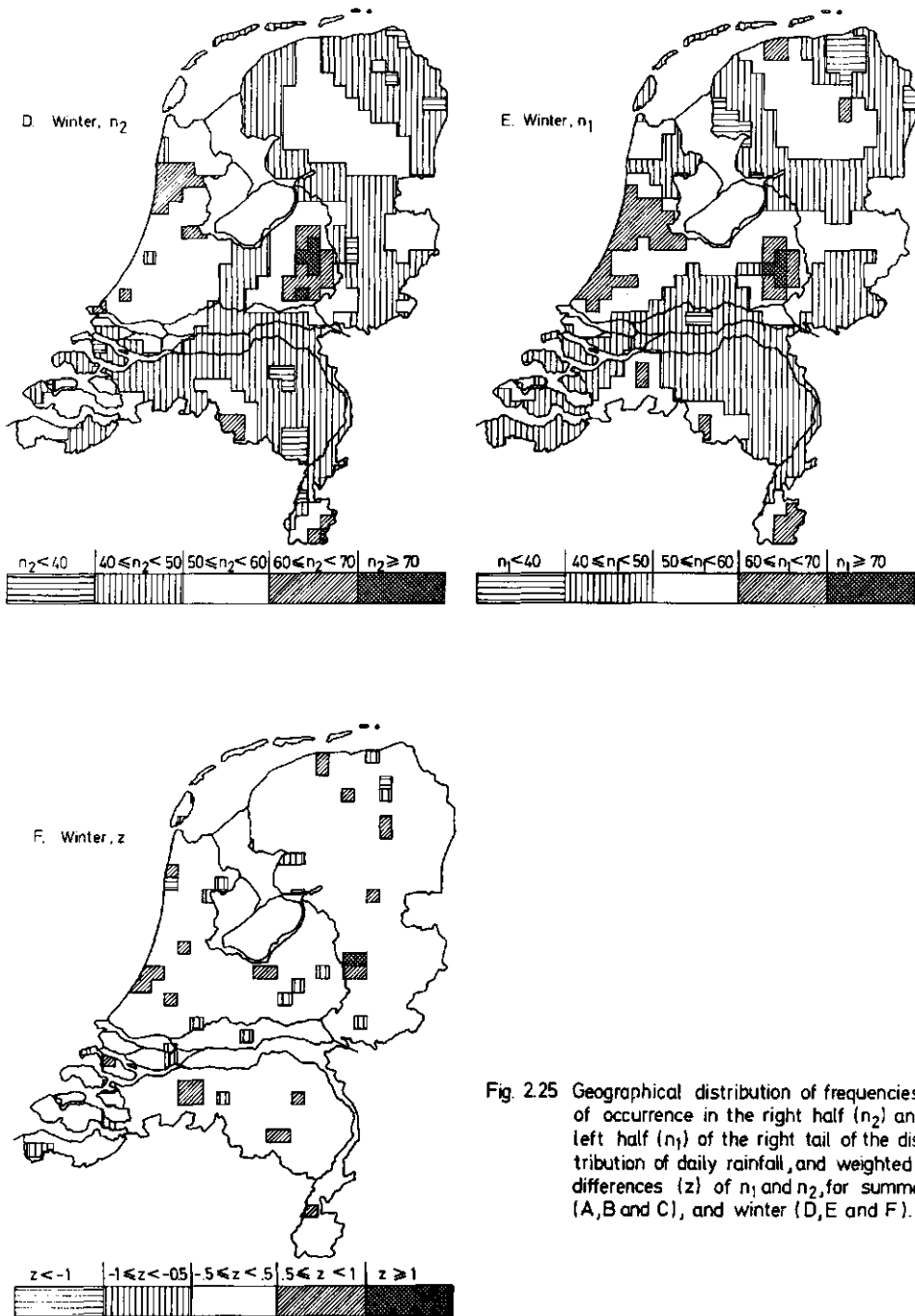


Fig. 2.25 Geographical distribution of frequencies of occurrence in the right half (n_2) and left half (n_1) of the right tail of the distribution of daily rainfall, and weighted differences (z) of n_1 and n_2 , for summer (A, B and C), and winter (D, E and F).

3. STATISTICAL AREAL REDUCTION FACTOR ARF

3.1. INTRODUCTION

In this chapter variability in space of hourly and daily rainfall is considered over a length scale of up to, say, 50 km. This length scale differs from that considered in Chapter 2, in which the distribution of rainfall over the whole of the Netherlands was considered. In this chapter discussion is confined to space variability in rainfall within periods of one hour and of one day by studying the quotient of the mean areal rainfall with a given low exceedance probability and the point rainfall with the same exceedance probability. This quotient is called the statistical areal reduction factor (ARF).

The statistical ARF is a function of the size of the area A , the duration D of the time increment of rainfall recording and the recurrence time T

$$\text{ARF}(A,D,T) = x_A(D,T)/x_S(D,T), \quad (3.1)$$

where

$x_S(D,T)$: the rainfall amount at point S for duration D
and with recurrence time T

$x_A(D,T)$: the areal rainfall amount, being the mean of
 $x_S(D,T)$ over all points S of a region V with
area A .

The recurrence time T is defined by a quantile x_p with $F(x_p)=p$ as

$$T = \frac{1}{1-F(x_p)} = \frac{1}{1-p}, \quad (3.2)$$

where $F(x)$ is the cdf of x . Obviously, ARF will decrease as A and T increase and as D decreases. In this study, A and T in Equation 3.1 are dropped; in some cases D will remain as a suffix to ARF. Thus, ARF_1 and ARF_{24} are hourly and daily values respectively.

Although for very low recurrence times, ARF will exceed one (Nguyen et al., 1981), ARF is usually less than one. Design dimensions of drainage networks serving large areas can be reduced, if a critical point rainfall is used as an input to the design. A critical rainfall is a rainfall event of a certain duration, exceeded by a given frequency. In general, a reduction in design because of the size of the drainage area cannot be made only on the basis of variability in time and space of rainfall. Certain geomorphological and land use characteristics of the drainage area and of the orientation of the catchment with respect to prevailing winds must also be considered. In design of drainage networks, the following procedures are often used with respect to areal reduction.

Rural drainage in the Netherlands

In the Netherlands with its flat topography, the waterways draining the polders are dimensioned in such a way that excesses of water will have a low and predetermined frequency of occurrence. For rural areas, the first stage in the drainage process is the flow of groundwater towards the ditches surrounding small parcels of land. This flow is assumed to be constant, given a minimum allowable depth of the groundwater table. Under the assumption of stationary flow, critical flows have been determined for given depths of the groundwater table and for various land uses and soil types, critical flow meaning such a flow that an excess of it is undesirable. The assumption of stationary flow is probably not only adopted because of its simplicity, but also because winter rainfall is used in the design of rural drainage. Winter rainfall is to a large extent caused by the passage of fronts, which leads to rainfall of long duration. For arable land, an acceptable critical flow is $0.08 \text{ m}^3 \cdot \text{s}^{-1} \cdot \text{km}^{-2}$ given a minimum depth of groundwater table of 0.50 m; for pasture land, the same flow is considered acceptable but a minimum depth of groundwater table of 0.30 m is assumed (Werkgroep Afvoerberekeningen, 1979). These are empirical values, however, corresponding to a daily rainfall of about 7 mm. As waterways should be able to convey the upstream flow, given certain allowable exceedances of the polder level, the dimensions of the waterways in all parts of the network can be determined. Thus critical rainfall is not used directly in the design of rural drainage. As a

consequence, reductions because of areal size are empirically verified reductions of the *discharge* to be conveyed by the drainage network. For example, an equation for the reduction factor f of the discharge if areal size exceeds 10 000 ha is (Cultuurtechnische Vereniging, 1971)

$$f = 1.60 - 0.15^{10} \log A, \quad (3.3)$$

where

A: areal size (ha).

This purely empirical approach, which does not take into account the dynamic character of the runoff process, seems to satisfy requirements in the flat parts of the Netherlands where storage in groundwater and surface water tends to suppress short-period fluctuations in discharge. The design of drainage systems in glass-covered horticultural and in sloping rural areas, however, requires a non-stationary approach in which the actual input of areal precipitation should be considered.

Urban drainage in the Netherlands

In the design of urban drainage, a critical depth of rainfall is often used, and also a certain storm profile is assumed. Finally, the capacity of the drainage network to convey flow from the upstream area must be checked. A reduction in the rainfall input because of areal size is not applied. However, for larger areas such a reduction could be applied by multiplying the critical rainfall depth by ARF.

In this chapter the following issues are dealt with:

- In Section 3.2 prediction of areal rainfall by means of kriging is discussed, in particular whether the IRF-0 theory is adequate for making kriging predictions of areal rainfall, and whether different predictors of areal rainfall produce different results.

- In Section 3.3, ARF_{24} is estimated by various methods for each of three areas of about 1000 km^2 in the Netherlands (Figure 3.1). Several estimators of ARF have been proposed, based on annual maxima series of both point and areal rainfall (e.g., USWB, 1957-1960; and NERC, 1975, Vol. 2); on POT series of both point and areal rainfall (e.g., Bell, 1976); and on the marginal distribution of point rainfall (e.g., Roche, 1963; Rodríguez-Iturbe and Mejía, 1974; Buishand, 1977b and c). The estimates by these three methods are compared, and also with earlier estimates of ARF_{24} for the Netherlands (Kraijenhoff, 1963; Buishand, 1977c).
- In Section 3.3, attention is also paid to the dependence of ARF on location, on season, and on exceedance frequency of rainfall, particularly whether the three areas in the Netherlands vary with regard to ARF_{24} , and whether these estimates of ARF_{24} differ from those for other countries; whether ARF_{24} differs between seasons, and whether annual maxima of both point and areal rainfall occur in the same season; and whether ARF_{24} depends on frequency of exceedance.
- Section 3.4 deals with the dependence of ARF on duration of rainfall and on areal size, and in particular whether estimates of ARF_1 for the Netherlands differ from those for other countries; and whether ARF calculated from the marginal distributions of rainfall varies with duration of rainfall at fixed return period and areal size.
- In Section 3.5, a variable related to ARF, the storm-centred areal reduction factor SRF, is discussed. This reduction factor SRF is defined as

$$SRF = x_A / x_{\max} , \quad (3.4)$$

where

x_{\max} : local maximum point rainfall over a certain time period (e.g., one specific day)

x_A : simultaneous areal rainfall over area A bounded by an isohyet.

The relationship between ARF and SRF is discussed.

The rainfall series used concerning the 29-year period 1951-1979 are given in Appendix B.1 and the location of the rainfall stations is shown in Figure 3.1.

3.2. PREDICTION OF AREAL RAINFALL

Most estimators of ARF require information on mean areal rainfall. Areal rainfall may be predicted from the arithmetic mean of point samples provided that these are approximately evenly distributed throughout the area, and there are no orographic effects (Buishand and Velds, 1980). Other predictors of areal rainfall include:

- the isohyet method;
- the Thiessen method;
- an extension of the method of optimum interpolation (De Bruin, 1975);
- the Kalman filter method (Bras and Colón, 1978);
- the kriging method (e.g., Journel and Huijbregts, 1978).

The kriging method, the optimum interpolation method, and the Kalman filter method result in best linear unbiased predictors (BLUP), where 'best' is used in the sense that prediction variances are minimized (see Section 2.4.1). As the kriging predictor requires only a minimum set of assumptions (most notably the variance of the regionalized variable $Z(u)$ need not exist), discussion in this section is confined to the kriging predictor.

The adequacy of the IRF-0 theory for obtaining a kriging prediction of areal rainfall, is discussed in Section 3.2.1 and in Section 3.2.2 the kriging predictor is compared with the commonly used arithmetic mean predictor and the Thiessen predictor.

Throughout this section only daily rainfall series are used, as there is insufficient hourly rainfall data for the Hupsel catchment area to obtain reliable estimates of the semi-variances or

generalized covariances. Discussion is restricted to monthly maxima of daily rainfall, occurring on days with maximum arithmetic mean of the available point samples.

3.2.1. *The order k and the estimation of the semi-variogram*

It has been assumed in the present application that the regionalized variable $Z(u)$ is stationary in the mean. The mean summer and winter daily rainfall at each rainfall station in the three areas considered (Figure 3.1) on days with a monthly maximum of areal rainfall are given in Figure 3.2; the respective areas are approximated by rectangles. As no clearly defined drift is shown, an IRF-0 model seems to be adequate.

For area 1, for each of the 29 available January and August rainfall maxima, the order k has been determined with the computer programme AKRIP (Kafritsas and Bras, 1981) for IRF- k point and block kriging. As suggested by Delfiner (1976), in AKRIP the order k is determined by kriging the data points, on the assumption that in turn $k = 0, 1$, and using for both values of k the same neighbouring points for the kriging of a data point and the same generalized covariance function: $K(h) = -h$. In this chapter only intrinsic random functions of order one or zero are considered, because 12 data points are insufficient for the identification of higher order random functions. The order that results in the smallest kriging error at a data point should be given the grade 1, and the other the grade 2. The grades of both orders should be averaged over all points kriged and the order with the smallest average grade should be chosen.

Quite contrary to what is generally accepted, in a substantial number of cases, the order k was estimated to be one (see Table 3.1). The estimate of the order k depends to some extent on the number of neighbouring data points used to krig each data point separately (see also Table 3.1). The kriging algorithm was applied to each data point, with all the remaining points as its neighbourhood.

Table 3.1. Number of years (29 in total) with order k for rainfall maxima in January and August (area 1), determined by the computer programme AKRIP (Kafritsas and Bras, 1981)

Number of neighbouring points	Order k		
	k = 0	k = 1	ex aequo
January: 11 (all)	12	12	5
6	19	7	3
August : 11 (all)	14	7	8
6	14	9	6

When the grades are equal the coefficients C , α_1 , and α_3 of the polynomial generalized covariance functions

$$K(h) = C\delta + \alpha_1 h \quad (C \geq 0, \quad \alpha_1 \leq 0) \quad (3.5a)$$

and

$$K(h) = C\delta + \alpha_1 h + \alpha_3 h^3, \quad (C \geq 0, \quad \alpha_1 \leq 0, \quad \alpha_3 \geq 0) \quad (3.5b)$$

for order $k = 0$ and 1 , respectively, have to be determined. Because it is possible to equate one or more of the coefficients in Equation 3.5a and Equation 3.5b to zero, the resulting number of possible choices for $K(h)$ is three and seven, respectively. Given the order k , AKRIP creates generalized increments by kriging a data point τ , using a generalized covariance function that is appropriate to any order k : $K(h) = -h$. The resulting kriging error can be directly observed; denote its square for data point τ to be kriged by $s_{K,\tau}^2$. The theoretical prediction variance, $\sigma_{K,\tau}^2 = \sum_i \sum_j \lambda_i \lambda_j K(u_i - u_j)$ is obtained by using the desired, more specific generalized covariance function according to Equation 3.5a or Equation 3.5b.

On repeating the procedure for several data points, the sum of squares Q may be obtained of the differences between the squared kriging errors $s_{K,\tau}^2$ and the theoretical prediction variances $\sigma_{K,\tau}^2$

$$Q = \sum_{\tau} [s_{K,\tau}^2 - \sigma_{K,\tau}^2]^2. \quad (3.6)$$

The coefficients of $K(h)$ can then be obtained by regression. The results can be used to create new generalized increments and to find new sets of coefficients (for each permissible model of $K(h)$), and so on, until the coefficients stabilize. From the generalized covariances thus determined, the one is selected that has the ratio

$$r = \frac{\sum_{\tau} s_{K,\tau}^2}{\sum_{\tau} \sigma_{K,\tau}^2} \quad (3.7)$$

closest to unity. This provides the ultimate choice of k , in case of equal grades: for each k the selected generalized covariance function is used to redetermine the grades. Because of Equation 2.36, the ratio r is always equal to one, if $k=0$ and $K(h)=C\delta$. Thus, the procedure should be used cautiously, as $K(h)=C\delta$ is often selected incorrectly, especially for August maxima. Therefore, where these grades were equal, the structure identification part of the programme was rerun, using as generalized covariance functions both $K(h)=C\delta$ and $K(h)=-h$. The final result was that k was equal to zero in 15 and 18 out of 29 cases for January and for August, respectively.

In the following, it is assumed that k is equal to zero. This is also in accordance with the work of Chua and Bras (1980), who for a plain area of 550 km^2 in the USA, assumed the IRF-0 theory to be adequate to predict daily areal rainfall from 10 point samples. In 8 out of the 9 cases studied, this was also the case for a mountainous area of 4400 km^2 , ranging in height from 2350 to 3660 m, and sampled at 21 to 29 points. Moreover, the structure identification in the IRF- k theory proceeds iteratively. Therefore, this theory is not particularly suitable for the routine calculations of mean areal rainfall, involved in the calculation of ARF.

Further arguments in favour of the IRF-0 theory are provided by the sample semi-variograms as estimated by the multi-realization approach; these semi-variograms increase roughly linearly with the distance h (Figures 3.3, 3.4, and 3.5). It is known that

the IRF-0 theory is valid, for a regionalized variable $Z(u)$ having a linear semi-variogram (Section 2.4.1). To the sample semi-variograms, linear population semi-variograms $\gamma(h)$ have been fitted according to Equation 2.26a

$$\gamma(h) = C\delta + \alpha_1 h, \quad (3.8)$$

where

C, α_1 : non-negative coefficients

δ : 0 ($h=0$) or 1 ($h \neq 0$).

In the single-realization approach, as opposed to the multi-realization approach, for each event (monthly rainfall maximum in this case) separately, a sample semi-variogram is estimated according to Equation 2.25. To this a population semi-variogram $\gamma(h)$ is fitted, which is used in the prediction of areal rainfall for that particular event. In the multi-realization approach, as applied here, monthly maxima for all years of record and one particular month are grouped together, and a mean sample semi-variogram is estimated. Subsequently, a function $\gamma(h)$ is fitted, which is used in the prediction of areal rainfall for all maxima within the group.

An argument in favour of the multi-realization approach is that it does not seem unreasonable to group monthly maxima for one particular month of the year together for all years of record. In addition, the use of the multi-realization approach is almost unavoidable, because there are not enough sample points available to estimate the semi-variogram for each event separately. Using the well-known property (Kendall and Stuart, 1977; p. 258) of the variance estimator \underline{s}^2

$$\text{var } \underline{s}^2 \cong 2\sigma^4/n, \quad (3.9)$$

where n is the number of samples, it follows that $N(h)$ in Equation 2.25 should exceed 40, for the squared coefficient of variation of the estimator $\gamma(h)$ to be less than 5%. However, the use of Equation 3.9 is rather restrictive. The regionalized variable $Z(u)$ is assumed to be independent and normally distributed, and second order sta-

tionary. Furthermore, the one realization $z(u)$ which is sampled is thought of as to constitute the whole population, if only sampled exhaustively. This, in fact, is contrary to the concept of a stochastic function $Z(u)$.

Similarly, Gandin (1965) presented the required minimum number of sample points to obtain a given accuracy, by considering the normalized semi-variogram $g(h)$

$$g(h) = \gamma(h)/\sigma^2, \quad (3.10)$$

where σ^2 is the point variance $\text{var}[z(u)]$. With a second order stationary $z(u)$, the variance of the estimator $\hat{g}(h)$ equals

$$\text{var}[\hat{g}(h)] = \text{var}[\underline{r}(h)], \quad (3.11)$$

where $r(h)$ is the estimate of the correlation coefficient $\rho(h)$ at distance h . With normally distributed variables, this variance is approximately (Kendall and Stuart, 1977; p. 258)

$$\text{var}[\underline{r}(h)] \cong \frac{(1-\rho^2(h))^2}{N(h)}. \quad (3.12)$$

By using Equation 3.11 and Equation 3.12, $N(h)$ can be presented as a function of $\text{var}[\hat{g}(h)]$ and of $g(h)$, and from Equation 3.12 it can be seen that $N(h)$ increases with h .

With 12 sample points, there are 66 data pairs. As indicated by the semi-variograms, the realizations $z(u)$ are not second order stationary, but intrinsic only. Thus clearly, a single-realization approach would not permit reliable estimation of the semi-variogram. This, in fact, is a further argument in favour of using the IRF-0 theory, because the present IRF-k algorithms have been developed for the single-realization approach. Chua and Bras (1980) also concluded that a multi-realization approach was necessary. For the plain area they analysed, in about half of the 35 events, the single-realization approach did not permit detection of the semi-variogram structure. For the remaining events, the single-realization semi-variograms were either spherical (ten events) or

linear (seven events). For one event both a spherical and a linear semi-variogram seemed to fit, and six events showed a nugget effect.

The sample semi-variograms for monthly rainfall maxima stratified according to month are presented in Figures 3.3, 3.4, and 3.5. These have been calculated by using Equation 2.25 but adapted to the multi-realization approach, which means averaging over the 29 years of record

$$\hat{\gamma}(h) = \frac{1}{29} \sum_{j=1}^{29} \hat{\gamma}_j(h) = \frac{1}{29} \sum_{j=1}^{29} \frac{1}{2N(h)} \sum_{i=1}^{N(h)} [z(u_i) - z(u_i+h)]^2, \quad (3.13)$$

where

$\hat{\gamma}_j(h)$: single-realization sample semi-variogram for monthly maximum in year j .

Distance classes of 5 km up to 35 km have been considered. For area 1 in Figure 3.1, the sample standard deviations of the values of the single-realization sample semi-variograms which were averaged, are presented in Figure 3.3. It has been verified whether less variation between the single-realization sample semi-variograms for each particular month may result from further classification of monthly maxima according to rainfall depth, because it is known that with increasing areal rainfall the coefficient of variation decreases. This is confirmed by the results presented in Figure 3.6, in which the coefficient of variation is the ratio of the sample estimate of the standard deviation of point rainfall, and the estimated mean areal rainfall (equal to the arithmetic mean of the point rainfalls).

Two classifications according to rainfall depth have been attempted: one on the basis of mean areal rainfall in exceedance of 15 mm or not; and the other on the basis of maximum point rainfall in exceedance of 20 mm or not (thus placing more emphasis on 'spottiness' of rainfall). However, these classifications did not result in any noteworthy reduction in variation between the single-realization $\hat{\gamma}_j(h)$ to be averaged, and did not result in different limiting behaviour of the semi-variograms with regard to distance.

Therefore, classification according to rainfall depth has been omitted, and linear population semi-variograms have been fitted by ordinary regression under restriction of the observed semi-variances for all realizations on their distances h , for $h \leq L/2$, where L is the maximum distance between sample points. The choice of the linear semi-variogram model was based on visual inspection of Figures 3.3, 3.4, and 3.5. The resulting OLS estimates of the coefficients C and α_1 in Equation 3.8 are presented in Table 3.2. The estimates of C/α_1 are also presented because these ratios, and not C only, as suggested by Chua and Bras (1980), completely determine the kriging weights for a given configuration of sample points, when the semi-variogram model according to Equation 3.8 is used.

As may be expected, values of \hat{C} and $\hat{\alpha}_1$ tend to be high in summer and low in winter. On the other hand, the annual pattern of parameter values is not particularly even. Thus, classifying months according to their respective values of $\hat{C}/\hat{\alpha}_1$ yields rather odd groups of months, which also differ for the three respective areas. This is probably caused by sample variability between single-realization semi-variograms (Appendix A.4).

Table 3.2. OLS estimates of C (mm^2) and α_1 ($\text{mm}^2 \cdot \text{km}^{-1}$) in Equation 3.8 and of the ratio C/α_1 (km) for monthly maxima of daily rainfall for three areas in the Netherlands

Month	Area 1			Area 2			Area 3		
	\hat{C}	$\hat{\alpha}_1$	$\hat{C}/\hat{\alpha}_1$	\hat{C}	$\hat{\alpha}_1$	$\hat{C}/\hat{\alpha}_1$	\hat{C}	$\hat{\alpha}_1$	$\hat{C}/\hat{\alpha}_1$
Jan.	1.3	0.2	6.0	1.3	0.5	2.6	4.3	0.2	17.2
Feb.	1.4	0.2	7.4	2.7	0.1	39.1	1.5	0.3	5.3
March	0.9	0.3	2.9	2.1	0.1	25.8	0.6	0.3	1.9
April	0.2	0.5	0.3	0	0.4	0	3.9	0.4	10.2
May	3.9	0.7	5.8	0.0	0.7	0.0	6.8	0.9	7.1
June	1.3	1.3	1.1	11.9	0.7	16.1	13.5	1.3	10.8
July	16.8	1.9	8.9	6.4	2.3	2.8	18.4	2.4	7.8
Aug.	19.7	6.3	3.1	44.7	0.7	67.7	18.9	2.3	8.2
Sept.	7.8	1.6	4.9	13.1	1.3	10.1	7.0	1.1	6.4
Oct.	2.6	1.0	2.6	4.6	1.3	3.6	2.9	0.7	4.4
Nov.	0.6	0.8	0.8	6.2	0.1	68.7	3.1	0.3	11.1
Dec.	5.2	0.3	15.3	9.1	0.0	302.3	7.6	0.1	151.2

It is unlikely that these differences have been caused by anisotropy. For the Netherlands, anisotropy of the correlation function $\rho(h)$ for 10-day and monthly rainfall has been demonstrated by Buis-hand and Velds (1980). For the relatively small areas considered here, anisotropy of the semi-variograms for daily rainfall is not expected. Stol (1972), investigating $\rho(h)$ for daily rainfall in an area of about 2000 km² found no indications for anisotropy.

Further, it is unlikely that differences between areas have been caused by differences in the quality of the measurements. Well-scrutinized measurements from the Royal Netherlands Meteorological Institute (KNMI) obtained by means of one type of daily rainfall measuring device only have been used. Differences in quality of measurements will lead to systematic differences in estimated semi-variograms for each area, as demonstrated by Gandin (1965). Consider, for example, a random error ε , according to

$$\underline{f}_i^* = \underline{f}_i + \varepsilon_i, \quad (3.14)$$

where

\underline{f}_i^* : measured rainfall at station i

\underline{f}_i : actual rainfall at station i

ε_i : random measurement and observational error with expectation zero and variance σ^2 at station i .

Assume also that the errors are uncorrelated with actual rainfall, and uncorrelated with random errors at other stations, then such errors lead to an increase in the nugget effect by σ^2 .

If only systematic measurement and observational errors occur, according to

$$\underline{f}_i^* = \beta_i \underline{f}_i, \quad (3.15)$$

where

β_i : factor, indicating the systematic error at station i ,
and if $\beta_i = \beta_j = \beta$, then $E[\hat{\gamma}^*(h)] = \beta\gamma(h)$.

Thus errors according to Equation 3.14 and Equation 3.15 would lead to systematic differences between the estimates of C and α_1 in Equation 3.8 for different areas. Such systematic differences do not seem to be apparent in Table 3.2, although \hat{C} values for area 1 are rather low, and $\hat{\alpha}_1$ values for area 2 are low. These, however, seem to be caused by a pattern of sample points in area 1 relatively well suited to the estimation of C , and by the effect of wide tidal inlets in area 2.

Another physical cause of differences between the three areas, which is reflected to some degree in Table 3.2, is the relatively frequent occurrence of convective rainfall during summer in the east and south-east of the Netherlands, as a result of high surface temperatures. Along the coast, convective rainfall is suppressed during spring and early summer, because of relatively low sea temperatures. During autumn, however, the relatively warm sea enhances the development of showers along the coast (Buishand and Velds, 1980).

Thus, it cannot be conclusively stated that the IRF-0 theory is adequate to predict areal rainfall. As reported by Delhomme (1978) and by Chua and Bras (1980), the IRF-0 theory seems to be adequate to predict areal rainfall over climatologically homogeneous areas. Yet the results of this study are not in accordance with this. Apparently, the issue of structure identification requires further investigation, both statistical and physical. As k was set at zero, calculations were simple. Contrary to the IRF- k theory, where estimation of the generalized covariance is carried out for each realization separately, the semi-variogram to be used in the IRF-0 theory can be estimated by the multi-realization approach. As only few data points were available, a more reliable estimation of the semi-variogram was possible. On the other hand, variation both between months and between areas in the semi-variograms in the multi-realization approach is large.

3.2.2. Comparison of the kriging, Thiessen, and arithmetic mean predictors

The mean areal rainfall Z_V over a region V with area A , where $Z_V = \frac{1}{A} \int_V Z(u) du$, can be predicted by a linear combination of the point samples

$$\hat{z}_V = \sum_{i=1}^N \lambda_i z(u_i), \quad (3.16)$$

where

λ_i : weighting factor

N : total number of sample points $u_i \in V$.

The unbiasedness and minimum variance conditions of the prediction obtained with Equation 3.16 lead to the kriging Equations 2.23

$$\begin{cases} \Gamma \lambda + \mu 1_N = r \\ 1_N' \lambda = 1, \end{cases} \quad (3.17a)$$

$$(3.17b)$$

where in the present application $r' = (\bar{\gamma}(u_1; V), \dots, \bar{\gamma}(u_N; V))$.

Such mean semi-variances $\bar{\gamma}(u_i; V)$, where one of a pair of points remains fixed at location u_i , and the other point sweeps V , can be calculated numerically according to the method proposed by Bras and Rodríguez-Iturbe (1976). In this method, V is approximated by a rectangle V' , which is then split into four subrectangles by axes passing through u_i and parallel to the sides of V' ; then

$$\bar{\gamma}(u_i; V) = \frac{1}{A} \left[\sum_{i=1}^4 \int_0^{L_i} \gamma(h) f_i(h) dh \right], \quad (3.18)$$

where

L_i : largest distance in subrectangle i

$f_i(h)$: pdf of distance h between the fixed point u_i and a random point in subrectangle i .

The single integral in Equation 3.18 can be easily calculated numerically.

Here auxiliary functions are used (Journel and Huijbregts, 1978). These are analytical functions which yield $\bar{\gamma}(u;V)$ for certain simple geometric forms of the regions u and V , and given a certain semi-variogram model, for example, linear or exponential. Although there are several auxiliary functions, in this study, following the notation of Journel and Huijbregts (1978), use is made of $H(a;b) = \bar{\gamma}(u;V)$, where V is a rectangle with sides a and b and u is a point, that is one of V 's vertices. The function $H(a;b)$ is defined as (Journel and Huijbregts, 1978; p. 113)

$$H(a;b) = \frac{1}{3}(a^2+b^2)^{\frac{1}{2}} + \frac{b^2}{6a} \ln\left\{\frac{a+(a^2+b^2)^{\frac{1}{2}}}{b}\right\} + \frac{a^2}{6b} \ln\left\{\frac{b+(a^2+b^2)^{\frac{1}{2}}}{a}\right\}. \quad (3.19)$$

After approximating V by a rectangle V' , V' is split into four subrectangles, and for each of these $H(a;b)$ is calculated. Weighted, by the area of the corresponding subrectangle, means of these yield $\bar{\gamma}(u_i;V)$, apart from the nugget effect C in Equation 3.8. Then this nugget effect, which is a constant value for all sample points in V , is added to the weighted mean $\bar{H}(a;b)$ to obtain $\bar{\gamma}(u_i;V)$.

Solving Equations 3.17a and b yields the kriging weights, which are presented in Appendix B.2 for each of the three areas and for each month separately. All weights are positive. With all sample points inside V , negative weights are only to be expected in point interpolation if shadow effects occur. The kriging weights for January and for August, and the arithmetic mean weights and Thiessen weights are presented in Table 3.3.

Kriging weights tend to correlate well with the area of the Thiessen polygons, especially when the nugget effect \hat{C} of the semi-variogram is relatively unimportant. The kriging weights are equal to the arithmetic mean weights, if $\hat{\alpha}_1 = 0$. Differences in kriging weights for maxima of daily rainfall in different months are rather small.

Table 3.3. Kriging weights for predicting mean areal rainfall for monthly maxima of daily rainfall for three areas in the Netherlands¹

Area 1				Area 2				Area 3			
KNMI code no.	<u>Kriging</u> Jan. Aug.	Thies- sen		KNMI code no.	<u>Kriging</u> Jan. Aug.	Thies- sen		KNMI code no.	<u>Kriging</u> Jan. Aug.	Thies- sen	
223	.0904	.0833	.0345	733	.0477	.0714	.0537	542	.0826	.0842	.1036
225	.0877	.0913	.1171	736	.0709	.0909	.0471	543	.0934	.0907	.0804
226	.0750	.0751	.0790	743	.0623	.0820	.0604	558	.0739	.0766	.0959
229	.0547	.0514	.0458	746	.1064	.0972	.0684	564	.0904	.0897	.0634
230	.0735	.0719	.0786	749	.0763	.0737	.0834	565	.0623	.0573	.0480
233	.0807	.0784	.0950	751	.1515	.1054	.1750	567	.0983	.1011	.0937
435	.0751	.0689	.0616	752	.1821	.1160	.1987	570	.1051	.1119	.1478
436	.0671	.0665	.0228	754	.0376	.0596	.0386	571	.0933	.0988	.1065
437	.1143	.1187	.1162	755	.0979	.0838	.1054	573	.0947	.0936	.0840
438	.1106	.1176	.1406	756	.0658	.0807	.0652	578	.0955	.1000	.1166
441	.1082	.1114	.1453	758	.0624	.0751	.0578	579	.0581	.0522	.0361
454	.0628	.0605	.0636	760	.0391	.0642	.0464	580	.0524	.0438	.0241

¹ Arithmetic mean weights would be 0.0833 regardless of month or area.

Mean areal rainfall predicted by each of the three methods can be compared by evaluating their prediction variances. When predicting mean values over an area, the prediction variance equals

$$\sigma_E^2 = 2 \sum_{i=1}^N \bar{y}(u_i; V) - \bar{y}(V; V) - \sum_{i=1}^N \sum_{j=1}^N \lambda_i \lambda_j \bar{y}(u_i - u_j). \quad (3.20)$$

In comparing Equation 3.20 with Equation 2.22, it should be noted that for a point V, $\bar{y}(V; V)$ vanishes. The resulting minimum variance σ_K^2 of the kriging prediction equals (see Equation 2.24)

$$\sigma_K^2 = \sum_{i=1}^N \lambda_i \bar{y}(u_i; V) + \mu - \bar{y}(V; V), \quad (3.21)$$

or in matrix notation, following Corsten (1982)

$$\sigma_K^2 = -\bar{y}(V;V) + r' \Gamma^{-1} r - (1 - 1_N' \Gamma^{-1} r) (1_N' \Gamma^{-1} 1_N)^{-1} (1 - 1_N' \Gamma^{-1} r), \quad (3.22)$$

where (as in Equation 2.33) the last term is closely related to the variance of the estimate of the stationary expectation $E[Z_V]$, and the sum of the remaining terms on the right-hand side is an estimate of the residual variance of Z_V with regard to the best linear approximation. Note that r in Equation 3.22 is r from Equation 3.17: $r = \bar{y}(u_1; V)$.

To calculate σ_E^2 and σ_K^2 , use has been made of Equations 3.20 and 3.22, respectively. The $\bar{y}(u_1; V)$ in Equation 3.20, denoted as r in Equation 3.22, have been obtained previously. To calculate $\bar{y}(V; V)$, the auxiliary function $F(a; b)$ has been used (Journel and Huijbregts, 1978; p. 113)

$$\begin{aligned} F(a; b) = & (a^2 + b^2)^{\frac{1}{2}} \left(\frac{1}{5} - \frac{1}{15} \frac{a^2}{b^2} - \frac{1}{15} \frac{b^2}{a^2} \right) + \frac{1}{15} \left(\frac{a^3}{b^2} + \frac{b^3}{a^2} \right) + \\ & + \frac{1}{6} \frac{a^2}{b} \ln \{ (b + (a^2 + b^2)^{\frac{1}{2}}) / a \} + \frac{1}{6} \frac{b^2}{a} \ln \{ (a + (a^2 + b^2)^{\frac{1}{2}}) / b \}. \end{aligned} \quad (3.23)$$

The results are presented in Table 3.4. In most cases the Thiessen mean prediction variance $\sigma_{E,T}^2$ is less than $\sigma_{E,A}^2$, the arithmetic mean prediction variance. The arithmetic mean can be a very inefficient predictor, if a region is characterized by a few very large Thiessen polygons. If, however, there is virtually no spatial coherence (high values of $\hat{C}/\hat{\sigma}_1$ in Table 3.2), then areal rainfall is more efficiently predicted by the arithmetic mean than by the Thiessen method.

Table 3.4. Prediction variances σ_E^2 (mm^2) and efficiencies (%) with respect to the minimum variance σ_K^2 for three predictors of areal mean values for monthly maxima of daily rainfall for three areas in the Netherlands

Month	Area 1					Area 2					Area 3				
	Arithmetic		Thiessen		Kriging	Arithmetic		Thiessen		Kriging	Arithmetic		Thiessen		Kriging
	mean					mean					mean				
	$\sigma_{E,A}^2$	eff.	$\sigma_{E,T}^2$	eff.	σ_K^2	$\sigma_{E,A}^2$	eff.	$\sigma_{E,T}^2$	eff.	σ_K^2	$\sigma_{E,A}^2$	eff.	$\sigma_{E,T}^2$	eff.	σ_K^2
Jan.	0.27	87	0.27	87	0.23	0.83	49	0.43	94	0.40	0.53	89	0.51	92	0.47
Feb.	0.25	89	0.25	87	0.22	0.33	90	0.35	85	0.30	0.31	75	0.25	95	0.23
March	0.29	82	0.27	88	0.23	0.30	83	0.28	88	0.25	0.27	64	0.18	97	0.17
April	0.40	75	0.34	87	0.30	0.65	37	0.26	93	0.24	0.58	83	0.51	94	0.48
May	0.81	87	0.81	87	0.71	1.00	37	0.39	93	0.37	1.20	79	1.00	95	0.95
June	1.02	77	0.90	87	0.79	2.08	76	1.77	90	1.59	1.98	84	1.77	94	1.66
July	2.75	90	2.84	87	2.48	3.85	49	2.03	94	1.90	3.14	80	2.65	94	2.51
Aug.	6.21	83	5.85	88	5.13	4.69	95	5.42	82	4.45	3.15	80	2.69	94	2.53
Sept.	1.79	86	1.76	88	1.54	2.99	68	2.23	92	2.04	1.32	77	1.07	95	1.02
Oct.	0.92	82	0.85	88	0.75	2.26	52	1.26	94	1.18	0.69	72	0.52	96	0.50
Nov.	0.65	76	0.57	87	0.50	0.65	95	0.75	82	0.62	0.45	84	0.40	94	0.38
Dec.	0.68	94	0.73	87	0.63	0.79	100	1.04	76	0.79	0.66	99	0.75	88	0.66

Denote the kriging prediction of mean areal rainfall for a maximum in month i and year j by $\hat{x}_{i,j}^K$, and let $\hat{x}_{i,j}^T$ and $\hat{x}_{i,j}^A$ be the Thiessen and arithmetic mean predictions, respectively. The latter two predictions have been compared with the kriging predictions by calculating differences $V_{i,j}$ according to

$$V_{i,j} = \hat{x}_{i,j}^K - \hat{x}_{i,j}^T, \quad (3.24a)$$

or

$$V_{i,j} = \hat{x}_{i,j}^K - \hat{x}_{i,j}^A, \quad (3.24b)$$

respectively. The mean $V_{i.} = \sum_j V_{i,j} / n$, where n is the number of years of record gives an indication of possible systematic differences between kriging predictions and the Thiessen and arithmetic mean predictions. The relative magnitude of such differences may be obtained from, for example

$$V_{i.}^! = \frac{1}{n} \sum_{j=1}^n \{ \hat{x}_{i,j}^K - \hat{x}_{i,j}^T / \hat{x}_{i,j}^K \}, \quad (3.25)$$

where

n : number of years of record ($n=29$).

The results are presented in Table 3.5.

Table 3.5. Absolute differences V_i (mm) and relative differences V_i' (%) between kriging predictions of mean monthly maximum rainfall, and Thiessen and arithmetic mean predictions for three areas in the Netherlands

Month	Area 1				Area 2				Area 3			
	Thiessen		Arithmetic		Thiessen		Arithmetic		Thiessen		Arithmetic	
			mean				mean				mean	
	V_i	V_i'	V_i	V_i'	V_i	V_i'	V_i	V_i'	V_i	V_i'	V_i	V_i'
Jan.	-0.34	1.21	0.70	1.14	0.21	0.97	0.68	3.03	-0.26	0.85	0.88	1.09
Feb.	-0.58	1.38	0.74	1.10	-0.54	1.53	-0.31	1.98	-0.52	0.85	0.83	1.49
March	-1.13	1.28	0.67	1.81	-0.68	1.54	-0.02	1.90	-0.32	0.68	1.61	1.91
April	-0.24	1.28	0.74	1.67	-0.15	0.76	1.93	5.29	-0.95	1.66	1.17	2.39
May	-0.45	1.89	0.88	1.58	-0.17	1.51	1.78	7.41	-2.10	1.76	2.86	2.89
June	0.66	1.57	2.46	2.33	-0.58	2.15	-2.04	4.54	-0.08	1.78	-1.48	2.08
July	-1.90	2.39	1.21	2.94	-0.29	1.56	-3.21	7.80	-1.12	2.10	-1.21	2.26
Aug.	-3.10	2.54	3.95	3.99	-0.46	3.53	-1.25	3.03	0.10	1.58	2.58	2.89
Sept.	-0.34	1.89	1.00	2.18	0.98	1.66	-1.20	4.00	-0.02	0.78	1.10	1.95
Oct.	-0.57	2.19	0.49	1.85	-0.42	1.27	-2.06	4.82	-0.32	1.26	1.39	2.02
Nov.	-1.59	1.32	-0.59	1.22	-1.32	2.20	0.35	1.20	-0.76	0.92	0.96	1.13
Dec.	-0.60	1.14	1.10	1.06	-0.46	2.93	-0.04	0.45	-1.52	1.59	0.61	0.51

Thus, as reported earlier by Delhomme (1978), the differences between kriging and Thiessen predictions of areal rainfall are rather small. Results of the arithmetic mean predictor are less satisfactory. In the present application, the Thiessen predictions tend to be higher than the respective kriging predictions, and the arithmetic mean predictions tend to be lower.

Although in general the kriging predictions do not differ greatly from the Thiessen and arithmetic mean predictions (Table 3.5), the efficiency of the other two predictors can be quite low. In

August, when prediction variances are highest, the efficiency of the Thiessen predictor is 0.88, 0.82, and 0.94 for areas 1, 2, and 3, respectively; and for the arithmetic mean predictor 0.83, 0.95, and 0.80 for areas 1, 2, and 3, respectively. The efficiency of the Thiessen predictor does not vary very much for the three areas, but that of the arithmetic mean predictor does.

3.3. ARF FOR DAILY RAINFALL AND ITS DEPENDENCE ON LOCATION, SEASON, AND RETURN PERIOD

In Section 3.3.1, methods to estimate ARF are presented and estimates of ARF for three areas in the Netherlands are presented in Section 3.3.2. Finally, in Section 3.3.3 the variance of ARF_{24} is estimated, in order to determine whether the various methods for estimating ARF produce different estimates of ARF_{24} . This variance is also used in the discussion on the dependence of ARF on certain factors.

As defined by Equation 3.1, ARF is

$$ARF(A,D,T) = x_A(D,T)/x_S(D,T),$$

implying that ARF is at least a function of duration of rainfall D , of return period T , and of areal size A . Other factors likely to effect ARF are location, season, and storm type. In this discussion D is fixed at 24-hour intervals where observations were taken only at specified times, at 7.55 h UTC daily. Thus, attention is restricted to location, season, and return period, although the results also indicate that there is a decrease in ARF with areal size.

The degree to which ARF depends on location is not certain. On the one hand, ARF values as determined for the United Kingdom (NERC, 1975; Vol. 2) have been recommended for use in countries as far apart as the Netherlands (Buishand and Velds, 1980) and New Zealand (Tomlinson, 1980); and values determined for the USA (USWB, 1957-1960) have been recommended for use in Australia (Pattison (ed.), 1977). On the other hand, Bell (1976) has concluded that for the

United Kingdom, there may be a slight tendency for ARF_{24} to increase with latitude. For the USA, Myers and Zehr (1980) suggest that ARF is dependent on location. Thus it would seem that there are substantial differences in ARF_{24} values for very distinct climatological regions. This is supported by the comparatively low values of ARF_{24} for several tropical African countries reported by Vuillaume (1974). The dependence of ARF_{24} on location is considered in Section 3.3.3 particularly with reference to three areas in the Netherlands of approximately equal areal size. Estimates of ARF_{24} are compared with those for other countries.

The dependence of ARF on season has received little attention. From the effect of climate on ARF already mentioned, it may be inferred that there is a seasonal effect on ARF_{24} . In this section consideration is given to whether ARF_{24} varies with season and whether annual maxima of both point and areal rainfall occur in the same season.

The effect of return period on ARF has been investigated by Bell (1976), using data for the United Kingdom. In Bell's study, which was a follow-up to NERC (1975) in which it was assumed that the dependence of ARF on return period was of no practical value, evidence was found for a decrease in ARF with return period. Therefore, in the present study it was decided to investigate the dependence of ARF on frequency of exceedance.

3.3.1. *Methods to estimate ARF*

In this section, methods to estimate ARF are discussed which are based on annual maxima series of both point and areal rainfall, on POT series of both point and areal rainfall, and on the marginal distribution of point rainfall, respectively. Methods used to estimate ARF in previous studies in the Netherlands are also discussed.

a. Estimation of ARF from annual maxima series

Two methods to estimate ARF from annual maxima series are described, the USWB (1957-1960) and the NERC (1975) method. Neither method uses the complete probability distributions of annual maxima, but

only their expectations and, consequently, the exceedance probabilities of the expectations. If, for instance the annual maxima follow a Gumbel distribution, then the ARF values correspond to a 2.33-year return period. In the following discussion on both methods, N is the total number of rainfall stations in a region, and n is the length of the period of record (year).

In the first of these methods (USWB, 1957-1960), the maximum value $x_A(j)$ in year j of mean areal rainfall of a given duration is determined. The mean of the annual maxima of areal rainfall is denoted by \bar{x}_A . For all rainfall stations i ($i=1, \dots, N$), the maximum value $x_{S,i}(j)$ in year j of point rainfall of this duration is determined. The mean of the annual maxima of point rainfall at location i is denoted by $\bar{x}_{S,i}$. The areal mean of the annual maxima of point rainfall is calculated as

$$\bar{x}_S = \frac{1}{N} \sum_{i=1}^N \bar{x}_{S,i}.$$

Thus, ARF is estimated as

$$\text{ARF} = \bar{x}_A / \bar{x}_S.$$

In the second method (NERC, 1975), for each year j , the maximum value $x_A(j)$ of areal rainfall of a given duration is determined, and for all rainfall stations the simultaneous point rainfall is denoted by $x'_{S,i}(j)$ ($i=1, \dots, N$). For all rainfall stations i the maximum value $x_{S,i}(j)$ in year j of point rainfall of this duration is determined. For each pair (i,j) the following ratio is calculated

$$q(i,j) = x'_{S,i}(j) / x_{S,i}(j).$$

Thus, ARF is estimated as

$$\text{ARF} = \frac{1}{N} \sum_{i=1}^N \frac{1}{n} \sum_{j=1}^n q(i,j) / (nN).$$

b. Estimation of ARF from peaks-over-threshold (POT) series

Bell (1976) used the following method to estimate ARF from POT series. The frequency curves (rainfall versus return period) of peaks of point rainfall of a given duration for each rainfall station are determined. The point rainfall frequency curve is then derived by averaging these curves. Also, the areal rainfall frequency curve for this duration of rainfall is determined. The estimate of ARF for a given return period is the ratio of the ordinates of the areal and point rainfall frequency curve, respectively, corresponding to that return period. This method makes full use of the probability distribution of peaks.

c. Estimation of ARF from the marginal distribution of point rainfall

Estimation of ARF from the marginal distribution of point rainfall was first suggested by Roche (1963). In contrast to the methods described above, which require data from relatively dense, rainfall measuring networks in order to predict areal rainfall, this method and that of Rodríguez-Iturbe and Mejía (1974), only use point rainfall at paired sample points. However, Roche's method is rather complicated and in a subsequent publication Brunet-Moret and Roche (1966) have proposed another method which makes use of the marginal distribution of both point and areal rainfall. This method which has been used by Vuillaume (1974) and Le Barbe (1982), counts the number of occurrences of pairs of (x_A, x_S) values in certain classes of rainfall depth. This leads to a description of the empirical bivariate (x_A, x_S) frequency distribution. Adding up over x_S classes gives the empirical marginal frequency distribution of areal rainfall, and adding up over x_A classes gives the empirical marginal frequency distribution of point rainfall.

As data sets which permit the calculation of areal rainfall are usually restricted in record length, but rather long records of point rainfall are likely to be available, Brunet-Moret and Roche recommend that the empirical marginal frequency distribution of point rainfall be corrected as follows. The longest rainfall record

available within the region should be used to fit a pdf of point rainfall according to a certain model, thus permitting the estimation of quantiles of point rainfall: $\hat{x}_{S,p}$. This pdf should then be used to replace, for each class of point rainfall depth, the observed number of point rainfalls with the expected number. As a consequence, the number of observed areal rainfalls is also corrected. Then the number of exceedances of a certain threshold value of x_A can easily be determined by integrating the corrected bivariate frequency distribution. The number of exceedances of this particular threshold value of x_A is then transformed into a quantile estimate: $\hat{x}_{A,p}$. Thus ARF, is estimated as

$$ARF = \hat{x}_{A,p} / \hat{x}_{S,p}.$$

Another method for estimating ARF that uses essentially the marginal distribution of point rainfall is that used by Rodríguez-Iturbe and Mejía (1974), and Buishand (1977b,c). Rainfall at a point with co-ordinate vector u during period t is denoted by $x_S(u,t)$. Rodríguez-Iturbe and Mejía assumed that the point rainfall process $\{x_S(u,t)\}$ has expectation μ_S and variance σ_S^2 , and is stationary and isotropic. The volume of rainfall $\underline{h}(t)$ over the region V with area A is

$$\underline{h}(t) = \int_V x_S(u,t) du.$$

Furthermore,

$$E[\underline{h}(t)] = \mu_A A \quad (\text{with } \mu_A = E[x_A]).$$

Time-space covariance is

$$\begin{aligned} \text{cov}[\underline{h}(t), \underline{h}(t+\Delta t)] &= E[\underline{h}(t)\underline{h}(t+\Delta t)] - \{E[\underline{h}(t)]\}^2 \\ &= E[\int_V x_S(u_1,t) du_1 \int_V x_S(u_2,t+\Delta t) du_2] - \mu_A^2 A^2 \\ &= \int_V \int_V \{E[x_S(u_1,t)x_S(u_2,t+\Delta t)] - \mu_A^2\} du_1 du_2. \end{aligned}$$

If $\Delta t=0$,

$$\text{cov}[\underline{h}(t), \underline{h}(t)] = \text{var}[\underline{h}(t)] = \sigma_h^2 = \int_V \int_V \{E[x_S(u_1,t)x_S(u_2,t)] - \mu_A^2\} du_1 du_2.$$

Because the rainfall process is stationary, $\mu_S = \mu_A$. Consequently,

$$\begin{aligned}\sigma_h^2 &= \int_V \int_V \{E[\underline{x}_S(u_1, t) \underline{x}_S(u_2, t) - \mu_S^2] du_1 du_2 \\ &= \sigma_S^2 \int_V \int_V r(u_1; u_2) du_1 du_2,\end{aligned}\quad (3.26)$$

where

$r(u_1; u_2)$: spatial correlation coefficient between rainfall at points with co-ordinate vector u_1 and u_2 , respectively.

Consequently,

$$\sigma_h^2 = A^2 \sigma_S^2 \bar{r}(V; V), \quad (3.27)$$

and

$$\text{var}[\underline{x}_A] = \sigma_A^2 = \sigma_S^2 \bar{r}(V; V), \quad (3.28)$$

where

$\bar{r}(V; V)$: mean of the correlation coefficient between rainfall at points, each independently sweeping the area V .

If the point rainfall process is Gaussian, the areal process will also be Gaussian, and as implied in Equation 3.28, a reduction factor equal to $[\bar{r}(V; V)]^{1/2}$ will relate identical return periods. This reduction factor does not vary with return period.

Unlike Rodríguez-Iturbe and Mejía, Buishand (1977c) assumed that both point and areal rainfall follow a gamma distribution with expectation and variance μ_S and σ_S^2 , and μ_A and σ_A^2 , respectively, and

$$\mu_A = \mu_S, \quad (3.29a)$$

$$\sigma_A^2 = f \sigma_S^2. \quad (3.29b)$$

Furthermore, instead of $f = \bar{r}(V; V)$, Buishand (1977c) uses the approximation $f = r(E[h])$.

ARF is estimated by Buishand (1977c) by fitting for each month of the year, a Gumbel distribution to the monthly maxima series, and by determining the point rainfall $\hat{x}_{S,p}$ for the relevant rainfall duration and return period. Then by using the gamma distribution fitted to the point rainfalls by the method of moments,

$$\Pr\{\underline{x}_S \leq \hat{x}_{S,p}\} \quad (3.30)$$

is determined. The gamma distribution for areal rainfall, with parameters determined by Equation 3.29a and Equation 3.29b, is used to find $\hat{x}_{A,p}$ according to

$$\Pr\{\underline{x}_A \leq \hat{x}_{A,p}\} = \Pr\{\underline{x}_S \leq \hat{x}_{S,p}\}.$$

Thus, ARF is estimated as

$$ARF = \hat{x}_{A,p} / \hat{x}_{S,p}.$$

Buishand's method is used in this study with the following minor modifications:

- use is made of POT series which are assumed to be exponentially distributed;
- use is made of $f = \bar{r}(V;V)$, although in this case with a linear correlation-distance function $r(h)$, both $f = \bar{r}(V;V)$ and $f = r(E[h])$ yield the same result;
- application of the ML estimation procedure of the parameters of the gamma distribution of point rainfalls, as given in Buishand (1977a).

d. Methods used to estimate ARF in earlier studies in the Netherlands

Statistical areal reduction factors for the Netherlands have been estimated from daily rainfall data over the 1932-1956 period by Kraijenhoff (1963). For a group of 30 rainfall stations evenly distributed throughout the Netherlands, areal rainfall has been predicted by the isohyet method for circular areas of 10, 50, 100, 250, and 500 km² around these stations for summer days with rain-

fall in excess of 40 mm at least at one of the stations. For each areal size considered, areal rainfall was plotted as a function of the point rainfall of equal ranking on double logarithmic paper. By the method of least squares, straight lines were fitted (Figure 3.7). Along each line in Figure 3.7, ARF decreases with increasing rainfall depth, and therefore with increasing return period. This method is somewhat similar to that of Bell (1976), described earlier.

3.3.2. *Estimates of ARF_{24} for three areas of 1000 km² in the Netherlands*

a. ARF_{24} estimated from annual maximum series

For the areas 1, 2, and 3 indicated in Figure 3.1, ARF_{24} has been estimated by both the USWB (1957-1960) and the NERC (1975) method, for the summer, winter, and the complete year. The results are presented in Table 3.12.

b. ARF_{24} estimated from POT series

For the areas 1, 2 and 3 indicated in Figure 3.1, POT series have been extracted from the daily point and areal rainfall records, for summer, winter, and the complete year. Thresholds have been selected that resulted on average in two peaks per year or season. In order to assure independence of the peaks, these have to be separated by at least one day without rain in the area considered. The mean POT series of point rainfall for a given area were obtained from the means of peaks of equal ranking of all records of point rainfall for that area. Exponential probability distribution functions according to

$$f(q) = \frac{1}{\beta} \exp[-(q-q_0)/\beta], \quad (3.31)$$

where

q_0, β : positive parameters of location and scale, respectively,

were fitted to the POT series of areal rainfall and to the mean POT series of point rainfall. As in Section 2.2, ML estimates of β and q_0 in Equation 3.31 were calculated according to Equation 2.2 and 2.3 and the fit of the exponential probability distribution functions was checked by calculating realizations of the test statistic \underline{T} according to Equation 2.8. The realizations of \underline{T} and the ML estimates $\hat{\beta}$ and \hat{q}_0 are presented in Table 3.6. The exponential distribution seems to fit the POT series sufficiently well. Plots of the empirical distribution functions and the fitted distribution functions are presented in Figure 3.8. The plotting positions are according to Equation 2.4.

Table 3.6. ML estimates $\hat{\beta}$ (mm) and \hat{q}_0 (mm) from Equation 3.31 and realizations of the test statistic \underline{T} to assess the fit of the exponential distribution function to POT series of areal and point rainfall in three areas of the Netherlands

	Areal rainfall			Point rainfall		
	Area			Area		
	1	2	3	1	3	3
Summer						
$\hat{\beta}$	5.8	6.2	7.9	7.7	7.8	10.3
\hat{q}_0	18.4	17.6	18.0	19.4	19.6	19.3
T	119.7	136.0	95.9	100.5	109.3	98.1
Winter						
$\hat{\beta}$	6.2	6.3	5.2	6.5	6.9	5.5
\hat{q}_0	15.6	15.0	15.8	16.5	15.8	16.6
T	87.6 ^{oo}	135.7	94.5	89.4	105.5	95.0
Year						
$\hat{\beta}$	6.2	5.6	7.9	7.9	7.3	9.4
\hat{q}_0	21.2	21.5	20.6	22.6	23.2	22.6
T	103.9	133.9	100.0	100.3	106.7	94.6

^{oo} Indicates values inside the critical region for $\alpha = 0.05$.

ARF values can now be estimated from the frequency curves

$$\hat{q} = \beta \ln(T/T_0) + \hat{q}_0, \quad (3.32)$$

where

$1/T_0$: mean annual number of threshold exceedances (=2).
Given T , β and \hat{q}_0 being estimated, and $1/T_0$ being fixed in advance, the peaks of areal and point rainfall, \hat{q}_A and \hat{q}_S , respectively, can be estimated, and ARF is estimated as their ratio. In Table 3.12, ARF₂₄ estimates for a 1.78-year return period are presented, as return periods T_p for peak exceedances are related to return periods T_a for annual maxima by $T_a \cong 1/[1 - \exp(-1/T_p)]$ (Langbein, 1949). This result is exact if the annual number of exceedances is Poisson distributed (Beran and Nozdryn-Plotnicki, 1977). ARF values corresponding to various other return periods are presented in Table 3.7. In Table 3.7, ARF₂₄ for $T = \infty$ has been estimated as the ratio of the parameter estimates β in Equation 3.32 for areal and point rainfall, respectively.

Table 3.7. ARF₂₄ estimated according to the method of Bell (1976) for three areas in the Netherlands for the summer, the winter and the complete year

Return period T	Summer			Winter			Year		
	Area			Area			Area		
	1	2	3	1	2	3	1	2	3
0.5	0.950	0.897	0.933	0.950	0.953	0.953	0.938	0.924	0.912
1	0.906	0.876	0.889	0.951	0.944	0.949	0.909	0.897	0.895
2	0.877	0.862	0.864	0.951	0.939	0.947	0.889	0.877	0.884
5	0.852	0.849	0.844	0.952	0.934	0.944	0.871	0.859	0.874
10	0.839	0.843	0.833	0.952	0.932	0.943	0.861	0.849	0.869
25	0.826	0.836	0.823	0.952	0.929	0.941	0.851	0.839	0.864
∞	0.747	0.797	0.771	0.954	0.915	0.932	0.787	0.769	0.834

c. ARF₂₄ estimated from the marginal distribution of point rainfall

For each month of the year and for each area, the empirical distribution functions of daily areal and point rainfall were determined.

Those of point rainfall were determined from all rainfall records within the area considered. Shifted rainfall amounts were not considered, although in many applications it is advisable to do so (Buishand, 1977a). But then, in view of the assumption made in Equation 3.29a, areal rainfall should have been calculated as a linear combination of shifted point rainfalls instead of, more logically, a shifted linear combination of point rainfalls. Rainfall is assumed to occur in the centre of the measurement intervals.

Areal rainfall was predicted by kriging with the IRF-0 theory. Sample semi-variances of daily point rainfall were determined for all days with at least 0.5 mm rainfall at one or more rainfall stations. The sample semi-variances and the fitted ($H \leq L/2$) linear semi-variance models for January and for August are presented in Figures 3.9 to 3.11. OLS estimates of C and α_1 in Equations 3.8 are presented in Table 3.8. The resulting kriging weights are listed in Appendix B.3 for each of the three areas and for each month separately.

Table 3.8. OLS estimates \hat{C} (mm^2) and $\hat{\alpha}_1$ ($\text{mm}^2 \cdot \text{km}^{-1}$) of the linear semi-variogram model, and ratio $\hat{C}/\hat{\alpha}_1$ (km) for all days with at least 0.5 mm of rainfall at one or more rainfall stations for three areas in the Netherlands; comparison between the mean point rainfall $\hat{\mu}_S$ (mm) and the mean kriging predictions of areal rainfall $\hat{\mu}_A$ (mm)

Month	Area 1					Area 2					Area 3				
	\hat{C}	$\hat{\alpha}_1$	$\hat{C}/\hat{\alpha}_1$	$\hat{\mu}_S$	$\hat{\mu}_A$	\hat{C}	$\hat{\alpha}_1$	$\hat{C}/\hat{\alpha}_1$	$\hat{\mu}_S$	$\hat{\mu}_A$	\hat{C}	$\hat{\alpha}_1$	$\hat{C}/\hat{\alpha}_1$	$\hat{\mu}_S$	$\hat{\mu}_A$
Jan.	0.55	0.060	9.2	2.18	2.18	0.55	0.056	9.8	1.96	1.97	0.71	0.068	10.5	2.31	2.33
Feb.	0.43	0.070	6.2	1.74	1.75	0.71	0.038	18.7	1.66	1.66	0.63	0.062	10.0	1.88	1.89
March	0.48	0.060	8.1	1.53	1.53	0.51	0.046	11.2	1.46	1.46	0.53	0.066	8.0	1.73	1.75
April	0.56	0.078	7.3	1.58	1.59	0.48	0.082	5.8	1.45	1.45	0.79	0.132	6.0	1.90	1.91
May	0.89	0.162	5.5	1.50	1.51	0.77	0.132	5.8	1.44	1.44	1.92	0.227	8.5	1.94	1.95
June	2.04	0.263	7.7	1.78	1.81	2.64	0.184	14.3	1.89	1.86	3.66	0.328	11.2	2.29	2.30
July	3.01	0.370	8.1	2.35	2.36	4.03	0.331	12.2	2.20	2.16	5.40	0.369	14.7	2.74	2.77
Aug.	3.46	0.736	4.7	2.86	2.88	7.11	0.392	18.1	2.58	2.55	4.31	0.443	9.7	2.96	2.98
Sept.	2.69	0.400	6.7	2.67	2.67	2.52	0.378	6.7	2.34	2.35	1.55	0.289	5.4	2.26	2.28
Oct.	1.29	0.238	5.4	2.57	2.58	1.69	0.222	7.6	2.41	2.41	1.49	0.090	16.5	2.11	2.12
Nov.	0.82	0.137	6.0	2.88	2.88	0.82	0.115	7.1	2.66	2.69	1.12	0.070	16.0	2.50	2.52
Dec.	0.90	0.085	10.6	2.55	2.56	1.30	0.035	36.8	2.21	2.21	1.28	0.058	22.0	2.65	2.66

A comparison of Tables 3.8 and 3.2 shows that both \hat{C} and $\hat{\sigma}_1$ tend to be smaller in Table 3.8. As $\hat{C}/\hat{\sigma}_1$ varies less between months in Table 3.8, the kriging weights in Appendix B.3 show less variation throughout the year than their counterparts in Appendix B.2 for monthly rainfall maxima. As there are no months with very low $\hat{C}/\hat{\sigma}_1$ values, the variation between rainfall stations is also less, as shown in Appendix B.3. In months with similar $\hat{C}/\hat{\sigma}_1$ values in Tables 3.2 and 3.8, the resulting kriging weights are also more or less the same (area 1: May, July; area 2: June; area 3: June). Prediction of the areal rainfall by kriging implies that $\hat{\mu}_A \neq \hat{\mu}_S$, even though the assumption in Equation 3.29a still holds. The differences are negligible, however, see also Table 3.8.

Gamma probability distribution functions have been fitted to the empirical distribution functions of point and areal rainfall according to

$$f(x) = \lambda(\lambda x)^{v-1} \exp(-\lambda x) / \Gamma(v), \quad (0 < x < \infty) \quad (3.33)$$

where

$\Gamma(\cdot)$: the gamma function

λ, v : positive parameters of scale and shape, respectively.

As a first approximation, the parameters λ and v in Equation 3.33 have been estimated according to the method of moments (MM)

$$\hat{\lambda} = \bar{x} / s^2, \quad (3.34a)$$

$$\hat{v} = \bar{x}^2 / s^2, \quad (3.34b)$$

where \bar{x} and s^2 are the sample mean and variance, respectively. As MM estimators are very inefficient compared with ML estimators, $\hat{\lambda}$ and \hat{v} have only been used as starting values in the calculation of ML estimates.

If rainfall amounts not exceeding a certain threshold value are counted only, the likelihood $L^*(\lambda, v)$ in accordance with Buishand (1977a) can be expressed as

$$L^*(\lambda, v) = \frac{\lambda^{nv}}{(\Gamma(v))^n} \left\{ \int_0^\epsilon \exp(-\lambda x) x^{v-1} dx \right\}^n \frac{\lambda^{mv}}{(\Gamma(v))^m} \exp(-\lambda \sum_{i=1}^m x_i) \prod_{i=1}^m x_i^{v-1}, \quad (3.35)$$

where

x_i ($i=1, \dots, m$): observations $> \varepsilon$ ($\varepsilon=0.95$ mm)

n : number of observations $< \varepsilon$.

The integral in Equation 3.35 can be approximated for small ε by

$$\int_0^\varepsilon \exp(-\lambda x) x^{v-1} dx \cong \int_0^\varepsilon (1-\lambda x) x^{v-1} dx = \frac{\varepsilon^v}{v} \left(1 - \frac{\lambda v \varepsilon}{v+1}\right). \quad (3.36)$$

For ε equal to 0.95 mm, the resulting relative error in the integral is about 0.1%. The ML estimates, $\hat{\lambda}_S^*$ and \hat{v}_S^* , were calculated by using the Newton-Raphson procedure, as given in Buishand (1977a). The results are presented in Table 3.10.

Parameters of the pdf of areal rainfall were estimated by

$$\hat{\lambda}_A^* = \hat{\lambda}_S^*/f, \quad (3.37a)$$

and

$$\hat{v}_A^* = \hat{v}_S^*/f, \quad (3.37b)$$

where $f = \bar{r}(V;V)$, as in Section 3.3.1. In calculating the reduction factor f , the parameters in the linear correlation-distance function

$$r(h) = \rho_0 + \theta h, \quad (0 \leq \rho_0 \leq 1, \theta \leq 0) \quad (3.38)$$

were estimated for areas 1, 2, and 3. As only distances h less than about 40 km were considered, a linear correlation-distance function has been fitted (Van Montfort, 1968; De Bruin, 1975; Buishand, 1977b). Table 3.9 gives the OLS estimates $\hat{\rho}_0$ and $\hat{\theta}$, $\bar{r}(V;V)$ (calculated with the auxiliary function $F(a;b)$ according to Equation 3.23), and the residual standard deviation s_r . An exponential correlation-distance function $r(h) = \rho_0 \exp(-\theta h)$ did not give a better fit. Plots of the estimated correlation coefficients and the fitted linear models for January and for August are shown in Figures 3.12, 3.13, and 3.14.

With the number of samples in this study, according to Equation 3.12 the following should hold approximately: $s_r \cong 0.006$ (winter) and $s_r \cong 0.015$ (summer). The rather large values of s_r in Table 3.9 are probably caused by autocorrelation and non-normality of the observations. A cube root transformation of the observations resulted in

substantially lower values of s_r : $s_r \cong 0.012$ (winter) and $s_r \cong 0.014$ (summer). Probably because of autocorrelation, winter values of s_r remain high.

Table 3.9. OLS estimates $\hat{\rho}_0(-)$ and $\hat{\theta}$ (km^{-1}), mean correlation coefficients $\bar{r}(V;V)$ (-) according to the linear correlation-distance function (Equation 3.38), and residual standard deviation $s_r(-)$ for daily rainfall for three areas in the Netherlands

Month	Area 1				Area 2				Area 3			
	$\hat{\rho}_0$	$\hat{\theta}$	$\bar{r}(V;V)$	s_r	$\hat{\rho}_0$	$\hat{\theta}$	$\bar{r}(V;V)$	s_r	$\hat{\rho}_0$	$\hat{\theta}$	$\bar{r}(V;V)$	s_r
Jan.	.965	-.0026	.922	.013	.954	-.0025	.907	.014	.967	-.0025	.925	.015
Feb.	.962	-.0024	.922	.016	.962	-.0028	.910	.015	.962	-.0023	.923	.013
March	.963	-.0030	.913	.012	.964	-.0029	.910	.013	.959	-.0030	.909	.015
April	.957	-.0028	.911	.013	.942	-.0029	.887	.027	.957	-.0053	.868	.019
May	.920	-.0045	.846	.037	.908	-.0057	.800	.045	.875	-.0037	.813	.039
June	.922	-.0053	.835	.031	.917	-.0031	.859	.024	.916	-.0057	.820	.037
July	.907	-.0057	.813	.022	.878	-.0046	.791	.046	.910	-.0064	.802	.048
Aug.	.868	-.0068	.756	.058	.853	-.0067	.727	.039	.876	-.0067	.763	.027
Sept.	.916	-.0044	.843	.045	.921	-.0056	.815	.028	.933	-.0053	.843	.027
Oct.	.960	-.0036	.900	.018	.955	-.0036	.888	.017	.966	-.0031	.914	.025
Nov.	.957	-.0030	.907	.018	.963	-.0033	.901	.013	.958	-.0027	.913	.022
Dec.	.956	-.0017	.928	.013	.961	-.0028	.908	.019	.970	-.0020	.936	.014

With $f = \bar{r}(V;V)$ from Table 3.9, the parameters of the pdfs of areal rainfall have been estimated by Equations 3.37a and 3.37b and the results are presented in Table 3.10. The adequacy of the estimates was checked by calculating realizations D_{\max} of the Kolmogorov Smirnov test statistic for single observations $> \epsilon$

$$D_{\max} = \max\{|F_0(x_A) - F_N(x_A)|\}, \quad (3.39)$$

where

$F_0(x_A)$: the fitted gamma cdf

$F_N(x_A)$: the edf according to $F_N(x_A) = k/N$, where k is the number of observations $< x_A$ (multiples of .1 mm), $N = n + m$, and n, m as defined in Equation 3.35.

Realizations D_{\max} of the test statistic are also presented in Table 3.10. Critical values of the test statistic for the exponential distribution were obtained from Pearson and Hartley (1972). This is not quite correct as critical values of the test statistic depend on v . In addition, the term 'test' is somewhat misleading here, as the fit was only assessed for $x_A > \epsilon$. Nevertheless, Figures 3.15 to 3.17 show, together with Table 3.10, that the fit of the gamma distribution function is satisfactory.

Table 3.10. ML parameter estimates $\hat{\nu}_S^*$ (-) and $\hat{\lambda}_S^*$ (mm^{-1}), and $\hat{\nu}_A^*$ (-) and $\hat{\lambda}_A^*$ (mm^{-1}), for the gamma distribution functions of daily point and daily areal rainfall respectively, and realizations D_{\max} of the Kolmogorov Smirnov statistic for the fit of the distribution of areal rainfall for three areas in the Netherlands

Month	Area 1					Area 2					Area 3				
	$\hat{\nu}_S^*$	$\hat{\lambda}_S^*$	$\hat{\nu}_A^*$	$\hat{\lambda}_A^*$	D_{\max}	$\hat{\nu}_S^*$	$\hat{\lambda}_S^*$	$\hat{\nu}_A^*$	$\hat{\lambda}_A^*$	D_{\max}	$\hat{\nu}_S^*$	$\hat{\lambda}_S^*$	$\hat{\nu}_A^*$	$\hat{\lambda}_{\max}^*$	D
Jan.	.330	.148	.358	.160	.017	.330	.164	.364	.181	.017	.327	.138	.354	.149	.033°
Feb.	.245	.137	.265	.149	.023	.265	.156	.292	.171	.015	.252	.131	.273	.142	.024
March	.247	.156	.271	.171	.027	.254	.167	.280	.184	.016	.268	.149	.295	.164	.030
April	.229	.140	.252	.154	.018	.229	.152	.258	.171	.009	.257	.131	.296	.151	.028
May	.189	.122	.223	.144	.017	.229	.152	.286	.190	.021	.230	.116	.283	.143	.021
June	.158	.086	.189	.103	.031	.147	.076	.171	.088	.023	.185	.079	.226	.096	.031
July	.192	.080	.237	.098	.037°	.179	.079	.226	.100	.014	.220	.079	.274	.099	.022
Aug.	.220	.076	.291	.100	.029	.196	.075	.270	.103	.027	.242	.080	.318	.105	.027
Sept.	.189	.070	.224	.083	.030	.185	.077	.227	.094	.026	.201	.087	.239	.103	.030
Oct.	.208	.080	.231	.089	.030	.191	.078	.215	.088	.020	.201	.094	.220	.103	.020
Nov.	.336	.115	.370	.127	.032	.312	.115	.347	.128	.031	.315	.123	.345	.135	.018
Dec.	.319	.123	.344	.133	.026	.301	.133	.332	.146	.030	.286	.107	.305	.114	.022

° Indicates values inside the critical region for $\alpha = 0.10$.

°° Indicates values inside the critical region for $\alpha = 0.05$.

The adequacy of the method for obtaining the pdf of areal rainfall having been assessed, ARF values representative for the whole of the Netherlands were determined by combining the point rainfall records from the three areas. Then, ML estimates $\hat{\nu}_S^*$ and $\hat{\lambda}_S^*$ of the pdf according to Equation 3.33 of point rainfall were determined. Estimates $\bar{\rho}_0$ and $\bar{\theta}$ of a mean correlation-distance function according to Equation 3.38 were determined as the arithmetic mean of the $\hat{\rho}_0$ and $\hat{\theta}$ values in Table 3.9. As pointed out in Section 3.3.1, POT series of point rainfall are required for the determination of $\Pr\{x_S < x_{S,p}\}$ (Equation 3.30). The POT series were assumed to have an exponential distribution. The mean number of peaks per month was chosen to be one. The parameters q_0 and β of the exponential distribution functions, and also their fit were assessed in the usual way. The results are presented in Table 3.11; for January and for August the POT series and the fitted exponential distributions are shown in Figure 3.18.

Table 3.11. Parameter values for estimating ARF_{24} , realizations of the lack of fit statistic \underline{T} with respect to the exponential distribution

Period	\hat{v}_S^* (-)	$\hat{\lambda}_S^*$ (mm ⁻¹)	$\hat{\rho}_0$ (-)	$\hat{\theta}$ (km ⁻¹)	\hat{q}_0 (mm)	$\hat{\beta}$ (mm)	\underline{T}
Jan.	0.328	0.149	0.962	-0.0025	10.3	4.3	49.8
Feb.	0.253	0.140	0.962	-0.0025	8.4	4.9	53.3
March	0.256	0.157	0.962	-0.0030	8.4	4.2	59.5
April	0.237	0.139	0.952	-0.0037	9.2	4.6	56.0
May	0.214	0.128	0.901	-0.0046	9.2	5.4	51.3
June	0.163	0.080	0.918	-0.0047	12.1	7.7	47.1
July	0.197	0.079	0.898	-0.0056	13.8	9.1	47.3
Aug.	0.219	0.077	0.866	-0.0067	15.5	8.5	51.5
Sept.	0.191	0.077	0.923	-0.0051	13.1	7.9	51.8
Oct.	0.199	0.083	0.960	-0.0034	12.1	8.6	52.8
Nov.	0.321	0.117	0.959	-0.0030	11.3	6.5	62.6
Dec.	0.300	0.120	0.962	-0.0022	10.6	7.2	42.9
Summer	0.194	0.084	0.897	-0.0055	20.1 ¹	8.5 ¹	99.8
Winter	0.265	0.123	0.960	-0.0029	16.8 ¹	5.8 ¹	94.6
Year	0.232	0.105	0.927	-0.0043	23.1 ¹	8.1 ¹	95.9

¹ Corresponding to two threshold exceedances per period, on the average.

The reduction factor was obtained as $\bar{r}(V;V)$ with the parameter estimates from Table 3.11, and estimates \hat{v}_A^* and $\hat{\lambda}_A^*$ were obtained by using Equations 3.37a and 3.37b. For each month separately, ARF_{24} was calculated for areas of 25, 100, 250, and 1000 km², and return periods of 1, 1.78, 5, 10, and 50 years. Figure 3.19 shows the resulting eye-fitted curves for January and for August. Curves for the winter and summer are shown in Figure 3.20, and curves for the complete year including the 0.5-year return period ARF_{24} in Figure 3.21. In Table 3.12, estimates of ARF_{24} from Figure 3.20 and Figure 3.21 are compared with ARF_{24} estimates according to other methods described previously.

Table 3.12. Four estimates of ARF_{24} corresponding to a 2.33-year return period for annual maxima, and to an area of about 1000 km²

Season	Bell ¹ (1976)	NERC ¹ (1975)	USWB ¹ (1957-1960)	Marginal distribution
Summer	0.871	0.853	0.860	0.878
Winter	0.946	0.943	0.951	0.946
Year	0.886	0.866	0.871	0.902

¹ Averaged over the three areas.

3.3.3. Variance of ARF for daily rainfall

Table 3.12 can only be interpreted if the variance of ARF_{24} is known. $Var(ARF_{24})$ was determined according to the method proposed by Bell (1976). If a peak quantile q is estimated by using Equation 3.32, with parameter estimates by Equations 2.2 and 2.3, then the estimation variance can be shown (NERC, 1975; Vol. 1, p. 195) to be

$$var(\hat{q}) = \frac{\beta^2}{n} \left\{ \frac{(1-G)^2}{n-1} + G^2 \right\}, \quad (3.40)$$

where

$$G: \ln(T/T_0).$$

Equation 3.40 was used to estimate the variance of estimates of quantiles of point and areal rainfall, \hat{q}_S and \hat{q}_A , respectively, and

$$var(ARF) = var(\hat{q}_A/\hat{q}_S). \quad (3.41)$$

The variance of this ratio is approximately equal to (Kendall and Stuart, 1977; Vol. 1, p. 247)

$$\{E(\hat{q}_A)/E(\hat{q}_S)\}^2 \{cv^2(\hat{q}_A) + cv^2(\hat{q}_S) - 2cc^2(\hat{q}_A, \hat{q}_S)\}, \quad (3.42)$$

where

$E(\hat{q}_A)$, $E(\hat{q}_S)$: expectation of \hat{q}_A and \hat{q}_S , respectively, for a given return period

cv: coefficient of variation
cc: coefficient of covariation.

A reasonable estimate of $\text{cov}(\hat{q}_A, \hat{q}_S)$ in the coefficient of co-variation appearing in Equation 3.42 is not available, because there are only three areas. Bell (1976), who estimated ARF_{24} with data for nine areas, determined a correlation coefficient r

$$r = \text{cov}(\hat{q}_A, \hat{q}_S) / (\text{var}(\hat{q}_A) \text{var}(\hat{q}_S))^{1/2}, \quad (3.43)$$

where \hat{q} stands for a 'standardized' peak according to

$$\hat{q} = (\hat{q} - \hat{q}_e) / \hat{q}_e,$$

where \hat{q}_e is the estimate of the 'true' or population value q for the given return period, as obtained from the frequency analysis carried out in NERC (1975). The correlation coefficient varied with return period, the minimum value being 0.76. Thus $r=0.70$ and $r=0.80$ were inserted in Equation 3.42 and the standard deviation estimates obtained are given in Table 3.13.

Table 3.13. Standard deviation of ARF_{24} according to Equation 3.42 for different values of the return period T and of the correlation coefficient r in Equation 3.43

r	T	Area 1			Area 2			Area 3		
		Year	Summer	Winter	Year	Summer	Winter	Year	Summer	Winter
0.7	1	0.017	0.019	0.021	0.015	0.018	0.022	0.020	0.023	0.018
	2	0.028	0.030	0.034	0.026	0.030	0.036	0.032	0.036	0.030
	5	0.038	0.040	0.046	0.035	0.040	0.047	0.043	0.046	0.042
	10	0.043	0.045	0.053	0.040	0.046	0.054	0.048	0.050	0.048
	25	0.049	0.049	0.059	0.046	0.051	0.060	0.054	0.055	0.054
0.8	1	0.014	0.016	0.017	0.013	0.015	0.018	0.016	0.019	0.015
	2	0.023	0.025	0.028	0.021	0.025	0.029	0.026	0.029	0.025
	5	0.031	0.033	0.038	0.029	0.033	0.039	0.035	0.037	0.034
	10	0.035	0.037	0.043	0.033	0.037	0.044	0.040	0.041	0.039
	25	0.040	0.040	0.048	0.037	0.042	0.049	0.044	0.045	0.044

Table 3.13 suggests that the standard deviation of ARF_{24} is independent of season, but varies with return period. For a return period of 2 years, it may be safely assumed that the standard deviation of ARF_{24} is 0.03, or about 3 to 3.5%. Thus from Table 3.12 it can be concluded that the various methods for estimating ARF_{24} do not produce practically different results and that the three areas of about the same size do not vary with respect to ARF_{24} . Figure 3.22 shows the estimates of ARF_{24} in this study according to NERC (1975), and the USWB (1957-1960) and NERC (1975) estimates of ARF_{24} as a function of areal size. The difference between the estimates in this study and those of NERC (1975), which stem from a similar climatic region and which were derived by the same method, are about one standard deviation. As can be seen from Table 3.14, differences with earlier estimates of ARF_{24} from Dutch rainfall records are moderately small for large areal sizes.

Table 3.14. Comparison of estimates of ARF_{24} from Dutch rainfall records

Investigator	Rainfall		Area (km^2)	ARF_{24}	ARF_{24} according to Figures 3.19 and 3.20
	Depth (mm)	Period			
Kraijenhoff (1963)	40	Summer	50	0.968	0.915
	40	Summer	250	0.928	0.898
	40	Summer	500	0.918	0.883
Buishand (1977a)	19	July	100	0.926	0.942
	19	July	1000	0.895	0.911
	32	July	100	0.900	0.919
	32	July	1000	0.866	0.879

For small areas the estimates from Figure 3.20 differ considerably from those of Kraijenhoff (1963), see Figure 3.23. When the yearly values of ARF_{24} from Figure 3.21 are compared with those of NERC (1975), differences are also found: for a 1.78-year return period and an area of $25 km^2$, according to NERC (1975), $ARF_{24} = 0.966$, but according to Figure 3.21, $ARF_{24} = 0.946$; for areas of about $150 km^2$ both estimates are the same, and for larger areas the estimates from Figure 3.21 exceed those of NERC (1975).

The low values of ARF_{24} in this study for small areas are probably due to the large discontinuity of the fitted correlation-distance functions at the origin. In a late stage in this study it was realized that such a large discontinuity is not physically plausible. The correlation coefficients for daily rainfall for the three rainfall stations in the Hupsel catchment area, all about 1.5 km apart, are between 0.97 and 0.98. For the rainfall data used in the study of short distance variability of rainfall by Denkema (1970), correlation coefficients for distances of 4 m are about 0.999 (summer), 0.997 (winter), and 0.998 (year).

Thus, it appears that the correlation-distance function should model a smoother decrease of the correlation coefficients at small distances. A possible correlation-distance function could be the mixture of two exponential functions, $r(h) = \rho_0 \exp(-\theta_1 h) + (1 - \rho_0) \exp(-\theta_2 h)$ (see Rhenals-Figueroa et al., 1974; p. 133), to be referred to in the text as double exponential correlation-distance function.

This double exponential correlation-distance function does not provide a much better fit (residual standard deviation for the summer season is 0.025, as against 0.027 for the linear model), but does result in higher ARF_{24} estimates for smaller areas. The resulting ARF_{24} values corresponding to a 1.78-year return period have been plotted in Figure 3.19, 3.20, and 3.21.

These ARF_{24} values have also been plotted for a return period corresponding to a daily rainfall depth of 40 mm in summer in Figure 3.23. For small areas they differ less from those of Kraijenhoff (1963) than the estimates derived under the assumption of a linear correlation-distance function. The higher values of ARF_{24} for all areal sizes in Kraijenhoff (1963) may be due to the fact that areal rainfall was determined by the isohyet method, which implies another way of smoothing. Moreover, his data covered the period 1932-1956 whereas the present study is based on 1951-1979 data. Also, areal rainfall was considered for circular areas of 10, 50, 100, 250, and 500 km², centred around 30 rainfall stations evenly distributed throughout the Netherlands. In the present study, three rectangular areas of 1000 km² have been considered.

When comparing estimates of ARF_{24} for different seasons and return periods, Table 3.7 and Figure 3.20 show, in conjunction with Table 3.13, that ARF_{24} does depend on season and return period. Winter values of ARF_{24} , however, appear to be independent of return period.

Table 3.15 shows that annual maxima of both point and areal rainfall tend to occur in summer, and, averaged over the three areas, the maximum areal rainfall occurs in winter in only 33% of all years, and maxima of point and areal rainfall occur on the same day in 49% of all years. Although winter maxima are generally smaller than summer maxima, Figure 3.24 shows that if the annual maximum occurs in the winter, such maxima are not necessarily small. The differences shown in Figure 3.24 between the three areas may be explained by the fact that areas 1 and 2 are near the coast and area 3 is further inland and somewhat hilly.

Table 3.15. Seasonal distribution (%) of annual maxima of daily point rainfall, given the season of occurrence of the areal maximum for the three areas

Maximum of areal rainfall	Maximum of point rainfall	Area		
		1	2	3
Summer	Summer	89	89	90
	Winter	11	11	10
Winter	Winter	64	67	53
	Summer	36	33	47

3.4. ARF FOR HOURLY RAINFALL

Estimates of ARF_1 are only available for the USA (USWB, 1957-1960) and the United Kingdom (NERC, 1975). It is not surprising that few studies have been carried out on ARF_1 because in comparison with ARF_{24} , methods to estimate ARF_1 require data from dense rainfall measuring networks. Few such networks exist. In the Netherlands during the period October 1969 to October 1974, three rainfall recorders were in operation in the Hupselse Beek experimental

catchment area (5 km^2). In the present study only the first four years of record have been used. With so few data, ARF_1 can only be estimated from the marginal distribution of hourly point rainfall, together with additional data from sources outside the network. The De Bilt series, 1906-1982, were used to obtain both the marginal distribution of hourly point rainfall and the distribution of threshold exceedances, and the Soesterberg series, 1974-1982, for additional data on the correlation-distance function.

In this section, consideration is given to whether the pdf of areal rainfall can be obtained from the pdf of point rainfall by using Equations 3.29a and 3.29b which relate the first two moments of areal and point rainfall (Section 3.4.1). In Section 3.4.2, ARF_1 is estimated and consideration is given to whether estimates of ARF_1 for the Netherlands differ from those for other countries, and whether ARF calculated from the marginal distributions of rainfall varies with duration of rainfall at fixed return period and areal size.

3.4.1. *The distribution of hourly areal rainfall*

In order to investigate whether the pdf of hourly areal rainfall can be obtained from the pdf of hourly point rainfall, firstly the edf of hourly point rainfall was obtained by combining the records of the three rainfall stations in the Hupselse Beek catchment area. To the edf, a gamma distribution function according to Equation 3.33 was fitted, using the procedure set out in Section 3.3.2. As the recorders in the Hupselse Beek catchment area measure rainfall in 0.12 mm units, ϵ in Equation 3.35 was taken to be 0.18 mm. Then, the relative error because of the approximation in Equation 3.36 is about 0.01%. The ML estimates \hat{v}_S^* and $\hat{\lambda}_S^*$ of the parameters in Equation 3.33 are given in Table 3.16.

The edf of areal rainfall, and also the edf of point rainfall were determined from only those hourly periods for which no data were missing. Areal rainfall was estimated by averaging point rainfalls. As the three rainfall stations are evenly distributed throughout the area so that the distance between stations is about the same

(1100 to 1700 m), all stations will receive about the same kriging weights, irrespective of the semi-variogram (but with equal weights in case of a pure nugget effect). Furthermore, a reliable estimate of the semi-variogram seems impossible with only three pairs of sample points, all about the same distance apart. The factor f in Equation 3.29b, relating the variance of areal and point rainfall, was estimated as the mean of the correlation coefficients between hourly rainfalls at the three stations. Table 3.16 gives f in Equation 3.29b and the resulting ML estimates \hat{v}_A^* and $\hat{\lambda}_A^*$ of the parameters in the pdf of hourly rainfall. Realizations D_{\max} of the Kolmogorov Smirnov test statistic are also shown in Table 3.16. Figure 3.25 shows, together with Table 3.16, that the fit of the gamma distribution is satisfactory.

Table 3.16. Estimates $\hat{v}_A^*(-)$ and $\hat{\lambda}_A^*(\text{mm}^{-1})$ of the parameters in the pdf of hourly areal rainfall, obtained from the ML point rainfall parameter estimates $\hat{v}_S^*(-)$ and $\hat{\lambda}_S^*(\text{mm}^{-1})$, and from the variance reduction factor f ; Kolmogorov Smirnov test statistic D_{\max} to assess the fit of the pdf of areal rainfall

Month	\hat{v}_S^*	$\hat{\lambda}_S^*$	f	\hat{v}_A^*	$\hat{\lambda}_A^*$	D_{\max}
Jan.	0.0694	1.240	0.841	0.0825	1.474	0.006
Feb.	0.0574	1.132	0.898	0.0639	1.261	0.004
March	0.0671	0.983	0.924	0.0727	1.064	0.006
April	0.0480	0.486	0.922	0.0521	0.527	0.010
May	0.0329	0.400	0.905	0.0363	0.442	0.005
June	0.0262	0.315	0.889	0.0295	0.355	0.007
July	0.0304	0.293	0.879	0.0346	0.333	0.003
Aug.	0.0162	0.293	0.823	0.0197	0.356	0.006
Sept.	0.0284	0.389	0.859	0.0331	0.453	0.008
Oct.	0.0173	0.776	0.904	0.0191	0.859	0.002
Nov.	0.0660	0.719	0.945	0.0699	0.761	0.012
Dec.	0.0529	1.223	0.927	0.0571	1.319	0.006

3.4.2. Estimates of ARF_1

The parameters v_S and λ_S of the pdf of hourly point rainfall were estimated from the hourly rainfall records for De Bilt. In the ML

estimation procedure, ε in Equation 3.35 was set at 0.45 mm. The ML estimates \hat{v}_S^* and $\hat{\lambda}_S^*$ are given in Table 3.17. A linear correlation-distance function according to Equation 3.38 was fitted to the three correlation coefficients for the Hupselse Beek catchment and the correlation coefficient between hourly rainfalls at De Bilt and Soesterberg. The OLS estimates of ρ_0 and θ in Equation 3.38 are also presented in Table 3.17, and also the ML estimates \hat{q}_0 and $\hat{\beta}$ of the exponential distribution function fitted to POT series of hourly rainfall extracted from the De Bilt records.

Table 3.17. Parameter values used for estimating ARF_1 ; realizations of the lack of fit statistic \underline{T} to the exponential distribution

Month	\hat{v}_S^* (-)	$\hat{\lambda}_S^*$ (mm ⁻¹)	$\hat{\rho}_0$ (-)	$\hat{\theta}$ (km ⁻¹)	\hat{q}_0 (mm)	$\hat{\beta}$ (mm)	\underline{T} (-)
Jan.	.0667	.700	.873	-.022	3.0	1.0	138.3
Feb.	.0534	.688	.940	-.031	2.8	1.1	134.6
March	.0519	.697	.946	-.015	2.9	1.0	140.8
April	.0442	.591	.970	-.034	3.2	1.5	125.9
May	.0324	.421	.932	-.018	4.6	3.1	105.4 ^{°°}
June	.0315	.334	.978	-.064	5.8	4.6	92.6 ^{°°}
July	.0321	.306	.940	-.043	6.9	3.7	139.0
Aug.	.0331	.286	.883	-.042	6.8	5.1	168.0
Sept.	.0390	.401	.914	-.038	5.1	2.4	161.2
Oct.	.0494	.486	.937	-.022	4.2	2.0	98.9 ^{°°}
Nov.	.0650	.597	1.000	-.042	3.7	1.3	149.1
Dec.	.0714	.650	.960	-.024	3.3	1.1	169.5
Summer	.0332	.340	.937	-.042	9.2	4.6	261.8 [°]
Winter	.0571	.621	.950	-.027	4.9	1.6	214.3 ^{°°}
Year	.0452	.483	.937	-.035	9.7	4.3	249.1 ^{°°}

° Indicates values inside the critical region for $\alpha = 0.10$.

°° Indicates values inside the critical region for $\alpha = 0.05$.

The mean number of threshold exceedances is one for each month, and two for each year or season, and peaks are separated by an interval of at least ten hours, as indicated in Section 2.5.3. The validity of the assumption of exponentially distributed peaks has been assessed by the test statistic \underline{T} according to Equation 2.8. Table 3.17 also gives the realizations T . The winter, summer, and year series show poor fit. This could have been improved, had only one exceedance for each year been allowed which would have yielded for the winter series only a T critical at the 10% level. However, as interest is in low return period events, these results are accepted. Figure 3.26 shows the POT series of hourly point rainfall and also the fitted exponential distributions for January, August, summer, winter, and the complete year.

ARF_1 has been estimated for areas of 10, 50, 100, and 250 km², and return periods of 1, 1.78, 5, and 10 years. Figure 3.27 shows ARF_1 for January and August as a function of area and return period, and Figure 3.28 shows ARF_1 for winter and summer. ARF_1 and ARF_{24} for the complete year are shown in Figure 3.21. ARFs corresponding to a 0.5-year return period are shown in this figure, but ARF_1 values corresponding to a 5- and 10-year return period are not shown, because these require the extreme right tail of the fitted distributions, which is not accurately known.

Figure 3.21 shows that ARF increases with rainfall duration. The ARF_1 estimates in the present study for the Netherlands are somewhat lower than those reported in USWB (1957-1960) and NERC (1975) (see Table 3.18). Apart from different estimation methods, both the USWB (1957-1960) and NERC (1975) studies were based on more data obtained from dense rainfall measuring networks. Both USWB (1957-1960) and Bell (1976) show that there is a large variation in ARF_1 values derived from different areas. Lack of data rather than climatological differences could be the reason of the differences in ARF_1 values shown in Table 3.18.

Table 3.18. Comparison of ARF_1 estimates in the present study for the Netherlands with those from USWB (1957-1960) for the USA and NERC (1975) for the United Kingdom

Area (km ²)	ARF_1		
	Present study	USWB (1957-1960)	NERC (1975)
100	0.76	0.83	0.79
250	0.66	0.73	0.72

3.5. STORM-CENTRED AREAL REDUCTION FACTOR SRF

The storm-centred areal reduction factor SRF which is similar to the statistical areal reduction factor ARF is defined as (Equation 3.4)

$$SRF = x_A / x_{\max}$$

where

x_{\max} : local maximum point rainfall over a certain time period (e.g., one specific day)

x_A : simultaneous areal rainfall over area A bounded by an isohyet.

SRF is used in the derivation of statistical estimates of probable maximum precipitation: theoretically, the greatest depth of precipitation that can occur in a particular drainage basin for a particular duration in a particular season. It may also be of use in simulation studies. But, as pointed out by Holland (1967), the requirement to develop a relationship between point and areal rainfall is "... in the engineering context the need to match frequencies or periods of return (p. 194)."

While ARF relates point and areal rainfall of equal exceedance probability and without any assumption of simultaneousness, SRF relates point and areal rainfall over the same time span and consequently with almost certainly different exceedance probabilities. ARF intrinsically refers to fixed areas, whereas SRF is quite often determined from isohyet patterns occurring within a larger area (referred to as moving target area SRF).

When a fixed area is considered, a densely-gauged experimental catchment may be selected. This may lead to accurate estimates of SRF, but also has the disadvantage that very often the point rainfall maximum occurs near the edge of the catchment, or even outside it, so that the presumed maximum is not the maximum at all. As SRF is often derived under the assumption of circular isohyets, it may be cumbersome both to verify this assumption, and to estimate x_A , when a fixed area is used. In principle, however, whether a moving target area or a fixed area is used is immaterial, but the possibility with a fixed area that the true maximum is not recognized may have the consequence that different estimates of SRF are obtained.

In general, SRF is equal to or less than ARF, see also Figure 3.29 (from Bell, 1976). The smaller the area and the shorter the period during which rainfall totals are considered (for example, SRF and ARF values for a particular month instead of the complete year), the closer the values of SRF and ARF will be. By extending both the period and the area, the probability of non-simultaneousness of point and areal maxima will increase. This will generally lead to ARF values which are high compared to SRF values, but this depends also on the criteria according to which the days are selected for estimating SRF.

According to Eagleson (1970), the difference $x_{\max} - x_A$ in general

- (i) increases with area;
- (ii) decreases with total rainfall depth (which causes an increase of the coefficient of variation with decrease of total rainfall depth (Figure 3.6);
- (iii) decreases with duration;
- (iv) is greater for convective and orographic precipitation than for cyclonic precipitation.

Therefore, the ratio SRF of x_A and x_{\max} will generally show opposite behaviour.

An insight into the dependence of SRF on A can be obtained from depth-area curves, "Curves showing, for a given duration, the relation of maximum average depth to size of area within a storm or storms" (USWB, 1947; p. 252), or from minimum-rainfall curves, which are similar to the depth-area curves, "... except that ordi-

nates represent minimum instead of average depths within the areas" (USWB, 1947; p. 297). The equation representing a minimum-rainfall curve can be written so as to represent a depth-area curve. Such an equation gives x_A as a function of A . When the equation is divided by x_{\max} , the result is SRF as a function of A . Table 3.19 contains expressions for SRF derived from published equations representing depth-area and minimum-rainfall curves.

Table 3.19. Expressions for the storm-centred areal reduction factor SRF, deduced from equations representing depth-area and minimum-rainfall curves

Investigator	SRF	Duration	General remarks
Horton (1924)	$1 - \alpha A^{\frac{1}{2}} + 0.5\alpha^2 A - \dots$ ¹	one day	heavy rainfall in the eastern USA; moving target area
Huff and Stout (1952)	$1 - \alpha A^{\frac{1}{2}}$	30 min-18 hours	small, densely-gauged networks in Illinois (USA); thunderstorm rainfall
Chow (1953, 1954)	$1 - \alpha A^{\frac{1}{2}} + \beta A - \dots$	not specified	applied to data from one of Huff and Stout's networks
Boyer (1957)	$1 - \alpha A^{\frac{1}{2}} + 0.41\alpha^2 A - \dots$ ²	6-48 hours	great storms over the central plains of the USA; moving target area
Kraijenhoff (1958)	$1 - \alpha A + \beta A^2 - \dots$ ³	one day	heavy summer rainfall in the Netherlands; moving target area
Woolhiser and Schwalen (1959)	$1 - \alpha A^{3/5}$	one day	thunderstorm rainfall over a small, densely-gauged network in Arizona (USA)
Court (1961)	$1 - \alpha A + 2/3\alpha^2 A^2 - \dots$ ⁴	not specified	applied to convective rainfall of less than two hours duration over a small, densely-gauged network in southern Arizona (USA), by Fogel and Duckstein (1969)
Smith (1974)	$1 - \alpha A$	one day	thunderstorm rainfall in southern Arizona (USA)
Nicks and Igo (1980)	$1 - \alpha A + \alpha\beta A^2$	⁵ up to 24 hours	large (3885 km ²), densely-gauged network in Oklahoma (USA); verified with other USA rainfall data

¹ Taylor expansion of $\text{SRF} = \exp(-\alpha A^\beta)$, with $\beta \approx 0.50$.

² This expression follows from Boyer's SRF = $\frac{1.68}{A/\alpha'} \{1 - \exp(-1.09(A/\alpha')^{\frac{1}{2}})(1.09(A/\alpha')^{\frac{1}{2}} + 1)\}$, after a Taylor expansion, followed by some simplifications, as noted by Chow (1958).

³ Taylor expansion of $\text{SRF} = \frac{\gamma'\alpha'}{A} \{1 - \exp(-A/\alpha')\} + \frac{(1-\gamma')\beta'}{A} \{1 - \exp(-A/\beta')\}$.

⁴ Taylor expansion of $\text{SRF} = \frac{\alpha'}{A} \{1 - \exp(-A/\alpha')\}$.

⁵ Their original expression is approximated as follows

$$\text{SRF} = 1 - \left(\frac{D\gamma'}{\alpha' + \beta'A} \right) A = 1 - \frac{D\gamma'}{\alpha'} \left(\frac{A}{1 + \frac{\beta'}{\alpha'} A} \right) = 1 - \alpha \frac{A}{1 + \beta A} \approx 1 - \alpha A (1 - \beta A) = 1 - \alpha A + \alpha\beta A^2; D \text{ denotes the duration of rainfall.}$$

None of the expressions in Table 3.19, except for that of Nicks and Igo (1980) which has duration as an independent variable, contains explicitly the following above-mentioned factors: total rainfall depth (*ii*); duration (*iii*); and the nature of the precipitation (*iv*). Thus, they should be used only for those circumstances under which they have been derived.

Many approximations have been used in Table 3.19, notably the Taylor expansions mentioned in the footnotes, and the replacement by x_{\max} of all such quantities as the measured x_{\max} , the 'true', that is interpolated, x_{\max} , and the maximum areal rainfall at the eye of the storm over ten square miles. Close examination of these studies, and similar approximations used by Court (1961) indicate that the approximations in Table 3.19 are acceptable. Table 3.19 shows that, basically, there are two expressions for SRF

$$\text{SRF} = 1 - \alpha A^{\frac{1}{2}} + \dots, \quad (3.44a)$$

and

$$\text{SRF} = 1 - \alpha A + \dots. \quad (3.44b)$$

A general relationship between ARF and SRF can only be derived on the basis of many assumptions. Firstly, an equation for the depth-area curve needs to be postulated, for example, one of the equations referred to in Table 3.19. As the coefficient α in Table 3.19 may depend on x_{\max} , this dependence also needs to be postulated. SRF can then be estimated, and for certain depth-area relationships, the correlation-distance function can be obtained from the work of Stol (1981a,b,c), on the assumptions that this relationship is the same for all storms and that storms occur randomly and are uniformly distributed in space, with at most one storm occurring during one interval of precipitation measurement (for example, one day). Stol (1981a,b,c) has obtained the correlation-distance function as a space average over straight lines passing through the location of maximum rainfall. By spatially averaging the correlation-distance function, one finds $f = \bar{r}(V;V)$. Then, from the pdf of point rainfall, the pdf of areal rainfall can be obtained, and ARF estimated. In such a comparison, SRF is compared with ARF corresponding to a certain return period.

A more general approach uses only the pdf of point rainfall, the pdf of maximum rainfall x_{\max} , and the correlation-distance function as estimated, without assumptions on the depth-area relationship. Then, as seen before, ARF is determined completely, and SRF can be found as follows (Smith, 1974). A minimum-rainfall relationship gives the minimum rainfall $x_s(h)$ along an isohyet at distance h from the rainfall maximum as a function of A . Its inverse gives A as a function of $x_s(h)$. A dimensionless inverse may be written as $A_*(x_*)$, which gives the dimensionless area $A_* = A/A_{\text{tot}}$ (see Figure 3.30) as a function of the dimensionless rainfall depth $x_* = x_s(h)/x_{\max}$. Note that $A_*(0)=1$, and $A_*(1)=0$. As $0 \leq x_* \leq 1$, $1-A_*(x_*)$ can be seen as the cdf of x_* .

Let the random variable x_s represent point rainfall depth at point S within an area, then the probability of the event $\{x_s \leq d\}$ can be expressed as (see Figure 3.30)

$$P\{x_s \leq d\} = P\{x_{\max} \leq d\} + P[\{x_{\max} > d\} \cap \{S: x_s \leq d\}]. \quad (3.45)$$

The last event in Equation 3.45 indicates the possibility that, although $x_{\max} > d$, S is so remote from the rainfall maximum as to cause $x_s \leq d$. Because $1-A_*(x_*)$ is a cdf

$$P\{S: x_s \leq d\} = 1 - A_*(d/x_{\max}). \quad (3.46)$$

Combining Equations 3.45 and 3.46 yields

$$P\{x_s \leq d\} = P\{x_{\max} \leq d\} + \int_{y=d}^{\infty} [1 - A_*(d/y)] dP\{x_{\max} < d\},$$

or

$$P\{x_s \leq d\} = 1 - \int_{y=d}^{\infty} A_*(d/y) p_{x_{\max}}(y) dy, \quad (3.47)$$

where

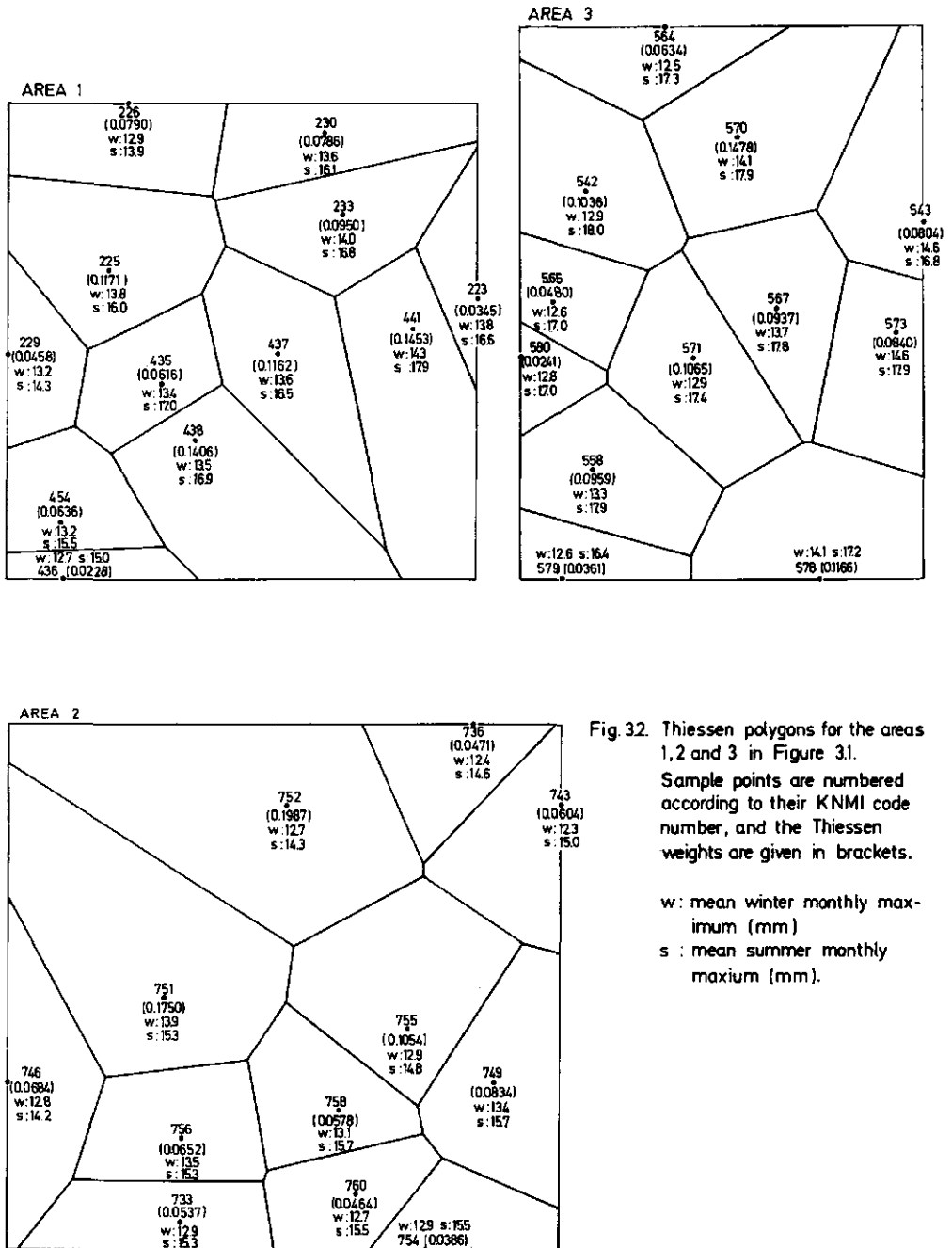
$p_x(\cdot)$: pdf of x .

According to Equation 3.47, the dimensionless depth-area relationship $A_*(x_*)$ can be determined from the pdfs of centre depth and point rainfall, and SRF can be determined from $A_*(x_*)$.

Also similar to ARF is the epicentre coefficient (Kraijenhoff, 1963; Galéa et al., 1983), the ratio of the maximum point rainfall over an area for a given return period and duration, and the quantile estimate of point rainfall for that return period and duration. The epicentre coefficient is always at least one, and increases with area and return period, and decreases with duration. Estimates of epicentre coefficients also depend heavily on network density. Kraijenhoff (1963) related the minimum and maximum point rainfall depth to return period and to the point rainfall depth with the same return period for summer days with measured rainfall at a particular rainfall station in excess of 40 mm (see Figure 3.31). From this figure, epicentre coefficients and a related quantity with regard to minimum rainfall can easily be estimated. Because of the low density of the rainfall measuring network, estimates of the epicentre coefficients from Figure 3.31 will be rather lower than those from Galéa et al. (1983) for France. For daily summer rainfall, an area of 50 km², and a 10-year return period, according to Figure 3.31 the epicentre coefficient is 1.14, but according to Galéa et al. (their Figure 3), it is 1.56.



Fig. 3.1. Location of rainfall stations and areas considered in Chapter 3.



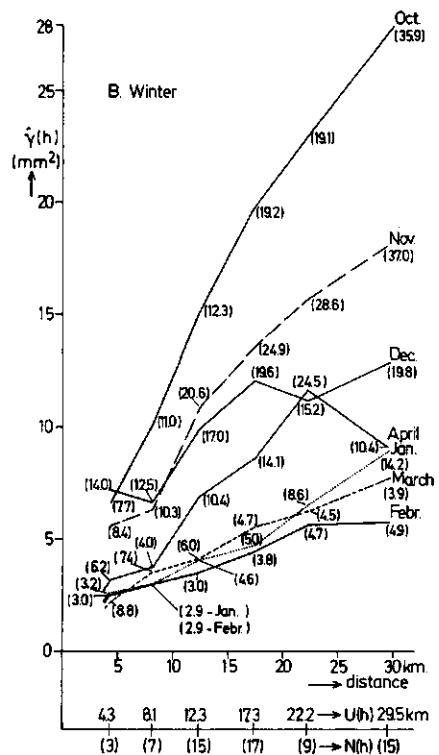
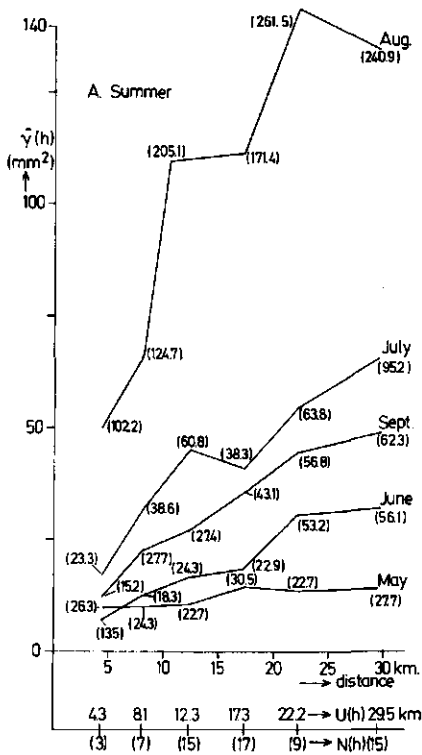


Fig. 3.3. Multi-realization sample semi-variograms. Monthly maxima of daily rainfall. Area 1.

Sample standard deviations of the results are given in brackets.

$U(h)$: location of centres of distance classes

$N(h)$: number of pairs of sample points within a distance class.

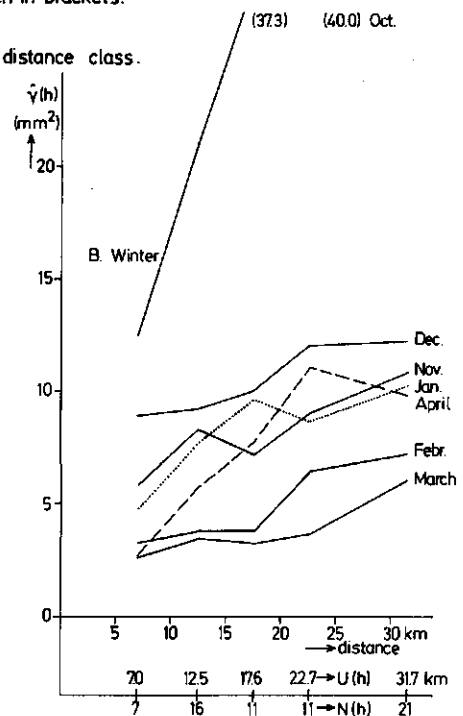
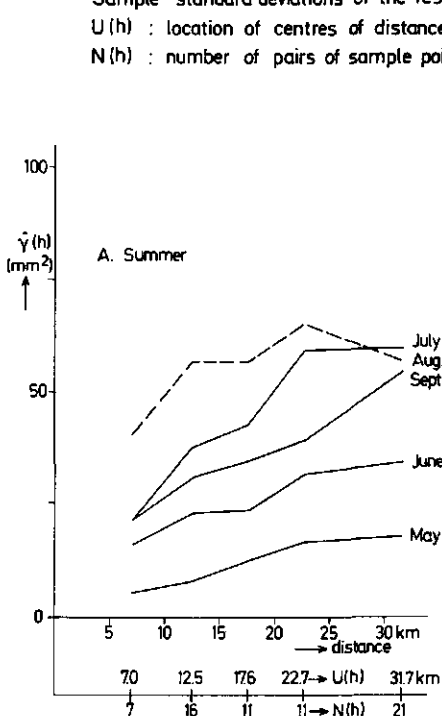


Fig. 3.4. Multi-realization sample semi-variograms. Monthly maxima of daily rainfall. Area 2.

$U(h)$: location of centres of distance classes

$N(h)$: number of pairs of sample points within a distance class.

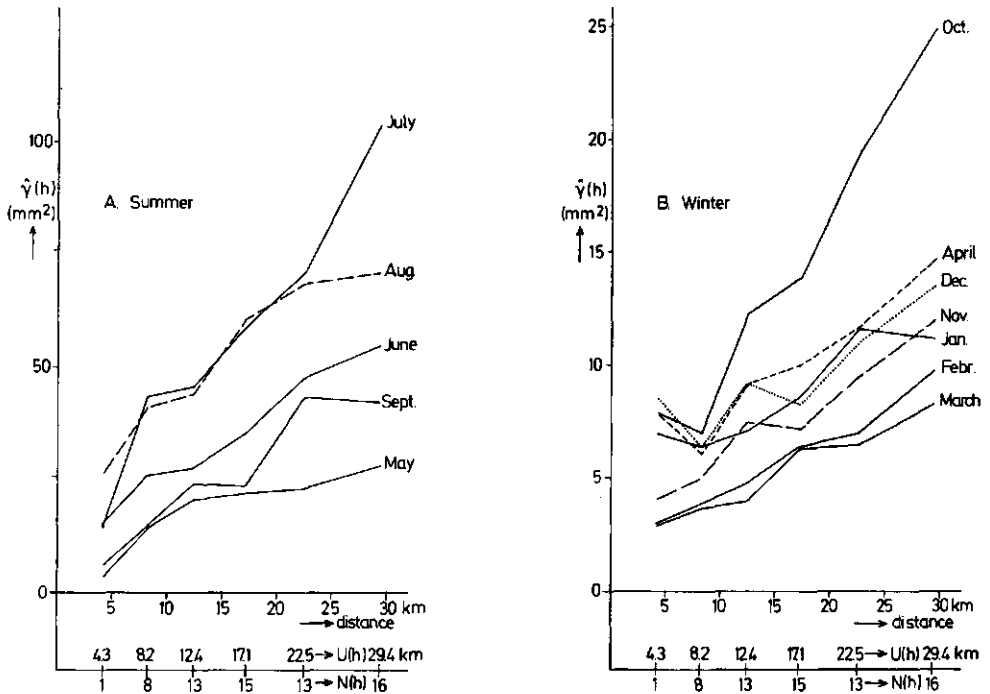
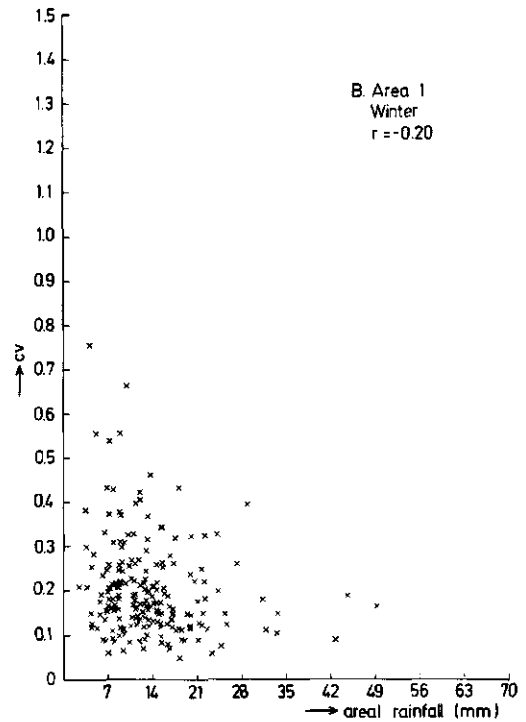
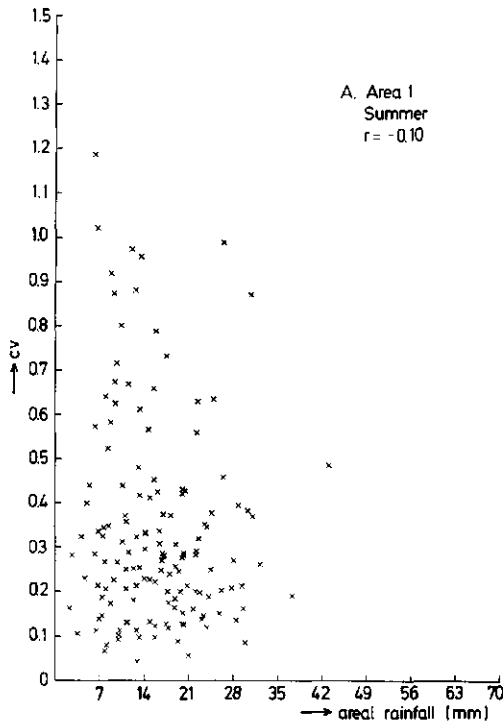


Fig. 35. Multi-realization sample semi-variograms. Monthly maxima of daily rainfall. Area 3.

$U(h)$: location of centres of distance classes

$N(h)$: number of pairs of sample points within a distance class.



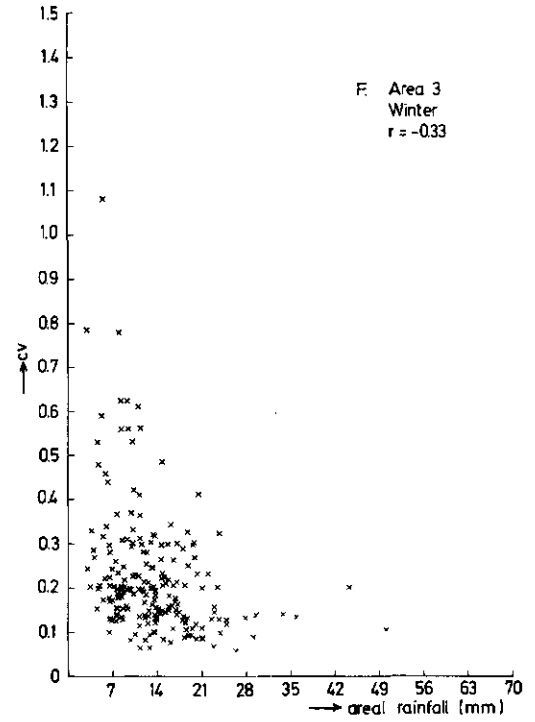
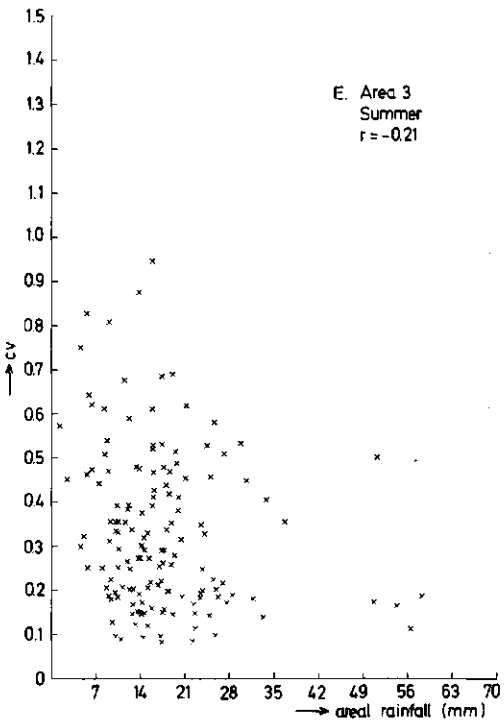
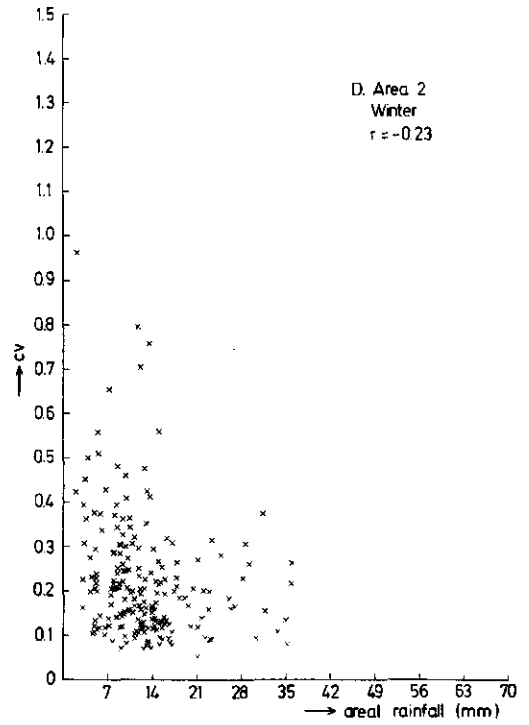
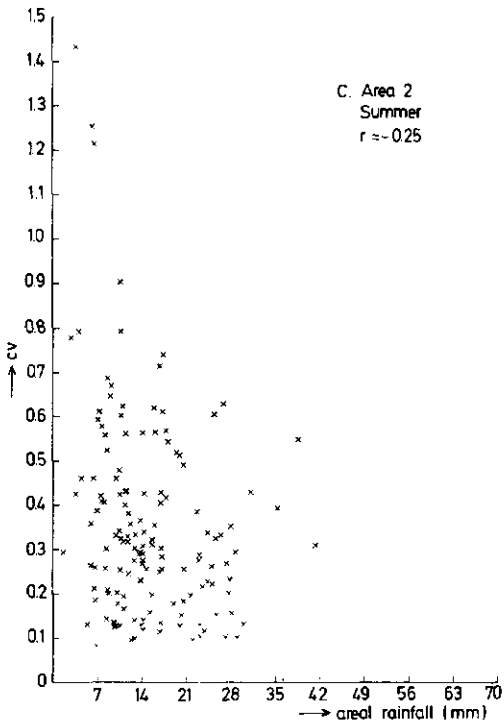


Fig. 3.6. Coefficient of variation cv for monthly maxima of daily rainfall, plotted against mean areal rainfall, r is the correlation coefficient between cv and mean areal rainfall.

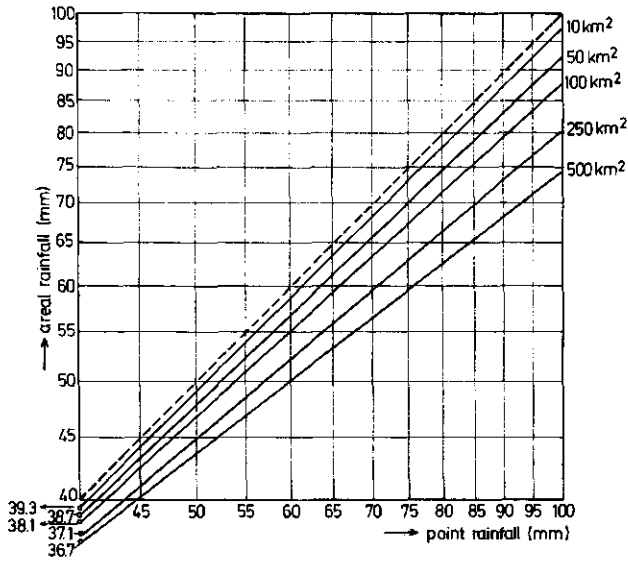
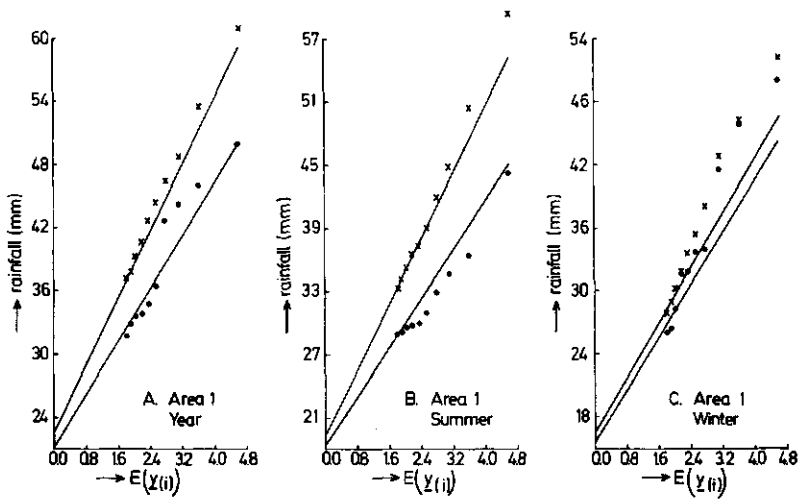


Fig. 3.7. Regression lines relating areal daily summer rainfalls to point rainfalls of equal return period, according to Krajenhoff (1963).



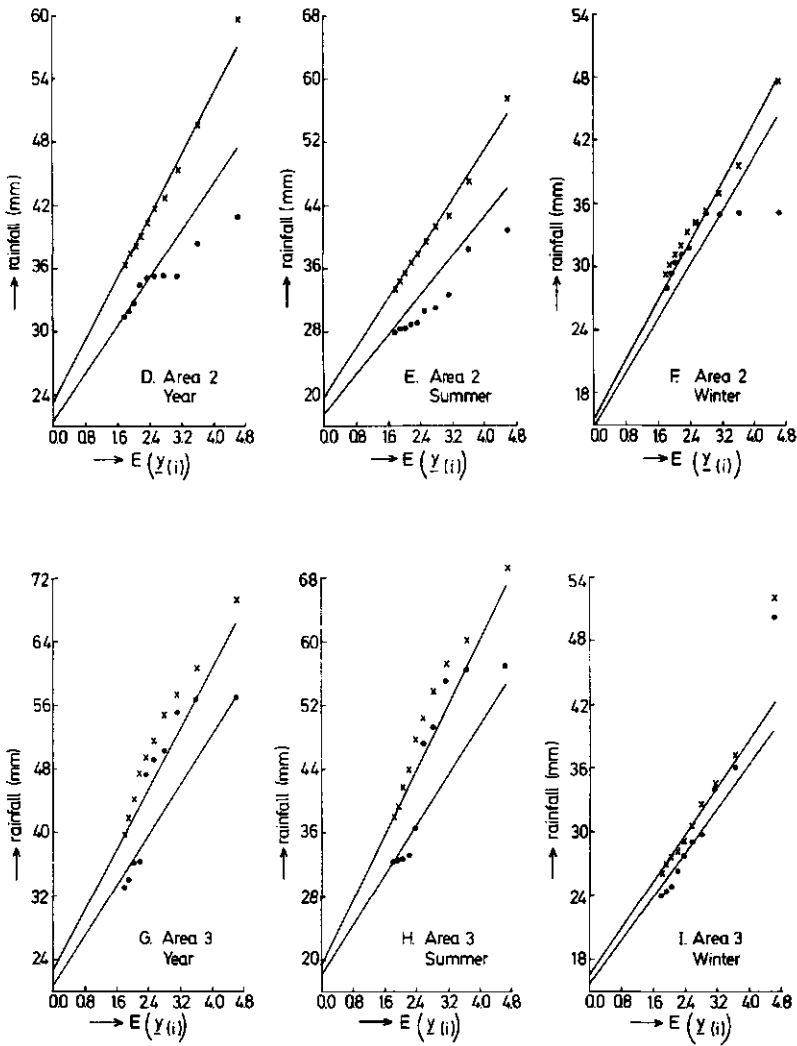


Fig. 3.8. Ten highest peaks (out of 58) from POT series of daily areal rainfall (•) and daily point rainfall (x), and fitted exponential distribution functions for the three areas considered in the derivation of ARF_{24} .

Plotting position $E(Y(i)) = \sum_{j=1}^i (n+1-j)^{-1}$

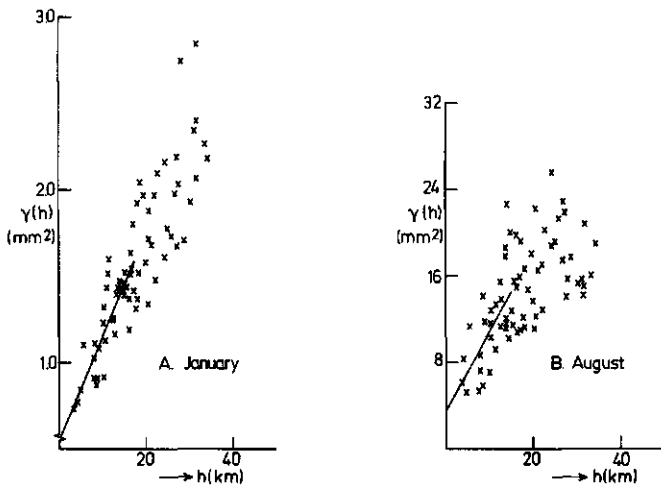


Fig.3.9. Sample semi-variances and fitted linear $\gamma(h)$ model ; area 1.

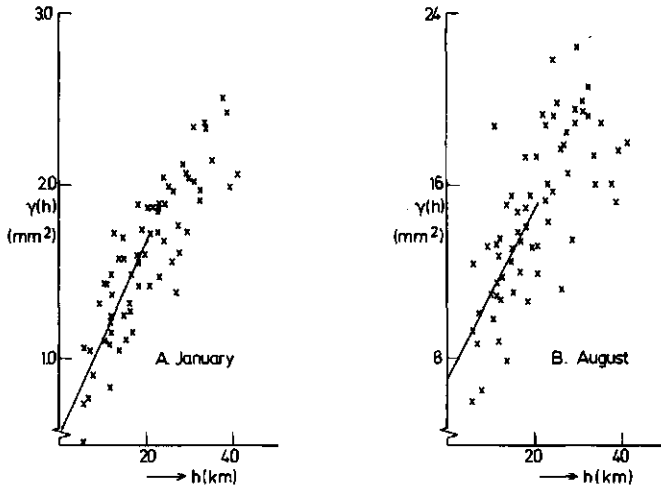


Fig. 3.10. Sample semi-variances and fitted linear $\gamma(h)$ model ; area 2.

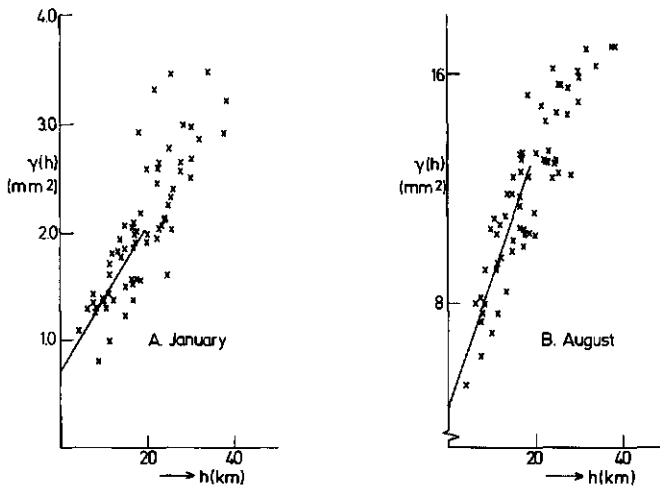


Fig. 3.11. Sample semi-variances and fitted linear $\gamma(h)$ model, area 3.

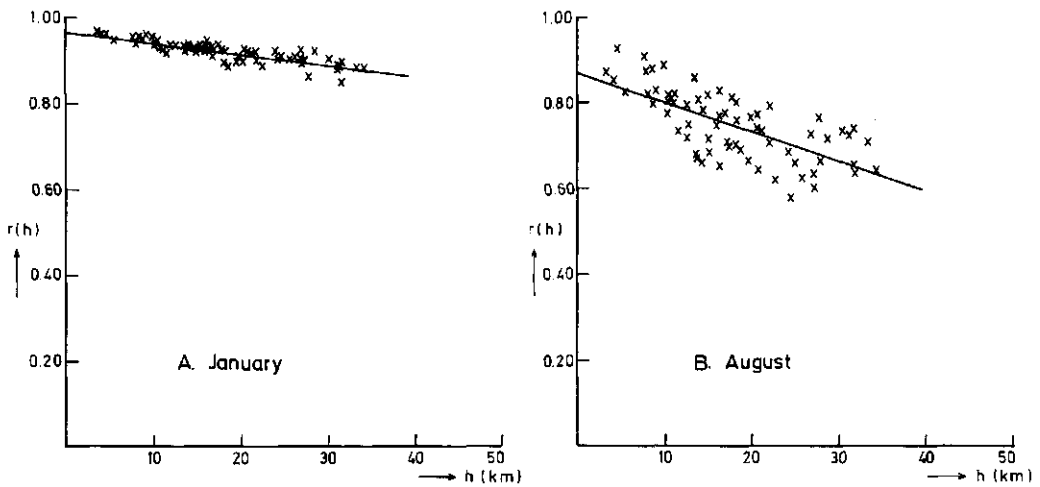


Fig. 3.12. Calculated correlation coefficients and fitted linear correlation-distance function $r(h)$ for area 1.

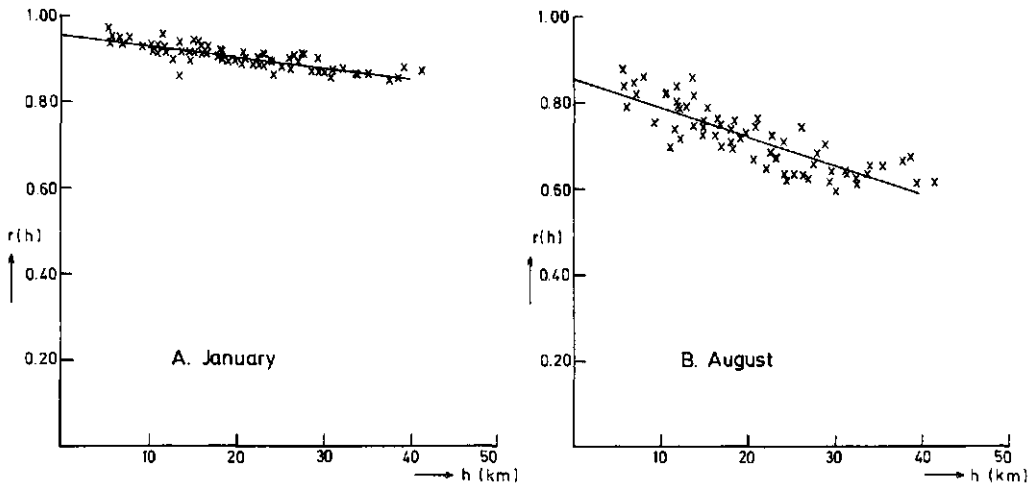


Fig. 3.13. Calculated correlation coefficients and fitted linear correlation-distance function $r(h)$ for area 2.

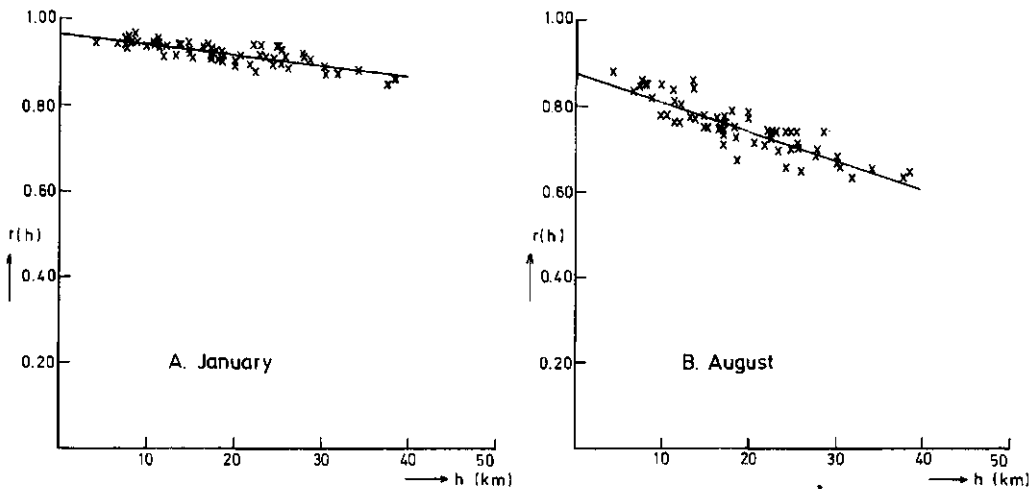


Fig. 3.14. Calculated correlation coefficients and fitted linear correlation-distance function $r(h)$ for area 3.

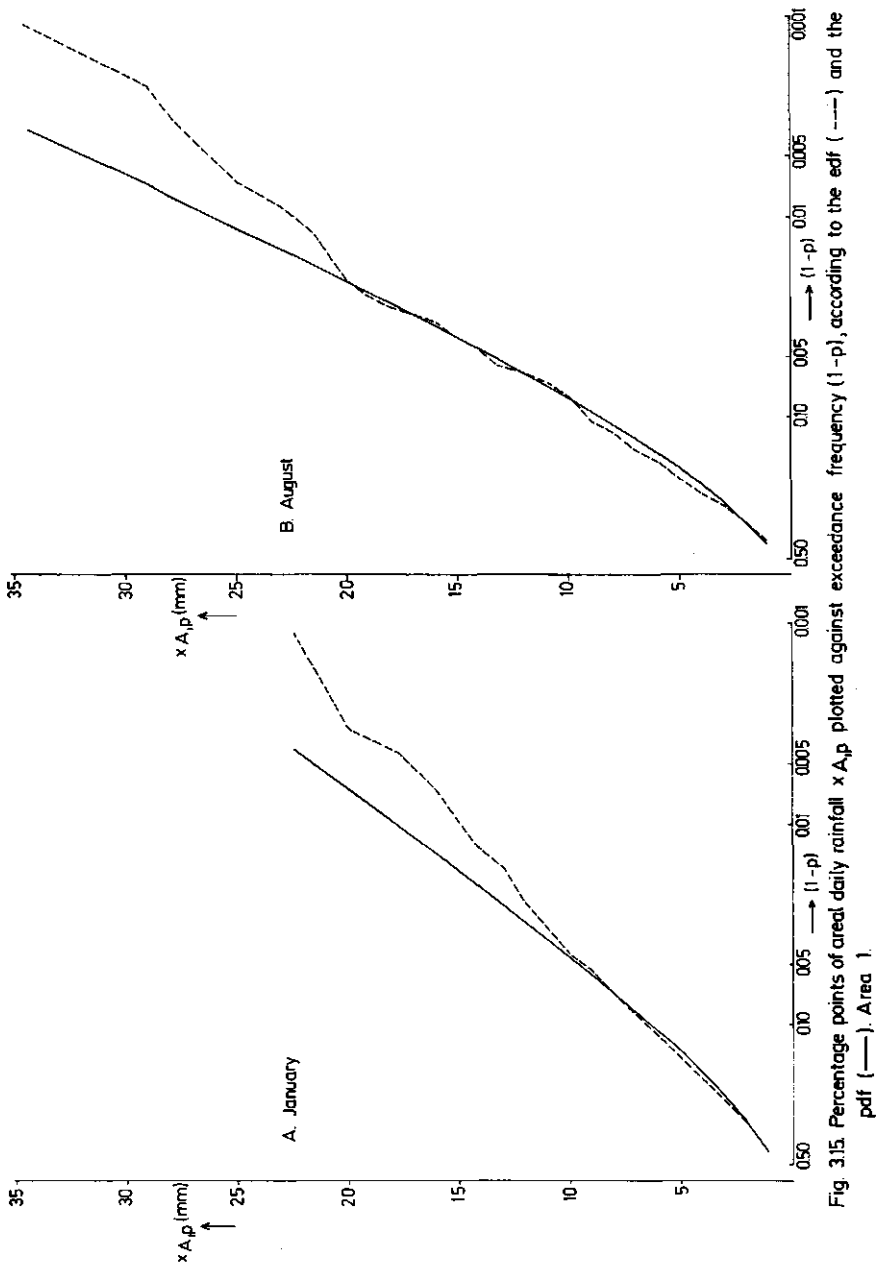


Fig. 3.15. Percentage points of areal daily rainfall $x A_p$ plotted against exceedance frequency $(1-p)$, according to the edf (---) and the pdf (—). Area 1

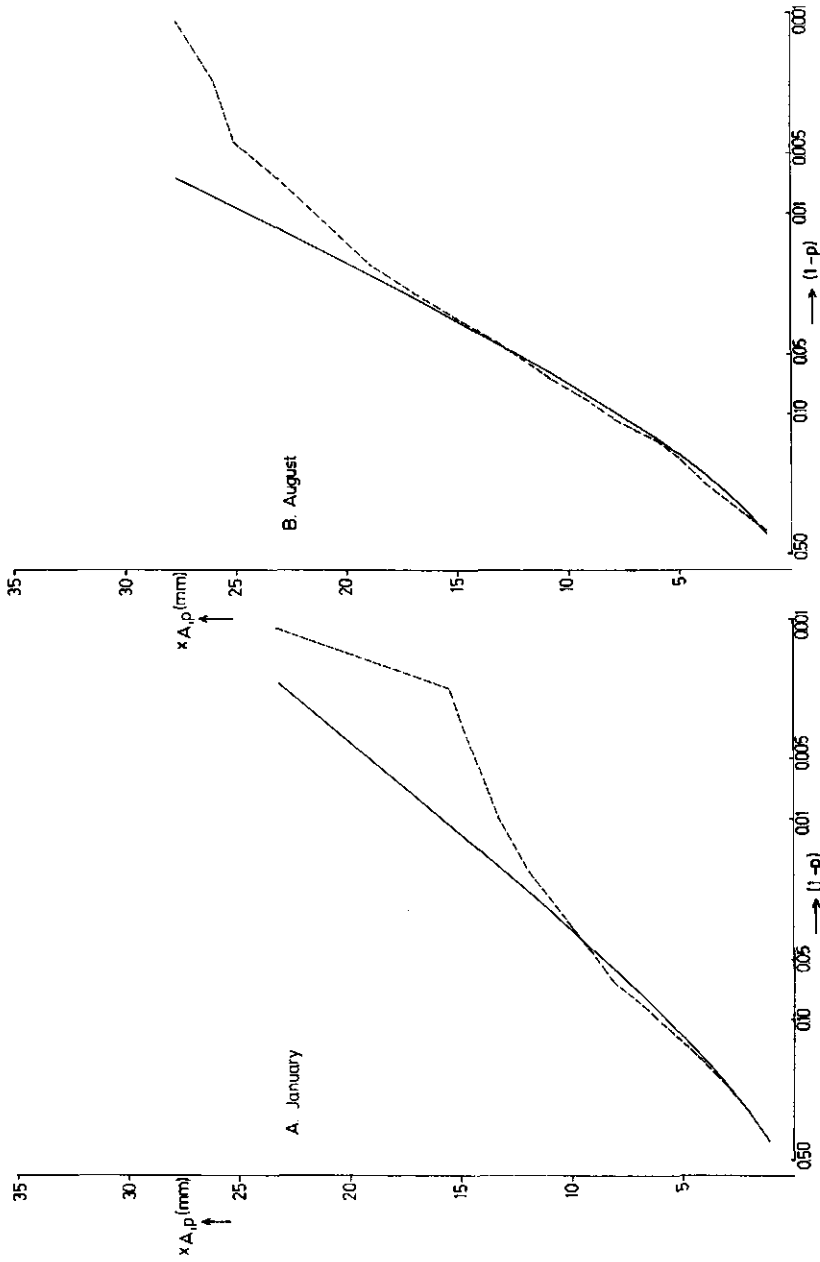
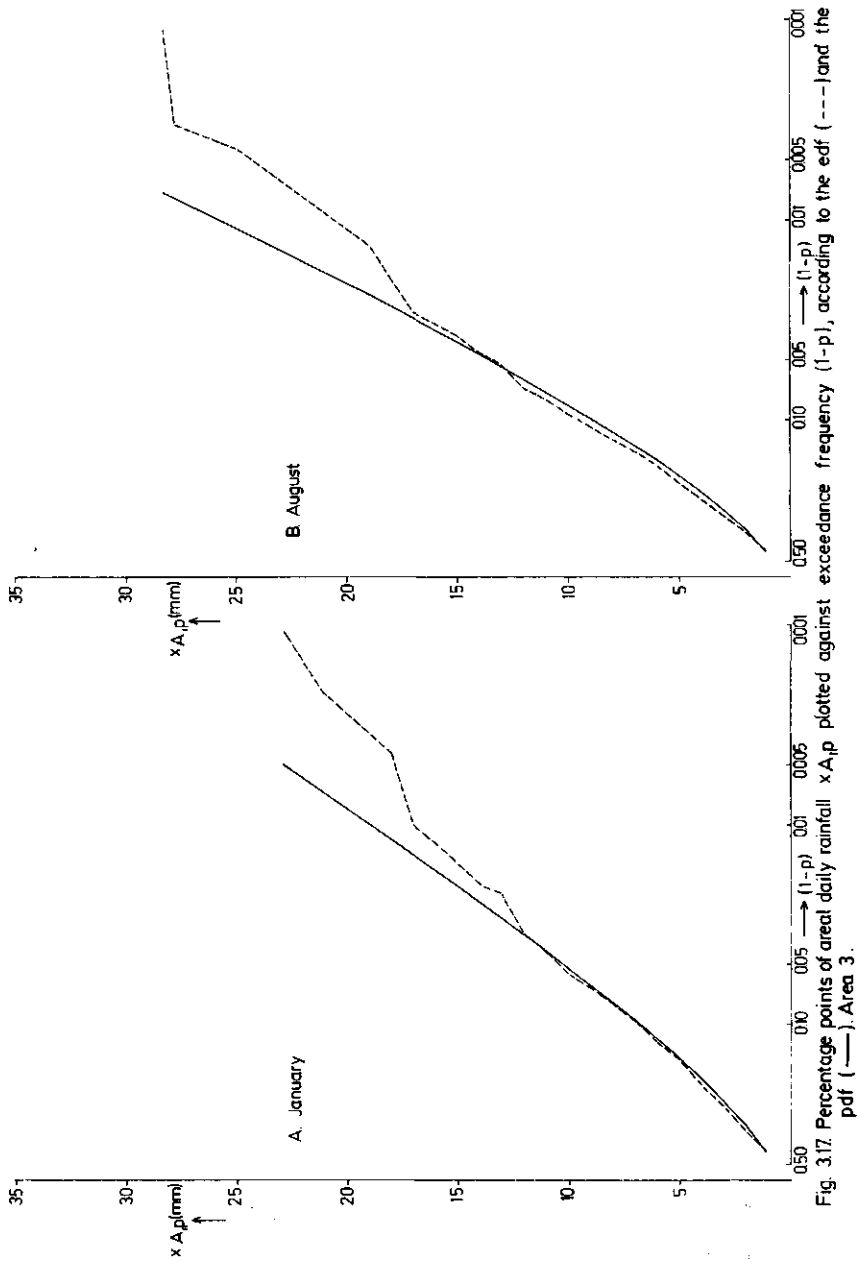


Fig. 3.16 Percentage points of areal daily rainfall $x A_p$ plotted against exceedance frequency $(1-p)$, according to the edf (---) and the pdf (—). Area 2.



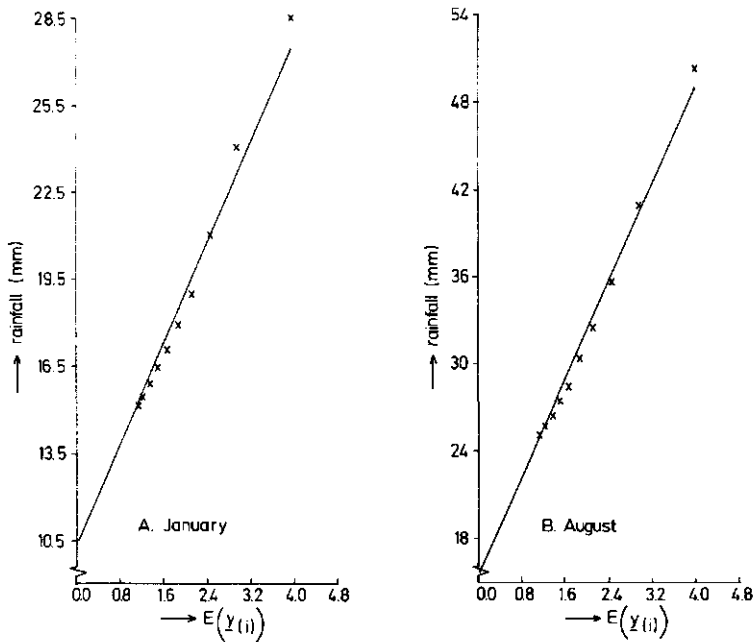


Fig. 3.18. Ten highest peaks (out of 29) from POT series of daily point rainfall, and fitted exponential distribution functions. The POT series have been derived by averaging over the individual POT series of all rainfall series in the three areas considered.

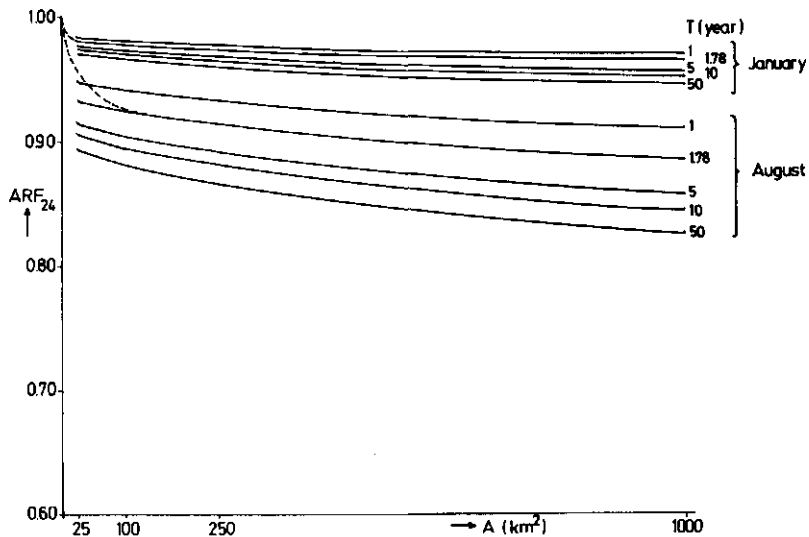


Fig. 3.19. ARF_{24} for January and August as a function of areal size A and return period T . (----: for a double exponential correlation-distance function).

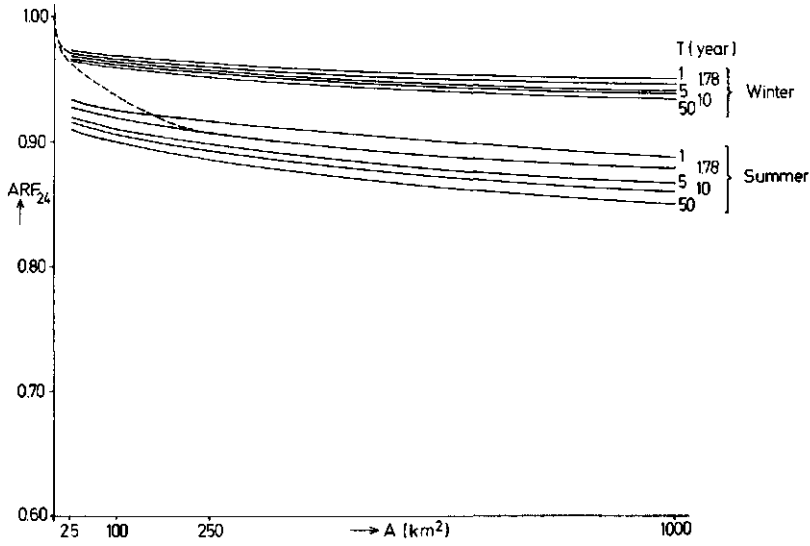


Fig. 3.20. ARF_{24} for summer and winter as a function of areal size A and return period T .
(----: for a double exponential correlation-distance function).

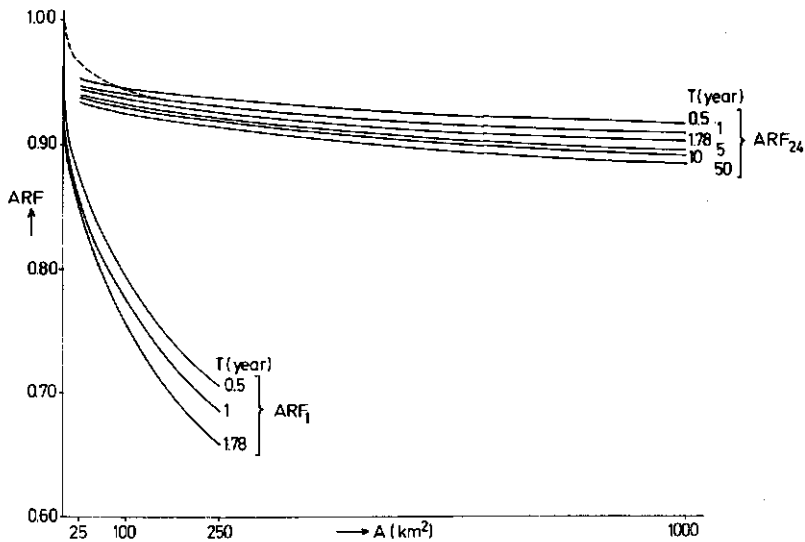


Fig. 3.21. ARF_{24} and ARF_1 for the complete year as a function of areal size A and return period T .
(----: for a double exponential correlation-distance function).

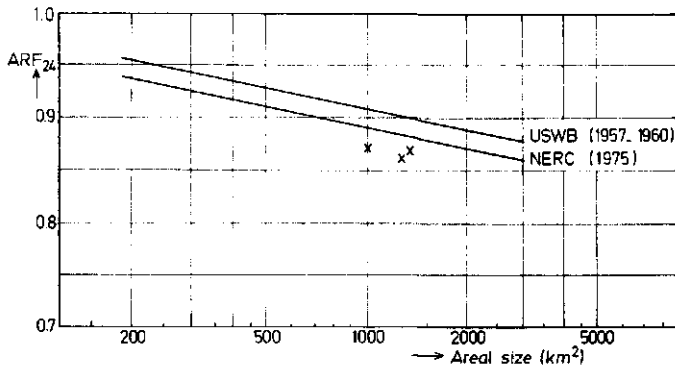


Fig. 3.22. Estimates of $ARF_{24}(x)$ according to NERC (1975) for areas 1, 2 and 3, and the USWB (1957-1960) and NERC (1975) estimates of ARF_{24} (corresponding to a 178-year return period for peak exceedances).

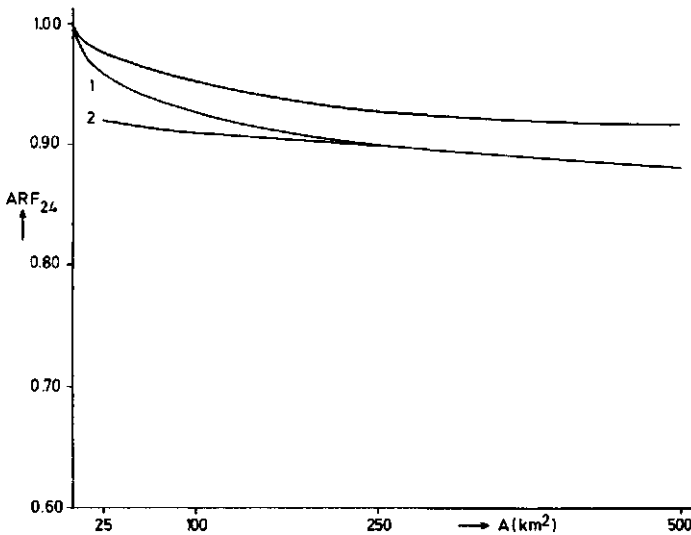


Fig. 3.23. ARF_{24} estimates according to Kraijenhoff (1963) for a daily rainfall depth in summer of 40 mm, compared to estimates from the marginal distribution of point rainfall for a double exponential (1) and a linear correlation - distance function (2).

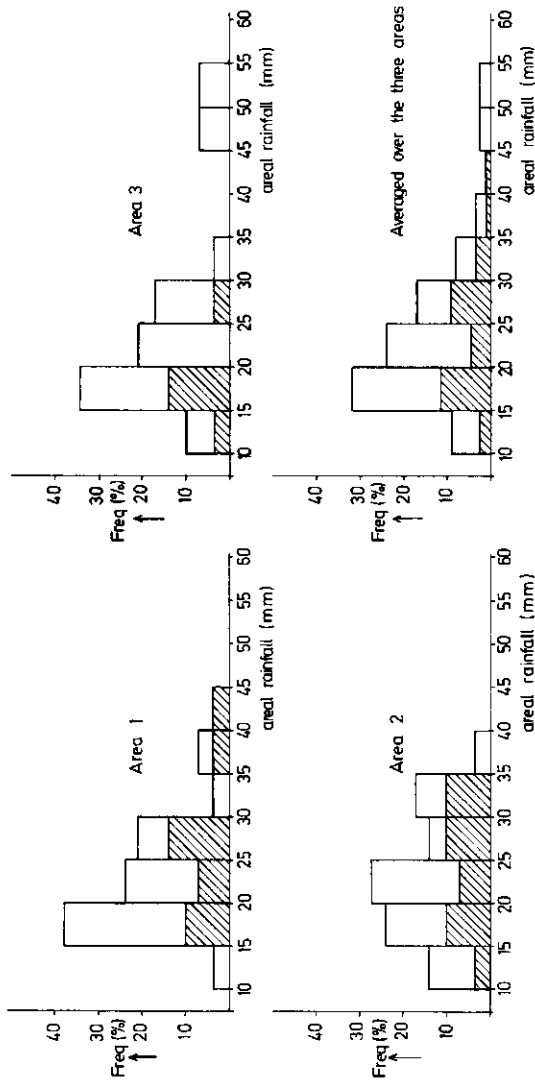


Fig. 3.24. Frequency distribution of daily maxima of areal rainfall; the contribution of winter maxima is hatched.

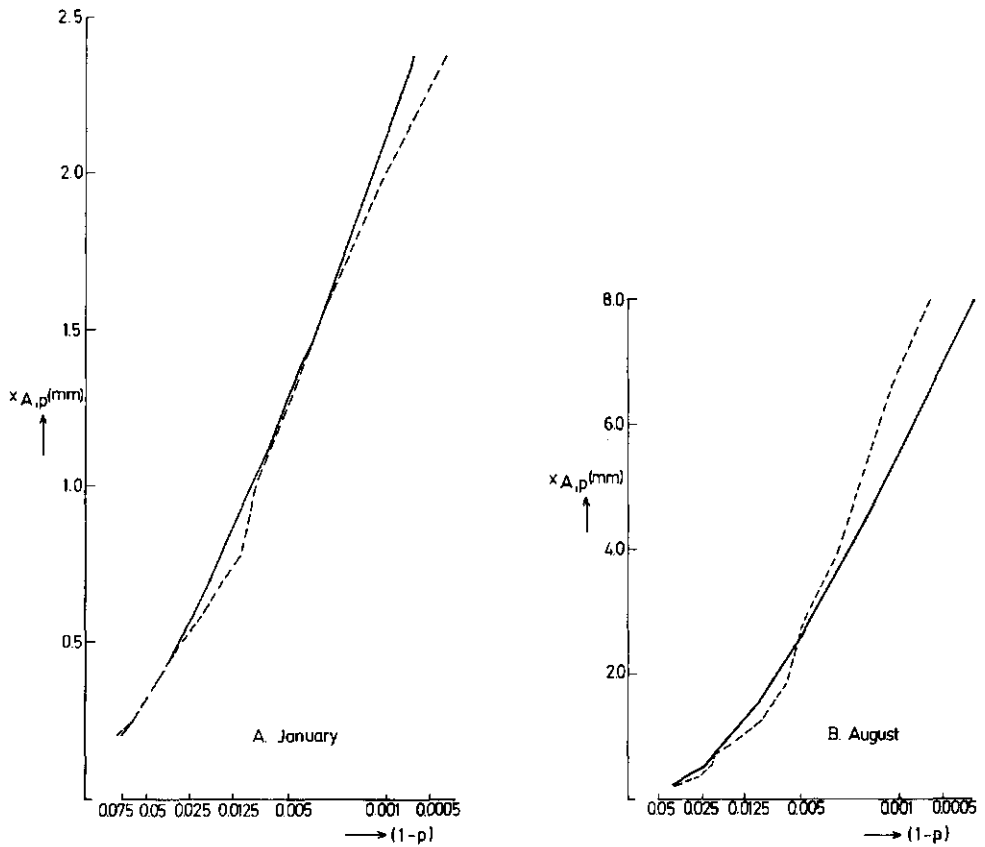
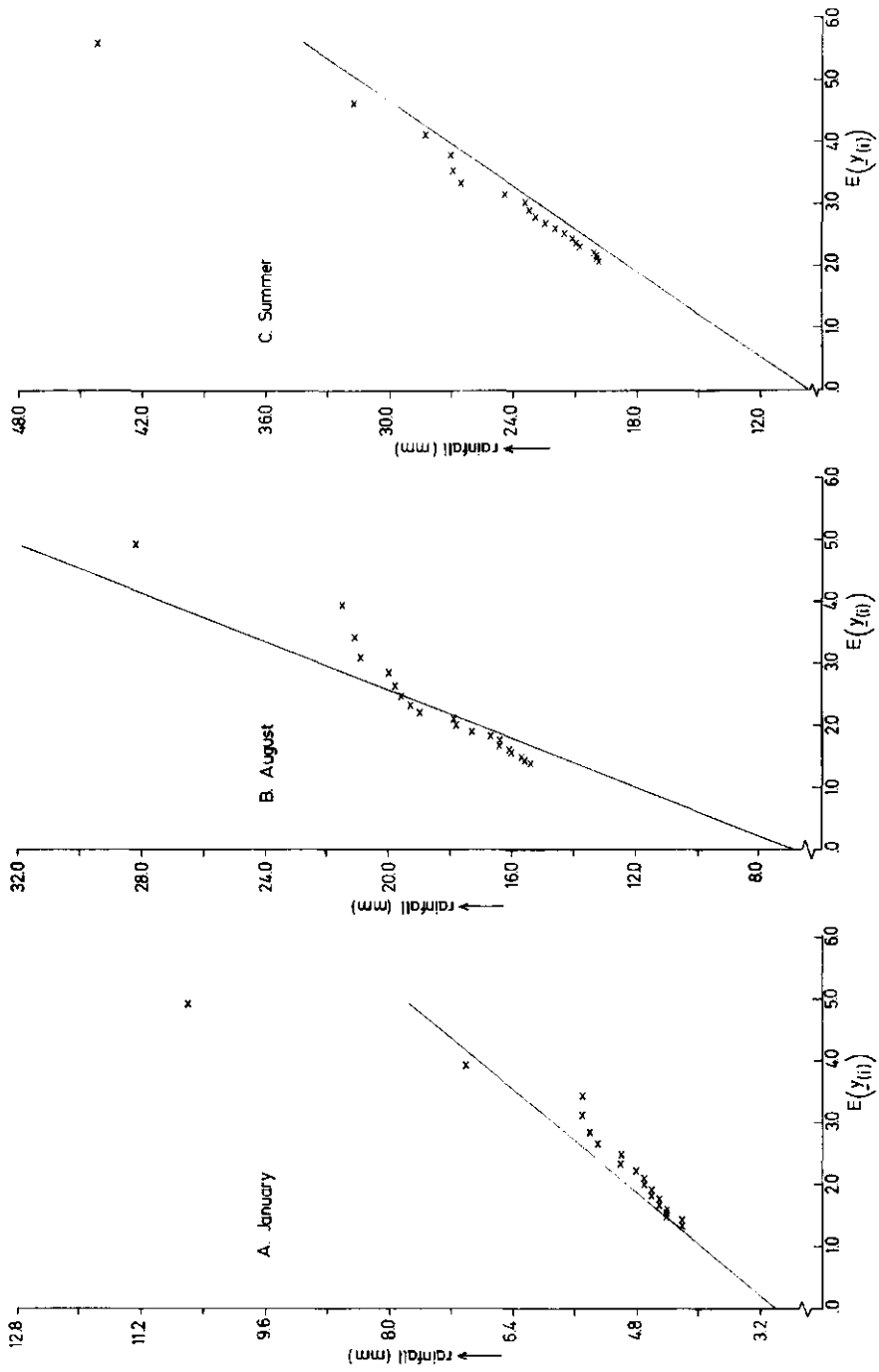


Fig. 3.25. Percentage points of areal hourly rainfall $x_{A,p}$ plotted against exceedance frequency $(1-p)$, according to the edf (---) and the pdf (—).



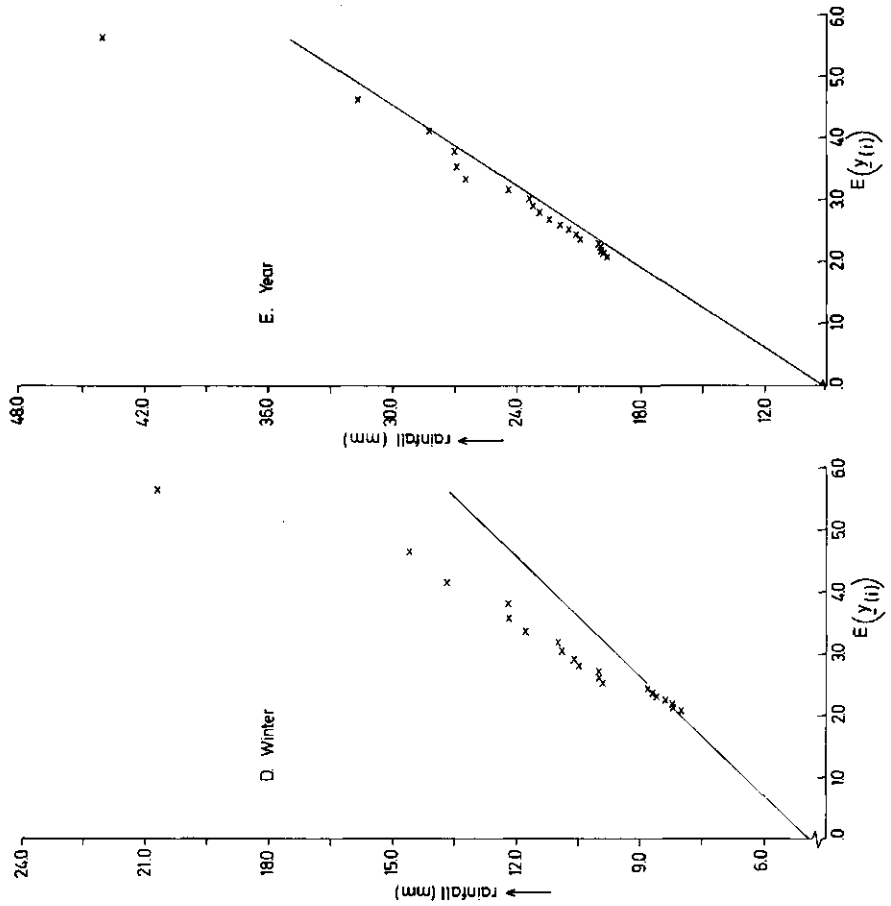


Fig. 3.26. Twenty highest peaks of POT series of hourly rainfall and fitted exponential pdfs, for January (A) and August (B) with an average of one exceedance each month, and for the summer (C), the winter (D), and the complete year (E) with an average of two exceedances each season or year.

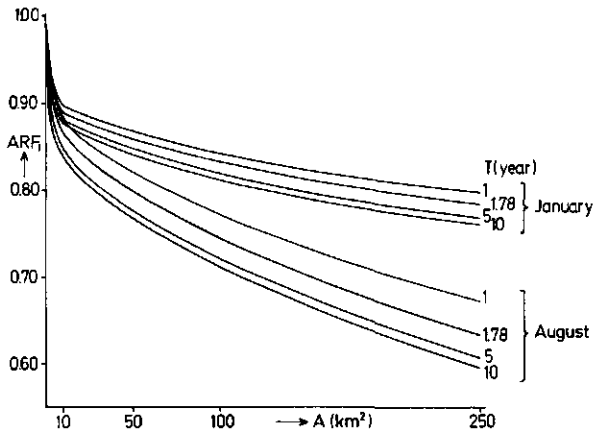


Fig. 3.27. ARF_i for January and August as a function of areal size A and return period T .

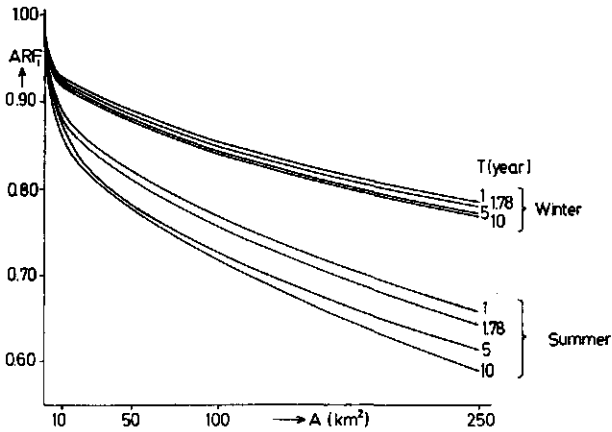


Fig. 3.28. ARF_i for summer and winter as a function of areal size A and return period T .

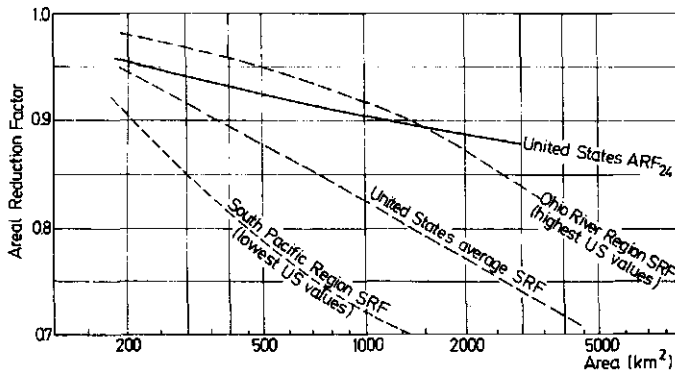


Fig. 3.29. Comparison of ARF_{24} and SRF values for the USA (from Bell, 1976).

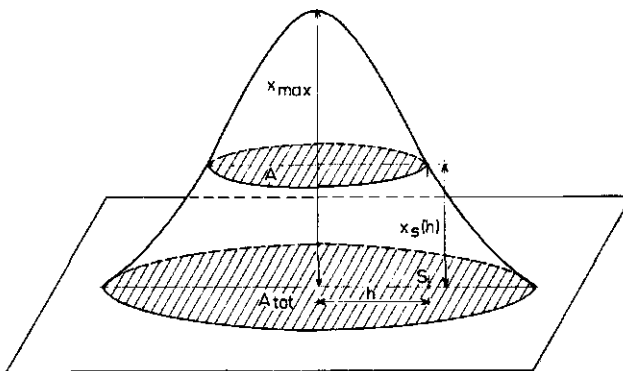


Fig. 3.30. Hypothetical depth - area relationship.

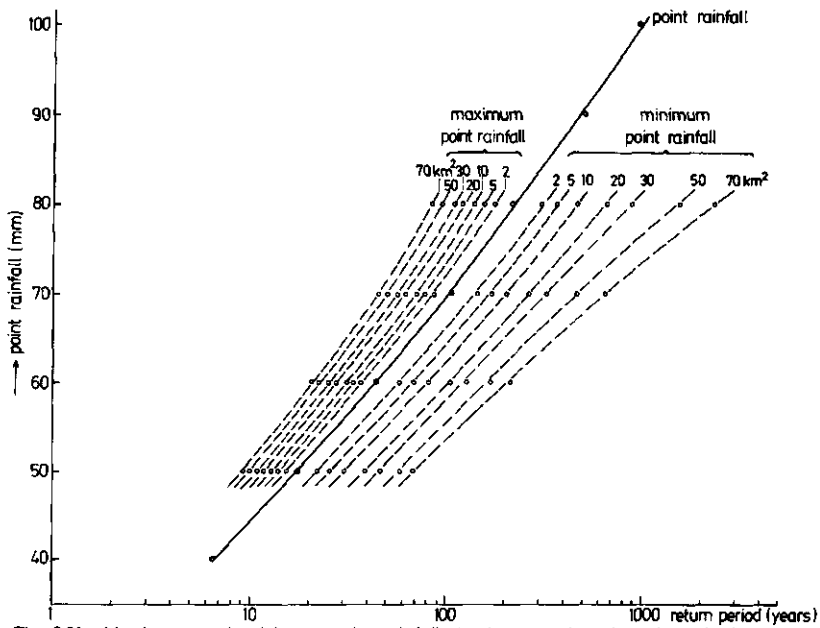


Fig. 331. Maximum and minimum point rainfall depths as a function of areal size and return period, according to Kraijenhoff (1963).

4. SUMMARY AND CONCLUSIONS

Rainfall data for the Netherlands have been used in this study to investigate aspects of heterogeneity of rainfall, in particular local differences in rainfall levels, time trends in rainfall, and local differences in rainfall trend. The possible effect of urbanization and industrialization on the distribution of rainfall has also been studied. Consideration has been given to whether local differences in rainfall justify a partition of the Netherlands into regions. Finally, the degree of areal reduction which is possible in hydrological design because of variation of rainfall in time and space has been investigated.

A statistical analysis of these aspects is useful because they frequently appear in the hydrological literature. The statistical analysis presented in this thesis uses hydrological concepts, such as the statistical areal reduction factor, and attention is focused on moderately low return period events. Only rainfall levels and trends in rainfall have been investigated and not more complicated aspects, such as, trends in the variance of rainfall. Further, rainfall variations in time and space have been analysed separately.

Estimates of the levels of the rainfall characteristics used in the investigation of homogeneity in time and space are given in Section 2.2. These are annual frequencies of exceedance during the summer or the winter period of a certain threshold value and the total annual rainfall (Tables 2.1 and 2.2). The expected daily rainfall has also been estimated for return periods in excess of half a year (Table 2.4, Figure 2.2). Time trends in rainfall averaged over the Netherlands have been estimated. For the period 1951-1979, the time trend is negative for the summer period; and for the period 1906-1979, the time trend is positive for the winter period (Table 2.5). Time trends in rainfall series were found to be related to the occurrence of circulation types (Figure 2.4).

In Section 2.4 local differences in these rainfall characteristics have been investigated using the kriging method that gives the

best linear unbiased predictor. As may be expected, there are local differences, both in rainfall level (Figure 2.7), and in time trends in the rainfall series which were reduced by the annual mean (Figure 2.9). Many of the rainfall series investigated exhibit inhomogeneities (Table 2.7). Two possible causes of these inhomogeneities, changes in the frequency of occurrence of circulation types and anthropogenic activities, such as urbanization and industrialization, are discussed in Section 2.6.

A possible partition of the Netherlands into regions is investigated by using rainfall data for the period 1951-1979. Earlier studies on the geographical distribution of certain rainfall characteristics in the Netherlands are presented in Section 2.5.1. The model to test the statistical significance of the partitions used in this study is presented in Section 2.5.2.

One of the proposed partitions, an a posteriori partition based on mean annual rainfall (Figure 2.11D), is in agreement with the resulting spatial patterns of the levels of the rainfall characteristics considered (Table 2.10). Also, the level of hourly rainfall was found to be related to mean annual rainfall (Figure 2.18A), but, with a simple urban runoff model with a time-step of one hour, no differences were found between the number and quantity of overflow for 12 rainfall stations, classified according to this partition (Section 2.5.3).

These partitions into regions are not satisfactory for rainfall trends, except for an a posteriori partition based on time trends for the period 1951-1979 (Figure 2.12). But both the geographical distribution of trends and the degree of trend in some long-term rainfall records are not in agreement with this partition. Apparently, the changes in rainfall pattern are recent. Because the partition is based on trends in reduced rainfall series (reduced by the annual mean), the changes are also local. Thus on the basis of data used in this study, it was not possible to devise a satisfactory partition of the Netherlands for rainfall trends. With regard to rainfall level it is suffice to assume that the design rainfall at a given location is proportionate to the mean sum-

mer or winter rainfall; therefore, a partition of the Netherlands into regions is not necessary. This has already been suggested in Buishand and Velds (1980).

The influence of urbanization and industrialization on precipitation (urban effects) has been investigated by using the method of Lowry (1977), which allows for changes in frequency of occurrence of circulation types. In Section 2.6, this method is discussed and the findings of other studies on the occurrence, causes, and magnitude of urban effects are presented. In Section 2.6.1, the occurrence of urban effects is discussed, for instance, on the basis of changes in mean daily rainfall for 32 rainfall stations between the industrialized and urbanized period (1956-1979) and the non-industrialized period (1932-1955), with a stratification of days according to season and circulation type (according to Hess, 1977), see Figure 2.22. Although the results were sometimes inconclusive and not always in accordance with the hypothesis of an urban effect, there are indications of urban effects for the zonal circulation type and for three of the meridional circulation types (Tables 2.16 and 2.17; Figure 2.22). Moderate rainfalls were also found to be affected (Table 2.17, where a threshold value for daily rainfall of 15 mm has been considered), and urban effects in the summer period increase with rainfall depth.

In Chapter 3 consideration is given to the degree of areal reduction which is possible in hydrological design because of variations of rainfall in time and space. Use has been made of the IRF-0 kriging theory, and semi-variograms were estimated by the multi-realization approach. The applicability of the IRF-0 theory to predict the mean areal rainfall is discussed in Section 3.2.1. Contrary to what had been expected, in a substantial number of cases the estimated order of the intrinsic random function differs from zero (Table 3.1). Further research is needed on the structure identification, both on the statistical aspects (estimation of the order k of the intrinsic random function and of the coefficients of the generalized covariance model) and on the physical aspects (semi-variogram or generalized covariance model to be

expected under certain assumptions regarding rainfall). The variation in semi-variogram estimates for individual rainfall events was found to be large (Figure 3.3). In Section 3.2.2, the kriging predictor of areal rainfall is compared with the more commonly used arithmetic mean and Thiessen predictor. All three predictors yield similar results (Table 3.5), but the kriging predictor is more efficient (Table 3.4).

Methods to estimate the statistical areal reduction factor (ARF) are presented in Section 3.3.1. With the methods proposed in USWB (1957-1960), NERC (1975), Bell (1976), and Rodríguez-Iturbe and Mejía (1974) and Buishand (1977c), the areal reduction factor for daily rainfall (ARF_{24}) has been estimated for three areas each of about 1000 km^2 in the Netherlands, for the summer period, the winter period, and the complete year. In Section 3.3.3, the variance of ARF_{24} is estimated. All four estimators of ARF_{24} were found to produce similar results (Table 3.12), and the three areas considered do not clearly differ with respect to ARF_{24} . These estimates of ARF_{24} are somewhat lower than those of USWB (1957-1960) for the United States and those of NERC (1975) for the United Kingdom (Figure 3.22), and they are in reasonable agreement with earlier estimates of ARF_{24} for the Netherlands (Table 3.14). For small areas, ARF_{24} is underestimated by the method which uses the marginal distribution of point rainfall and the fitted correlation-distance function. This is also evidenced by the higher ARF_{24} values in Kraijenhoff (1963). ARF_{24} depends heavily on season and return period (Table 3.7). Averaged over the three areas, the maximum areal rainfall occurs in the winter period in 33% of the years considered.

In Section 3.4 ARF for hourly rainfall (ARF_1) is estimated. As a function of areal size and return period, ARF_1 has been estimated for the summer and the winter period (Figure 3.28) and for the complete year (Figure 3.21). These ARF_1 estimates are somewhat lower than those of USWB (1957-1960) and NERC (1975) (Table 3.18), probably because few hourly rainfall data were available for this study. Especially the correlation-distance function for *hourly* rainfalls could not be estimated very satisfactorily.

The storm-centred areal reduction factor (SRF) is discussed in Section 3.5. Models for SRF based on a literature survey of minimum-rainfall curves are presented in Table 3.19. For equal areal size, SRF values from network data are generally lower than ARF values (Figure 3.29). The smaller the areal size and the shorter the period for which rainfall totals are considered, the closer SRF and ARF values.

In this study, rainfall variations in time and space have been analysed separately. Because of this simplification of the problem, the results presented in Chapter 3 may be of less relevance to practical design issues related to areal rainfall. Areal reduction is partly caused by spatial differences in rainfall patterns in time. This aspect of areal reduction is not taken into account, when time aggregates of rainfall over a measurement interval are considered, and rainfall depths over consecutive intervals are assumed to be independent. For this reason, the degree of areal reduction applicable to regional transport systems of sewerage water cannot be determined by using the statistical areal reduction factor.

When rainfall variations in time and space are analysed as being interdependent, the need for knowledge and understanding of meteorology increases because the rainfall events described have first to be classified. Further, instead of the univariate statistical methods as used almost exclusively in this study, multivariate methods are required. However, at present, data from a dense network of rainfall recorders, necessary for such an investigation, are not available for the Netherlands.

Further research on the causes of homogeneities in rainfall series is necessary. Although this study of homogeneity has been restricted to rainfall records of good and even quality, many rainfall series are statistically inhomogeneous, and local differences in trend often seem inexplicable. To explain this, meteorological knowledge and knowledge of the station history of rainfall series used is essential.

SAMENVATTING EN CONCLUSIES

In deze studie zijn met behulp van Nederlandse neerslaggegevens aspecten van de heterogeniteit van de neerslag onderzocht, met name plaatselijke verschillen in het niveau van de neerslag, trends in het neerslagverloop en plaatselijke verschillen in trend. De mogelijke invloed van verstedelijking en industrialisatie op de neerslagverdeling is eveneens bestudeerd. Aandacht is besteed aan de vraag of plaatselijke verschillen in neerslag een opsplitsing van Nederland in deelgebieden rechtvaardigen. Tenslotte is onderzocht de mate waarin gebiedsreductie mogelijk is in sommige ontwerpen als gevolg van de variatie van de neerslag naar tijd en plaats.

De bovenvermelde aspecten komen geregeld ter sprake in de hydrologische literatuur, hetgeen een statistische behandeling ervan zinvol maakt. Deze statistische behandeling maakt gebruik van hydrologische begrippen zoals de statistische gebiedsreductiefactor, en vooral gebeurtenissen met een betrekkelijk korte herhalings-tijd zijn beschouwd. Alleen het niveau van de neerslag en trends daarin zijn onderzocht, en niet gecompliceerdere aspecten, zoals trends in de variantie van de neerslag. Ook zijn de variaties naar tijd en plaats steeds afzonderlijk behandeld.

In Paragraaf 2.2 is het niveau geschat van de neerslagkenmerken waarvan de homogeniteit naar tijd en plaats is onderzocht: jaarlijkse aantallen dagneerslagen groter dan een zekere drempelwaarde in de zomer- of winterperiode, en de jaarneerslag (Tabellen 2.1 en 2.2). Ook is voor herhalingstijden langer dan een half jaar de verwachte dagneerslagsom geschat (Tabel 2.4, Figuur 2.2). Trends in het over Nederland gemiddelde neerslagverloop zijn bepaald. Voor de periode 1951-1979 is de trend voor de zomerperiode negatief; voor de periode 1906-1979 is de trend voor de winterperiode positief (Tabel 2.5). Trends in het verloop van neerslagkenmerken blijken gerelateerd aan het optreden van circulatietypen (Figuur 2.4).

In Paragraaf 2.4 zijn plaatselijke verschillen in deze neerslagkenmerken onderzocht, waarbij gebruik is gemaakt van de kriging methode, ter verkrijging van de beste lineaire zuivere voorspeller. Zoals te verwachten is, zijn er plaatselijke verschillen, zowel in het niveau van de neerslag (Figuur 2.7), als in trends in verschilreeksen (Figuur 2.9); deze verschilreeksen ontstaan door aftrekken van het jaargemiddelde. Veel van de onderzochte neerslagreeksen blijken statistisch niet homogeen te zijn (Tabel 2.7). Twee mogelijke verklaringen van de geconstateerde afwijkingen van homogeniteit, veranderingen in de frequentie van voorkomen van circulatietypen en antropogene activiteiten zoals verstedelijking en industrialisatie, zijn onderzocht in Paragraaf 2.6.

Een mogelijke opdeling van Nederland in deelgebieden is onderzocht met behulp van neerslaggegevens voor de periode 1951-1979. Eerder onderzoek naar de geografische verdeling van bepaalde neerslagkenmerken in Nederland is vermeld in Paragraaf 2.5.1. Het hier gebruikte toetsingsmodel is vermeld in Paragraaf 2.5.2.

Een van de voorgestelde gebiedsindelingen, een a posteriori indeling gebaseerd op gemiddelde jaarneerslag (Figuur 2.11D), is in overeenstemming met de ruimtelijke patronen van de niveaus van de beschouwde neerslagkenmerken (Tabel 2.10). Ook het niveau van uurneerslagsommen blijkt samen te hangen met de gemiddelde jaarneerslag (Figuur 2.18A), maar met behulp van een eenvoudig stedelijk afvoermodel met een tijdstap van een uur konden geen verschillen in aantallen en hoeveelheden van overstorten worden aangetoond tussen 12 volgens deze gebiedsindeling geklassificeerde neerslagstations (Paragraaf 2.5.3).

Voor trends in het neerslagverloop voldoen deze gebiedsindelingen niet, behalve een a posteriori indeling gebaseerd op trends voor de periode 1951-1979 (Figuur 2.12). Voor enkele langjarige reeksen blijken de geografische verdeling van trends en de mate van trend echter niet overeen te stemmen met deze gebiedsindeling. Blijkbaar gaat het om recente veranderingen in het neerslagpatroon. Aangezien de gebiedsindeling gebaseerd is op trends in verschilreeksen, gaat het hier om lokale veranderingen. Met behulp van de

in deze studie gebruikte gegevens kon de vraag naar een opdeling van Nederland in gebieden voor trends in het neerslagverloop dan ook niet worden beantwoord. Met betrekking tot het niveau van de neerslag is het voldoende om de ontwerpneerslag voor een bepaalde plaats evenredig te veronderstellen met de normaalwaarde van de seizoensneerslag en hoeft Nederland niet in gebieden te worden opgedeeld. Deze suggestie is al gedaan in Buishand en Velds (1980).

De invloed van verstedelijking en industrialisatie op de neerslag (stedelijke effecten) is bestudeerd volgens de in Lowry (1977) gepresenteerde methode, waarbij wordt gecorrigeerd voor veranderingen in frequentie van voorkomen van circulatietypen. In Paragraaf 2.6 is Lowry's methode gepresenteerd, en is verslag gedaan van resultaten van elders verricht onderzoek naar het voorkomen, de oorzaken en de omvang van stedelijke effecten. In Paragraaf 2.6.1 is het voorkomen van stedelijke effecten nagegaan, onder andere aan de hand van de verandering van de gemiddelde dagneerslag voor de geïndustrialiseerde en verstedelijkte periode (1956-1979) ten opzichte van de niet-geïndustrialiseerde periode (1932-1955) voor 32 neerslagstations, waarbij onderscheid is gemaakt naar seizoen en circulatietype (volgens Hess, 1977), zie Figuur 2.22. Alhoewel de resultaten soms onduidelijk zijn en niet altijd in overeenstemming met de hypothese van stedelijke effecten, zijn er voor het zonale hoofdcirculatietype en voor drie meridionale circulatietypen aanwijzingen voor het bestaan van stedelijke effecten (Tabellen 2.16 en 2.17; Figuur 2.22). Alhoewel de effecten zich ook uitstrekken tot matige neerslagen (zie Tabel 2.17, waar is uitgegaan van een drempelwaarde voor de dagneerslag van 15 mm), nemen gedurende de zomerperiode de stedelijke effecten toe met de neerslaghoeveelheid.

In Hoofdstuk 3 is aandacht geschonken aan de mate waarin gebiedsreductie mogelijk is in sommige ontwerpen als gevolg van de variatie van de neerslag naar tijd en plaats. Er is gebruik gemaakt van de IRF-0 kriging theorie, en semi-variogrammen zijn geschat met behulp van de meervoudige-realisatiebenadering. De toepasbaarheid van de IRF-0 theorie voor het bepalen van gebiedsgemid-

delden van de neerslag is nagegaan in Paragraaf 3.2.1. In tegenstelling tot wat verwacht werd, is in vrij veel van de onderzochte gevallen de geschatte orde van de intrinsieke toevalsfunctie ongelijk nul (Tabel 3.1). Het verdient aanbeveling toekomstig onderzoek onder andere te richten op deze zogenaamde structuurverkenning, zowel op de statistische aspecten (het schatten van de orde k van de intrinsieke toevalsfunctie en van de coëfficiënten van het gegeneraliseerde covariantiemodel) als op de fysische aspecten (het te verwachten semi-variogram of gegeneraliseerd covariantiemodel onder zekere veronderstellingen met betrekking tot de neerslag). De variatie tussen semi-variogram schattingen voor afzonderlijke neerslaggebeurtenissen is groot (zie Figuur 3.3). In Paragraaf 3.2.2 is de voorspeller van het gebiedsgemiddelde door kriging vergeleken met twee gebruikelijke voorspellers van het gebiedsgemiddelde, het rekenkundig gemiddelde en het Thiessen gemiddelde. Toepassing van kriging leidt hier niet zozeer tot resultaten die gemiddeld sterk verschillen ten opzichte van de resultaten van andere methoden (Tabel 3.5), maar tot efficiëntere voorspellingen (Tabel 3.4).

Enige schatters van de statistische gebiedsreductiefactor ARF zijn gepresenteerd in Paragraaf 3.3.1. Met behulp van de schatters volgens USWB (1957-1960), NERC (1975), Bell (1976) en volgens Rodríguez-Iturbe en Mejía (1974) en Buishand (1977c) is in Paragraaf 3.3.2 voor een drietal gebieden in Nederland van ongeveer 1000 km^2 ARF_{24} , de gebiedsreductiefactor voor dagsommen van de neerslag, geschat, zowel voor het gehele jaar, als voor de zomer- en winterperiode afzonderlijk. In Paragraaf 3.3.3 is de variantie van ARF_{24} geschat. Alle vier genoemde schatters van ARF_{24} blijken praktisch dezelfde resultaten op te leveren (Tabel 3.12), en de drie beschouwde gebieden verschillen niet duidelijk met betrekking tot ARF_{24} . Deze schattingen van ARF_{24} zijn iets lager dan de schattingen in USWB (1957-1960) voor de Verenigde Staten en in NERC (1975) voor het Verenigd Koninkrijk (Figuur 3.22), en stemmen redelijk overeen met eerdere schattingen van ARF_{24} voor Nederland (Tabel 3.14). Voor kleine gebiedsgrootten onderschat de methode die gebruik maakt van de marginale kansverdeling van puntneerslagen en het aangepaste correlatieverloop ARF_{24} . Dit blijkt

ook uit de hogere ARF_{24} waarden in Kraijenhoff (1963). ARF_{24} is sterk afhankelijk van seizoen en herhalingstijd (Tabel 3.7). Gemiddeld over de drie gebieden valt in 33% van de jaren het jaar-maximum van de gebiedsneerslag gedurende de winterperiode.

In Paragraaf 3.4 is ARF voor uurneerslagen (ARF_1) geschat. Als functie van de gebiedsgrootte en de herhalingstijd is ARF_1 weergegeven in Figuur 3.21 voor het gehele jaar, en in Figuur 3.28 voor de zomer- en winterperiode. De in deze studie geschatte ARF_1 waarden zijn lager dan die in NERC (1975) en USWB (1957-1960) (zie Tabel 3.18), waarschijnlijk als gevolg van de geringe hoeveelheid beschikbare uurneerslaggegevens voor deze studie. Vooral het ruimtelijk correlatieverloop van uurneerslagen kon niet erg bevredigend worden geschat.

In Paragraaf 3.5 is aandacht besteed aan de bui-gecentreerde gebiedsreductiefactor (SRF). Enige modellen voor SRF, gebaseerd op in de literatuur vermelde modellen voor het neerslagverloop langs een isohyeet, als functie van de afstand van die isohyeet tot het neerslagcentrum, zijn vermeld in Tabel 3.19. Op metingen gebaseerde SRF waarden blijken in het algemeen lager te zijn dan ARF waarden (Figuur 3.29). SRF en ARF liggen dicht bij elkaar naarmate de gebiedsgrootte kleiner is en de periode waarbinnen neerslagsommen beschouwd worden, korter is.

In deze studie zijn de variatie naar tijd en de variatie naar plaats steeds afzonderlijk behandeld. Vanwege deze vereenvoudiging kunnen de resultaten in Hoofdstuk 3 van minder belang zijn voor sommige met de gebiedsneerslag samenhangende ontwerpproblemen. Gebiedsreductie wordt gedeeltelijk veroorzaakt doordat het neerslagverloop in de tijd binnen een neerslaggebeurtenis van plaats tot plaats verschilt. Doordat de neerslag wordt gesommeerd over een waarnemingsinterval, en doordat er geen samenhang tussen in opeenvolgende waarnemingsintervallen gevallen neerslaghoeveelheden wordt verondersteld, blijft dit aspect van de gebiedsreductie buiten beschouwing. Hierdoor kan de mogelijke gebiedsreductie voor regionale afvalwatertransportsystemen niet met de gebiedsreductiefactor worden beantwoord.

Wanneer de variaties van de neerslag naar tijd en plaats in hun onderlinge samenhang worden behandeld, zal de noodzaak om meteorologische kennis toe te passen toenemen, omdat dan neerslaggebeurtenissen worden beschreven, die eerst in klassen moeten worden ingedeeld. In plaats van de in deze studie bijna uitsluitend toegepaste statistische methoden voor enkelvoudige kenmerken, zijn dan statistische methoden voor meervoudige kenmerken nodig. Op dit moment zijn in Nederland de voor een dergelijk onderzoek benodigde neerslaggegevens van een dicht netwerk van regenschrijvers overigens nog niet beschikbaar.

Ook nader onderzoek naar de oorzaken van inhomogeniteiten in neerslagreeksen is noodzakelijk. Hoewel het hier verrichte homogeniteitsonderzoek zich beperkte tot een selectie van neerslagreeksen van goede en van gelijkmatige kwaliteit, zijn statistisch gezien veel neerslagreeksen inhomogeen, en lijken plaatselijke verschillen in trend vaak onverklaarbaar. Meteorologisch inzicht en kennis van de stationsgeschiedenis van de beschouwde neerslagstations zijn ook daarom eerste vereisten.

APPENDIX A. DATA AND SUPPLEMENTARY RESULTS OF THE STUDY ON HOMOGENEITY

A.1. DUTCH RAINFALL STATIONS USED IN THE STUDY OF HOMOGENEITY OF RAINFALL RECORDS

In this appendix, the names are given of the rainfall stations in the data sets used in the study of homogeneity of rainfall records. The KNMI code number is given in brackets after the name of the station, and comments on missing data are presented as footnotes to the end of the appendix.

A.1.1. Data set 140: daily rainfall records (1951-1979) of 140 KNMI rainfall stations distributed evenly throughout the Netherlands (data from KNMI magnetic tape REGEN).

Hollum (10)	Onnen (158)	Vroomshoop (345)
Schiermonnikoog (12)	Eelde (161)	Kraggenburg (346)
Petten (16)	Niekerk (162)	Urk (347)
Den Burg (17)	Marum (166)	Emmeloord (348)
Cocksdoorp (19)	Enkhuizen ³ (221)	Nagele (352)
Dokkum (67)	Hoorn (222)	Blokzijl (353)
Lemmer (Tacozijsl) (74)	Overveen (225)	Dedemsvaart (354)
Oldeholtspade (75)	Schagen (228)	Kuinre (356)
Kornwerderzand (76)	Zaandijk (230)	Lemmer (Buma) ⁴ (359)
Stavoren (80)	Bergen (234)	Groot Ammers ⁵ (434)
Gorredijk (82)	Castricum (235)	Sassenheim (436)
Ezumazijl (84)	Medemblik (236)	Lijnsden (437)
Leeuwarden (85)	De Haukes (238)	Hoofddorp (438)
Groningen (139)	Den Oever (239)	Oude Wetering (439)
Assen (140)	Kreileroord (240)	Scheveningen (440)
Ter Apel ¹ (144)	Marken (246)	Amsterdam (441)
Zoutkamp (145)	Kolhorn (252)	Boskoop (442)
Sappemeer (148)	Wapenveld (329)	Gouda (443)
Roodeschool (151)	Zwolle (330)	Katwijk aan de Rijn (444)
Winschoten (153)	Emmen (333)	Rotterdam (445)
Eenrum ² (154)	Rheezerveen (339)	Delft ⁶ (449)
Vlagtwedde (156)	Zweelo (341)	Numansdorp (450)

Bergschenhoek (453)	Almelo (664)	Oudenbosch (828)
Mookhoek ⁷ (455)	Enschede (665)	Herwijnen (830)
Oostvoorne (456)	Winterswijk (666)	Bergen op Zoom (832)
Aalsmeer (458)	Doetinchem (667)	Oosterhout (833)
Dordrecht (459)	Hengelo (668)	Chaam (834)
Dirksland (462)	Borculo ¹³ (669)	Andel (835)
Wassenaar (466)	Twente (670)	Ginneken (838)
Poortugaal ⁸ (467)	Gendringen (673)	Hoogerheide (839)
Leiden (469)	Rekken (674)	Nieuwendijk (840)
Ouddorp ⁹ (471)	Oldenzaal (676)	Gilze Rijen (843)
Nijmegen (539)	Deventer ¹⁴ (677)	Capelle ¹⁸ (844)
Arnhem ¹⁰ (541)	Almen (678)	Helmond ¹⁹ (896)
Apeldoorn (543)	Lettele ¹⁵ (681)	Gemert (899)
Nijkerk ¹¹ (547)	Vlissingen (733)	Nuland (901)
De Bilt (550)	Sint Kruis (740)	Eindhoven (902)
Bussum (556)	Terneuzen (742)	Megen ²⁰ (903)
Lunteren (558)	Axel (745)	Deurne ²¹ (908)
Tiel (562)	Krabbendijke ¹⁶ (747)	Dinther (911)
Hulshorst (564)	Vrouwenpolder (751)	Leende (912)
Harskamp ¹² (571)	Haamstede ¹⁷ (752)	Eersel ²² (915)
Beekbergen (573)	Middelburg (756)	Vaals (968)
Oosterbeek (578)	Sint Annaland (759)	Stramproij (970)
Veenendaal (579)	's-Heerenhoek (760)	Beek (973)
Geldermalsen (584)	Cadzand (763)	Buchten (974)
Hilversum (586)	Tilburg (827)	

A.1.2. Data set D14: long-term daily rainfall records (1906-1979) of 14 KNMI rainfall stations distributed evenly throughout the Netherlands.

Den Helder/De Kooy (9/25)	Heerde (328)	Kerkwerpe ²⁴ (737/743/46)
West Terschelling (11)	Denekamp ²³ (331)	Axel (745)
Groningen (139)	Hoofddorp (438)	Oudenbosch (828)
Ter Apel (144)	Winterswijk (666)	Roermond ²⁵ (961)
Hoorn (222)	Vlissingen (733)	

Before 1951, data are from the KNMI magnetic tape CODE2X. For the period 1951-1979, data are from the KNMI magnetic tape REGEN. Records of the stations West Terschelling, Heerde and Kerkwerpe

showed some gaps for the period 1951-1953. In these cases use was made of the CODE2X tape for supplementary data.

A.1.3. Data set D32: daily rainfall records (1932-1979) of 32 KNMI rainfall stations; 17 in the Rijnmond area, and 15 evenly distributed throughout the rest of the Netherlands (data from magnetic tapes CODE2X and REGEN, and from punch card lists).

The data set includes all stations listed in Section A.1.2 plus the following stations:

Schellingwoude ²⁶ (223)	Oude Wetering (439)	Lisse ³⁰ (454)
Zandvoort ²⁷ (229)	Amsterdam (441)	Mookhoek ³¹ (455)
Castricum (235)	Boskoop (442)	Oostvoorne (456)
Dwingelo (327)	Delft ²⁹ (449)	Leiden (469)
Cruquius/Heemstede ²⁸ (435)	IJsselmonde (451)	Zegveld ³² (470)
Sassenheim (436)	Bergschenhoek (453)	Arnhem ³³ (541)

A.1.4. Data set H12: hourly rainfall records and the period of observation for 12 KNMI rainfall stations.

De Bilt ³⁴ (260), 1906-1982	Schiphol (240), 1971-1980
Den Helder/De Kooy (235), 1957-1980	Leeuwarden (270), 1 June 1974-1980
Beek (380), 1957-1980	Rotterdam (344), 1974-1980
Vlissingen (310), 1 May 1958-1980	Soesterberg ³⁵ (265), 1 June 1974-1982
Eelde (280), 1957-1980	Twente ³⁶ (290) 1 June 1974-1980
Valkenburg (210), 1 May 1972-1980	Volkel (375), 1 June 1974-1980

¹ Missing: Aug. 1955, supplemented by Vlagtwedde.

² Missing: March 1964, supplemented by Ulrum.

³ Missing: Feb. 1951, supplemented by Hoorn.

⁴ Missing: Dec. 1958, supplemented by Lemmer (Tacozijsl).

⁵ Missing: Jan. 1953, supplemented by Oud Alblas.

⁶ Missing: Feb. 1951, supplemented by Naaldwijk.

⁷ Missing: Feb. 1953, supplemented by Numansdorp.

⁸ Missing: June, July 1951, supplemented by IJsselmonde.

⁹ Missing: Feb. 1953, supplemented by Brielle.

- ¹⁰ Missing: Sept. 1955, supplemented by Arnhem (data from yearbook).
- ¹¹ Missing: 11-28 Feb. 1955, supplemented by Lunteren.
- ¹² Missing: 21-28 Feb. 1955 and Dec. 1955 supplemented by Beekbergen.
- ¹³ Missing: 14 May 1978, supplemented by Borculo (data from yearbook).
- ¹⁴ Missing: Dec. 1952, supplemented by Deventer (data from yearbook).
- ¹⁵ Missing: Oct. 1952, supplemented by Lettele (data from yearbook).
- ¹⁶ Missing: 6-28 Feb. 1953, supplemented by Kapelle.
- ¹⁷ Missing: Feb. 1953, supplemented by Vrouwenpolder.
- ¹⁸ Missing: Jan., Feb. 1951, supplemented by Oosterhout.
- ¹⁹ Missing: Aug. 1951, supplemented by Gemert.
- ²⁰ Missing: Feb. 1960, supplemented by Oss.
- ²¹ Missing: July 1969, supplemented by Helmond.
- ²² Missing: July 1952, supplemented by Eersel (data from yearbook).
- ²³ Missing: 211 days in 1956-1959, supplemented by Weerselo.
- ²⁴ Missing: Jan., Feb. 1954, supplemented by Noordgouwe.
- ²⁵ Missing: March, Nov. 1971, supplemented by Beesel.
- ²⁶ Missing: Jan. 1945, 1-10 March 1947 and Feb. 1957, supplemented by Marken.
- ²⁷ Missing: Aug. 1944, supplemented by Overveen.
- ²⁸ Missing: Nov., Dec. 1948, Dec. 1973 and Jan. 1974, supplemented by Lisse.
- ²⁹ Missing: Feb. 1951, supplemented by Naaldwijk.
- ³⁰ Missing: Dec. 1945, supplemented by Sassenheim.
- ³¹ Missing: June 1945, supplemented by Oud Beijerland and Feb. 1953, supplemented by Numansdorp.
- ³² Missing: April 1945, Feb. 1956, supplemented by Gouda.
- ³³ Missing: Sept. 1955, supplemented by Arnhem (data from yearbook).
- ³⁴ Missing: Apr. 1945, not supplemented.
- ³⁵ Missing: 25 April-18 June 1981, not supplemented.
- ³⁶ Missing: 3-7 Jan. 1976, not supplemented.

A.2. PROPERTIES OF THE TRANSFORMATION ACCORDING TO EQUATION 2.9 APPLIED TO POISSON VARIATES

Consider a transformation

$$x = \sqrt{\tilde{x} + \sqrt{(\tilde{x} + 1)}}. \quad (\text{A.2.1})$$

Its variance stabilizing effect on Poisson variates can be easily verified by calculating the first and second moment of \underline{x} by

$$E(\underline{x}^k) = \sum_{\tilde{x}=0}^{\infty} \frac{e^{-\lambda} \lambda^{\tilde{x}}}{\tilde{x}!} (\sqrt{\tilde{x} + \sqrt{(\tilde{x} + 1)}}), \quad (\text{A.2.2})$$

where

$$\lambda = E\tilde{x}; \text{ note } \text{var}\underline{x} = E\underline{x}^2 - (E\underline{x})^2.$$

The summation in Equation A.2.2 converges rapidly enough to make calculation by computer feasible. For values of λ ranging from 1 to 50, the variance calculated with Equation A.2.2 ranges from 0.940 to 1.001.

As a secondary effect \underline{x} tends to be normally distributed; this is particularly useful because the distribution of the statistics to test homogeneity of a series is usually derived for independent normally distributed variates. In Chapter 2, the independence of the variates is quite well satisfied. This tendency to a normal distribution of \underline{x} has been verified by comparing the distribution functions of

$$\underline{x}_{29}^2 = \frac{1}{2} \sum_{k=1}^{29} (\underline{x}_{2k-1} - \underline{x}_{2k})^2, \quad (\text{A.2.3})$$

and χ_{29}^2 , by calculating the Kolmogorov Smirnov statistic D , that is the maximum absolute value of the difference between the edf (Equation A.2.3) and the cdf of χ_{29}^2 , where the edf has been simulated by 1000 samples of 58 independent Poisson variates \tilde{x}_j each. The results for different values of λ are given in Table A.2.1. The expectation and variance of χ_{29}^2 are 29 and 58, respectively.

Table A.2.1. The Kolmogorov Smirnov statistic D and the first two moments of \underline{X}^2 for different values of λ

λ	\underline{X}^2		D
	mean	variance	
1	27.3	38.9	0.108 ^{oo}
5	29.1	68.1	0.045
15	28.9	61.4	0.027
50	29.1	61.5	0.024

^{oo} Inside the critical region for $\alpha = 0.05$.

Although for $\lambda = 1$, D is rather large, for all values of λ the edf of \underline{X}^2 produces a virtually straight line when plotted on Gauss paper (see Figure A.2.1). Thus, for a Poisson variate \underline{X} , it can be assumed that \underline{X} is normally distributed.

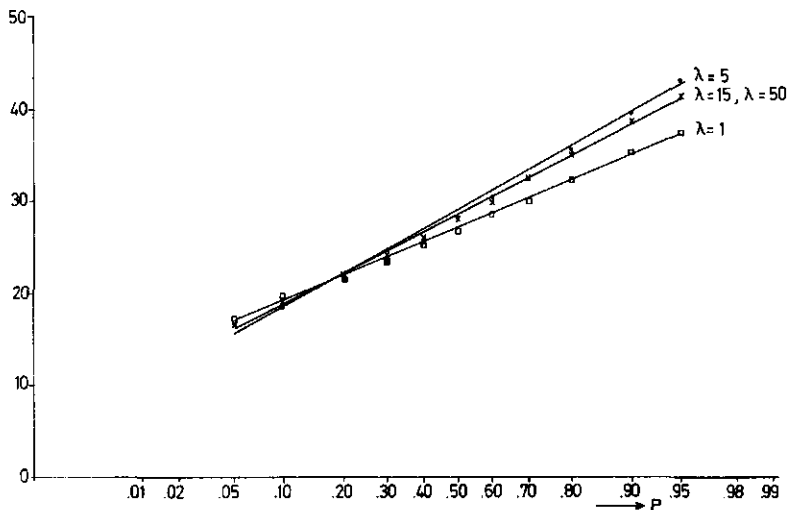


Fig.A.2.1. The edf of \underline{X}^2 for different values of λ . The lines were fitted by eye.

A.3. PROPERTIES OF WEIGHTED RESCALED ADJUSTED PARTIAL SUMS

In the notation in Section 2.3, it can be shown that under the null hypothesis $\delta = 0$ in Equations 2.10 and 2.11 (Anis and Lloyd, 1976)

$$(\underline{S}_k^{**})^2 \sim \underline{\beta}(\frac{1}{2}, \frac{1}{2}n-1), \quad (\text{A.3.1})$$

from which it follows that $\text{var}(\underline{S}_k^{**}) = \frac{1}{n-1}$ ($k=1, \dots, n-1$), that is independent of k .

It follows from Equation A.3.1 that under the null hypothesis

$$(n-2) \frac{(\underline{S}_k^{**})^2}{1 - (\underline{S}_k^{**})^2} \sim \frac{(n-2)\underline{\beta}(\frac{1}{2}, \frac{1}{2}n-1)}{1 - \underline{\beta}(\frac{1}{2}, \frac{1}{2}n-1)} \sim \underline{t}_{n-2}^2. \quad (\text{A.3.2})$$

Since Worsley's test statistic \underline{W} is defined as $\max |\underline{Z}_k|$, with $\underline{Z}_k \sim \underline{t}_{n-2}$ (Worsley, 1979), it may be concluded that under the null hypothesis

$$\underline{W} = (n-2)^{\frac{1}{2}} \underline{M} / (1 - \underline{M}^2)^{\frac{1}{2}}. \quad (\text{A.3.3})$$

A.4. VARIANCE OF THE SEMI-VARIANCE ESTIMATOR

Let $\underline{X} = (\underline{X}_1, \underline{X}_2, \underline{X}_3, \underline{X}_4)$ be simultaneously normally distributed with expectation vector 0 and covariance matrix $\Sigma = (\sigma_{ij})$, then

$$E(\underline{X}_1 \underline{X}_2 \underline{X}_3 \underline{X}_4) = \sigma_{12} \sigma_{34} + \sigma_{13} \sigma_{24} + \sigma_{14} \sigma_{23}. \quad (\text{A.4.1})$$

This may be proved by using characteristic functions (Anderson, 1958; p. 38, 39), and as a consequence

$$\begin{aligned} & E[\{Z(u_1+h)-Z(u_1)\}^2 \{Z(u_2+h)-Z(u_2)\}^2] = \\ & = E[\{Z(u_1+h)-Z(u_1)\} \{Z(u_1+h)-Z(u_1)\} \{Z(u_2+h)-Z(u_2)\} \{Z(u_2+h)-Z(u_2)\}] = \\ & = \text{Var}[Z(u_1+h)-Z(u_1)] \text{Var}[Z(u_2+h)-Z(u_2)] + \\ & + 2\text{Cov}^2[\{Z(u_1+h)-Z(u_1)\}, \{Z(u_2+h)-Z(u_2)\}], \end{aligned} \quad (\text{A.4.2})$$

where $Z(u)$ is an intrinsic random function, defined on a transect V of length L , and $V \in \mathbb{R}^1$, and the increments $\{Z(u+h)-Z(u)\}$ are normally distributed.

General results are

$$\begin{aligned} & \text{Cov}[\{Z(u_1+h)-Z(u_1)\}, \{Z(u_2+h)-Z(u_2)\}] = \text{Cov}[Z(u_1+h), Z(u_2+h)] - \\ & - \text{Cov}[Z(u_1+h), Z(u_2)] - \text{Cov}[Z(u_1), Z(u_2+h)] + \text{Cov}[Z(u_1), Z(u_2)] = \\ & = -2\gamma(u_1-u_2) + \gamma(u_1-u_2+h) + \gamma(u_1-u_2-h), \end{aligned} \quad (\text{A.4.3})$$

and

$$\text{Var}[\{Z(u_1+h)-Z(u_1)\}] = \text{Var}[\{Z(u_2+h)-Z(u_2)\}] = 2\gamma(h). \quad (\text{A.4.4})$$

Inserting Equations A.4.3 and A.4.4 into Equation A.4.2 leads to

$$\begin{aligned} & E[\{Z(u_1+h)-Z(u_1)\}^2 \{Z(u_2+h)-Z(u_2)\}^2] = \\ & = 4\gamma^2(h) + 2[\gamma(u_1-u_2+h) + \gamma(u_1-u_2-h) - 2\gamma(u_1-u_2)]^2, \end{aligned} \quad (\text{A.4.5})$$

where

$$4\gamma^2(h) = \{E\{Z(u_1+h)-Z(u_1)\}^2\}^2.$$

Thus

$$\begin{aligned} \text{Cov}[\{Z(u_1+h)-Z(u_1)\}^2, \{Z(u_2+h)-Z(u_2)\}^2] &= \\ &= 2[\gamma(u_1-u_2+h)+\gamma(u_1-u_2-h)-2\gamma(u_1-u_2)]^2. \end{aligned} \quad (\text{A.4.6})$$

Let $\hat{\gamma}_V(h)$ be the sample semi-variogram in case of complete information on V of the realization $z(u)$ of $Z(u)$. Then, because of Equation A.4.6

$$\begin{aligned} 4E\{\text{Var}[\hat{\gamma}_V(h)]\} &= \frac{1}{(L-h)^2} \int_0^{L-h} \int_0^{L-h} 2[\gamma(u_1-u_2+h)+ \\ &+ \gamma(u_1-u_2-h)-2\gamma(u_1-u_2)]^2 du_1 du_2. \end{aligned}$$

If one assumes a linear population semi-variogram $\gamma(h)=\alpha h$, then

$$\begin{aligned} \text{Var}[\hat{\gamma}_V(h)] &= \frac{1}{(L-h)^2} \int_0^{L-h} \int_0^{u_1} [\gamma(u_1-u_2+h)+\gamma(u_1-u_2-h)-2\gamma(u_1-u_2)]^2 du_1 du_2 = \\ &= \frac{4\alpha^2}{(L-h)^2} \int_0^{L-h} \int_{\sup(0, (u_1-h))}^{u_1} [h-u_1+u_2]^2 du_1 du_2. \end{aligned}$$

Thus for $h \leq L/2$

$$\text{Var}[\hat{\gamma}_V(h)] = \left(\frac{4}{3}\frac{h^3}{L-h}\right) - \frac{1}{3}\left(\frac{h^4}{(L-h)^2}\right)\alpha^2, \quad (\text{A.4.7})$$

and for $h > L/2$

$$\text{Var}[\hat{\gamma}_V(h)] = (2h^2 + \frac{1}{3}(L-h)^2 - \frac{4}{3}h(L-h))\alpha^2. \quad (\text{A.4.8})$$

Specifically, for $h \rightarrow 0$, $\text{Var}[\hat{\gamma}_V(h)]/[\gamma(h)]^2 \approx \frac{4h}{3L}$, while for $h=L/2$

$$\text{Var}[\hat{\gamma}_V(h)]/[\gamma(h)]^2 = 1.$$

As a numerical illustration, a random walk $Z(u)$ was considered, simulated on an interval $[0, L]$, and starting at the origin

$$Z(u_i) = Y_0 + \dots + Y_i, \quad i=0, 1, \dots, N-1, \quad (\text{A.4.9})$$

where the Y_i are standard normal variates and the N points u_i are equidistant at distance 1, thus

$$\begin{cases} E[Z(u) - Z(u+h)] = 0 \\ \gamma(h) = \frac{1}{2}h, \end{cases} \quad h=0, 1, \dots, N-1.$$

For each of 500 realizations of random walks $Z(u)$ on $[0, 140]$ the quantity $\hat{\gamma}_V(h)$ as well as the ratio of the experimental variance of $\hat{\gamma}_V(h)$ to $[\gamma(h)]^2$ for the first 2, the first 50, and all 500 realizations have been calculated for $h=1, 10, 70$ and 139. These ratios are presented in Figure A.4.1. It may be concluded that for $n=500$ realizations, the ratios $\text{Var}[\hat{\gamma}_V(h)]/[\gamma(h)]^2$ are very close to the expected values, which are 0.0952 ($h=10$), 1 ($h=70$) and about 2 ($h=139$). For a small number of realizations ($n=2$) the results are rather unpredictable.

Thus, if only one realization out of the infinitely many possible is considered the possibility of statistical inference rapidly decreases with increasing h . When more realizations on V of the same process $Z(u)$ are known, the situation is more favourable. Using the above simulation results, the ratio was calculated

$$|\hat{\gamma}_V(h) - \gamma(h)| / \gamma(h), \quad (\text{A.4.10})$$

where $\hat{\gamma}_V(h)$ was calculated for the first realization or averaged over the first 2, the first 50, or all 500 realizations. From Figure A.4.2, it can be seen that for these mean $\hat{\gamma}_V(h)$, the ratio according to Equation A.4.10 rapidly decreases with increasing n .

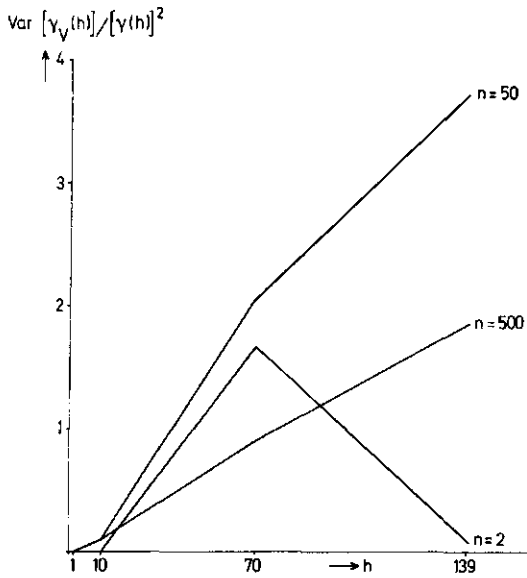


Fig.A.4.1. $\text{Var}[\gamma_V(h)] / [\gamma(h)]^2$ as function of h and n .

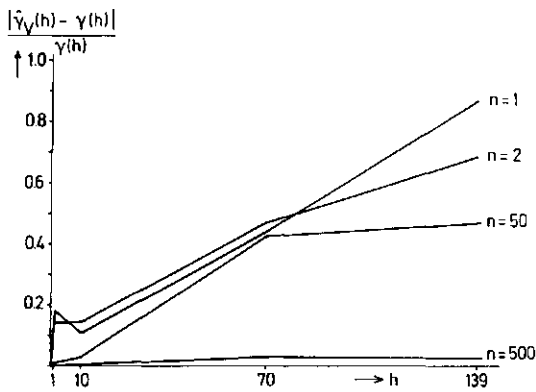


Fig.A.4.2. $|\hat{\gamma}_V(h) - \gamma(h)| / \gamma(h)$ as function of h and n .

A.5. RESULTS OF HOMOGENEITY TESTS AND CLASSIFICATION OF RAINFALL STATIONS IN DATA SET D140

Table A.5.1 gives the results of homogeneity tests for rainfall characteristics for rainfall stations in data set D140. The Table should be read as follows:

- 0: only R critical
- 1: only T critical
- 2: only M critical
- 3: both R and T, but not M critical
- 4: both R and M, but not T critical
- 5: both T and M, but not R critical
- 6: all three statistics critical.

The sign of these numbers in Table A.5.1 indicates the direction of the trend or jump.

In addition, the classification of each station according to the six proposed partitions of the Netherlands on the basis of rainfall level and rainfall trend is also given in Table A.5.1. The six partitions are as follows:

- partitions (i), (ii), (iii), and (iv) on the basis of rainfall level, discussed in Section 2.5.1 and shown in Figure 2.11;
- partition (v) on the basis of rainfall trend, discussed in Section 2.5.3 and shown in Figure 2.12;
- partition (vi) on the basis of urbanization and industrialization, discussed in Section 6.1 and shown in Figure 2.24.

Table A.5.1. Results of homogeneity tests on rainfall characteristics and classification of rainfall stations in data set D140

Rainfall station code number	Results of homogeneity tests on rainfall characteristic							Partition					
	F_1^S	F_{15}^S	F_{25}^S	F_1^W	F_{15}^W	F_{25}^W	R	(i)	(ii)	(iii)	(iv)	(v)	(vi)
10								1	2	2	3	3	2
12		-1					-2	1	2	2	3	3	2
16				3		0		1	2	2	3	3	2
17	0							1	2	2	3	1	2

Rainfall station code number	Results of homogeneity tests on rainfall characteristic							Partition					
	F_1^S	F_{15}^S	F_{25}^S	F_1^W	F_{15}^W	F_{25}^W	R	(i)	(ii)	(iii)	(iv)	(v)	(vi)
19								1	2	2	3	3	2
67							0	2	2	2	1	3	2
74	-6	0		-6	-1	-5	-3	2	3	3	3	2	2
75				0		-5		3	3	3	1	1	2
76				-6				2	2	2	2	2	2
80	0			0				2	3	3	2	2	2
82							4	3	3	3	1	3	2
84	-4							2	2	2	3	3	2
85	-1	-6		-6	-1		-6	2	3	3	3	2	2
139		-1	0	-6				3	3	3	3	2	2
140		0		-5			-4	3	3	2	3	2	2
144						-1		5	3	2	2	2	2
145	5	0			6		6	2	2	2	3	3	2
148	5					-5	0	3	3	3	2	3	2
151	5				2		6	2	2	2	2	3	2
153	0			-6	-6		-6	3	3	3	2	3	2
154	5				2			2	2	2	3	3	2
156				-5				5	3	2	2	3	2
158		-6	-1	-5	-6		0	3	3	2	2	2	2
161		-5	-6	0	0	-4		3	3	2	3	2	2
162				0				3	3	3	3	3	2
166							2	3	3	3	1	3	2
221				5		1	5	1	3	3	3	3	2
222	0			0				1	3	3	3	2	2
225							2	1	2	2	3	2	2
228			0					1	2	2	3	3	2
230		-1	0	0		1		1	1	1	3	2	1
234		-1		4			4	1	2	2	3	2	2
235							2	1	2	2	3	2	2
236			6				6	1	3	3	3	1	2
238							5	1	2	2	3	1	2
239				-5				1	2	2	3	1	2

Rainfall station code number	Results of homogeneity tests on rainfall characteristic							Partition					
	F_1^S	F_{15}^S	F_{25}^S	F_1^W	F_{15}^W	F_{25}^W	R	(i)	(ii)	(iii)	(iv)	(v)	(vi)
240			1		1		5	1	3	3	3	1	2
246			0				-1	1	3	3	3	3	2
252			0					1	3	3	3	3	2
329				-1	-6		-5	3	3	3	1	3	2
330	2	0	0	5			0	3	3	1	3	3	2
333		-6	0	-2	0		-6	5	3	3	3	2	2
339					-1	-5	-6	5	3	3	3	2	2
341			-3				-6	5	3	3	3	2	2
345		0	-6		-6	-1	-5	5	3	3	3	2	2
346				-5	-1	-4		2	3	1	3	3	2
347								2	3	3	3	1	2
348		1	1			-1		2	3	1	3	1	2
352		1					0	2	3	3	3	1	2
353				5				2	3	1	3	1	2
354					-1	-1	-6	3	3	3	3	2	2
356				4				2	3	1	3	1	2
359	-5			-6			-6	2	3	1	3	1	2
434	1	5		6			5	4	3	1	3	1	1
436					2			1	1	1	3	3	1
437	-5				2			1	1	1	1	2	1
438	0							1	1	1	1	2	1
439					2			1	1	1	1	2	1
440								1	2	2	1	3	2
441					4		-2	1	1	1	1	3	1
442	-4							1	1	1	1	2	1
443	-2	0						1	1	1	1	1	1
444							5	1	2	2	3	3	2
445			1		-6			1	1	1	1	3	1
449			0					1	1	1	1	3	1
450				5	6	4	6	1	2	2	3	1	2
453				5				1	1	1	1	3	1
455		5				5	5	1	3	3	3	1	1

Rainfall station code number	Results of homogeneity tests on rainfall characteristic							Partition					
	F_1^S	F_{15}^S	F_{25}^S	F_1^W	F_{15}^W	F_{25}^W	R	(i)	(ii)	(iii)	(iv)	(v)	(vi)
456	1		0					1	2	2	3	1	2
458		-6						1	1	1	1	2	1
459		6	0	6	1		6	1	3	1	3	1	1
462	5			1	1		1	1	2	2	3	1	2
466		0		1			1	1	2	2	1	3	2
467				6			1	1	3	1	1	3	1
469		0					5	1	1	1	1	3	1
471								1	2	2	2	1	2
539					0		-5	5	3	3	3	2	2
541	2							5	1	1	1	1	2
543							-6	4	1	1	1	3	2
547	-1			-2			-4	4	3	3	3	3	2
550		1						4	3	3	3	1	2
556					0		0	4	3	1	1	3	2
558		1		6	0			4	3	3	1	1	2
562	6		1	6		-6		4	3	3	3	1	2
564	-5			-6	-6		-6	4	3	3	3	3	2
571				5				4	1	1	1	3	2
573								4	1	1	1	3	2
578	0				0			4	1	1	1	1	2
579					2	0		4	3	3	3	1	2
584	4	4	6	2			5	4	3	3	3	1	2
586			5				0	4	3	1	1	3	2
664	-4	-4	-6			-5	-1	5	3	3	3	2	2
665						-5		5	1	1	3	2	2
666				-1	-6			5	1	1	3	2	2
667								5	3	3	3	3	2
668	2				0	-5		5	3	3	3	2	2
669						-1		5	3	3	3	2	2
670	-5			-2	-6	-1	-5	5	1	1	3	2	2
673	-1		-6	-6	-5		-6	5	3	3	2	2	2
674								5	1	1	3	2	2

Rainfall station code number	Results of homogeneity tests on rainfall characteristic							Partition					
	F_1^S	F_{15}^S	F_{25}^S	F_1^W	F_{15}^W	F_{25}^W	R	(i)	(ii)	(iii)	(iv)	(v)	(vi)
676	-5		-1			-5	-1	5	1	1	3	2	2
677							-1	4	3	3	3	3	2
678		-2						5	3	3	3	3	2
681			0					3	3	3	3	3	2
733				-2				1	2	2	2	1	2
740	5					2	0	1	2	2	3	1	2
742		-6	-1			4		1	2	1	3	2	1
745						4		1	2	1	3	2	1
747			-1					1	2	1	3	2	1
751					6			1	2	2	2	1	2
752		4					3	1	2	2	2	1	2
756						5		1	2	2	2	1	2
759			0	3	1		0	1	2	2	3	1	2
760		0					0	1	2	2	2	3	2
763		6				1	3	1	2	2	2	1	2
827		1					0	4	3	3	2	1	2
828							-6	4	3	3	3	2	2
830	0	5			4		6	4	3	3	3	1	2
832						2	-6	1	2	2	3	2	2
833	0	4					4	4	3	3	3	1	2
834		0		0				4	3	3	3	1	2
835	0	2		6	4			4	3	3	3	1	2
838					2			4	3	3	3	3	2
839			0		1			1	2	2	3	3	2
840		0		0	0			4	3	3	3	1	2
843	4							4	3	3	3	1	2
844	0	1	1		0		1	4	3	3	3	1	2
896	0		0					5	3	3	2	1	2
899		4		2			1	1	3	3	2	1	2
901	5			1	2		6	4	3	3	3	1	2
902			1	2			2	5	3	3	2	1	2
903	1					2		4	3	3	3	1	2

Rainfall station code number	Results of homogeneity tests on rainfall characteristic							Partition					
	F_1^S	F_{15}^S	F_{25}^S	F_1^W	F_{15}^W	F_{25}^W	R	(i)	(ii)	(iii)	(iv)	(v)	(vi)
908	0	-4	-3					5	3	3	2	2	2
911							0	4	3	3	3	1	2
912	0						-1	5	3	3	2	3	2
915	0	1					0	5	3	3	3	1	2
968							-1	5	1	1	1	2	1
970			0		-2		-1	5	3	3	2	2	1
973		0			-5		-1	5	3	1	3	2	1
974	-6	-5	-6		0		-6	5	3	3	2	2	1

A.6. DEGREE OF INDUSTRIALIZATION AND URBANIZATION OF THE RAINFALL STATIONS IN DATA SET D32

Table A.6.1. The degree of urbanization and industrialization of the rainfall stations in data set D32

Rainfall station	Pollution data available from year	Grid area ¹	Emissions (10 ³ t/y)			Inhabitants (x1000) (CBS, 1980)
			Sulphur dioxide	Carbon monoxide	Hydrocarbons	
Amsterdam	1975	G5	1.6	11.1	3.7	718.6
Arnhem	1977	N6	2.0	3.2	1.7	127.0
Axel	1978	I3	0.0	0.3	0.2	11.9
Bergschenhoek	1974	I8	0.1	2.9	0.7	6.7
Boskoop	1974	K10	0.0	0.8	0.4	13.4
Castricum	1975	D9	0.1	1.9	0.7	22.8
Cruquius/Heemstede	1975	C4	0.1	1.2	1.0	26.9
Delft	1974	G9	1.4	4.6	1.5	83.7
Denekamp	1977	U7	0.0	0.2	0.3	11.8
Den Helder/De Kooy	1975	E18	0.1	1.0	0.8	61.3
Dwingelo	n.a. ²					3.6
Groningen	n.a. ²					160.6
Heerde	1977	O15	0.1	0.8	0.6	17.5
Hoofddorp	1975	D3	0.1	2.0	0.5	76.0
Hoorn	1975	I11	0.1	1.4	0.5	37.3
Kerkwerpe	1978	I12	0.0	0.1	0.1	2.4
Leiden	1974	I12	0.2	5.1	3.9	102.7
Lisse	1974	J14	0.0	1.7	0.5	19.2
Mookhoek	1974	K3	0.1	2.3	0.4	8.1
Oostvoorne	1974	D7	5.8	8.6	0.7	7.0
Oudenbosch	1978	F10	0.0	0.9	0.3	11.9
Oude Wetering	1974	K13	0.0	1.5	0.4	12.7
Roermond	n.a. ²					37.2
Sassenheim	1974	J14	0.0	1.7	0.5	12.5
Schellingwoude	1975	H5	0.1	0.5	0.4	718.6
Ter Apel	n.a. ²					16.5

Rainfall station	Pollution data available from year	Grid area ¹	Emissions (10 ³ t/y)			Inhabitants (x1000) (CBS, 1980)
			Sulphur dioxide	Carbon monoxide	Hydrocarbons	
Vlissingen	1978	D7	0.2	1.0	0.6	44.9
West Terschelling	n.a. ²					4.6
Winterswijk	1977	Y6	0.1	0.7	0.5	27.4
IJsselmonde	1974	J6	0.2	8.1	1.7	582.4
Zandvoort	1975	B5	0.0	0.7	0.4	16.4
Zegveld	1975	B5	0.0	0.0	0.2	1.8

¹ Map references: Emission registrations, published by the Ministry of Public Health and Environmental Hygiene (Ministerie van Volksgezondheid en Milieuhygiëne). These are issued for each province of the Netherlands. Those for the provinces Zuid-Holland and Noord-Holland are included in the references.

² n.a.: data not available.

APPENDIX B. DATA AND SUPPLEMENTARY RESULTS OF THE STUDY ON ARF

B.1. RAINFALL RECORDS USED IN THE DETERMINATION OF ARF

The following records were used to estimate ARF_1 :

- data from three recording rainfall stations in the Hupsel catchment area;
- hourly rainfall records from De Bilt (1906-1982) and Soesterberg (1974-1982).

Records used to estimate ARF_{24} are presented in Table B.1.1.

Table B.1.1. Records used to estimate ARF_{24} (period of observation: 1951-1979)

Area	Areal size ¹ (km ²)	Name rainfall station	Code number (KNMI)	Days without observations	Periods of gap(s) (code no. of station supplying supplementary data)
1	990	Schellingwoude	223	28	Feb. 1957 (441)
		Overveen	225	0	
		Wijk aan Zee	226	31	Jan. 1953 (225)
		Zandvoort	229	0	
		Zaandijk	230	0	
		Zaandam	233	92	June-Aug. 1958 (230)
		Cruquius/Heemstede	435	61	Dec. 1973-Jan. 1974 (438)
		Sassenheim	436	0	
		Lijnsden	437	0	
		Hoofddorp	438	0	
		Amsterdam	441	0	
		Lisse	454	0	
2	1270	Vlissingen	733	0	
		Brouwershaven	736	90	Oct. 1952; Feb.-March 1953 (751)
		Noordgouwe	743	59	Feb.-March 1953 (751)
		Westkapelle	746	0	
		Wilhelminadorp	749	0	
		Vrouwenpolder	751	0	
		Haamstede	752	28	Feb. 1953 (751)
		Ovezande	754	0	
		Kortgene	755	90	Jan.-March 1953 (751)
		Middelburg	756	0	
		Wolphaartsdijk	758	31	Jan. 1951 (749)
		's-Heerenhoek	760	0	
3	1360	Putten	542	0	
		Apeldoorn	543	0	
		Lunteren	558	0	
		Hulshorst	564	0	
		Voorthuizen	565	0	
		Kootwijk	567	31	Nov. 1953 (543)
		Elspeet	570	0	
		Harskamp	571	39	21-28 Feb. 1955; Dec. 1955 (573)
		Beekbergen	573	0	
		Oosterbeek	578	0	
		Veenendaal	579	0	
		Barneveld	580	81	Nov.-Dec. 1955; 10-30 Sept. 1956 (565)

¹ Calculated according to USWB (1957-1960) as the total areal extent of 12 (number of rainfall records used) circles, each with radius equal to the mean distance between rainfall stations. These mean distances have been established using the Thiessen polygons from Figure 3.2.

B.2. KRIGING WEIGHTS FOR AREAL MEANS OF MONTHLY MAXIMA

The kriging weights, multiplied by the number of stations (12), are given in Tables B.2.1 to B.2.3.

Table B.2.1. Kriging weights for area 1

Month	KNMI code number of rainfall station											
	223	225	226	229	230	233	435	436	437	438	441	454
Jan.	1.08	1.05	0.90	0.66	0.88	0.97	0.90	0.81	1.37	1.33	1.30	0.75
Feb.	1.09	1.04	0.90	0.68	0.89	0.98	0.93	0.81	1.35	1.29	1.28	0.77
March	1.06	1.10	0.90	0.61	0.86	0.94	0.82	0.80	1.43	1.42	1.34	0.72
April	1.00	1.20	0.90	0.56	0.85	0.89	0.63	0.80	1.50	1.59	1.41	0.68
May	1.08	1.05	0.90	0.66	0.88	0.97	0.90	0.81	1.37	1.33	1.30	0.75
June	1.02	1.16	0.90	0.58	0.85	0.90	0.71	0.80	1.48	1.53	1.38	0.69
July	1.10	1.02	0.90	0.69	0.90	0.99	0.94	0.81	1.33	1.27	1.27	0.78
Aug.	1.06	1.10	0.90	0.62	0.86	0.94	0.83	0.80	1.42	1.41	1.34	0.73
Sept.	1.08	1.06	0.90	0.64	0.88	0.96	0.88	0.80	1.39	1.35	1.31	0.75
Oct.	1.05	1.11	0.90	0.61	0.86	0.93	0.81	0.80	1.44	1.43	1.35	0.72
Nov.	1.02	1.17	0.90	0.57	0.85	0.90	0.68	0.80	1.48	1.55	1.39	0.69
Dec.	1.11	1.00	0.90	0.74	0.93	1.01	0.97	0.83	1.27	1.20	1.23	0.81

Table B.2.2. Kriging weights for area 2

Month	KNMI code number of rainfall station											
	733	736	743	746	749	751	752	754	755	756	758	760
Jan.	0.57	0.85	0.75	1.28	0.92	1.82	2.19	0.45	1.17	0.79	0.75	0.47
Feb.	0.80	1.09	0.95	1.21	0.86	1.37	1.54	0.63	1.02	0.95	0.87	0.70
March	0.75	1.06	0.91	1.25	0.86	1.46	1.68	0.57	1.05	0.93	0.85	0.64
April	0.55	0.75	0.72	1.26	0.95	1.93	2.33	0.45	1.22	0.72	0.69	0.43
May	0.55	0.75	0.72	1.26	0.95	1.93	2.33	0.45	1.22	0.72	0.69	0.43
June	0.70	1.03	0.87	1.27	0.86	1.55	1.80	0.52	1.08	0.90	0.83	0.60
July	0.57	0.86	0.75	1.28	0.91	1.81	2.18	0.45	1.17	0.79	0.75	0.47
Aug.	0.86	1.09	0.98	1.17	0.88	1.26	1.39	0.72	1.01	0.97	0.90	0.77
Sept.	0.65	0.98	0.83	1.28	0.87	1.64	1.93	0.49	1.11	0.87	0.81	0.55
Oct.	0.58	0.88	0.76	1.28	0.91	1.79	2.14	0.45	1.16	0.81	0.76	0.48
Nov.	0.86	1.09	0.98	1.17	0.88	1.27	1.40	0.71	1.01	0.97	0.90	0.77
Dec.	0.96	1.04	1.01	1.05	0.96	1.07	1.11	0.91	1.00	0.99	0.97	0.93

Table B.2.3. Kriging weights for area 3

Month	KNMI code number of rainfall station											
	542	543	558	564	565	567	570	571	573	578	579	580
Jan.	0.99	1.12	0.89	1.08	0.75	1.18	1.26	1.12	1.14	1.15	0.70	0.63
Feb.	1.02	1.07	0.95	1.07	0.66	1.22	1.39	1.22	1.11	1.23	0.59	0.47
March	1.05	1.03	1.02	1.04	0.62	1.23	1.47	1.28	1.09	1.27	0.52	0.37
April	1.00	1.10	0.91	1.08	0.70	1.20	1.32	1.17	1.13	1.19	0.65	0.56
May	1.01	1.08	0.93	1.07	0.68	1.22	1.36	1.20	1.12	1.21	0.61	0.51
June	1.00	1.10	0.90	1.08	0.71	1.20	1.31	1.16	1.13	1.18	0.65	0.56
July	1.01	1.09	0.92	1.08	0.68	1.21	1.35	1.19	1.12	1.20	0.62	0.52
Aug.	1.01	1.09	0.92	1.08	0.69	1.21	1.34	1.19	1.12	1.20	0.63	0.53
Sept.	1.02	1.08	0.94	1.07	0.67	1.22	1.37	1.21	1.12	1.22	0.60	0.49
Oct.	1.03	1.06	0.96	1.06	0.65	1.23	1.41	1.23	1.11	1.24	0.57	0.45
Nov.	1.00	1.10	0.90	1.08	0.71	1.20	1.31	1.16	1.13	1.18	0.66	0.57
Dec.	0.99	1.08	0.93	1.04	0.92	1.06	1.08	1.02	1.07	1.03	0.90	0.89

B.3. KRIGING WEIGHTS FOR AREAL MEANS OF DAILY RAINFALL

The kriging weights, multiplied by the number of stations (12), are given in Tables B.3.1 to B.3.3.

Table B.3.1. Kriging weights for area 1

Month	KNMI code number of rainfall station											
	223	225	226	229	230	233	435	436	437	438	441	454
Jan.	1.10	1.02	0.90	0.69	0.90	0.99	0.94	0.81	1.32	1.27	1.27	0.78
Feb.	1.09	1.05	0.90	0.66	0.88	0.97	0.91	0.81	1.37	1.32	1.29	0.76
March	1.10	1.03	0.90	0.68	0.90	0.98	0.93	0.81	1.34	1.28	1.28	0.77
April	1.09	1.04	0.90	0.67	0.89	0.98	0.92	0.81	1.35	1.30	1.28	0.76
May	1.08	1.06	0.90	0.65	0.88	0.96	0.89	0.80	1.38	1.34	1.30	0.75
June	1.10	1.03	0.90	0.68	0.89	0.98	0.93	0.81	1.34	1.29	1.28	0.77
July	1.10	1.03	0.90	0.68	0.90	0.98	0.93	0.81	1.34	1.28	1.28	0.77
Aug.	1.08	1.07	0.90	0.64	0.87	0.96	0.88	0.80	1.39	1.36	1.31	0.74
Sept.	1.09	1.04	0.90	0.67	0.89	0.97	0.91	0.81	1.36	1.31	1.29	0.76
Oct.	1.08	1.06	0.90	0.65	0.88	0.96	0.89	0.80	1.38	1.34	1.30	0.75
Nov.	1.09	1.05	0.90	0.66	0.88	0.97	0.90	0.81	1.37	1.32	1.30	0.75
Dec.	1.11	1.02	0.90	0.70	0.91	0.99	0.95	0.82	1.31	1.25	1.26	0.78

Table B.3.2. Kriging weights for area 2

Month	KNMI code number of rainfall station											
	733	736	743	746	749	751	752	754	755	756	758	760
Jan.	0.65	0.98	0.82	1.28	0.87	1.64	1.93	0.49	1.11	0.87	0.81	0.55
Feb.	0.72	1.04	0.88	1.26	0.86	1.52	1.76	0.54	1.07	0.91	0.84	0.61
March	0.66	0.99	0.84	1.28	0.87	1.62	1.90	0.49	1.10	0.88	0.82	0.56
April	0.61	0.93	0.78	1.28	0.89	1.72	2.05	0.46	1.14	0.84	0.78	0.51
May	0.61	0.93	0.78	1.28	0.89	1.72	2.05	0.46	1.14	0.84	0.79	0.51
June	0.69	1.02	0.86	1.27	0.86	1.57	1.83	0.51	1.08	0.90	0.83	0.58
July	0.67	1.00	0.84	1.27	0.86	1.60	1.88	0.50	1.09	0.89	0.82	0.57
Aug.	0.71	1.04	0.88	1.26	0.86	1.52	1.77	0.54	1.07	0.91	0.84	0.61
Sept.	0.62	0.94	0.79	1.28	0.88	1.70	2.03	0.47	1.13	0.84	0.79	0.52
Oct.	0.63	0.95	0.80	1.28	0.88	1.68	2.00	0.47	1.12	0.85	0.80	0.53
Nov.	0.62	0.95	0.80	1.28	0.88	1.69	2.01	0.47	1.13	0.85	0.80	0.52
Dec.	0.79	1.08	0.95	1.22	0.86	1.38	1.56	0.62	1.03	0.95	0.87	0.69

Table B.3.3. Kriging weights for area 3

Month	KNMI code number of rainfall station											
	542	543	558	564	565	567	570	571	573	578	579	580
Jan.	1.00	1.10	0.91	1.08	0.71	1.20	1.32	1.16	1.13	1.18	0.65	0.56
Feb.	1.00	1.10	0.91	1.08	0.70	1.21	1.32	1.17	1.13	1.19	0.65	0.55
March	1.01	1.09	0.92	1.08	0.69	1.21	1.35	1.19	1.12	1.20	0.63	0.52
April	1.02	1.07	0.94	1.07	0.67	1.22	1.38	1.21	1.12	1.22	0.60	0.49
May	1.01	1.09	0.92	1.08	0.69	1.21	1.34	1.18	1.12	1.20	0.63	0.53
June	1.00	1.10	0.90	1.08	0.71	1.20	1.31	1.16	1.13	1.18	0.66	0.57
July	0.99	1.11	0.89	1.08	0.73	1.19	1.28	1.13	1.13	1.16	0.68	0.61
Aug.	1.00	1.10	0.91	1.08	0.70	1.21	1.32	1.17	1.13	1.19	0.64	0.55
Sept.	1.02	1.07	0.95	1.07	0.66	1.22	1.39	1.22	1.11	1.23	0.59	0.47
Oct.	0.99	1.12	0.89	1.08	0.74	1.18	1.27	1.12	1.14	1.15	0.69	0.62
Nov.	0.99	1.12	0.89	1.08	0.74	1.18	1.27	1.13	1.14	1.15	0.69	0.62
Dec.	0.99	1.13	0.88	1.08	0.77	1.17	1.23	1.10	1.14	1.13	0.72	0.66

REFERENCES

- Abdy, P.R., and Dempster, M.A.H., 1974. Introduction to optimization methods. Chapman and Hall, London.
- Abrahamse, A.P.J., and Koerts, J., 1969. A comparison between the power of the Durbin-Watson test and the power of the BLUS test. *Journal of the American Statistical Association* 64: 938-948.
- Anderson, T.W., 1958. An introduction to multivariate statistical analysis. Chapman and Hall, London.
- Anis, A.A., and Lloyd, E.H., 1976. The expected value of the adjusted rescaled Hurst range of independent normal summands. *Biometrika* 63: 111-116.
- Barry, A.G., and Perry, A.N., 1973. Synoptic climatology. Methods and applications. Methuen & Co., London.
- Bell, F.C., 1969. Generalized rainfall-duration-frequency relationships. *Journal of the Hydraulics Division (ASCE)* 95: 311-327.
- Bell, F.C., 1976. The areal reduction factor in rainfall frequency estimation. Report 35, Institute of Hydrology, Wallingford.
- Beran, M.A., and Nozdryn-Plotnicki, M.J., 1977. Estimation of low return period floods. *Hydrological Science Bulletin* 22: 275-282.
- Boer, J.H., and Feteris, P.J., 1969. The influence of the sea on the distribution of lightning and rain over a coastal area. *Annalen der Meteorologie (Neue Folge)* 4: 109-111.
- Boyer, M.C., 1957. A correlation of the characteristics of great storms. *Transactions American Geophysical Union* 38: 233-238.
- Bornstein, R.D., and Oke, T., 1980. Influence of pollution on urban climatology. *Advances in Environmental Sciences and Engineering* 3: 171-202.
- Braak, C., 1933. Het klimaat van Nederland. A (vervolg). Neerslag. Eerste gedeelte. Neerslag volgens zelfregistreerende en gewone regenmeters, regenkaarten (The climate of the Netherlands. A (continued). Precipitation. First part. Precipitation, observed with selfrecording and ordinary raingauges, rainfall maps). KNMI Mededelingen en Verhandelingen 34a, Koninklijk Nederlands Meteorologisch Instituut, De Bilt.

- Braak, C., 1945. Invloed van den wind op regenwaarnemingen (Influence of the wind on rainfall measurements). KNMI Mededelingen en Verhandelingen 48, Rijksuitgeverij, 's-Gravenhage.
- Braham, R.R., 1979. Comments on 'Urban, topographic and diurnal effects on rainfall in the St. Louis region'. *Journal of Applied Meteorology* 18: 371-375.
- Bras, R.L., and Rodríguez-Iturbe, I., 1976. Evaluation of the mean square error involved in approximating the real average of a rainfall event by a discrete summation. *Water Resources Research* 12: 181-184.
- Bras, R.L., and Colón, R., 1978. Time-averaged areal mean of precipitation estimates and network design. *Water Resources Research* 14: 878-888.
- Brunet-Moret, Y., and Roche, M., 1966. Etude théorique et méthodologique de l'abattement des pluies. *Cahiers ORSTOM. Série Hydrologie* 3(4): 3-13.
- Buishand, T.A., 1977a. Stochastic modelling of daily rainfall sequences. *Communications Agricultural University* 77-3, Veenman & Zonen, Wageningen.
- Buishand, T.A., 1977b. De variantie van de gebiedsneerslag als functie van puntneerslagen en hun onderlinge samenhang (The variance of the amount of rainfall on an area related to point rainfall amounts). *Communications Agricultural University* 77-10, Veenman & Zonen, Wageningen.
- Buishand, T.A., 1977c. Het gebiedsgrootte-effect bij dagneerslagen. Mimeograph, Department of Mathematics of the Agricultural University, Wageningen.
- Buishand, T.A., 1979. Urbanization and changes in precipitation, a statistical approach. *Journal of Hydrology* 40: 365-375.
- Buishand, T.A., 1981. The analysis of homogeneity of long-term rainfall records in the Netherlands. KNMI Scientific Report 81-7, Koninklijk Nederlands Meteorologisch Instituut, De Bilt.
- Buishand, T.A., 1982a. Some methods for testing the homogeneity of rainfall records. *Journal of Hydrology* 58: 11-27.
- Buishand, T.A., 1982b. Maandsommen en jaarsommen van enkele langjarige neerslagreeksen in Nederland (Monthly and annual amounts of long-term rainfall records in the Netherlands). KNMI Technical Report 26, Koninklijk Nederlands Meteorologisch Instituut, De Bilt.

- Buishand, T.A., 1983. De kansverdeling van D-uurlijkse neerslag-sommen ($D = 1, 2, 4, 6, 12, 24$ of 48) in Nederland (The distribution of D-hour precipitation amounts ($D = 1, 2, 4, 6, 12, 24$ or 48) in the Netherlands). KNMI Scientific Report 83-5, Koninklijk Nederlands Meteorologisch Instituut, De Bilt.
- Buishand, T.A., and Velds, C.A., 1980. Neerslag en verdamping. Koninklijk Nederlands Meteorologisch Instituut, De Bilt.
- Bijvoet, H.C., and Schmidt, F.H., 1958. Het weer in Nederland in afhankelijkheid van circulatietypen. Deel 1. KNMI Wetenschappelijk Rapport 58-4, Koninklijk Nederlands Meteorologisch Instituut, De Bilt.
- Bijvoet, H.C., and Schmidt, F.H., 1960. Het weer in Nederland in afhankelijkheid van circulatietypen. Deel 2. KNMI Wetenschappelijk Rapport 60-1, Koninklijk Nederlands Meteorologisch Instituut, De Bilt.
- CBS, 1979. 80 jaar statistiek in tijdreeksen. 1899-1979 (Historical series of the Netherlands. 1899-1979). Staatsuitgeverij, 's-Gravenhage.
- CBS, 1980. Regionaal statistisch zakboek 1980. (Regional pocket yearbook 1980). Staatsuitgeverij, 's-Gravenhage.
- Chow, V.T., 1953. Discussion of 'Area-depth studies for thunderstorm rainfall in Illinois' by F.A. Huff and G.E. Stout. Transactions American Geophysical Union 34: 628-630.
- Chow, V.T., 1954. Discussion on rainfall studies using rain-gage networks and radar. Transactions American Society of Civil Engineers 119: 274-275.
- Chow, V.T., 1958. Discussion of 'A correlation of the characteristics of great storms' by M.C. Boyer. Transactions American Geophysical Union 39: 124-125.
- Chua, S.H., and Bras, R.L., 1980. Estimation of stationary and non-stationary random fields: kriging in the analysis of orographic precipitation. Ralph M. Parsons Laboratory Report 255, Massachusetts Institute of Technology, Cambridge (Massachusetts).
- Corsten, L.C.A., 1982. Geregionaliseerde stochastische functies. Department of Mathematics of the Agricultural University, Wageningen.
- Court, A., 1961. Area-depth rainfall formulas. Journal of Geophysical Research 66: 1823-1831.

- CTGREF, 1979. Analyse des pluies de 1 à 10 jours sur 300 postes métropolitains. Centre Technique du Génie Rural des Eaux et des Forêts, Antony.
- Cultuurtechnische Vereniging, 1971. Cultuurtechnisch vademecum. Cultuurtechnische Vereniging, Utrecht.
- De Bruin, H.A.R., 1975. Over het interpoleren van de neerslaghoogte. KNMI Wetenschappelijk Rapport 75-2, Koninklijk Nederlands Meteorologisch Instituut, De Bilt.
- Delfiner, P., 1976. Linear estimation of non stationary spatial phenomena. In: Guarascio, M., David, M., and Huijbregts, C. (ed.), 1976. Advanced geostatistics in the mining industry. D. Reidel Publishing Company, Dordrecht.
- Delhomme, J.P., 1978. Kriging in the hydrosiences. *Advances in Water Resources* 1: 251-266.
- Denkema, A., 1970. Representativiteit van een puntmeting. KNMI Wetenschappelijk Rapport 70-6, Koninklijk Nederlands Meteorologisch Instituut, De Bilt.
- Deij, L.J.L., 1968. Enige opmerkingen over de neerslagmeting en de neerslagverdeling naar tijd en plaats in ons land (Some notes on the measuring of precipitation and its partition in time and space in the Netherlands). In: Committee for hydrological research T.N.O. Proceedings and Informations 14, T.N.O., 's-Gravenhage.
- Durbin, J.D., 1961. Some methods of constructing exact tests. *Biometrika* 48: 41-55.
- Eagleson, P.S., 1970. Dynamic hydrology. McGraw-Hill, New York.
- Feller, W., 1951. The asymptotic distribution of the range of sums of independent random variables. *Annals of Mathematical Statistics* 22: 427-432.
- Fogel, M.M., and Duckstein, L., 1969. Point rainfall frequencies in convective storms. *Water Resources Research* 5: 1229-1237.
- Galéa, G., Michel, C., and Oberlin, G., 1983. Maximal rainfall on a surface the epicentre coefficient of 1- to 48-hour rainfall. *Journal of Hydrology* 66: 159-167.
- Gandin, L.S., 1965. Objective analysis of meteorological fields. Israel Program for Scientific Translations, Jerusalem.
- Hartman, Ch.M.A., 1913. Het klimaat van Nederland. A. Neerslag. KNMI Mededelingen en Verhandelingen 15, Koninklijk Nederlands Meteorologisch Instituut, De Bilt.

- HEC, 1977. Storage, treatment, overflow, runoff model STORM. Hydrologic Engineering Center, US Army Corps of Engineers, Davis.
- Hershfield, D.M., 1961. Rainfall frequency atlas of the United States. Weather Bureau Technical Paper 40, US Department of Commerce, Washington D.C.
- Hershfield, D.M., 1979. Secular trends in extreme rainfalls. *Journal of Applied Meteorology* 18: 1078-1081.
- Hess, P., 1977. Katalog der Grosswetterlagen Europas. Deutsche Wetterdienst, Offenbach am Main.
- Holland, D.J., 1967. The Cardington rainfall experiment. *Meteorological Magazine* 96: 193-202.
- Horton, R.E., 1924. Discussion of 'The distribution of intense rainfall and some other factors in the design of storm-water drains' by Frank A. Marston. *Proceedings American Society of Civil Engineers* 50: 660-667.
- Huff, F.A., and Changnon, S.A., 1973. Precipitation modification by major urban areas. *Bulletin American Meteorological Society* 54: 1220-1232.
- Huff, F.A., and Stout, G.E., 1952. Area-depth studies for thunderstorm rainfall in Illinois, *Transactions American Geophysical Union* 33: 495-498.
- Huff, F.A., and Vogel, J.L., 1979. Reply to comments on 'Urban, topographic and diurnal effects on rainfall in the St. Louis region' by R.R. Braham. *Journal of Applied Meteorology* 18: 375-378.
- Johnson, N.L., and Kotz, S., 1970. Distributions in statistics - Continuous univariate distributions-2. John Wiley & Sons, New York.
- Journel, A.G., and Huijbregts, Ch.J., 1978. Mining geostatistics. Academic Press, New York.
- Kafritsas, J., and Bras, R.L., 1981. The practice of kriging. Ralph M. Parsons Laboratory Report 263, Massachusetts Institute of Technology, Cambridge (Massachusetts).
- Kendall, M.G., and Stuart, A.D., 1977. The advanced theory of statistics. Three-volume edition: Volume 1. Distribution theory. Charles Griffin & Company Limited, London.
- KNMI, 1972. Klimaatatlas. Staatsuitgeverij, 's-Gravenhage.

- KNMI/RIV, 1982. Chemical composition of precipitation over the Netherlands. Annual Report 1981. Koninklijk Nederlands Meteorologisch Instituut, De Bilt.
- Können, G.P., 1983. Het weer in Nederland. Thieme, Zutphen.
- Kraijenhoff, D.A., 1958. Discussion of 'A correlation of the characteristics of great storms' by M.C. Boyer. Transactions American Geophysical Union 39: 125-127.
- Kraijenhoff, D.A., 1963. Areal distribution of extreme summer rainfall in the Netherlands. Mimeograph, Department of Hydraulics and Catchment Hydrology of the Agricultural University, Wageningen.
- Kraijenhoff, D.A., and Prak, H., 1979. Verstedelijking, industrie en zware zomerregens: een verkennende studie. (Urbanization, industrialization and heavy summer rainfalls: a reconnaissance). H_2O 12: 75-81.
- Kraijenhoff, D.A., Kroeze, J., and Arnold, G.E., 1981. Heftige regens leiden tot snelle afvoeren. Waterschapsbelangen 66: 64-68.
- Kruizinga, S., and Yperlaan, G.J., 1976. Ruimtelijke interpolatie van de dagtotalen van de neerslag. Een experimentele benadering (Spatial interpolation of daily rainfall totals). KNMI Wetenschappelijk Rapport 76-4, Koninklijk Nederlands Meteorologisch Instituut, De Bilt.
- Langbein, W.B., 1949. Annual floods and the partial-duration flood series. Transactions American Geophysical Union 30: 879-881.
- Le Barbe, L., 1982. Etude du ruissellement urbain à Ouagadougou. Essai d'interprétation théorique. Recherche d'une méthode d'évaluation de la distribution des débits de pointes de crues à l'exutoire des bassins urbains (Urban runoff survey at Ouagadougou (Upper-Volta). Attempt of theoretical interpretation. Research of an assessment method of the discharge peak flow distribution at the outlet of urban basins). Cahiers ORSTOM, Série Hydrologie 19: 135-204.
- Leenen, J.D., and Groot, S., 1980. Kwalitatieve en kwantitatieve aspecten van de afvoer van stedelijke gebieden. Speurwerkverslag, calibratie STORM-model. Technical Note 45, Department of Hydraulics and Catchment Hydrology of the Agricultural University, Wageningen.

- Lowry, W.P., 1977. Emperical estimation of urban effects on climate: a problem analysis. *Journal of Applied Meteorology* 16: 129-135.
- Mandelbrot, B.B., and Wallis, J.R., 1969. Computer experiments with fractional Gaussian noises. Part 1, averages and variances. *Water Resources research* 5: 228-241.
- Matheron, G., 1971. The theory of regionalized variables and its applications. Ecole Nationale Supérieure des Mines de Paris, Paris.
- McIntosh, D.H., and Thom, A.S., 1978. Essentials of meteorology. Wykeham Publications, London.
- Ministère de l'Intérieur, 1977. Circulaire no. 77-284/JN5. In: Instruction technique relative aux réseaux d'assainissement des agglomérations. Ministère de l'Intérieur, Paris.
- Ministerie van Volksgezondheid en Milieuhygiëne, 1978. Emissie-registratie 2. Rapport emissieregistratie Zuid-Holland. Staatsuitgeverij, 's-Gravenhage.
- Ministerie van Volksgezondheid en Milieuhygiëne, 1980. Emissie-registratie 3. Rapport emissieregistratie Noord-Holland. Staatsuitgeverij, 's-Gravenhage.
- Myers, V.A., and Zehr, R.M., 1980. A methodology for point-to-area rainfall frequency ratios. NOAA Technical Report NWS 24, US Department of Commerce, Washington D.C.
- NERC, 1975. Flood Studies Report (5 volumes). Natural Environment Research Council, London.
- Nguyen, V.T., Rouselle, J., and McPherson, M.B., 1981. Evaluation of areal versus point rainfall with sparse data. *Canadian Journal of Civil Engineers* 8: 173-178.
- Nicks, A.D., and Igo, F.A., 1980. A depth-area-duration model of storm rainfall in the Southern Great Plains. *Water Resources Research* 16: 939-945.
- Nonclerq, P., 1982. Le dimensionnement hydraulique des collecteurs d'eaux pluviales. Cebedoc. Liège.
- Oke, T.R., 1974. Review of urban climatology 1968-1973. WMO Technical Note 134, World Meteorological Organization, Geneva.
- Oke, T.R., 1979. Review of urban climatology 1973-1976. WMO Technical Note 169, World Meteorological Organization, Geneva.

- Oke, T.R., 1980. Climatic impacts of urbanization. In: Bach, W., Pankrap, J., and Williams, J. Interactions of energy and climate. D. Reidel Publishing Company, Dordrecht.
- Pattison, A. (ed.), 1977. Australian rainfall and runoff. Flood analysis and design. Institution of Engineers. Canberra.
- Pearson, E.S., and Hartley, H.O., 1972. Biometrika tables for statisticians, Volume 2. Cambridge University Press, Cambridge.
- Rhenals-Figueroa, A.E., Rodríguez-Iturbe, I., and Schaake Jr., J.C., 1974. Bidimensional spectral analysis of rainfall events. Ralph M. Parsons Laboratory Report 193, Massachusetts Institute of Technology, Cambridge (Massachusetts).
- Roche, M., 1963. Hydrologie de surface. Gauthier-Villars, Paris.
- Rodríguez-Iturbe, I., and Mejía, J.M., 1974. On the transformation of point rainfall to areal rainfall. Water Resources Research 10: 729-736.
- Rogers, R.R., 1979. A short course in cloud physics. Pergamon Press, Oxford.
- Schmidt, F.H., and Boer, J.H., 1962. Local circulation around an industrial area. Berichte des Deutschen Wetterdienstes 91: 28-31.
- Smith, R.E., 1974. Point processes of seasonal thunderstorm rainfall. 3. Relation of point rainfall to storm areal properties. Water Resources Research 10: 424-426.
- Stol, Ph.Th., 1972. The relative efficiency of the density of rain-gage networks. Journal of Hydrology 15: 193-208.
- Stol, Ph.Th., 1981a. Rainfall interstation correlation functions. I. An analytic approach. Journal of Hydrology 50: 45-71.
- Stol, Ph.Th., 1981b. Rainfall interstation correlation functions. II. Application to three storm models with the percentage of dry days as a new parameter. Journal of Hydrology 50: 73-104.
- Stol, Ph.Th., 1981c. Rainfall interstation correlation functions. III. Approximations to the analytically derived equation of the correlation function for an exponential storm model compared to those for a rectangular and a triangular storm. Journal of Hydrology 52: 269-289.
- Timmermans, H., 1963. The influence of topography and orography on the precipitation patterns in the Netherlands. KNMI Mededelingen en Verhandelingen 80, Staatsdrukkerij- en uitgeverijbedrijf, 's-Gravenhage.

- Tomlinson, A.I., 1980. The frequency of high intensity rainfalls in New Zealand, Part 1. National Water and Soil Conservation Organisation, Wellington.
- USWB, 1947. Thunderstorm rainfall. US Weather Bureau Hydrometeorological Report 5, US Department of Commerce, Washington D.C.
- USWB, 1957-1960. Rainfall intensity-frequency regime (5 volumes). US Department of Commerce, Washington D.C.
- Van Montfort, M.A.J., 1968. Enige statistische opmerkingen over neerslag en afvoer (Some statistical remarks on precipitation and runoff). In: Committee for hydrological research T.N.O. Proceedings and Informations 14, T.N.O., 's-Gravenhage.
- Vuillaume, G., 1974. l'Abattement des précipitations journalières en Afrique intertropicale. Variabilité et précision de calcul. Cahiers ORSTOM, Série Hydrologie 11: 205-240.
- Wallis, J.R., and O'Connell, P.E., 1973. Firm reservoir yield - How reliable are historic hydrological records? Hydrological Science Bulletin 18: 347-365.
- Werkgroep Afvoerberekeningen, 1979. Richtlijnen voor het berekenen van afwateringsstelsels in landelijke gebieden. Studiekring voor Cultuurtechniek, Drachten.
- Wind, G.P., 1963. Gevolgen van wateroverlast in de moderne landbouw (High soil moisture contents and modern farming). In: Committee for hydrological research T.N.O. Proceedings and Informations 9, T.N.O., 's-Gravenhage.
- Woolhiser, D.A., and Schwalen, H.C., 1959. Area-depth-frequency relations for thunderstorm rainfall in Southern Arizona. Technical Paper 527, University of Arizona, Tucson.
- Worsley, K.J., 1979. On the likelihood ratio test for a shift in location of Normal populations. Journal of the American Statistical Association 74: 365-367.
- Yperlaan, G.J., 1977. Statistical evidence of the influence of urbanization on precipitation in the Rijnmond area: In: Effects of urbanization and industrialization on the hydrological regime and on water quality. Proceedings of the Amsterdam Symposium, October 1977. IAHS-AISH Publication 123.

CURRICULUM VITAE

Jan Victor Witter was born on 1 September 1950 in the village of Poortugaal, near Rotterdam. He attended secondary school in Rotterdam, which he finished in 1969. He studied rural engineering at the Agricultural University, Wageningen. During his studies, in 1977 he carried out field-work in Venezuela on reservoir management. In 1978, he worked for the Surinam government on mathematical models of open channel flow and of salt intrusion in estuaries. In 1979, he graduated from the Agricultural University and between September 1979 and September 1983 worked as a research assistant in the Department of Hydraulics and Catchment Hydrology at the Agricultural University.